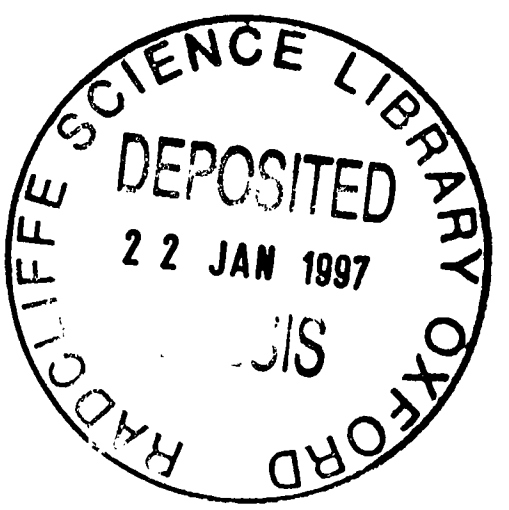
SYNAPTIC INTERACTION OF HIPPOCAMPAL GABAERGIC NEURONES

Stuart Robert Cobb

Green College, Oxford

Thesis submitted for the degree of Doctor of Philosophy at the University of Oxford

Trinity Term, 1996



II

Synaptic interaction of hippocampal GABAergic neurones

Stuart Robert Cobb
Green College, Oxford

Thesis submitted for the degree of Doctor of Philosophy at the University of Oxford
Trinity Term, 1996

ABSTRACT

Current concepts of hippocampal circuitry assume a large population of excitatory principal neurones whose activity is largely governed by a network of local-circuit GABAergic interneurones. The diversity of hippocampal local-circuit neurones and their synaptic control over principal cell activity was investigated *in vitro,* in order to define their synaptic connections and functional roles.

Single and dual intracellular recordings were made from local-circuit neurones and pyramidal cells in area CA1 of the rat hippocampal slice. Interneurones were tentatively distinguished from pyramidal cells based on their firing as well as their membrane properties. Intracellular labelling of recorded cells with the marker biocytin revealed a diversity of cell types based on differential dendritic and axonal morphology and synaptic connections.

The physiological data revealed that all types of interneurone tested evoked inhibitory postsynaptic potentials (IPSPs) in simultaneously recorded pyramidal cells. The IPSPs had fast rise and decay kinetics and the ones tested pharmacologically, were mediated by $GABA_A$ receptors. Similarly, individual interneurones were also shown to innervate other local-circuit interneurones in addition to pyramidal cells, the evoked effects being qualitatively similar in both types of postsynaptic targets.

The postsynaptic effect and functional role of one type of hippocampal interneurone, the basket cell, was investigated in greater detail. Basket cell-evoked IPSPs were reliable, but showed some frequency-dependent attenuation. Moreover, basket cell IPSPs were found to interact with intrinsic pyramidal cell conductances to elicit rebound depolarisations and facilitate action potential generation.

More detailed investigation showed that basket and axo-axonic cells were particularly effective in entraining pyramidal cell firing and sub-threshold membrane potential oscillations. Through these powerfully tuned mechanisms, sub-types of local-circuit interneurone provide a powerful mechanism to synchronise the activity of pyramidal cells.

These results demonstrate a remarkable diversity of GABAergic local-circuit neurones in the hippocampal CA1 area and suggest that specific subtypes of cell mediate different functions.

ACKNOWLEDGEMENTS

I would like to express my sincere gratitude to my co-supervisors, Professor Peter Somogyi and Dr. Eberhard Buhl for their teaching, advice and encouragement.

I would also like to thank the other lab members Zoltan Nusser, Txema Sanz, Imre Vida, Ole Paulsen, Rafael Lujan, David Roberts, Katalin Halasy, Diane Latawiec, Zai Ahmed, Gabor Tamas and Tibi Szilagy for creating a friendly and stimulating environment.

I thank the secretarial and technical staff for the excellent backup and in particular to Laura Lyford for frequent assistance and for putting up with me in her office. I thank Professor David Smith and all members of the MRC unit and Pharmacology Department for providing excellent facilities and am grateful to the Medical Research Council for providing financial support.

I am very grateful to Dr. Mario Cortina (Oxford University Statistical Service) for statistical advice.

Finally I would like to thank my family and friends for their encouragement and especially Cheryl for her love, understanding and support.

CONTENTS

Abstract	II
Acknowledgements	III
Contents	IV
Abbreviations	IX
Chapter 1. General introduction	1
1.1 Structure and function of the hippocampal formation	2
1.1.1 Microcircuitry of the hippocampus	2
1.1.2 Diversity of hippocampal GABAergic interneurones	4
1.2 Synaptic transmission	6
1.2.1 Glutamate as a neurotransmitter	6
1.2.2 GABA as a neurotransmitter	7
1.3 Neuronal integration at the cellular level	9
1.4 Objectives of thesis	11
Figure 1.1	12
Chapter 2. Experimental procedures	13
2.1 Hippocampal slice preparation	14
2.1.1 Animal procedures and anaesthesia	14
2.1.2 Brain sectioning	14
2.1.3 Solutions	15
2.2 Intracellular recordings and data analysis	15
2.3 Histological processing and anatomical evaluation	17
2.3.1 Processing of sections for light microscopy	17
2.3.2 Light microscopic evaluation of specimens	18
2.3.3 Processing of cells for electron microscopy	18
2.3.4 Electron microscopic evaluation of specimens	19
2.4 Materials	20
2.4.1 General	20

2.4.2 Pharmacological compounds 20
2.5 Distribution of shared materials 21
Table 2.1 22

Chapter 3. Anatomical and physiological identification of local-circuit interneurones in area CA1 of the rat hippocampus 23

3.1 Introduction 24
3.2 Materials and methods 25
3.3 Results 27
3.3.1 Morphologically heterogeneous population of CA1 interneurones 27
3.3.1.1 Axo-axonic cells 30
3.3.1.2 Basket cells 31
3.3.1.3 Dendritically terminating cells 32
3.3.1.4 Mixed cells 33
3.3.1.5 Statistical analysis of cell types based on differential synaptic target profiles 34
3.3.2 Physiological properties of pyramidal cell layer interneurones 36
3.3.3 Unitary synaptic responses evoked in postsynaptic pyramidal cells 37
3.4 Discussion 39
3.4.1 Diversity of local-circuit interneurones in the CA1 area 39
3.4.2 Laminar axonal distribution and synaptic termination patterns of local-circuit neurones in the CA1 area 40
3.4.2.1 Axo-axonic cells 41
3.4.2.2 Basket cells 43
3.4.2.3 Dendritically terminating cells 45
3.4.2.4 Mixed cells 47
3.4.3 Comparison of dendritic and axonal arbourisations 48
3.4.4 Functional implications 50
Figure 3.1 53
Figure 3.2 54
Figure 3.3 55
Figure 3.4 56

Figure 3.5 57
Figure 3.6 58
Figure 3.7 59
Figure 3.8 60
Figure 3.9 61
Figure 3.10 62
Table 3.1 63
Table 3.2 64

Chapter 4. Properties of unitary IPSPs evoked by anatomically identified basket cells in the rat hippocampus 65

4.1 Introduction 66
4.2 Materials and methods 68
4.3 Results 68
4.3.1 Physiological properties of pre- and postsynaptic cells 68
4.3.2 Anatomical definition of CA1 basket cells 69
4.3.3 Morphological features of basket cells 70
4.3.4 Postsynaptic targets of basket cells 71
4.3.5 Properties of unitary basket cell-mediated IPSPs 72
4.3.6 Voltage dependence and conductance of unitary IPSPs 73
4.3.7 Receptor pharmacology of unitary IPSPs 74
4.3.8 Summation of IPSPs and use-dependent depression 75
4.3.9 Reliability of unitary IPSPs 75
4.3.10 Postinhibitory facilitation and rebound action potentials 76
4.4 Discussion 77
4.4.1 Identification of pre- and postsynaptic neurones 77
4.4.2 Monosynaptic nature of unitary basket cell effects 78
4.4.3 Unitary basket cell IPSPs - some consensus data 79
4.4.4 Receptor pharmacology of basket cell-mediated IPSPs 80
4.4.5 Presynaptic control of basket cell-mediated GABA release 81
4.4.6 Unitary conductance and number of release sites 83
4.4.7 Inhibitory rebound 84
4.4.8 A distinct functional role for basket cells ? 85
Figure 4.1 86
Figure 4.2 87

Figure 4.3 88
Figure 4.4 89
Figure 4.5 90
Figure 4.6 91
Table 4.1 92

Chapter 5. Novel mechanisms of synchronising neuronal activity by individual local-circuit interneurones 93

5.1 Introduction 94
5.2 Materials and methods 96
5.3 Results 98
5.3.1 Identification of labelled neurones 98
5.3.2 Characteristics of unitary IPSPs 99
5.3.3 Effect of unitary IPSPs on action potential generation 99
5.3.4 Effect of unitary IPSPs on the timing of action potentials 100
5.3.5 Mechanisms underlying phasing of pyramidal cells 101
5.3.6 Synchronisation of pyramidal cell activity 103
5.4 Discussion 103
5.4.1 Basket cell mediated suppression of pyramidal cell firing 104
5.4.2 Unitary IPSPs control the timing of pyramidal cell activities 107
5.4.3 Mechanisms underlying inhibitory phasing of pyramidal cells 108
5.4.4 Functional implications 109
Figure 5.1 112
Figure 5.2 113
Figure 5.3 114
Figure 5.4 115
Figure 5.5 116
Figure 5.6 117

Chapter 6. Common sources of GABAergic inhibitory input to interneurones and pyramidal cells 118

6.1 Introduction 119
6.2 Materials and methods 120
6.3 Results 120

6.3.1 Basket cell - to - bistratified cell pair 121
6.3.1.1 Anatomical analysis 121
6.3.1.2 Synaptic coupling 122
6.3.2 Basket cell -to- fast-spiking interneurone pair 123
6.3.2.1 Anatomical analysis 123
6.3.2.2 Synaptic coupling 125
6.3.3 Stratum lacunosum-moleculare / radiatum border interneurone - to - bistratified cell pair 126
6.3.3.1 Anatomical analysis 126
6.3.3.2 Synaptic coupling 127
6.4 Discussion 128
6.4.1 Identification of pre- and postsynaptic neurones 128
6.4.2 Properties of postsynaptic responses 129
6.4.3 Sources of GABAergic input 131
6.4.4 Functional implications 132
Figure 6.1 134
Figure 6.2 135
Figure 6.3 136
Figure 6.4 137
Figure 6.5 138
Figure 6.6 139
Figure 6.7 140
Figure 6.8 141
Table 6.1 142

Chapter 7. General discussion 143

7.1 Overview 144
7.1.1 Diversity of GABAergic interneurones 145
7.1.2 Synaptic interaction of GABAergic interneurones 146
7.1.3 Distinct functional roles for different types of GABAergic interneurones ? 147
7.1.4 Modelling of hippocampal circuits 150
7.2 Technical consideration 150
7.3 Future directions 153
References 156

ABBREVIATIONS

ABC	avidin-biotinylated horseradish peroxidase complex
ACSF	artificial cerebrospinal fluid
AMPA	D,L-alpha-amino-3-hydroxy-5-methyl-4-isoxazole propionate
CNQX	6-cyano-7-nitroquinoxaline-2,3-dione
CNS	central nervous system
DAB	3,3'-diaminobenzidine
EPSC	excitatory postsynaptic current
EPSP	excitatory postsynaptic potential
fAHP	fast afterhyperpolarisation
GABA	gamma aminobutyric acid
GAD	glutamic acid decarboxylase
IPSC	inhibitory postsynaptic current
IPSP	inhibitory postsynaptic potential
L-AP5	L-2-amino-4-phosphonopentanoate
LTP	long term potentiation
mGluR	metabotropic glutamate receptor
NMDA	N-methyl-D-aspartate
PB	phosphate buffer
PBS	phosphate buffer saline
TB	tris buffer
TBS	tris buffered saline

Chapter 1. General introduction

1.1 Structure and function of the hippocampal formation - general overview

The Ammon's horn, also known as the hippocampus proper, together with adjoining structures, including the dentate gyrus, subicular complex and entorhinal cortex, make up the hippocampal formation and constitute a major component of the temporal lobe. Despite being part of the cerebral cortex however, the hippocampal formation may represent a phylogenetically older form of cortex, therefore is designated as archicortex, and is presumed to be distinct from neocortex. The hippocampus is generally regarded to be the best characterised cortical area. Its apparently "simple" cellular organisation and stereotyped circuitry has meant that the hippocampus has been a popular brain area for studies of basic mechanisms of synaptic function and key concepts in the organisation of cortical microcircuits. On a systems level however, the exact function of the hippocampus remains elusive. The hippocampus and adjoining structures are particularly seizure prone (Schwartzkroin, 1994) and also highly susceptible to neurodegenerative diseases (Robbins and Kumar, 1987). Damage to the hippocampus can have profound neuropsychological consequences. The hippocampus receives multimodal sensory input and it is considered to be important in certain aspects of learning and memory (Zola-Morgan and Squire, 1993), although the exact mnemonic functions performed and their underlying mechanisms remain poorly understood. If the information processing mediated by the hippocampal circuitry is to be explained in specific neuronal terms, then a prerequisite is to establish the microcircuitry which allows it to carry out its complex functions.

1.1.1 Microcircuitry of the hippocampal formation

The characteristic stereotyped and ordered structure of the hippocampal formation has meant that it has been of interest to anatomists for over a century. As a consequence, the neuronal components as well as the efferent, afferent and

intrinsic connections have been investigated in some detail (reviewed by Swanson et al., 1987; Brown and Zador, 1990; Amaral and Witter, 1995; Patton and McNaughton, 1995; Freund and Buzsáki, 1996). The hippocampus is comprised of two major cell types - a large and relatively homogeneous population of excitatory principal cells and a numerically more sparse, but highly heterogeneous population of inhibitory local-circuit neurones. The principal cells of the hippocampal formation are comprised of granule cells in the dentate gyrus and pyramidal cells in Ammon's horn. Within the hippocampus of the rat, there are an estimated 0.6 to 2.2 $x10^6$ granule cells and 400,000 pyramidal cells (Amaral and Witter, 1995; Squire et al., 1989). In both the dentate gyrus and Ammon's horn, the principal cell dendrites are similarly orientated and the cell bodies aligned and relatively tightly packed, so as to form a single sheet. This means that when the hippocampus is viewed in cross section, a characteristic laminar structure becomes apparent, the different laminae corresponding to different somato-dendritic domains of the component neurones. In addition, the intrinsic axonal pathways within the hippocampus generally respect these boundaries so that the area, as a whole, is highly structured not only in terms of the cytoarchitecture of the component neurones but also in terms of the connectivity patterns. The structured laminar organisation of the hippocampal formation, together with the major intrinsic connections are shown schematically on figure 1.1.

The major extrahippocampal inputs are highly structured, with selective termination zones within the hippocampus. The main cortical input fibres to the hippocampus originate from the entorhinal cortex (Ramon y Cajal, 1911; Lorente de Nó, 1934) and contralateral hippocampus (Blackstad, 1956). Subcortical inputs include the cholinergic (Petsche et al., 1962) and GABAergic (Köhler et al., 1984; Freund and Antal, 1988) inputs which originate in the medial septal nucleus, noradrenergic fibres from the locus coeruleus (Loy et al., 1980) and serotoninergic fibres from the raphé nuclei (Assaf and Miller, 1978; Halasy et al., 1992). Additional direct projections to the hippocampus include those from the

supramammillary nucleus (Segal and Landis, 1974) and several nuclei of the hypothalamus and thalamus (Wouterlood et al., 1990).

Within the hippocampal formation, the main intrinsic excitatory connections form a largely unidirectional pathway which courses throughout all regions and is referred to as the trisynaptic loop. The first stage in this loop is formed by the perforant path projection from cells in layer II of the entorhinal cortex which terminate on the distal portion of granule cell dendrites in the dentate gyrus. The granule cells, in turn, innervate pyramidal cells as well as interneurones (Frotscher, 1989) in the CA3 subfield of Ammon's horn, their axons forming what is referred to as the mossy fibre input, this representing the second stage in the trisynaptic loop. The CA3 pyramidal cells, in turn, project to the pyramidal cells of the CA1 subfield in what is known as the Schaffer collateral pathway (Schaffer, 1892; Li et al., 1994). Finally, the CA1 pyramidal cells project back to the deep layers of the entorhinal cortex, to some degree directly, and in part via the subicular complex (Amaral and Witter, 1995), so closing the loop. Although the perforant path input is considered to represent the major source of information flowing through the hippocampus, many other smaller excitatory loops and projections have been described, providing a basis for information flow to take place together with the trisynaptic pathway (Amaral and Witter, 1995).

1.1.2 Diversity of hippocampal GABAergic interneurones

As their name suggests, GABAergic interneurones form mainly local connections (but see Tóth and Freund, 1992; Sík et al., 1995) and provide local inhibition by releasing the inhibitory neurotransmitter, γ - aminobutyric acid (GABA). Immunocytochemical studies indicate that such local-circuit neurones form approximately 5.8 (Aika et al., 1994) to 11% (Woodson et al., 1989) of the total hippocampal cell population. In contrast to principal cells, hippocampal GABAergic interneurones show great morphological and neurochemical diversity. They may differ with respect to their content of various neuropeptides (Somogyi et

al., 1984; Kosaka et al., 1985; Nunzi et al., 1985; Sloviter and Nilaver, 1987; Deller and Leranth, 1990; Miettinen and Freund, 1992; Acsády et al., 1996a), calcium binding proteins (Kosaka et al., 1987; Nitsch et al., 1990; Gulyás et al., 1991; Miettinen et al., 1992; Tóth and Freund, 1992; Gulyás et al., 1996) and in their expression of neurotransmitter receptors (Baude et al., 1993; McBain and Dingledine, 1993; McBain et al., 1994). GABAergic interneurones also differ in their synaptic inputs (Gulyás et al., 1990; Halasy et al., 1992; Miettinen and Freund, 1992) as well as their synaptic target selectivity (Somogyi et al., 1983a, 1985; Halasy and Somogyi, 1993; Han et al., 1993; Gulyás et al., 1993a; Buhl et al., 1994a; Halasy et al. 1996). The morphological, neurochemical and physiological features of hippocampal interneurones have recently been comprehensively reviewed (Freund and Buzsáki, 1996).

That GABAergic interneurones show such variety, strongly suggests that different cells perform different functions within the hippocampal circuit. Although the division of function suggested by such heterogeneity remains to be fully established, some general rules regarding the functional significance of different types of interneurone are beginning to emerge. Indeed, it has been demonstrated that the axonal output of many types of GABAergic interneurone terminate in conjunction with the terminal field of specific excitatory input pathways (Gulyás et al., 1993a; Han et al., 1993, Buhl et al., 1994a) suggesting that specific cells may selectively influence excitatory inputs from particular pathways and regions. In addition, recent immunocytochemical studies have established specialised types of local-circuit neurones which selectively target other interneurones (Acsády et al., 1996b; Gulyás et al. 1996), suggesting that some interneurones may be dedicated specifically to control the activity of other interneurones, thus adding another level of complexity to the hippocampal microcircuitry.

1.2 Synaptic transmission

Cells in the adult brain mainly communicate with each other through specialised regions of functional contact, designated synapses (Sherrington, 1897, 1906). Synapses can be electrical (i.e. directly connected) or chemical in nature, although chemical synapses are considered to play a more important role in mammalian species (Brock et al., 1952; Eccles, 1982; but see Jefferys, 1995). A major distinction exists between chemical neurotransmission, which is mediated directly through ligand-gated ion channels (ionotropic neurotransmission) and metabotropic neurotransmission, which is conveyed through indirect biochemical second messenger systems (Eccles and McGeer, 1979). Ionotropic neurotransmission has a fast onset and a short duration, whilst metabotropic neurotransmission has a slower onset and is longer lasting (McCormick, 1990). Fast information processing in the mammalian brain is considered to be mediated through ionotropic receptors, which, within the hippocampus and other cortical areas, is predominantly mediated through the amino acid neurotransmitters glutamate and GABA. Glutamate is the major excitatory neurotransmitter whilst GABA is the main inhibitory neurotransmitter. This thesis mainly considers GABAergic neurotransmission, although both will be summarised here briefly.

1.2.1 Glutamate as a neurotransmitter

Fast glutamatergic EPSPs result from released glutamate, acting on ionotropic glutamate receptors. Ionotropic glutamate receptors are divided into NMDA (n-methyl-D-aspartate), kainate and AMPA (D,L-alpha-amino-3-hydroxy-5-methyl-4-isoxalone propinoic acid) subtypes based upon their pharmacological profile to specific agonists (see Watkins et al., 1990). Kainate and AMPA receptors act via similar ionic mechanisms (Nicoll, 1988) and are often referred to as non-NMDA receptors. However, recent evidence suggests that they may perform

different functional roles within the hippocampus (Chittajallu et al., 1996). Both open mixed cation channels which are mainly permeable to Na^+ and K^+ ions with a resulting reversal potential of about 0mV (see MacDermott and Dale, 1987). The fast kinetics of the receptor / channel complex leads to rapid depolarisation, thus the AMPA / kainate receptor mediated EPSPs are usually referred to as 'fast' EPSPs.

In contrast to the fast EPSPs mediated by AMPA / kainate receptors, the action of glutamate through NMDA receptors is more complex. When opened by glutamate, NMDA channels are permeable to Na^+, K^+ and, importantly, also to Ca^{2+} ions. However, at 'normal' resting membrane potentials, Mg^{2+} ions may block the ion channel and prevent the flux of ions through the pore. However, if the membrane potential is already depolarised, then the Mg^{2+} block is removed and the channel opens. Together, the voltage dependence of the Mg^{2+} block, the requirement for glutamate to bind to a receptor site and the slow kinetics of channel opening, means that NMDA channel opening is both voltage and ligand gated. This dual ligand and voltage-dependence is a key feature of NMDA receptors (see Ascher and Nowak, 1987) which, coupled to the relatively high calcium permeability of the receptor, provides an attractive mechanism through which synaptic efficacy may be controlled at certain synapses (reviewed by Bliss and Collingridge, 1993).

In addition to its action on ionotropic receptors, glutamate also has actions on metabotropic receptors (reviewed by Nakanishi, 1994; Pin and Duvoisin, 1995) which are not considered here.

1.2.2 GABA as a neurotransmitter

GABA was first shown to mediate IPSPs in crustacea (Kravitz et al., 1963a,b), following which, it has also been generally accepted that GABA is the major inhibitory transmitter in the hippocampus (Alger and Nicoll, 1979; Newberry and Nicoll, 1984a,b, 1985; Dutar and Nicoll, 1988). There are three major types of

GABA receptors which are referred to as $GABA_A$, $GABA_B$ (Bowery et al., 1987) and $GABA_C$ (Bormann and Feigenspan, 1995) receptors. Whilst ionotropic $GABA_A$ receptors directly gate chloride channels, metabotropic $GABA_B$ receptors are thought to be either positively coupled to potassium channels or negatively coupled to calcium channels through G-proteins (Nicoll and Dutar, 1990; Misgeld et al., 1995). Electrical stimulation of the Schaffer collateral pathway typically evokes an EPSP followed by a two-component IPSP, the early phase of which reverses at about -70mV and is sensitive to the chloride gradient, whilst the late phase reverses at about -90mV and is sensitive to the potassium concentration gradient (Newberry and Nicoll, 1984a,b). These early and late phases were subsequently shown to relate to $GABA_A$ and $GABA_B$ receptors, respectively. However, the increased chloride ($GABA_A$) and raised potassium ($GABA_B$) conductances can have quite different functional consequences, which lead to differences in effect other than just their time course. The conductance associated with the fast IPSP is high, compared to the longer lasting slow IPSP (see McCormick, 1990) and will efficiently shunt the currents flowing across a cell membrane without necessarily causing much change in membrane voltage. For this reason, computational scientists consider shunting inhibition to be well suited to carry out 'veto' functions, whereas hyperpolarising inhibition is better suited to modulate the overall excitability of a neurone (McCormick, 1990).

Many clinically useful drugs produce their effect by interacting with $GABA_A$ receptors (Lüddens and Wisden, 1991) which show great molecular diversity (reviewed by Sieghart, 1995; Möhler et al., 1996). Five different classes of $GABA_A$ receptor subunit, each with multiple variants, assemble to form pentameric $GABA_A$ receptors with differing pharmacological and biophysical properties (Verdoorn et al., 1990). Recent immunocytochemical evidence suggests that separate classes of GABAergic interneurones may differentially activate $GABA_A$ receptors with differing subunit composition (Nusser et al., 1996). In contrast to the $GABA_A$ receptor, much less is known about the metabotropic $GABA_B$ receptor,

which has not yet been cloned. Based on differential pharmacology (reviewed by Bonanno and Raiteri, 1993; Misgeld et al., 1995) and ionic mechanisms (Dunlap, 1981; Gähwiler and Brown, 1985; Newberry and Nicoll, 1984a; Pham and Lacaille, 1996; Robertson and Taylor, 1986; Thompson and Gähwiler, 1992), several distinct subtypes of receptor appear to exist, although little is known of their cellular location. Qian and Sejnowski (1990) proposed that $GABA_B$ receptors are particularly well placed to mediate hyperpolarising inhibition at dendritic spines, where the confined volume would render $GABA_A$ receptor mediated shunting inhibition ineffective. However, recent studies in neocortex show that GABAergic double bouquet cells, which predominantly terminate onto dendritic spines, evoke fast, putative $GABA_A$ mediated IPSPs (Tamás et al., 1996). In addition to their role in postsynaptic inhibition, $GABA_B$ receptors inhibit transmitter release via presynaptic mechanisms (Bowery et al., 1980; Lanthorn and Cotman, 1981; Ault and Nadler, 1982; Deisz and Prince, 1989; Thompson et al., 1993) which are considered to be important with respect to synaptic plasticity (Davies et al., 1991).

1.3 Neuronal integration at the cellular level

Information processing depends both on the synaptic connections between nerve cells in a network, and also on the electrical properties of each individual nerve cell. The electrical behaviour of a neurone is dictated by its biophysical properties (Mason and Larkman, 1990; Larkman et al., 1992; Mainen and Sejnowski, 1996) and by the presence and distribution of ionic currents which flow across the lipid membrane. These mostly occur through ion channels, gated either by ligands or voltage and are driven by electrochemical gradients, but ion transporters and active ionic pumps also contribute to membrane currents (Hille, 1984). Thus membrane properties in conjunction with the combination and placement of different ion pores and carriers shape the electrical properties of each nerve cell (McCormick, 1990). In the classical model of neuronal integration

excitatory and inhibitory postsynaptic potentials originate at points on the somato-dendritic surface. From there, the postsynaptic potentials spread electrotonically towards the soma and axon hillock, where upon integration they may lead to a critical threshold membrane potential that triggers a regenerative action potential (Fuortes et al., 1957). Although the electrotonic structure of the dendrites was thought to shape the kinetics and amplitude of postsynaptic potentials as they spread towards the soma (Rall, 1977), this passive model generally assumed fairly linear input-output characteristics and did not take into account, non-synaptic conductances or the interplay of synaptic currents. Considerable evidence indicates that regenerative processes can be evoked in dendrites themselves (Llinás and Nicholson,1971; Llinás, 1988). Indeed, dendrites of hippocampal pyramidal cells have been shown to exhibit a variety of characteristic firing properties, depending upon the relative contribution of several intrinsic conductances (Andreasen and Lambert, 1995). Synaptic activation of hippocampal pyramidal cells has been shown to initiate action potentials in the dendrites (Andersen and Lomo, 1966; Turner et al., 1989, 1991, 1993; Poolos and Kocsis, 1990; Herreras, 1990; Colling and Wheal, 1994). Nevertheless, two recent studies (Hausser et al., 1995; Spruston et al., 1995) provided convincing evidence that the threshold for the genesis of fast sodium action potentials is lowest at the axon initial segment and that dendritic action potentials are only apparent at very high stimulation strengths or as a result of backpropagation. It thus appears, that graded synaptic responses may undergo dendritic amplification through interacting with intrinsic dendritic conductances (Magee and Johnston, 1995a,b; Magee et al., 1995), but that the fast sodium action potentials are usually first generated at the axon initial segment (Spruston et al., 1995). When considering synaptic interactions between nerve cells, it is therefore important to take account of passive as well as active intrinsic properties of neurones, in addition to the synaptic response *per se*.

1.4 Objectives of thesis

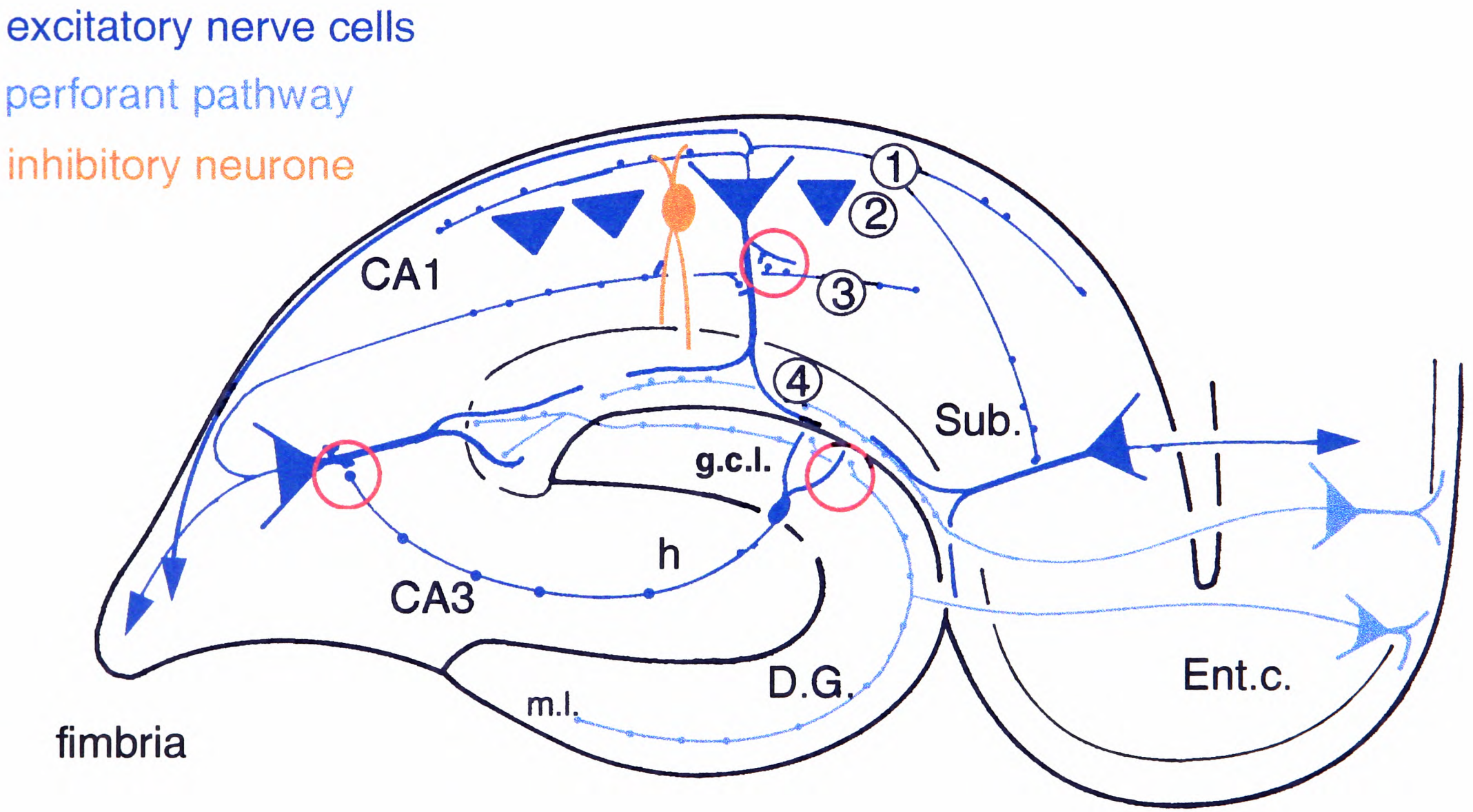
From this brief introduction to the structure, circuitry and most elementary concepts of synaptic neuronal communication within the hippocampus, it becomes evident that the processing of information within this brain area will depend upon a large number of factors. Defining the microcircuitry of the hippocampus is an important first step in identifying the hard wiring and connectivity rules of the system and may yield novel functional implications for the entire cortical mantle. To elucidate the governing principles underlying neuronal communication in the hippocampus, it is important to establish the types of synaptic interaction that take place between cells, the rules of the synaptic connections and the intrinsic active and passive properties of the neurones.

The specific objective of this thesis project was to contribute to the definition of the microcircuitry of the hippocampus and to characterise unitary interactions which take place between individual neurones, with particular reference to GABAergic interneurones. Indeed, it is hoped that investigating neuronal communication at this most fundamental level would reveal clues as to the functional role of key components in hippocampal GABAergic neurotransmission. Moreover, detailed anatomical scrutiny of the cells investigated helps to establish the exact neuronal elements taking part in the synaptic interactions and perhaps reveal novel and hitherto uncharacterised cell types. In order to test the hypothesis that GABAergic interneurones have distinct morphological and connectional properties as well as heterogeneous postsynaptic effects, perhaps reflecting specific functional roles, an experimental paradigm was adopted that allows the correlation of the morphology, efferent connectivity and postsynaptic effect of pairs of *identified* hippocampal neurones.

Figure 1.1 Schematic diagram showing major hippocampal connections in the transverse hippocampal slice. The hippocampal formation is divided into the entorhinal cortex, dentate gyrus, Ammon's horn and subicular complex. The three synaptic connections in the main trisynaptic pathways (see text) are indicated by red circles. The CA1 subfield is divided into stratum oriens (1), stratum pyramidale (2), stratum radiatum (3) and stratum lacunosum-moleculare (4).

Abbreviations: Ent. c., entorhinal cortex; Sub., subiculum; g.c.l., granule cell layer; h, hilus; m.l.; molecular layer; D.G., dentate gyrus; CA1 subfield; CA3 subfield.

Major hippocampal connections



Chapter 2. Experimental procedures

2.1 Hippocampal slice preparation

2.1.1 Animal procedures and anaesthesia

All experiments were performed on young adult female Wistar rats weighing 100-150g (Charles River, U.K.). The animals were housed in an animal holding facility, usually 4-5 rats per cage and allowed continuous access to food and water and kept on a 12 hour light/dark cycle. The rats were lightly anaesthetised with either ether or isoflurane by inhalation in a traditional ether jar apparatus. Following loss of consciousness, animals were more deeply anaesthetised by an intramuscular injection of ketamine (100 mg/kg) and xylazine (10 mg/kg). The level of anaesthesia was monitored by assessing the presence of reflex responses to tail or paw pinch stimuli. After cessation of pain reflexes, the abdominal cavity was opened and then incisions made in the diaphragm and along the sides of the rib cage to expose the heart. The pericardium was pulled away and the heart cannulated by pushing the cannula through the base of the left ventricle and up into the aorta. The right atrium was then immediately cut and the animals were intracardially perfused with approximately 30 ml of chilled artificial cerebrospinal fluid (ACSF) and their brains quickly removed and immersed in a beaker with chilled ACSF. All procedures were carried out in compliance with the provisions of the Animals (Scientific Procedures) Act 1986.

2.1.2 Brain sectioning

The hippocampi were dissected free by removing the surrounding cortex and subcortical areas. With the aid of a vibroslice (Campden Instruments, UK) 400 μm thick slices were cut in the horizontal plane. Hippocampal slices were then transferred to a recording chamber where they were maintained at 34-35° C on a nylon mesh at the interface between oxygenated ACSF and a humidified atmosphere saturated with 95% O_2/5% CO_2. The flow rate was adjusted to 1.5

ml/min and the slices were allowed to equilibrate for 45 minutes to 1 hour before commencing recording.

2.1.3 Solutions

The ACSF for electrophysiological recordings was composed of (in mM) 126 NaCl, 3.0 KCl, 1.25 NH_2P0_4, 24 Na HCO_3, 2.0 $MgSO_4$, 2.0 $CaCl_2$ and 10 glucose. During the initial stages of the experiments (perfusion, cutting, incubation) all NaCl (126 mM) was replaced by equiosmolar sucrose (256 mM), thus preventing passive chloride entry which has been suggested to be acutely responsible for neurotoxicity during slice preparation (Aghajanian and Rasmussen, 1989). Usually the slices remained 30 min in the sucrose solution before the perfusion medium was changed to normal ACSF. Drugs which were used in pharmacology experiments were kept as concentrated stocks which were diluted in ACSF and then bath applied.

2.2 Intracellular recordings and data analysis

Recording electrodes were pulled from standard wall borosilicate tubing, filled with 2% biocytin (Horikawa and Armstrong, 1988) in 1.5 M KCH_3SO_4 and bevelled to a DC resistance of 80-150 MΩ. Recordings were obtained in the pyramidal cell layer of the CA1 and CA3 subfields. Putative interneurones were identified due to their physiological characteristics, such as short-duration action potentials followed by large amplitude fast afterhyperpolarising potentials. Once a stable recording had been obtained a search was made for cells displaying the electrophysiological properties of pyramidal neurones. Action potentials in one record could give rise to artefacts in the other channel due to capacitive coupling between electrodes. Such capacitive coupling was either eliminated off-line (Miles, 1990) or alternatively, on-line using a modified Axoprobe (Axon Instruments, USA) amplifier (Mason et al., 1991). Synaptic coupling was tested using on-line

spike-triggered averaging, whilst eliciting firing in the interneurone with either depolarising current pulses or constant DC current injections. Firing rates in the interneurones were adjusted by varying the current intensity and, depending on the particular protocol, ranged between 0.3 Hz and >100 Hz. Recordings were obtained with either an Axoclamp or Axoprobe amplifier (both Axon Instruments) which were operated in bridge mode. Experimental data was acquired at 22kHz using a PCM instrumentation recorder and stored in digital form on videotapes. Data analysis was continued off-line by (re)digitising the data at 5-20 kHz using commercially available 12 Bit A/D boards (RC Electronics Computerscope, USA, and National Instruments Labmaster^{+}, UK) in conjunction with Axograph (Axon Instruments), RC Electronics Computerscope (RC Electronics) and WCP (courtesy of Dr. J. Dempster, University of Strathclyde, UK) software packages. Data used to determine kinetic and amplitude measurements were low-pass filtered at 1 or 2kHz. Traces used for autocorrelation and power spectrum analysis were high pass filtered at 1Hz. Unless indicated otherwise data is expressed as mean ± standard deviation.

Resting membrane potentials were determined following electrode withdrawal and are given as the difference between surface DC potential and the steady state membrane potential without bias current injection. Membrane time constants were obtained from small hyperpolarising current pulses as the time necessary to reach e^{-1} (63%) of the maximum voltage deflection. Likewise, input resistances were derived from Ohms law by dividing the maximal voltage deflection to small averaged hyperpolarising current pulses of known amplitude. Spike amplitudes were taken from baseline to the peak of the action potential, spike duration was measured at half-amplitude.

2.3 Histological processing and anatomical evaluation

2.3.1 Processing of sections for light microscopy

With few exceptions, when depolarising current pulses were employed, over the course of 1 hour, intracellular diffusion of biocytin from the electrode resulted in adequate filling of the recorded neurones. Following the recording, slices were sandwiched between two Millipore filters and fixed in 2.5% paraformaldehyde, 1.25% glutaraldehyde and 15% (v/v) picric acid in 0.1 M phosphate buffer (PB; pH 7.4), usually overnight. After fixation, the tissue was rinsed in phosphate buffer and infiltrated with 10% and then 20% sucrose solution. To increase the penetration of the reagents, slices were snap-frozen in liquid nitrogen and thawed in phosphate buffer. Slices were then embedded in 10% gelatine and the gelatine block placed in the same fixation solution for approximately one hour or until sufficiently hard for cutting. Taking care to keep the block flat, slices were re-sectioned on a vibratome at 50-60 μm thickness. After three 10-minute washes in phosphate buffer and two 10-minute washes in Tris-buffered saline (TBS; 0.05M, pH7.4), the sections were incubated overnight at 4°C with 1% avidin-biotinylated horseradish peroxidase complex (ABC, Vector laboratories; in TBS; 0.05M, pH7.4). Excess ABC reagent was removed by three 20-minute washes in TBS and two 20-minute washes in Tris-buffer (pH7.6). Sections were placed in 0.05% 3,3'-diaminobenzidine tetrahydrochloride (DAB) in Tris-buffer to equilibrate (10 minutes) before being developed for 10-15 minutes by adding 0.01% hydrogen peroxide. The reaction was carried out in the dark and the reaction progress monitored at regular intervals. After excess DAB was removed with further washes in tris-buffer (1x15 minutes) and phosphate buffer (2x10 minutes), sections were postfixed for 1 hour with 1% osmium tetroxide in phosphate buffer. Following a 10-minute rinse in phosphate buffer followed by

three 10-minute washes in distilled water, sections were block-stained in darkness for 40 minutes in a filtered 1% aqueous solution of uranyl acetate. Sections were then washed in distilled water (2x10-minutes) before being dehydrated between coverslips in an ascending series of ethanol solutions (50%, 70%, 95%,100%x2; 10 minutes in each). From the second absolute alcohol step, sections were transferred to propylene oxide (2x10-minutes). Material was then infiltrated overnight in Durcupan resin (Fluka) before being mounted onto glass slides and transferred to an oven (56°C, 48hours) to allow the resin to resin polymerise.

2.3.2 Light microscopic evaluation of specimens

Following their embedding into epoxy resin, all recovered cells were scrutinised at the light microscopic level to establish preliminary classification according to their salient morphological features (see chapter 3). When required, labelled cells were photographed and / or graphically reconstructed from serial 60 µm sections using a light microscope and drawing tube at x1,250 magnification. Where paired intracellular recordings had been made between synaptically coupled cell pairs, sites of potential synaptic contact were tentatively identified at the light microscopic level. In order to establish the overall postsynaptic target profile of individual cells, representative portions of axon rich tissue were re-embedded in Durcupan resin and serial ultrathin sections cut for electron microscopic evaluation.

2.3.3 Processing of sections for electron microscopy

Tissue was re-embedded by first removing the coverslip by pushing a razor blade between the thin layer of resin and the glass. With the aid of a binocular microscope, a small piece of the section was then cut out using a scalpel. The tip of the scalpel was then carefully inserted underneath to lift the section from the slide. Sometimes an anti-static gun was used to avoid the charged piece of cut tissue form sticking to nearby materials. The removed resin embedded material was then placed in the flat bottom of a polyethylene capsule (TAAB) which had been truncated to 5-

10mm in height. The capsule was then filled with fresh Durcupan resin and any bubbles allowed to dissipate before applying a coverslip over the open capsule top so to provide an optically smooth surface. After curing (overnight at 56°C), the coverslip and polyethylene capsule were removed with a razor blade, placed tissue-side up on a glass slide and viewed in the light microscope. Once the exact position and orientation of the tissue within the block was established, the block was placed in the specimen holder of the ultramicrotome and trimmed to form a small area of the tissue to be cut. Serial ultrathin sections (silver / grey) of approximately 60-80 nm in thickness were cut using a glass knife and an ultramicrotome (Reichert-Jung Ultracut E). The ultrathin sections were collected on formvar coated single-slot (2x1mm) copper grids and lead stained (Reynolds, 1963) to provide additional contrast.

2.3.4 Electron microscopic evaluation of specimens

All specimens were examined in a Philips CM 410 transmission electron microscope. Serial sections were scanned for opaque filled processes indicating the presence of electron dense precipitate. Labelled profiles were then followed in serial sections to find synaptic junctions. The identity of synaptic junctions was established based on the following criteria: (i) vesicle accumulation in the presynaptic axonal varicosity, (ii) rigid membrane apposition of pre- and postsynaptic elements with a characteristic widening of the extracellular space. (iii) the presence of a postsynaptic specialisation. The identity of postsynaptic structures were determined from characteristic ultrastructural features (see chapter 3). When the plain of the section was tangential to the junctional membranes, the synaptic cleft could be recognised by tilting the section using the goniometer of the electron microscope.

2.4 Materials

2.4.1 General

biocytin	Sigma, U.K.
3,3'-diaminobenzidine - tetrahydrochloride	Sigma, U.K.
Durcupan resin	Fluka, Switzerland
Gelatin	Sigma, U.K.
Formvar	TAAB, U.K.
glass capillaries	Clark Electromedical, U.K.
glutaraldehyde	TAAB, U.K.
hydrogen peroxide	Sigma, U.K.
Ketamine	Parke-Davis Veterinary, U.K.
$KCH_3 SO_4$	BDH, U.K.
NaOH	BDH, U.K.
osmium tetroxide	TAAB, U.K.
paraformaldehyde	TAAB, U.K.
picric acid	BDH, U.K.
propylene oxide	BDH, U.K.
Tris buffer	TAAB, U.K.
sucrose	BDH, U.K.
xylazine	Bayer, U.K.
uranyl acetate	EMscope, U.K.
Vectastain ABC kit	Vector labs, U.K.

2.4.2 Pharmacological compounds

The ionotropic glutamate receptor antagonists 6-cyano-7-nitroquinoxaline-2,3-dione (CNQX) and DL-2-amino-5-phosphonopentanoic acid (AP5) were obtained from Tocris Cookson, Bristol, U.K. Bicuculline hydrochloride was

purchased from Sigma, UK, and the $GABA_B$ receptor antagonist CGP 55845A was made available by Drs. Bittiger and Olpe, Ciba Geigy, Basle, Switzerland.

2.5 Distribution of shared materials

The substantial proportion of the results described in this thesis were obtained by the author. However, due to the interdisciplinary nature of the work described, a proportion of the materials and data were obtained by other co-workers. The relative contribution by myself and other persons, at each stage in the collection and analysis of data, are summarised in table 2.1.

Cell number	Cell code	recorded / labelled by:	Area	Classification	EM target profile ais	som	den	spn	?	EM evaluation by:	LM evaluation by:	Drawing by:	Physiological analysis by:
1	E23/01/92/1	E	CA1	basket	0	5	7	0	0	K	E		E
2	E28/01/92/1	E	CA1	basket	0	19	18	0	0	K	E		E
3	E06/02/92/1	E	CA1	basket	0	17	19	5	0	K	E		E
4	E22/07/92/1	E	CA3	mixed	3	6	6	2	0	K	E		E
5	E11/10/93/1	E	CA1	basket	0	7	5	0	0	K	E		E
6	E29/10/93/2	E	CA3	basket	0	14	2	0	0	K	E		E
7	S1/11/93/1	S	CA1	axo-axonic	10	0	0	0	1	K	S	R	S
8	S2/11/93/5	S	CA1	basket	2	5	2	0	0	K	S		S
9	E04/11/93/1	E	CA1	basket	0	5	6	0	0	K	E		
10	S16/11/93/1	S	CA1	bistratified							S		S
11	S16/11/93/4	S	CA1	basket	0	29	30	2	0	K/G	S	G	S
12	S17/11/93/2	S	CA1	mixed	9	8	5	0	6	T	S	R	S
13	S17/11/93/4	S	CA1	mixed							S		S
14	S18/11/93/2	S	CA1	bistratified							S		S
15	S23/11/93/2	S	CA1	SR cell							S	S	
16	S18/1/94/3	S	CA1	basket							S		
17	S17/5/94/3	S	CA1	not recovered							S		
18	S19/5/94/3	S	CA1	mixed	1	9	11	0	0	K	S		S
19	S27/5/94/1	S	CA1	basket							S		
20	S31/5/94/1	S	CA1	basket							S		
21	S3/6/94/1	S	CA1	basket							S		
22	S3/6/94/2	S	CA1	basket	0	5	6	0	0	K	S		S
23	S8/6/94/1	S	CA1	basket							S		S
24	S9/6/94/1	S	CA1	basket							S		S
25	S10/6/94/1	S	CA1	mixed	6	7	3	1	0	K	S		
26	S16/6/94/3	S	CA1	basket	0	5	5	0	0	K	S		S
27	S17/6/94/3	S	CA1	bistratified							S		S
28	S20/6/94/1	S	CA1	bistratified							S		S
29	S20/6/94/2	S	CA1	bistratified							S		
30	S20/6/94/3	S	CA1	basket	0	10	14	1	0	K	S	G	
31	S21/6/94/1	S	CA1	no axon							S		
32	S29/6/94/1	S	CA1	not recovered							S		S
33	S30/6/94/1	S	CA1	not recovered							S		S
34	S30/6/94/2	S	CA1	not recovered							S		
35	S05/7/94/1a	S	CA1	basket	0	6	6	0	0	K	S	K	S
36	S05/7/94/1b	S	CA1	bistratified							S	K	S
37	S07/7/94/1	S	CA1	not recovered							S		
38	S8/7/94/1	S	CA1	axo-axonic	12	0	0	0	0	T	S		S
39	S11/7/94/1	S	CA1	SR cell							S		
40	S12/7/94/1	S	CA1	mixed	4	10	9	1	0	K	S		S
41	S13/7/94/2	S	CA1	axo-axonic	11	0	0	0	0	S	S	T	S
42	S13/7/94/3	S	CA1	not recovered							S		S
43	S14/7/94/1	S	CA1	no axon							S		
44	S15/7/94/1	S	CA1	basket	0	5	5	0	0	K	S		S
45	S18/7/94/1	S	CA1	basket							S		
46	S19/7/94/1	S	CA1	not recovered							S		S
47	S21/7/94/1	S	CA1	not recovered							S		S
48	S21/7/94/2	S	CA1	basket							S		S
49	S16/9/94/2	S	CA1	mixed	1	8	3	0	1	S	S		S
50	S17/11/94/2	S	CA1	unidentified							S		S
51	S21/11/94/2	S	CA1	no axon							S		
52	S22/11/94/2	S	CA1	no axon							S		
53	S23/11/94/1	S	CA1	basket	0	7	6	0	0	K	S	S	S
54	S24/11/94/1	S	CA1	basket							S		S
55	S28/11/94/1	S	CA1	basket							S		S
56	S28/11/94/2	S	CA1	no axon							S		S
57	E29/11/94/1	E	CA1	axo-axonic	11	0	0	0	0	K	E		S
58	S29/11/94/2	S	CA1	not recovered							S		
59	S30/11/94/1	S	CA1	bistratified	0	0	8	2	0	K	S		
60	S01/12/94/1	S	CA1	bistratified							S		S
61	S01/12/94/2	S	CA1	bistratified							S		S
62	S05/12/94/1	S	CA1	mixed	0	16	7	0	0	K	S		S
63	S13/12/94/1	S	CA1	axo-axonic	11	0	0	0	0	K	S		S
64	S15/12/94/1	S	CA1	basket	0	5	1	0	2	P	S		S
65	IV07/06/95/1a	I	CA1	SR-LM							I	S	S
66	IV07/06/95/1b	I	CA1	bistratified	0	0	9	2	0	K	I	S	S

S - Stuart Cobb
E - Eberhard Buhl
K - Katalin Halasy
T Txema Sanz
I Imre Vida
P - Peter Somogyi
R - Rafa Lujan
G - Gabor Tamas

ais - axon initial segment
som - soma
den - dendrite
spn - dendritic spine
EM - electron microscopic
LM - light microscopic

Chapter 3. Anatomical and physiological identification of local-circuit interneurones in area CA1 of the rat hippocampus

3.1 Introduction

The basic cell types of the cerebral cortex were described in the pioneering Golgi impregnation studies of Ramon y Cajal (1893, 1911) and a more detailed account of hippocampal neurones given later by his former student, Lorente de Nó (1934). Both were early advocates of functional neuroanatomy, whereby specific functions were ascribed to different cell types based on morphological features of individual neurones and their known / presumed connectivity with others. Their early studies indicated two main populations of hippocampal neurones, a relatively homogenous population of principal cells (pyramidal cells in hippocampus and granule cells in the dentate gyrus) and a second, much more diverse population of non-principal cells. The evidence to suggest that pyramidal cells mediate excitation whilst non-pyramidal cells mediate inhibition did not come about until many decades later when Gray (1959) described type 1 and 2 synapses (asymmetrical and symmetrical respectively) based on characteristic ultrastructural features to which Eccles and colleagues (Andersen et al., 1963) promptly ascribed excitatory and inhibitory functions. To date, significant effort in the field has been devoted to identifying the different cell types which constitute the heterogeneous population of non-pyramidal cells in an attempt to classify them and to ascertain their functional roles within the cortical circuitry.

The aim of my initial experiments was to use combined physiological and anatomical techniques to identify and characterise local-circuit interneurones in the CA1 area of the rat hippocampus and to establish the type of synaptic response they evoke in their postsynaptic target neurones. The sampling of neurones was restricted to only those cells with somata located within stratum pyramidale of the CA1 area. Cells encountered were subsequently scrutinised on the basis of morphological characteristics, their efferent synaptic target profile and postsynaptic effect.

3.2 Materials and methods

Detailed description of the preparation of hippocampal slices, electrophysiological recording, biocytin labelling, and the subsequent correlated light and electron microscopic methods are given in chapter 2. In brief, intracellular recordings were obtained in 400μm transverse hippocampal slices of adult (>150g) female Wistar rats. Slices were maintained at 34-35°C on a nylon mesh at the interface between oxygenated artificial cerebrospinal fluid (ACSF, see 2.1.3) and a humidified atmosphere saturated with 95% O_2 and 5% CO_2. The flow rate was adjusted to 1.5-2ml min^{-1}. Micropipettes were filled with 2% biocytin in 1.5M KCH_3SO_4 and bevelled to a d.c. resistance ranging between 60-150MΩ. Putative interneurones were identified using previously established physiological criteria (Knowles & Schwartzkroin, 1981). When a stable recording was obtained, a search was made for synaptically coupled cells displaying the properties of hippocampal principal cells. The putative interneurone was triggered to fire action potentials by depolarising current injection and synaptic coupling tested using on-line spike-triggered averaging. Capacitive coupling was eliminated during the recording, using a modified axoprobe amplifier (section 2.2). Diffusion of biocytin during recordings generally resulted in adequate filling. Slices were processed for light and electron microscopy as described (section 2.3). The synaptic target profile of two cells (n= 24 synapses) were established by myself although the majority of electron microscopy was carried out both in the MRC Anatomical Neuropharmacology Unit and at Jozsef Attila university, Szeged, Hungary in collaboration with Dr K. Halasy's group. The synaptic target profile of a further two cells (numbers 12 and 38 on table 2.1) were carried out by T. Sanz (T. Sanz, unpublished observations).

All values are shown as mean ± standard deviation. Physiological parameters were compared by the non-parametric Mann Whitney U-test using

Statview 4.0 software (Abacus Concepts, Berkeley, CA, U.S.A.). To establish the presence of distinct cell classes based on their postsynaptic target profile, the proportion of synaptic output onto each of four postsynaptic elements (soma, dendrite, spine and axon initial segment) for each cell analysed was represented as a point in a 4 dimensional matrix. The 4 dimensional representation was then projected into a 2 dimensional x-y plot using non-linear mapping (stress <1%). The data were also plotted in a hierarchical form as a tree matrix dendrogram. Multi-dimensional matrix representations, cluster analysis and dendrograms were done in consultation with Dr. Mario Cortina (Oxford University Statistical Service) and constructed using the S+ package (StatSci, Seattle, WA, U.S.A.) as described by Venables and Ripley (1994).

3.3 Results

Intracellular recordings in the CA1 area of the rat hippocampal slice revealed 58 neurones (numbers 7,8,10-65 in table 2.1) with firing and salient membrane properties characteristic for local-circuit interneurones (Knowles and Schwartzkroin, 1981; Buhl et al., 1994b). Such features included short-duration, non-overshooting action potentials, which were followed by fast, deep afterhyperpolarisations and could be used to differentiate putative interneurones from pyramidal cells. Of the 58 recorded putative interneurones, 42 were adequately labelled with biocytin so that their morphological characteristics could be examined. Scrutinisation at the light microscopic level confirmed all suspected interneurones to share morphological features which are characteristic for many types of hippocampal interneurones and which are distinct from pyramidal cells. These included smooth or sparsely spiny dendrites which were frequently beaded, distinct dendritic branching patterns, and a dense local axon plexus. In contrast, pyramidal dendrites were highly spinous, had stereotyped branching patterns and the cells lacked the extensive, dense, local axonal arborization. Electron microscopic evaluation of interneurone axon terminals revealed them to consistently form so-called symmetrical (type 2) synaptic junctions with local postsynaptic target neurones. Moreover, individual local-circuit neurones were found to form synaptic contacts selectively with specific membrane domains of postsynaptic target neurones. In contrast to local-circuit interneurones, electron microscopic evaluation of pyramidal cell axon terminals showed them to form asymmetrical (type 1) synaptic contacts.

3.3.1 Morphologically heterogeneous populations of CA1 interneurones

Intracellular recording and subsequent visualisation revealed 42 fast-spiking cells with somata located within stratum pyramidale of the CA1 subfield. The shape

of cell bodies and the dendritic trees showed characteristic features of non-pyramidal cells described in earlier studies (Cajal, 1893, 1911, Lorente de Nó, 1934; Ribak and Seress, 1983; Somogyi et al., 1983a,b, 1985, Kawaguchi and Hama, 1987a,b, 1988; Nunzi et al., 1985; Lacaille et al., 1987, 1988a; Soriano and Frotscher, 1989; Scharfman et al., 1990; Soriano et al., 1990; Li et al., 1992; Halasy and Somogyi 1993; Han et al., 1993; Gulyás et al., 1993a,b, 1996; Buhl et al., 1994a,b, 1995; McBain et al., 1994; Sík et al., 1994, 1995; Buckmaster and Schwartzkroin 1995a,b; Ylinen et al., 1995b; Miles et al., 1996; Acsády et al., 1996b; Halasy et al., 1996; reviewed by Freund and Buzsáki, 1996). Interneurones generally had conical or ellipsoid somata which were usually radially elongated but were occasionally fusiform. Dendrites were mostly smooth, generally beaded to varying degrees and mostly originated form the upper or lower poles of the somata, thus forming an apical and basal tuft of dendrites. Occasionally, the dendritic arbour had multipolar appearances with dendrites extending horizontally. However, the dendritic orientation of most cells was parallel with the apical dendrites of pyramidal cells (Figure 3.1). Interestingly, the apical dendrites of filled neurones extended throughout the layers of the CA1 area to varying extents with close scrutiny of the respective cells showing that this anisotropic distribution of dendrites was not caused by the slicing procedure. Whilst the apical dendrites of some neurones ramified within both strata radiatum and lacunosum-moleculare, others extensively branched in stratum radiatum without extending significantly beyond the strata radiatum / lacunosum-moleculare border.

The axonal arbour of labelled cells was usually dense and contained within the CA1 area, forming horizontally elongated local axonal clouds which could extend laterally by up to 1mm. In most instances, the axon ramified within bands which corresponded to a specific layer(s) and / or afferent input domains of the CA1 area although, the degree to which individual axons 'respected' the laminar boundaries varied between cells (Figures 3.2, 3.3, 3.4, 3.5; summarised on figure 3.6). Due to the structured laminar organisation of pyramidal cells in the

hippocampus, the lamellar distribution of axonal clouds was found to closely correlate with the prevalence of synaptic target surface domains of their postsynaptic target neurones. A sample of randomly selected axon terminals (n=350) were electron microscopically examined and the postsynaptic target profile was established for 22 individual local-circuit interneurones (Table 3.1). Synaptic junctions, as opposed to non-junctional membrane appositions, were identified using the following criteria; (i) vesicle accumulation in the presynaptic axonal varicosity (when detectable); (ii) rigid membrane apposition between pre- and postsynaptic elements with a characteristic widening of the extracellular space; (iii) electron dense synaptic cleft material. Postsynaptic elements were identified by characteristic ultrastructural features (Peters et al., 1991) and comprised of somata, dendritic shafts, dendritic spines and axon initial segments (Figure 3.7). For the population of cells as a whole, the overall proportion of synapses onto each postsynaptic element is represented in histogram format in figure 3.8A-D. Such histograms showed an uneven distribution indicating that the cells do not form a homogenous population with respect to their postsynaptic target profile. Indeed, aided by previous studies (Somogyi et al., 1983a, 1985; Somogyi, 1989; Gulyás et al., 1993a; Han et al., 1993; Halasy and Somogyi, 1993; Buhl et al., 1994a,b, 1995; Halasy et al., 1996; Miles et al., 1996) and based on their synaptic target selectivity, local-circuit interneurones could be classified as (i) basket cells, preferentially innervating the perisomatic domain (soma and proximal dendrites) of their postsynaptic target neurones; (ii) axo-axonic cells, which *exclusively* targeted the axon initial segment domain of postsynaptic target neurones; and (iii) dendritically terminating neurones, which formed synapses with dendritic shafts and spines of postsynaptic target cells. In addition to these three classes of cell, a number of cells were encountered which innervated both the axon-initial segment and somatic / proximal dendritic domain of their postsynaptic target neurones and will be referred to as 'mixed cells'. The synaptic target profile for each group of cells is shown graphically in figure 3.8E-H and indicates that the cells can clearly be

differentiated on the basis of synaptic target selectivity towards particular membrane domains. Below, the respective cell groups will be described and discussed separately.

3.3.1.1 Axo-axonic cells

Axo-axonic cells in the hippocampus and neocortex form synapses exclusively with the axon initial segment of pyramidal neurones (Somogyi, 1977; Somogyi et al., 1982, 1983a, 1985; Soriano and Frotscher, 1989; Gulyás et al., 1993a; Buhl et al., 1994a,b). Five filled cells in this study were confirmed at the electron microscopic level (n=55 synapses) to exclusively form synapses with axon initial segments of pyramidal cells (Table 3.1). The main axon usually emerged from the cell body, giving rise to several main collaterals which were frequently myelinated before branching profusely to form a dense network of terminal branches studded with numerous boutons. A representative example of an axo-axonic cells is shown in figure 3.2. Generally, the axonal clouds of axo-axonic cells were restricted to the lower portion of stratum pyramidale and the subjacent stratum oriens. However, the identification of axo-axonic cells at the light microscopic level is complicated by the fact that, despite their axon generally forming a terminal cloud running parallel to the laminar boundaries of the CA1 subfield, there is often considerable or nearly complete overlap with the terminal cloud of basket cells (e.g. Figure 3.3) or cells with a mixed postsynaptic profile (Figure 3.5). This is due to the spatial overlap of axon initial segments and somata in the lower portion of the cell body layer. One conspicuous feature of axo-axonic cells which can be used to tentatively distinguish them from basket cells is that their axon commonly forms radially orientated rows of boutons (Buhl et al., 1994a; Gulyás et al., 1993a). In the CA1 area of the rat hippocampus however, the latter feature is not particularly prominent since many pyramidal cell axons are either bent or may take a relatively oblique trajectory.

Axo-axonic cell somata were conical in shape and gave rise to smooth, beaded dendrites. Several basal dendrites extended through stratum oriens and often penetrated the alveus. One or few apical dendrites usually traversed stratum radiatum, before branching profusely within stratum lacunosum-moleculare, forming a prominent apical dendritic tuft. When matching dendritic branching pattern and efferent target profile, the presence of such dendritic tufts formed a relatively reliable indicator for axo-axonic cells. Figure 3.1A shows an example of such striking characteristic dendritic features.

3.3.1.2 Basket cells

The most often encountered type of fast-spiking cells were basket cells (n=18) which had most of their axonal arbour concentrated within and around the cell body layer, thus suggesting a perisomatic placement of synapses onto their postsynaptic target neurones. A light microscopic reconstruction of a representative basket cell is given in figure 3.3 (see also figures 4.2, 4.3, 6.1, 6.4) which indicates the dendritic (red) and axonal (black) arborization within the CA1 subfield. In 9 of such cells tested at the electron microscopic level, evaluation of randomly selected synaptic profiles (n=169) confirmed these cells to preferentially target somata (54%), proximal dendrites (45%) and infrequently, dendritic spines (1%) of postsynaptic neurones (Table 3.1). Somata and dendrites were identified at the electron microscopic level based on their characteristic ultrastructural features (Peters et al., 1991). Representative examples of basket cell boutons forming symmetrical synapses onto postsynaptic somatic and dendritic membranes are given on figures 3.7A and 3.7C, respectively.

Although most basket cells were conspicuous at the light microscopic level by their axon terminal cloud mainly occupying stratum pyramidale (e.g. figures 3.3, 4.2, 4.3), a minority of basket cells (n=5) exhibited a broader axonal cloud which extended well into adjacent strata radiatum and oriens (for example see figure

6.4). However, evaluation of the postsynaptic target profile (n=25 synapses) of such an atypical 'wide axon' basket cell (20/06/94/1 in table 1) showed a similar selective innervation of somata (40%) and proximal dendritic shafts (56%), despite having a significant proportion of its axon in dendritic layers.

Unlike pyramidal cell dendrites which were highly spinous, basket cell dendrites were smooth and often beaded. The apical dendritic arbours of basket cells were usually extensive, several primary dendrites commonly fanning out in stratum radiatum, before branching in a dichotomous manner within stratum lacunosum-moleculare (Figure 3.1C-E). However, a few notable exceptions (n=3) exhibited completely different dendritic arborization patterns (Figure 3.1F).

3.3.1.3 Dendritically terminating cells

Pyramidal cell dendrites are known to receive inhibitory synaptic inputs (Somogyi et al., 1983b, Han et al., 1993; Halasy and Somogyi, 1993; Gulyás et al., 1993a; Buhl et al., 1994a, 1995; Halasy et al., 1996; Miles et al., 1996) although the cells which provide such dendritic synaptic input are only poorly characterised. Of the 42 recovered and morphologically characterised local-circuit interneurones, 12 cells had axons which preferentially ramified within dendritic layers of the CA1 subfield and had relatively few axon terminals in the pyramidal cell body layer. Of these, 10 cells preferentially innervated both stratum radiatum and stratum oriens and have been termed bistratified cells (Buhl et al., 1994a, 1996; Halasy et al., 1996; for example see figure 6.1). The remaining 2 cells had axons which selectively ramified mainly within stratum radiatum and will be referred to as stratum radiatum-terminating neurones (SR cells; Figure 3.4).

In contrast to basket cells, bistratified cells had relatively little axon within the pyramidal cell layer but, extensively ramified within stratum radiatum and stratum oriens. The axon of the bistratified cells, predominantly restricted to dendritic layers, is indicative of pyramidal cells receiving bistratified cell synapses

onto their dendrites. Electron microscopic analysis of randomly selected labelled axon terminals (n=21) was carried out on 2 of the 10 cells in this sample and confirmed these 2 bistratified cells to form type 2 (symmetrical) synapses exclusively with apical and basal dendritic shafts (81%) and spines (19%; Table 3.1). A more extensive sample from bistratified cells does however indicate that some of them may also target, to a lesser extent, neuronal somata (Halasy et al., 1996).

The bistratified cell somata were conical or ellipsoid in shape, with two tufts of smooth and often beaded vertically elongated dendrites extending from each pole. The basal dendrites ramified in stratum oriens and generally invaded the alveus. However, bistratified cells differed from basket cells in that their apical dendrites ramified within stratum radiatum but did not extend significantly into, nor branch within, stratum lacunosum-moleculare (Figure 3.1G,H).

Amongst the cells with axon in the dendritic layers, two labelled SR interneurones were similar to bistratified cells with respect to their dendritic arbour, but differed in their axons which preferentially ramified only within stratum radiatum. Illustrated in Figure 3.4 is a camera-lucida reconstruction of one such SR cell showing the location of the soma and dendrites (red) and the axonal arbour (black), which is predominantly confined to stratum radiatum. Although the postsynaptic profile of stratum radiatum cells has not been established at the electron microscopic level, such striking placement of the terminal axon field within a dendritic layer strongly suggests a dendritic placement of their synapses.

3.3.1.4 Mixed cells

In several instances (n=6), individual cells which, from their axonal and dendritic morphological characteristics, were considered to be basket or axo-axonic cells, were subsequently found to form synapses with dendritic, somatic and axon-initial segment domains of their postsynaptic targets, as detected by random electron

microscopic evaluation of postsynaptic profiles. Such 'mixed' postsynaptic target profiles were found in 6 of 22 (27%) cells examined at electron microscopic level (Table 3.1). The percentage of synapses formed with the axon initial domain of postsynaptic target neurones ranged from 5 to 41%.

The dendritic morphology of this class of 'mixed' cell with no apparent overall postsynaptic target preference appeared similar to basket and axo-axonic cells. Indeed, many cells had dendritic arbours which appeared to have both axo-axonic and basket cell features. A camera-lucida reconstruction of one such mixed cell is illustrated in figure 3.5 and shows multiple apical dendrites traversing stratum radiatum, before branching extensively within the molecular layer to form a prominent apical tuft. Similar to the axo-axonic cell shown in figure 3.2, the axon of this mixed cell also ramifies within and subjacent to the cell body layer. Despite these features suggesting that this cell could be an axo-axonic cell, evaluation of randomly selected postsynaptic profiles showed this cell to make only 41% of its synapses with axon initial segments, the remainder being onto somata (36%) and dendritic shafts (23%) The occurrence of mixed cells raises the question as to whether these cells constitute a distinct population in their own right or whether it simply indicates that GABAergic cell classes are overlapping categories of neurones. Statistical methods were therefore employed to address this issue.

3.3.1.5 Statistical analysis of cell types based on differential synaptic target profiles

Previous studies addressing different classes of local-circuit interneurone based on their efferent synaptic target profile have relied upon descriptive terms to distinguish different cell types (e.g. predominantly innervating particular cell types or membrane domains) or have constructed discriminatory rules (e.g. the percentage of synapses onto a particular domain must be greater or less than a certain value in order to belong to a particular class) to segregate cell types.

Although these methods are useful when first investigating differences or common features amongst populations of neurones, statistical methods can provide a more objective approach to determining whether distinct groups of cell exist within a particular population.

In the absence of an independent variable, multidimensional cluster analysis was employed in order to determine whether the sample of cells examined at the electron microscopic level did indeed contain distinct groups with respect to their postsynaptic target profile. The normalised (percentage) postsynaptic target profile for each cell sampled was represented in a 4 dimensional matrix, each of the four columns representing a different membrane domain. From this four dimensional plot, each data point (cell) was projected onto a two dimensional map (Figure 3.9A). From this graph, three distinct clusters of points became apparent, indicating that three separate populations of cell existed within the sample. The most concentrated cluster consisted of 5 data points (cells) which lay at the same position on the 2 dimensional plot, these corresponding to the axo-axonic cells, which, by exclusively innervating the axon initial segment, had identical postsynaptic target profiles. The second cluster contained only two data points but these were close together and clearly distinct form the other two clusters in the plot. These two points represented the two cells which had been classified as bistratified cells. The third cluster contained the most number of points and showed the greatest scatter. Nevertheless, this cluster of cells was clearly distinct from the other two. Interestingly, this third cluster contained both the basket cells and the mixed type cells, this result indicating that the mixed cells do not represent a distinct population and can not be distinguished from the basket cells in this sample. From the same 4 dimensional distance representation of the data set, the data was presented in a quantitative and hierarchical form as a tree matrix dendrogram (Figure 3.9B). On the basis of synaptic target profile, the dendrogram shows a hierarchical classification in which three cell types are clearly segregated by the first two branches of the dendrogram, the first differentiating the axo-axonic cells from the

basket and bistratified cells and the second differentiating the bistratified cells from the basket cells. Interestingly, subsequent branches fail to separate basket cells from mixed cells.

3.3.2 Physiological properties of pyramidal cell layer local-circuit neurones

The anatomical findings appear to indicate distinct classes of local-circuit interneurone. This raised the question, whether the differentiation of cell types on connectivity grounds is reflected in differences in salient membrane, firing and other biophysical properties ? Identifying differences in physiological properties between subtypes of local-circuit interneurone would be a valuable aid to tentatively identify interneurone subtypes already during electrophysiological recording, prior to histological processing of slices. To identify any such differences, 7 basket, 4 axo-axonic and 5 dendritically terminating cells were examined with respect to some of their basic biophysical properties, including cell input resistance, time constant (τ), action potential amplitude and action potential duration (measured at half-amplitude). Overall, the cells had an average input resistance of 63.9 $\pm$ 39.7MΩ, a membrane time constant of 14.3 $\pm$ 7.3ms. Action potentials were 54.5 $\pm$ 7.6mV in amplitude and had a mean duration of 0.55 $\pm$ 0.22ms. These data for each of the three cell types, together with their key anatomical features, are summarised in Table 3.2. For any of these parameters measured, no striking differences were apparent between the three cell types. Indeed, non-parametric statistical analysis (Mann-Whitney U-test) showed that, with respect to cell input resistance, membrane time constant and action potential amplitude, there were no significant differences between the three cell classes ($P>0.05$). However, the three groups of cells did differ significantly with respect to action potential duration. Action

potentials evoked in basket cells were of significantly shorter duration than those in axo-axonic cells, which, were in turn, shorter than those seen in dendritically terminating cells ($P<0.05$). The firing pattern of the cells was highly variable between individual cells. Depolarising current pulses evoked trains of action potentials could either result in little spike frequency adaptation, moderate, or strongly adaptation or could elicit bursting-type firing patterns. On a qualitative basis however, basket and axo-axonic cells were mostly regularly firing and showed only modest spike frequency adaptation whereas the dendritically terminating cells, with one exception, showed a moderate frequency adaptation (Figure 3.10A). However, like the other parameters above, the firing pattern of individual interneurones could not be used to reliably differentiate cell types during recording.

3.3.3 Unitary synaptic responses evoked in postsynaptic pyramidal cells

Synaptic coupling was observed in 60 of 115 paired intracellular recordings made between local-circuit interneurones and pyramidal cells in the hippocampal CA1 area, indicating a high degree of synaptic connectivity and suggesting a highly divergent output of individual interneurones. All cell types described above were shown by paired intracellular recording to evoke, hyperpolarising inhibitory postsynaptic potentials (IPSPs) in synaptically coupled pyramidal cells at membrane potentials in the range of -44.2 to -64.3mV (Figure 3.10B). In one case (cell number 57 in table 2.1), action potentials evoked in an axo-axonic cell elicited unitary IPSPs in a postsynaptic pyramidal cell, whilst activation of the same pyramidal cell elicited fast EPSPs in the axo-axonic cell (Figure 3.10Biv, mean amplitude 1.15mV at -60mV membrane potential) . The presence of such a loop indicates that axo-axonic cells participate in recurrent inhibition. Although the amplitude of IPSPs were evidently dependent upon the membrane potential of the

postsynaptic pyramidal cell (Figure 3.8C,D), even at depolarised membrane potentials close to action potential threshold, where the hyperpolarising effect was greatest, the amplitude of few averaged responses was greater than 1mV. Due to the high resistance of the sharp recording electrodes and the small amplitude of the synaptic responses measured, the signal to noise ratio was relatively low, so that synaptic responses were often undetectable in individual sweeps, but were clearly resolved upon spike triggered averaging of the postsynaptic trace (see methods). A sample of basket, bistratified and axo-axonic cells were compared with respect to the synaptic responses they evoked in postsynaptic pyramidal cells (n=18; Table 3.2). In the membrane potential range tested, basket, bistratified and axo-axonic cells all elicited hyperpolarising IPSPs (mean amplitude 586±369μV; membrane potential -57.2±5.6mV) in simultaneously recorded pyramidal cells. All synaptic responses had fast rise and decay kinetics (mean 10-90% rise time 6.0±4.8ms; mean decay time constant 32.0±15.6ms; mean IPSP duration measured at half-amplitude 40.6±30.5ms) and were monophasic, lacking a longer-lasting component, which might correspond to the activation of $GABA_B$ receptors (Newberry and Nicoll; 1985). The mean IPSP amplitude varied greatly between individual cell pairs, ranging from the level of detectability to more than 1.3mV. Similarly, the kinetic measurements also varied greatly between individual cell pairs. The mean IPSP amplitude and kinetic measurements for unitary responses evoked by each of the three cell types are given in table 3.2. No dramatic differences were apparent between basket, bistratified and axo-axonic cell-evoked responses. Indeed, with one exception, non-parametric statistical analysis failed to show significant differences between each of the three cell types, both in terms of IPSP amplitude and kinetic measurements ($P>0.05$; Mann-Whitney U-test). The one set of measurements, which did turn out to be statistically significant ($p<0.05$; Mann-Whitney U-test) was the mean IPSP amplitudes evoked by bistratified cells, which were larger than those evoked by axo-axonic cells. However, given the low number of observations obtained for both cell types (3 and 5), these results should

be viewed with caution, until a much larger sample is collected for each cell type. Moreover, the IPSP amplitude is not a good indication of synaptic strength as synaptic responses are dependent upon many factors such as the membrane potential, input resistance of the postsynaptic neurone, the gradient of the charge carrier(s) and possibly also dendritic filtering. Therefore, in the absence of conductance measurements, the comparative efficacy of synaptic responses evoked by interneurones targeting different membrane domains could not be established (see also chapter 6).

Relatively few synaptically coupled cell pairs were of sufficient quality to allow rigorous assessment of the evoked synaptic responses in conjunction with complete physiological and morphological analysis of both pre- and postsynaptic cells. This meant that a truly quantitative comparison between different cell types was severely restricted. For this reason, only the largest sample of synaptically coupled cell pairs, those with presynaptic basket cells, were collected for a more detailed investigation of their biophysical and pharmacological properties of unitary synaptic interactions with pyramidal cells. These results form chapter 4 of this thesis.

3.4 Discussion

3.4.1 Diversity of local-circuit interneurones in the CA1 area

Early studies using Golgi impregnation methods have provided detailed descriptions of non-principal cells and highlighted their great morphological diversity within the hippocampal formation (Ramon y Cajal, 1893; Lorente de No, 1934). However, in these early studies, the extensive axonal termination pattern for individual cells could not be fully established. Using the intracellular biocytin labelling technique (Horikawa and Armstrong, 1988), which permits a more complete reconstruction of dendritic and axonal processes of individual neurones,

the current experiments provide additional and novel data on the diversity of non-pyramidal cell types in the hippocampal CA1 area. However, even reconstruction from the 400μm thickness of the transverse hippocampal slice preparation resulted in the axonal and dendritic arborizations being only partial. Bearing this limitation in mind however, these results clearly demonstrate that this method is useful to examine and differentiate different cell types based on their morphological features.

A segregation of non-pyramidal cell types in the CA1 area is apparent, based on the remarkable laminar stratification of axon terminals. These marked differences in axonal morphology were accompanied by more subtle differences in dendritic morphology. Although all cells investigated in these experiments had their somata located within or adjacent to stratum pyramidale, it should be noted that non-pyramidal cells with somata located in dendritic layers also possess distinct dendritic and axonal arbours (Ramon y Cajal, 1989, 1911; Lorente de No, 1934; Kawaguchi and Hama, 1988; Kunkel et al., 1988; Lacaille and Schwartzkroin, 1988a; Tóth and Freund, 1992; Williams et al., 1994; Khazipov et al., 1995; Sík et al., 1995; Acsády et al., 1996a; Gulyás et al., 1996; Vida et al., 1997).

3.4.2 Laminar axonal distribution and synaptic termination patterns of local-circuit neurones in the CA1 area

These data indicate that individual local-circuit interneurones preferentially innervate the CA1 area of the rat hippocampus in a laminar specific manner as has been described previously in the dentate gyrus (Halasy and Somogyi, 1993; Han et al., 1993) and the CA3 and CA1 areas of the hippocampus (Gulyás et al., 1993a; Buhl et al., 1994a; Halasy et al., 1996). Due to the highly structured orientation of principal cells in the hippocampal formation (Lorente de No, 1934; Ramon y Cajal, 1893; Swanson et al., 1987), the observed staggered stratification of axonal termination fields for individual interneurones suggests that different cells may preferentially target different functional domains of the principal neurones and / or

co-stratify with specific excitatory afferent input pathways (Halasy and Somogyi, 1993; Han et al., 1993). Electron microscopic evaluation of the postsynaptic targets indeed indicated different local-circuit interneurones to selectively target dendritic, perisomatic or axon initial segment domains of pyramidal cells as described previously (Buhl et al., 1994a; Gulyás et al., 1993a; Halasy and Somogyi, 1993; Halasy et al., 1996; Miles et al., 1996; Seress and Ribak, 1985, 1990; Sík et al., 1995; Somogyi et al., 1983a,b, 1985; Soriano and Frotscher, 1989; Soriano et al., 1990). Moreover, by accurately targeting synapses towards specific functional cellular domains, these results indicate a striking division of labour amongst local-circuit interneurones (Buhl et al., 1994a; Gulyás et al., 1993a; Nicoll, 1994).

3.4.2.1 Axo-axonic cells

Axo-axonic cells were the most distinct type of GABAergic local-circuit interneurone in the CA1 area, by displaying a remarkably precise target selectivity, forming synapses exclusively with the axon initial segment domain of pyramidal cells. Indeed, the statistical analysis showed axo-axonic cells to be the most distinctive cell class based on their synaptic target profile. Similar electron microscopically determined postsynaptic target profiles have been described previously for axo-axonic cells in both the neocortex, dentate gyrus and hippocampus (Somogyi, 1977; Somogyi et al., 1982, 1983a, 1985; Kisvardáy et al., 1986a; Soriano and Frotscher, 1989; Freund et al., 1983; Halasy and Somogyi, 1993; Buhl et al., 1994a,b; Cobb et al., 1995). Earlier studies have shown these cells to contain GAD (Freund et al., 1983), GABA (Somogyi et al., 1985; Soriano and Frotscher, 1989) and the calcium binding protein parvalbumin (Katsumaru et al., 1988) but there is as yet no evidence that, in the hippocampus, axo-axonic cells express any of the known neuropeptide transmitters. Axo-axonic cells constitute a class of local-circuit neurone that is unique to cortical structures (Somogyi, 1989), but within cortical structures, appears ubiquitous, suggesting that they mediate a function which is fundamental to the operation of the cerebral cortex. Unlike other

local-circuit neurones, whose axon terminate in conjunction with excitatory inputs to the same cell, axo-axonic cells form synapses with what has been considered to be the final integration domain of pyramidal neurones. The axon initial segment represents the site where action potential threshold is lowest, and hence is intimately involved in the genesis of regenerative action potentials (Stuart and Sakmann, 1994; Hausser et al., 1995). Although *in vitro* experiments such as these cannot determine the functional role for individual types of local-circuit neurone within the hippocampus, it is reasonable to assume that as axo-axonic cells very accurately direct their efferent output to this strategic portion of the pyramidal cell membrane, they may be involved in modulating the output of pyramidal cells, as has been predicted (Somogyi et al., 1982; Douglas and Martin, 1990). Dual intracellular recording showed that individual axo-axonic cells evoke hyperpolarising IPSPs in synaptically connected pyramidal cells. The fast kinetics and reversal potential close to the chloride equilibrium potential were consistent with $GABA_A$ receptor mediated responses, as previously demonstrated (Buhl et al., 1994a) and were similar to effects mediated by somatic and dendritically terminating cells. The effect of axo-axonic cell-evoked IPSPs on action potential generation, timing and other dynamic membrane properties is considered in chapter 5 of this thesis.

Although the synaptic input onto axo-axonic cells was not investigated in these experiments, CA1 axo-axonic cells are known to be activated upon extracellular stimulation of fibre tracts presumably corresponding to the perforant path, Schaffer collaterals and axons at the stratum oriens / alveus border, indicating that axo-axonic cells may be activated in both feed-forward and feed-back manner (Buhl et al., 1994b). The results confirm the latter by showing an individual axo-axonic cell and pyramidal cell pair to be reciprocally connected (Figure 3.10B), as shown previously for basket cells (Buhl et al., 1994a).

3.4.2.2 Basket cells

The term 'basket cell' has previously appeared in the literature as a rather vague umbrella term, used to describe a variety of GABAergic local-circuit interneurones which reside in and around the cell body layer. Golgi impregnation studies revealed 'pericellular baskets' in neocortex (Ramon y Cajal, 1893) and the cells whose axons innervated the hippocampal pyramidal cell layer were termed basket cells (Lorente de No, 1934). The pericellular baskets are not produced by a single cell but are each comprised from the axons of several cells. Intracellular labelling studies have revealed a population of local-circuit interneurone to innervate selectively the perisomatic domain of principal cells and thus a new and more precise definition of basket cell (those cells selectively innervating somata and proximal dendrites) has emerged (Somogyi et al., 1983a, 1985; Gulyás et al., 1993a; Halasy and Somogyi, 1993; Han et al., 1993; Buhl et al., 1994a, 1995). However, the statistical analysis of the synaptic target profiles of the 22 cells examined at the electron microscopic level in these experiments showed that the mixed cells, which also formed synapses with axon initial segments, were, on these grounds, indistinguishable from the population of synaptically defined basket cells (those forming synapses with somata and proximal dendrites). This result implies that with regard to their efferent output, basket cells should be considered as cells which innervate soma and proximal processes including the axon initial segment.

The axonal arbours of basket cells in the CA1 area showed some variation but were mainly restricted to stratum pyramidale and neighbouring portions of strata radiatum and oriens. Most cells displayed a laminar distribution of their arbours, which was similar to those described for axo-axonic cells. Indeed, this similarity has occasionally resulted in misclassification of axo-axonic cells as basket cells in the literature (Freund and Buzsáki, 1996) and emphasises the necessity for rigorous electron microscopic examination of synaptic target profiles, if a reliable classification of a cell type is to be made. A minority of basket cells displayed

axonal arborization patterns which covered stratum pyramidale, but which extended significantly into the dendritic layers (e.g. Figure 6.4) as has been described for atypical basket cells in the CA3 area (Gulyás et al., 1993a). However, evaluation of the synaptic target profile of such 'wide axonal basket cells' showed that despite extensively ramifying within dendritic layers, its axon still selectively formed synapses with the perisomatic domain (40% of synapses onto cell bodies) of their target neurones.

Basket cells have been shown in other studies to contain the inhibitory transmitter GABA (Somogyi and Soltész, 1986; Halasy et al., 1996) as well as the neurochemical markers parvalbumin (Katsumaru et al., 1988; Kosaka et al., 1987; Sloviter, 1989; Sík et al., 1995) and cholecystokinin (Nunzi et al., 1985; Harris et al., 1985) which is probably co-localised with vasoactive intestinal peptide (Acsády et al., 1996a). It remains to be established whether the differences in dendritic and axonal morphologies seen in these experiments, reflect different sub-classes of basket cell with varying expression of neurochemical markers.

The somatic and proximal dendritic domain which basket cells innervate has traditionally been assumed to be an integration compartment, strategically placed between the dendritic input and the axonal output domain of cells. Based on this assumption, basket cells may gate the spread of excitation from the dendrites to the soma. The fast hyperpolarising synaptic responses recorded are most likely to represent the unattenuated shape of synaptic responses, as, unlike for the bistratified cell responses, the recording electrodes were located directly at the site of synaptic input. The physiology of basket cells and the responses they evoke in pyramidal cells are discussed in detail in the next chapter.

3.4.2.3 Dendritically terminating cells

The dendritically terminating cells were comprised of those whose axon ramified within strata radiatum and oriens, the bistratified cells, and those which had axons that selectively ramified in stratum radiatum, the SR cells. Bistratified cells are a recently described class of local-circuit interneurone whose axons co-stratify with the Schaffer collateral / commissural excitatory pathway to the CA1 area (Buhl et al., 1994a). Bistratified cells showed a synaptic target profile similar to those previously described for cells forming synapses exclusively with dendritic shafts and spines. Previous studies indicate that bistratified cells contain the neurotransmitter GABA (Buhl et al., 1994a) and the calcium binding protein calbindin (Sík et al., 1995). Using dual intracellular recording, the current experiments showed bistratified cells to evoke fast IPSPs in simultaneously recorded pyramidal cells, the kinetics of which are consistent with a $GABA_A$ receptor-mediated synaptic response and distinct from $GABA_B$ receptor-mediated effects (Dutar and Nicoll, 1988). These experiments failed to show any significant difference in the rise and decay kinetics of bistratified versus basket cell evoked IPSPs in pyramidal cells, in contrast to the previous findings (Buhl et al., 1994a; Miles et al., 1996). Slower kinetics would be expected from electrotonic attenuation (Rall, 1977), but might also result from dendrites expressing a different type of $GABA_A$ receptor (Wisden et al., 1992; Pearce, 1993). That no significant difference in the kinetics (in somatic records) was observed between dendritically and perisomatically terminating may be due to the number of cells sampled being very small, although alternative explanations include differences in the membrane properties of the postsynaptic pyramidal cells and variability in the exact placement of synapses onto different dendritic branches. The hyperpolarising nature of dendritically evoked responses are in agreement with other similar dual recording studies in the CA1 (Buhl et al., 1994a) and CA3 areas (Miles et al., 1996), but are in contrast to suggestion that the action of synaptically released GABA on dendritic

membrane may be depolarising (Alger and Nicoll, 1982a,b; Misgeld et al., 1986; Lambert et al., 1991; Staley et al., 1995).

Stratum radiatum cells have been described in the CA3 area of the guinea pig (Gulyás et al., 1993a) although, to the best of my knowledge, this is the first report of CA1 cell body layer local-circuit interneurones whose axons selectively ramify within stratum radiatum. The postsynaptic target profile of SR cells was not determined at the electron microscopic level. However, due to their selective ramification within the dendritic layer, it is likely that SR cells target apical dendrites, as shown in the CA3 area (Gulyás et al., 1993a). Like bistratified cells, SR cells co-stratify with the major Schaffer collateral and commissural pathways, perhaps selectively with axons from the CA3 area which predominantly project into stratum radiatum of the CA1 area (Li et al., 1992). However, by avoiding basal dendrites in stratum oriens, SR cells are less likely to influence recurrent input to CA1 neurones, which occurs mainly through basal dendrites (Lorente de No, 1934).

The dendrites of pyramidal cells receive excitatory input from several pathways which impinge upon them in a laminar fashion (see chapter 1). One attractive hypothesis concerning the function of cells that innervate dendritic regions is, that they may act to differentially modulate the efficacy of excitatory inputs arriving from segregated input pathways (Buhl et al., 1994a; Gulyás et al., 1993a; Halasy and Somogyi, 1993; Han et al., 1993). Such a mechanism would be achieved through both postsynaptic (Staley and Mody, 1992) as well as presynaptic mechanisms (Bowery et al., 1980; Lanthorn and Cotman, 1981; Ault and Nadler, 1982; Deisz and Prince, 1989). It is interesting to note that, in the pyramidal cell layer, no cells were encountered which selectively terminated in stratum lacunosum-moleculare in conjunction with the major perforant path input. Such cells are known to exist in the hippocampus but have their soma and dendrites mainly situated in stratum oriens, and are immunoreactive for both mGluR1α receptors and the peptide somatostatin (Köhler and Chan-Palay, 1982; Bakst et al., 1986; Kosaka et

al., 1988b; Kunkel and Schwartzkroin, 1988; Baude et al., 1993; Gulyás et al., 1993a; Buckmaster et al., 1994; McBain et al., 1994; Sík et al., 1995; Somogyi et al., 1984). Moreover, Vida et al. (1997) have recently described interneurones in the CA1 area with soma and dendrites located at the strata radiatum / lacunosum-moleculare border, which exclusively innervate stratum lacunosum-moleculare. It is therefore likely that cells selectively innervating stratum lacunosum-moleculare were not sampled in these experiments, as recordings were made only from cells with soma in stratum pyramidale.

3.4.2.4 Mixed cells

An unexpected result of this study was that individual local-circuit neurones were encountered which had a postsynaptic target profile including axon initial segments as well as somata / proximal dendrites. Strictly speaking, such mixed cells provide a significant somatic input to their target neurones and should be thus regarded as basket cells. Indeed, the statistical analysis failed to separate the mixed cells form the basket cells, suggesting that *on grounds of efferent connectivity*, they do not represent separate populations. With two exceptions (Soriano et al., 1990; Buhl et al., 1994b), most previous studies have shown axo-axonic cells to *exclusively* innervate axon initial segments of neocortical and hippocampal principal neurones in several species (Somogyi, 1977; Somogyi et al., 1983a, 1985; Halasy and Somogyi, 1993; Gulyás et al., 1993a). This notion supports the statistical data that mixed cells should be considered basket cells. However, the observation that some mixed cells (e.g. Figure 3.5) had a dendritic and axonal morphology which resembled that of axo-axonic cells, suggests that basket and axo-axonic cells may not form completely segregated, non-overlapping populations of neurones, with mixed cells representing those with intermediate properties. In the neocortex, basket cells were also found, occasionally, to target the AIS of principal cells (Somogyi et al., 1983b; Kisvardáy et al., 1985). This scenario may indicate that the situation in

the hippocampus reflects the early evolutionary segregation of perisomatically innervating GABAergic interneurones into two distinct, non-overlapping classes with distinct target preferences.

3.4.3 Comparison of dendritic and axonal arborizations

The dendritic morphology of the labelled local-circuit neurones shared characteristics common to previously described hippocampal non-pyramidal cells (Amaral, 1978; Ribak and Seress, 1983, 1988; Kosaka et al., 1985; Sloviter and Nilaver, 1987; Katsumaru et al., 1988; Soriano and Frotscher, 1989; Gulyás et al., 1992, 1993a; Tóth and Freund, 1992; Han et al., 1993; Buhl et al., 1994a,b). In contrast to the neocortex, the correlation between the laminar location of axonal bands and the postsynaptic structures (e.g. soma, dendrites) with which the cells formed synapses is readily apparent in view of the highly structured organisation of the hippocampal formation. A further correlation was that between the different classes of cell defined on the basis of their axonal arborization pattern (and their postsynaptic target profile), and their dendritic morphology, in particular, the extent to which their apical dendrites ramified within the molecular layer. Axo-axonic cell dendrites traverse stratum radiatum, rarely branching, until reaching stratum lacunosum-moleculare, suggesting that they receive a predominant portion of their efferent synaptic input via either the perforant path or the projection from the nucleus reuniens thalami (Wouterlood et al., 1990) and a disproportionately smaller contribution via the Schaffer collateral / commissural pathways. Conversely, bistratified and SR cell apical dendrites extensively ramified within stratum radiatum, but ended close to the border with stratum lacunosum-moleculare, suggesting that they receive mainly associational / commissural input and relatively little entorhinal input. It appears, that these features may represent either ends of a continuum, as basket cells appear to lie between the two extremes, suggesting that they receive substantial input form both efferent sources. It should be noted that this

conclusion is preliminary as the sample of cells obtained from these experiments was not adequate to carry out quantitative analysis of dendritic characteristics between different cells types. It is of interest to note that, nine cells from this sample, which were provided to Halasy and colleagues (1996) to complement a larger study, showed basket and bistratified cells to differ significantly with respect to the extent to which their dendrites ramified within stratum lacunosum-moleculare.

In contrast to the apical dendritic morphology, there were no obvious differences in basal dendritic arbours of the three types of local-circuit neurone examined. This suggests that basket, axo-axonic cells and dendritically terminating cells may all receive similar inputs in that region. The main afferents which arrive within stratum oriens are Schaffer collateral, commissural fibres from proximal to CA1 (CA3a) and recurrent excitatory collaterals from pyramidal cells in the CA1 area. The incidence of recurrent excitation between pyramidal cells is very low in the CA1 area (Thomson and Radpour, 1991) although, recurrent excitation to interneurones has been morphologically and physiologically demonstrated (Lacaille et al., 1987; Buhl et al., 1994a; Gulyás et al., 1993b; McBain et al., 1994; Blasco-Ibanez and Freund, 1995). In the CA3 area of the guinea pig, this connection is thought to consist of only one or two release sites on basal dendrites of each interneurone (Arancio et al., 1994; Gulyás et al., 1993b).

In Figure 3.10B an axo-axonic cell is also recurrently activated by a pyramidal cell, forming a reciprocal circuit. The functional significance for such bi-directional connectivity is not clear, although it is likely to shape firing patterns (Tarczy-Hornoch et al., 1996). Since the time required for the onset of recurrent inhibition in pyramidal cells is shorter than the latency of the action potential-induced depolarising afterpotential, repetitive firing / bursting of principal neurones can be prevented (Miles et al., 1996). The presence of recurrent innervation of bistratified cells has yet to be demonstrated physiologically.

3.4.4 Functional implications

The differences in the connections of distinct classes of GABAergic cells converging onto CA1 pyramidal cells suggest that each type of interneurone subserves a distinct functional role within the hippocampal network. The final outcome of GABA-mediated effects on pyramidal cells depend on (i) the location of the synapses on the postsynaptic cell, (ii) the pharmacological (receptor subunit specific) properties of GABA receptors mediating the effect and (iii) the passive as well as active membrane properties of the postsynaptic pyramidal cell. Previous results indicate that the postsynaptic mechanisms of perisomatically and dendritically terminating inhibitory cells appear to be different (Alger and Nicoll, 1982b; Pearce, 1993, Miles et al., 1996), and the control of GABA release from terminals has also been reported to be heterogeneous between different axons (Lambert and Wilson, 1993b). Based on the morphological information collected from these experiments, different cells appear to be specifically adapted to carry out quite different functions. By selectively innervating the dendrites in parallel with major excitatory afferent pathways, the bistratified and stratum radiatum-terminating cells are ideally placed to modulate incoming excitatory signals, perhaps mediating a downward re-scaling of Schaffer collateral / commissural EPSPs (Buhl et al., 1994a). Localised dendritic inhibition may be able to 'amputate' individual dendritic processes (Llinás and Nicholson, 1971), shunt NMDA receptor mediated conductances (Staley and Mody, 1992) or, by targeting individual dendritic spines, may exert a selective control of events at a single excitatory synapse. Alternatively, dendritically terminating interneurones may also control dendritic electrogenesis (Miles et al., 1996; Paulsen and Vida, 1996), including backpropagating action potentials (Stuart and Sakmann, 1994; Spruston et al., 1995; Buzsáki et al., 1996). Just as the morphology suggests that the dendritically terminating cells control the input domain of pyramidal cells, so does the anatomical finding that some cells exclusively innervate the output portion of pyramidal cells predestine the axo-axonic

cells to control their firing output. Thus the functional role for axo-axonic cells has long been assumed on anatomical (Somogyi et al., 1982; Buhl et al., 1994a,b) and theoretical grounds (Douglas and Martin, 1990) to be to govern action potential generation in the axon initial segment. Compared to axo-axonic cells and interneurones innervating dendritic regions, the functional role for the basket cells is perhaps less obvious. By forming somatic and proximal dendritic synapses close to the axon initial segment, the basket cells would at first appear to be well placed for controlling the spread of dendritic excitation to the axon initial segment and hence the firing output of the postsynaptic cell. However, that a specialised type of interneurone selectively innervates the exact site with the lowest action potential threshold makes this seem unlikely, although basket cells are known to interfere with somatic electrogenesis and can block sodium spikes (Cobb et al., 1995; Miles et al., 1996). The soma forms the linkage between the main excitatory input domain of the cell (the dendrites) and the output domain (the axon) and may therefore be viewed as a common integration domain, which combines efferent input received by the various dendrites and relays them to the axon initial segment. The function of basket cells may therefore be to gate the flow of excitation from the dendrites to the axon initial segment, rather than having a final veto as to whether an action potential is generated or not. The somata of hippocampal principal neurones are known to receive rhythmic IPSPs and are involved in rhythmic membrane potential changes (Soltész et al., 1993). The basket cells may thus phasically gate the transmission from the dendrites to the soma and therefore phase the activity of pyramidal cells. As each basket cell innervates many hundreds of pyramidal cells (Buhl et al., 1994a; Miles et al., 1996; Sík et al., 1995), such phasic activity may synchronise the activity of large populations of pyramidal cells. Tonic inhibition is also known to originate from synapses on the soma and proximal dendrites (Mody et al., 1994; Soltész et al., 1995; Miles et al., 1996). Thus, basket cells may be differentially active and subserve different functions under different behavioural states (Buzsáki et al., 1983, 1992; Buzsáki & Eidelberg, 1983; Lee et al., 1994; Bragin et al.,

1995; Ylinen et al., 1995b; Chrobak & Buzsáki, 1996; see also Freund and Buzsáki, 1996).

This chapter shows that local-circuit interneurones terminating onto both dendritic, perisomatic and axon initial segment domains essentially produce very similar postsynaptic effects when measured via a somatic sharp electrode. However, that no obvious differences are observed between the effects mediated by the three types of cell does not mean that they will subserve the same function under physiological conditions. Rather, the striking differences in morphology suggest that there are likely to be differences and that more subtle experimental paradigms have to be developed in order to test particular functions. An attempt towards addressing this issue is described in chapter 5 of this thesis.

Figure 3.1 Dendritic arbourisation pattern of intracellularly labelled local-circuit neurones and pyramidal cells in the hippocampal CA1 subfield. Light microscopic reconstructions of selected dendritic arbours showed most local-circuit neurones to have dendrites which were polarised and vertically orientated (A-E, G-I). Less commonly, cells were recovered which had a stellate appearance (F). Two pyramidal cells (J,K) were reconstructed for comparative purposes. Note that spines have been omitted from drawings. Lines on left indicate approximate position of laminar boundaries. Note the presence of prominent apical dendritic tufts in some cells (A,B) and the relative paucity of apical dendrite entering and branching within the molecular layer for others (F-I). Scale bar 100μm. S-LM, stratum lacunosum-moleculare; SR, stratum radiatum; SP, stratum pyramidale; SO, stratum oriens.

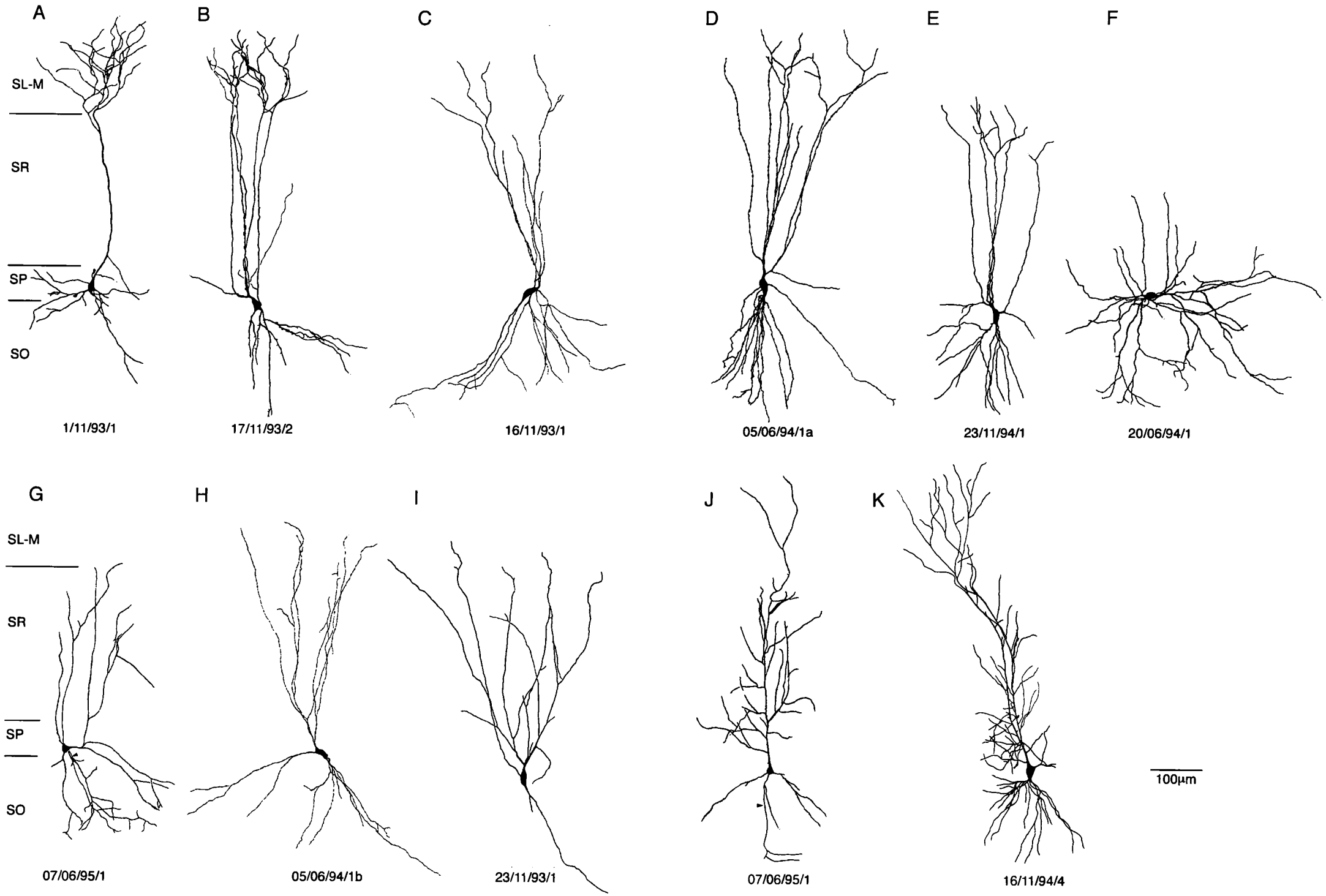

A
SL-M
SR
SP
SO
1/11/93/1
B
17/11/93/2
C
16/11/93/1
D
05/06/94/1a
E
23/11/94/1
F
20/06/94/1
G
SL-M
SR
SP
SO
07/06/95/1
H
05/06/94/1b
I
23/11/93/1
J
07/06/95/1
K
16/11/94/4
100µm

Figure 3.2 Intracellularly recorded and biocytin-filled axo-axonic cell in the CA1 area of the rat hippocampus. The light microscopic reconstruction of the soma and dendrites (red) was made for 5 X 60µm thick sections and shows the conical shaped cell body located in stratum pyramidale, giving rise to several smooth dendrites which traversed stratum radiatum and ramify within stratum lacunosum-moleculare. The distal apical dendrites were weakly filled and several appeared to be cut at the border of the slice so that the characteristic apical tuft in stratum lacunosum-moleculare is less apparent. Several basal dendrites emerged from the basal pole of the soma and extended through stratum oriens to the alveus where they fanned out and branched. The axon (black), partially reconstructed form 2 X 60µm sections, formed a dense band of terminal branches in the lower half of the cell body layer and in the subjacent portion of stratum oriens. The lateral extent of the axon was ~500µm. Evaluation of randomly selected postsynaptic profiles at the electron microscopic level (n=11) showed this cells to selectively form symmetrical type synapses exclusively with axon initial segments (100%). SL-M, stratum lacunosum-moleculare; SR, stratum radiatum; SP, stratum pyramidale; SO, stratum oriens.

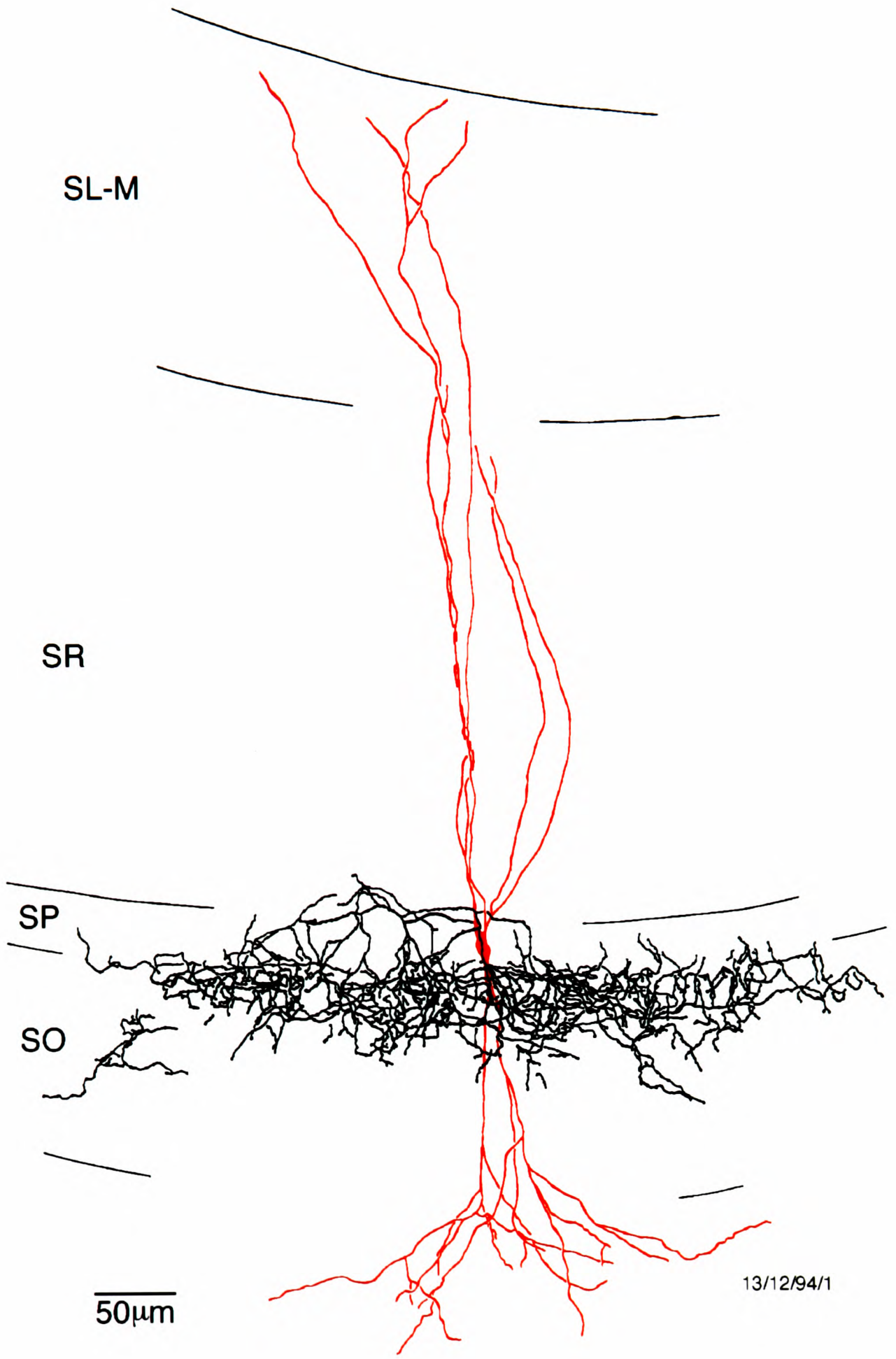

SL-M
SR
SP
SO
50µm
13/12/94/1

Figure 3.3 Light microscopic reconstruction of a typical basket cell from five sections (60μm each). This reconstruction shows the soma, dendrites (red) and axon (black). The soma is situated in stratum pyramidale, with basal dendrites ramifying in stratum oriens and apical dendrites extending through stratum radiatum before branching (though not extensively) in stratum lacunosum-moleculare. The axon emerges close to the apical pole of the soma, before extending laterally along stratum pyramidale, branching extensively and ramifying in stratum pyramidale as well as adjacent fringes of strata radiatum and oriens, suggesting a perisomatic innervation of its postsynaptic target neurones. Evaluation of randomly selected postsynaptic profiles at the electron microscopic level (n=13) confirmed this cells to selectively form symmetrical type synapses with somata (54%) and proximal dendritic shafts (46%).

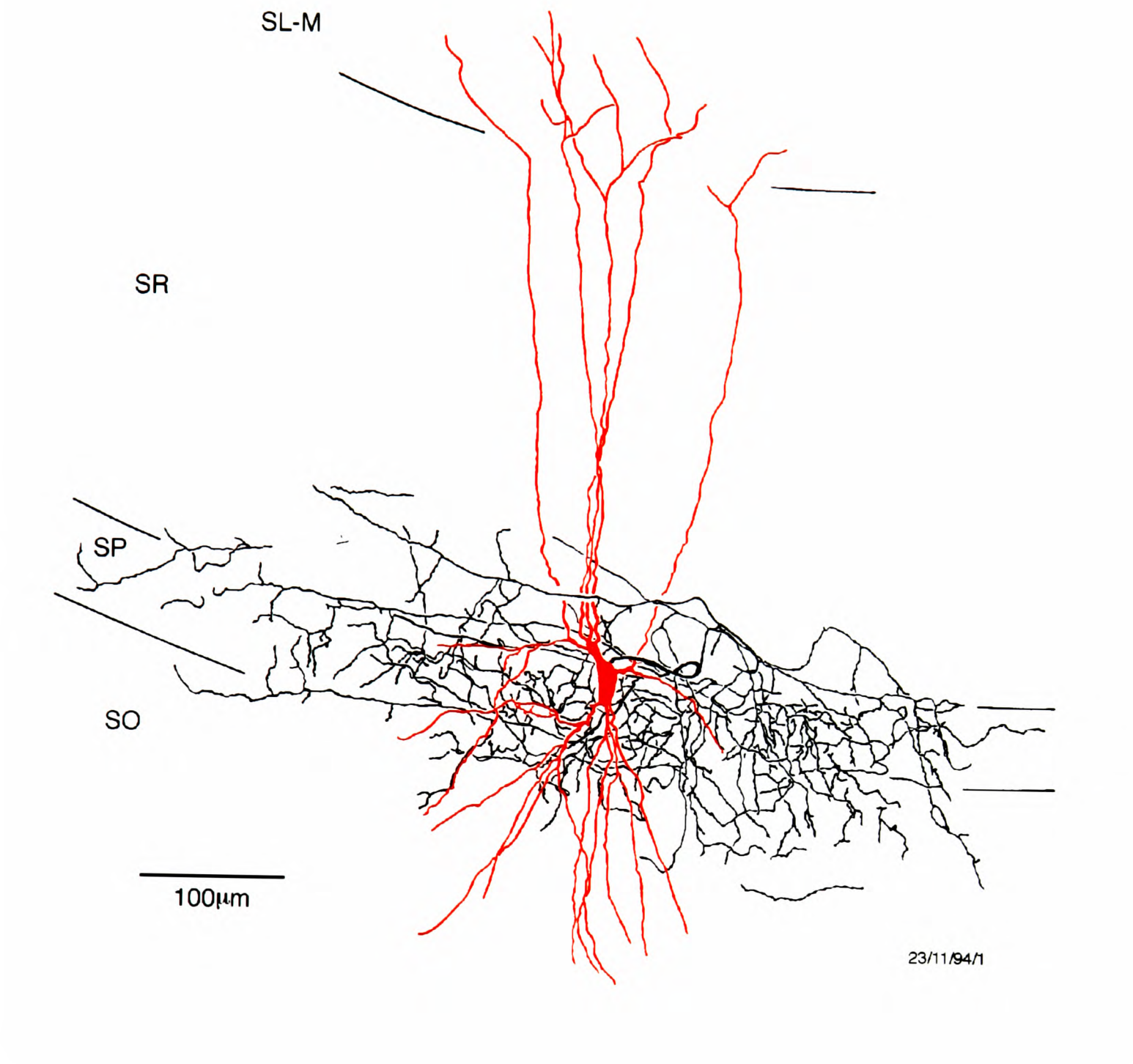
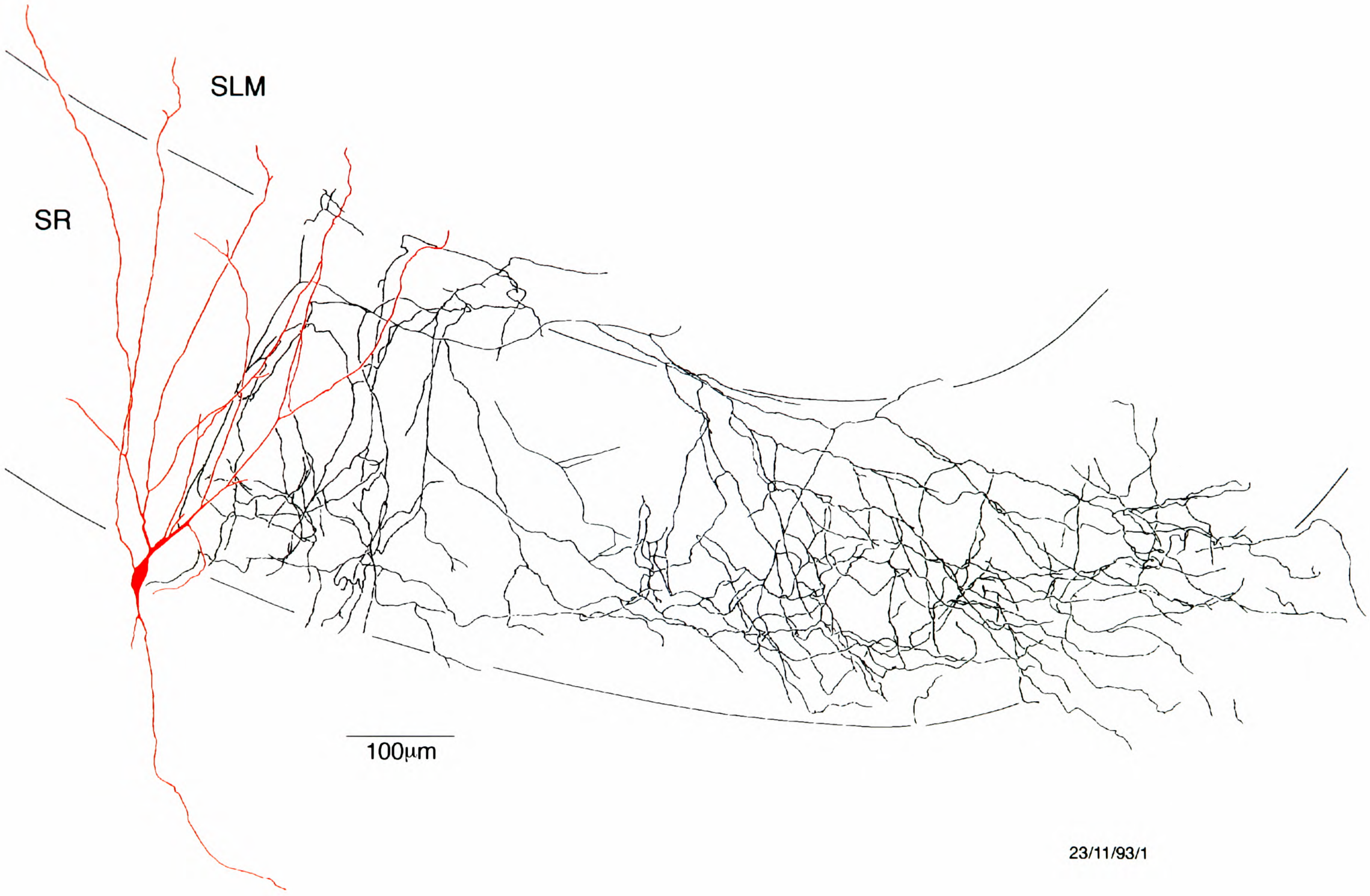

SL-M
SR
SP
SO
100µm
23/11/94/1

Figure 3.4 Light microscopic reconstruction of a stratum radiatum (SR) terminating interneurone in the CA1 area of the rat hippocampus. The soma (soma and dendrites in red) was located in stratum pyramidale from which multiple apical dendrites fanned out through stratum radiatum and slightly extended into stratum lacunosum-moleculare, where they terminated. A basal dendrite extended through stratum oriens and penetrated the alveus. The main axon (black) originated from the proximal portion of a primary apical dendrite and extended towards the border with stratum lacunosum-moleculare where it branched, forming several major collaterals which extend laterally along the CA1 subfield, frequently branching. The extensive axonal arbour ran laterally up to 1mm along the CA1 subfield but was predominantly restricted to stratum radiatum. The postsynaptic targets for this cell are unknown.



23/11/93/1

Figure 3.5 Light microscopic reconstruction of a biocytin labelled interneurone with a mixed-type postsynaptic target profile. The conical shaped soma (soma and dendrites in red) was located in stratum pyramidale from which radially orientated smooth beaded dendrites extended. The basal dendrites ramified within stratum oriens and extended into the alveus. Five main apical dendrites traversed stratum radiatum without branching or fanning out upon reaching stratum lacunosum-moleculare, forming a prominent apical dendritic tuft. The axon (black) formed a dense band of terminal branches in the lower half of the cell body layer and in the subjacent portion of stratum oriens. The lateral extent of the axon was ~600mm. Although the dendritic and axonal features of this cell were characteristic for axo-axonic cells, evaluation of randomly selected postsynaptic profiles at the electron microscopic level (n=22) showed this cells to selectively form symmetrical type synapses mostly with axon initial segments (41%), but also with somata (36%) and proximal dendritic shafts (23%). Thus, this cell had several features which characterise axo-axonic cells, but had a mixed efferent target profile (see text). SL-M, stratum lacunosum-moleculare; SR, stratum radiatum; SO, stratum oriens.

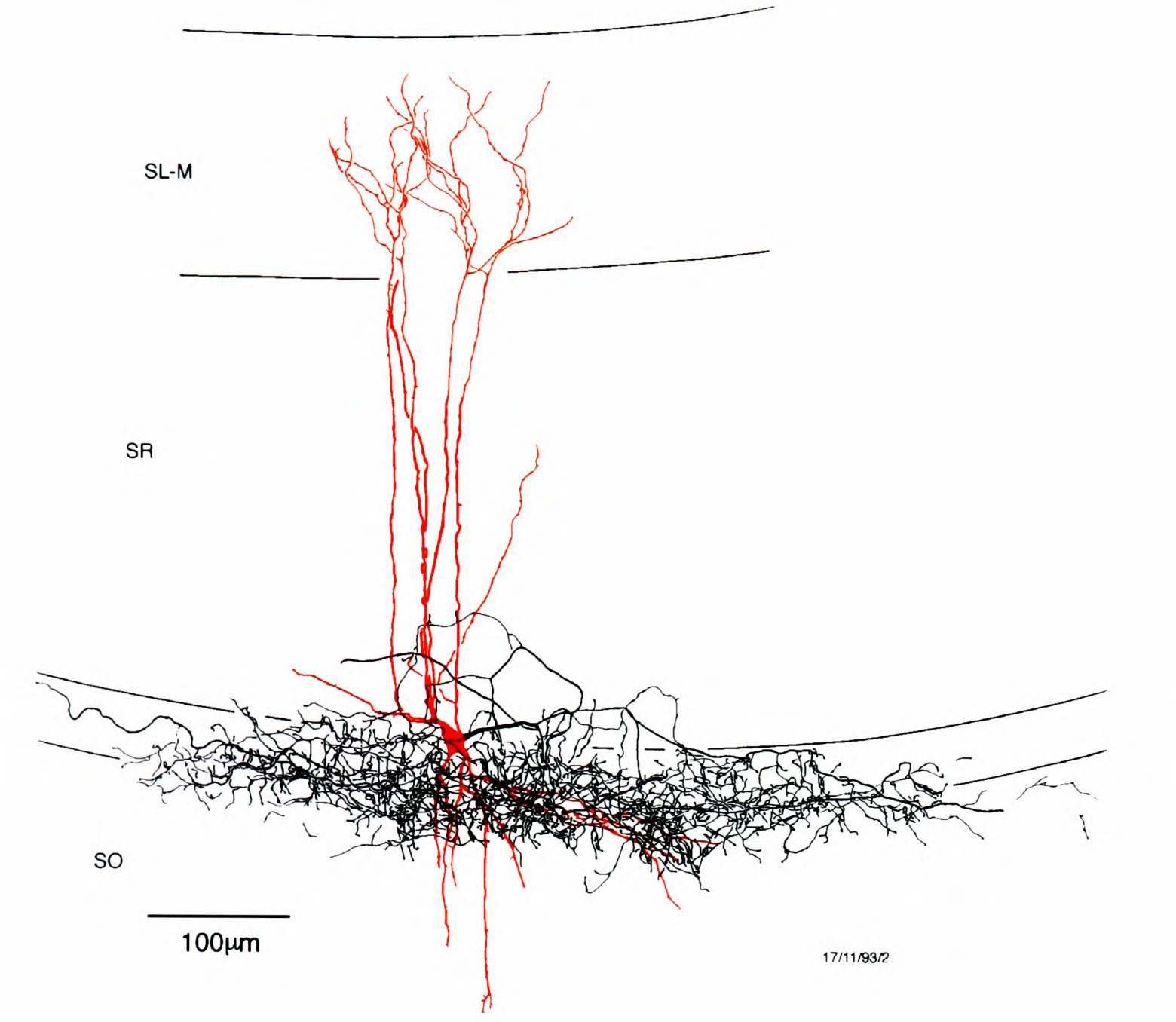

SL-M
SR
SO
100µm
17/11/93/2

Figure 3.6 Summary schematic diagram of the axonal arbourisation pattern and dendritic distribution of distinct subtypes of stratum pyramidale local-circuit interneurone in the CA1 area of the rat hippocampus. The vertical lines and filled circles represent typical laminar distribution of dendritic arbours and position of somata respectively. The hatched boxes indicate the laminar distribution of the axonal termination zone for each cell type. The lateral dimensions are not indicative of the lateral spread of dendritic and axonal arbours. On the left side the laminae of the CA1 subfield are indicated, and on the right, the main lamina-specific excitatory inputs are marked. AA, axo-axonic cell; B, basket cell; WB, wide axonal basket cell; BS, bistratified cell; SR cell, stratum radiatum-terminating cell; SL-M, stratum lacunosum-moleculare; SR, stratum radiatum; SP, stratum pyramidale; SO, stratum oriens.

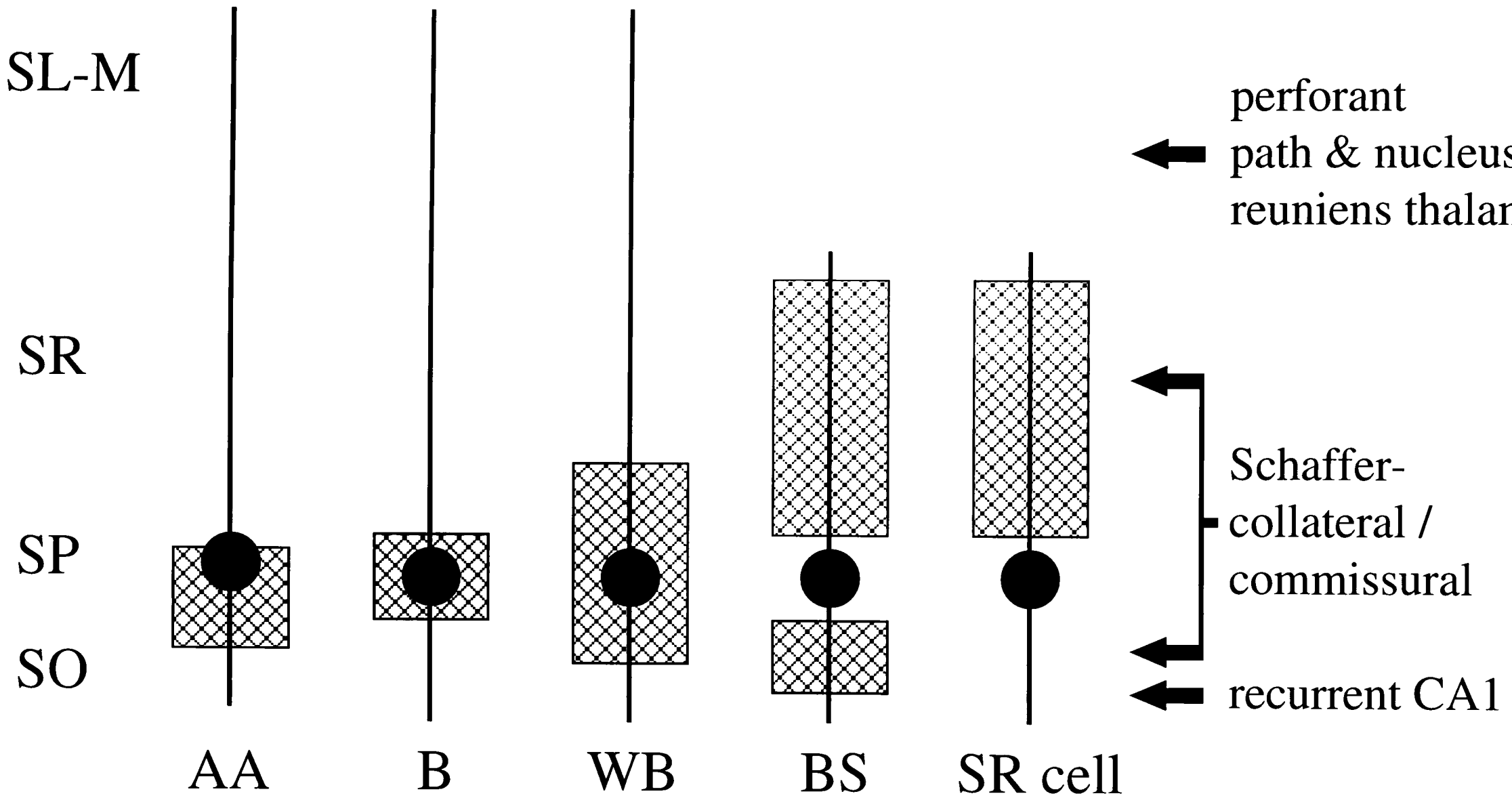

LAYER SPECIFIC
INPUT
SL-M
SR
SP
SO
perforant
path & nucleus
reuniens thalami
Schaffer-
collateral /
commissural
recurrent CA1
AA
B
WB
BS
SR cell

Figure 3.7 Electron micrographs of biocytin-filled cell axon terminals establishing synaptic junctions (arrows) with postsynaptic soma (so), axon initial segment (ais), dendritic shaft (d) and dendritic spine (sp). Presynaptic boutons (b) are readily identified by the presence of peroxidase reaction product. A-C shows labelled interneurone boutons forming type 2 (symmetrical) synapses whilst D shows a labelled pyramidal cell bouton forming a type 1 (asymmetrical) synapse. Note the widening of the extracellular space at the synaptic junctions. Presynaptic boutons in A-C originate from cell 16/09/94/2 in table 3.1, labelled bouton shown in D originates from labelled pyramidal cell 13/07/94/2P. Scale bars: A, 0.2μm; B-D, 0.5μm.

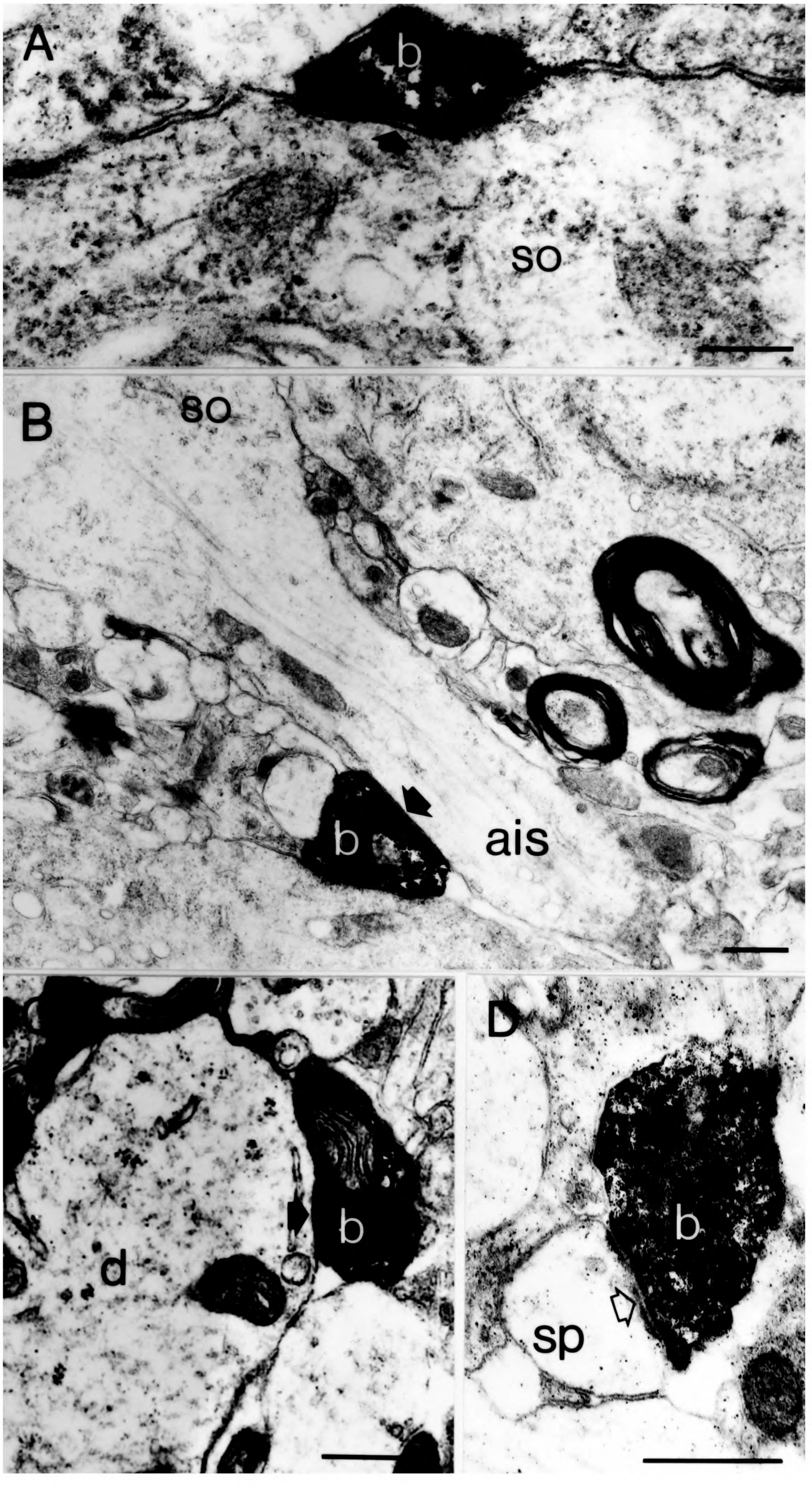
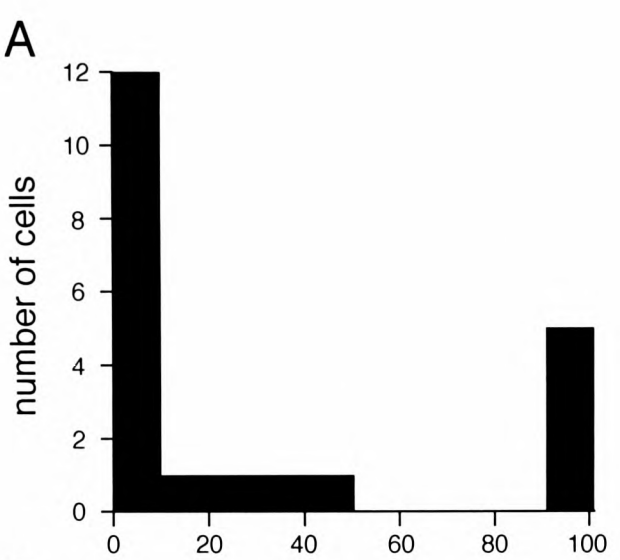
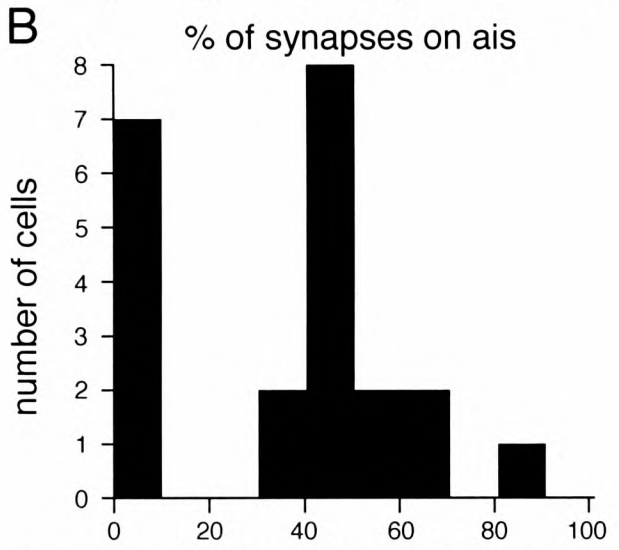
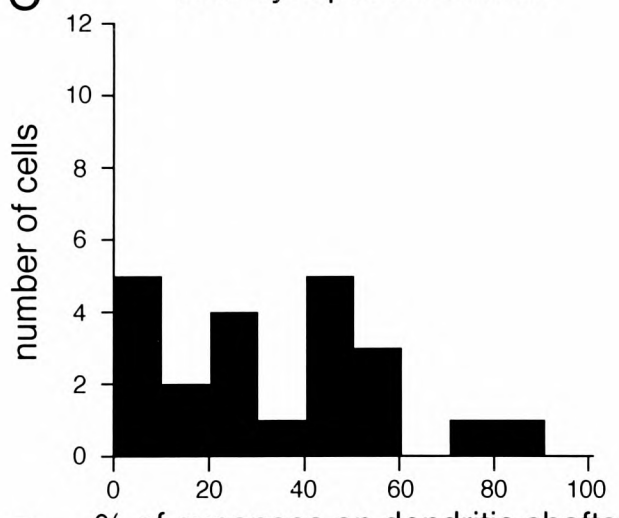

A
b
SO
B
SO
b
ais
d
b
D
b
sp

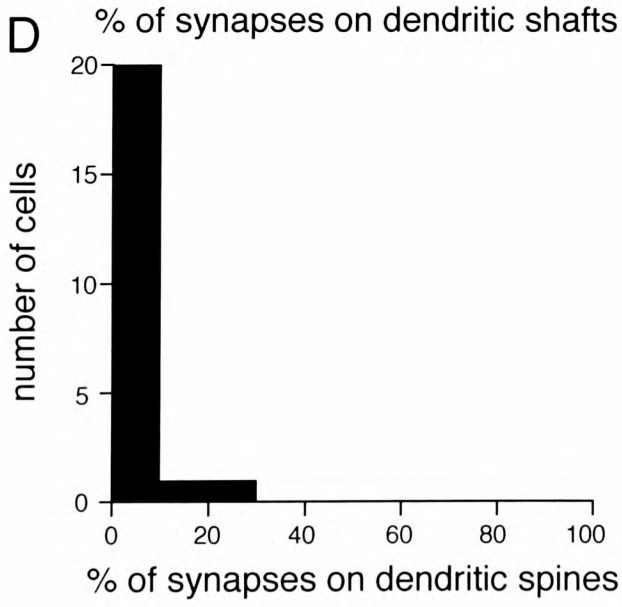
Figure 3.8 Histogram representation of postsynaptic target profiles.

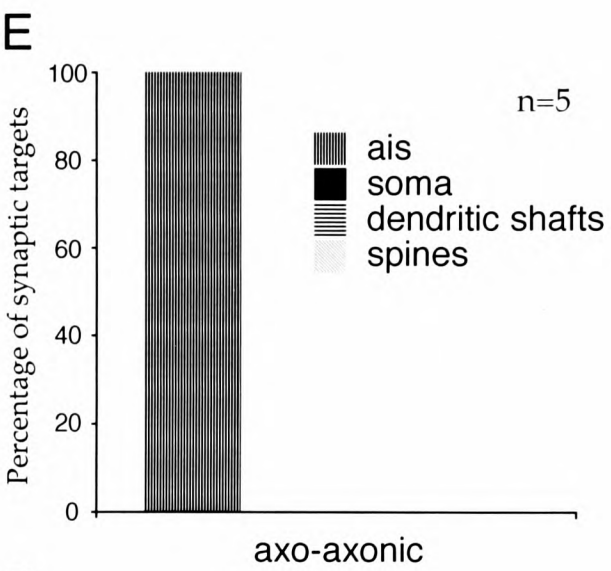
For each of the 22 cells sampled at the electron microscopic level (Table 3.1), the proportion of synaptic output onto axon-initial segments, somata, dendritic shafts and dendritic spines was represented (A-D respectively). Note that the proportion of synaptic output onto particular postsynaptic domains is not homogenous across all cells samples. Based in the selectivity of individual cells towards different combinations and proportions of postsynaptic elements, the cells could be classified into those which exclusively innervate action initial segments (axo-axonic cells, E), those which preferentially targeted soma and proximal dendritic shafts (basket cells, F), those which innervate dendritic shafts and spines (bistratified cells, G) and finally, those which showed less target selectivity and established synaptic junctions with axon initial segments, somata and dendrites (mixed cells, H).

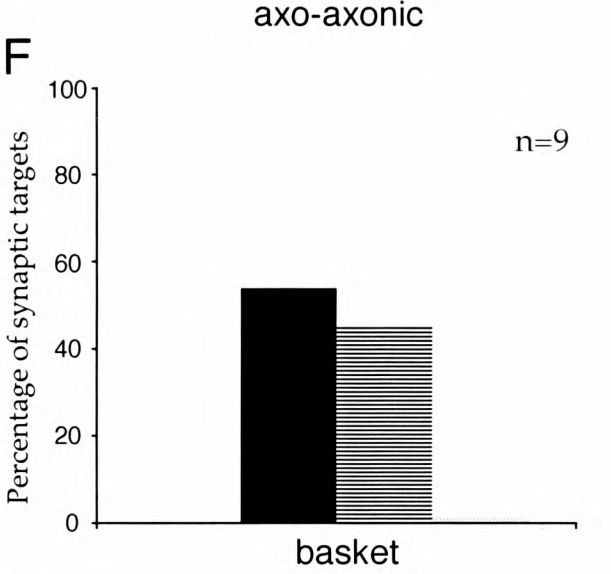

A
number of cells
% of synapses on ais

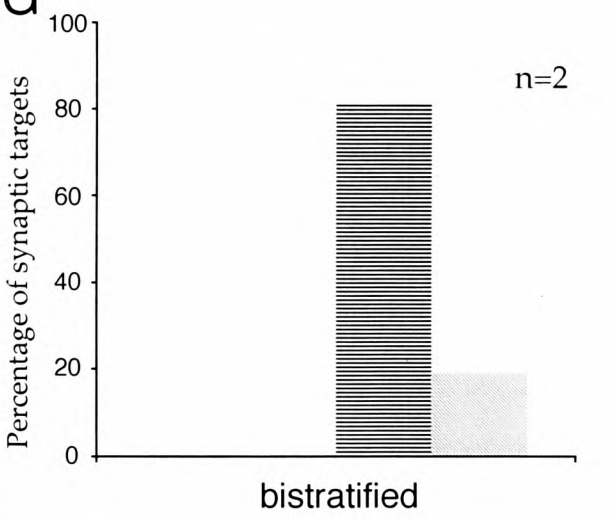

B
number of cells
% of synapses on soma


C
number of cells
% of synapses on dendritic shafts


D
number of cells
% of synapses on dendritic spines


E
Percentage of synaptic targets
n=5
ais
soma
dendritic shafts
spines
axo-axonic


F
Percentage of synaptic targets
n=9
basket


G
Percentage of synaptic targets
n=2
bistratified

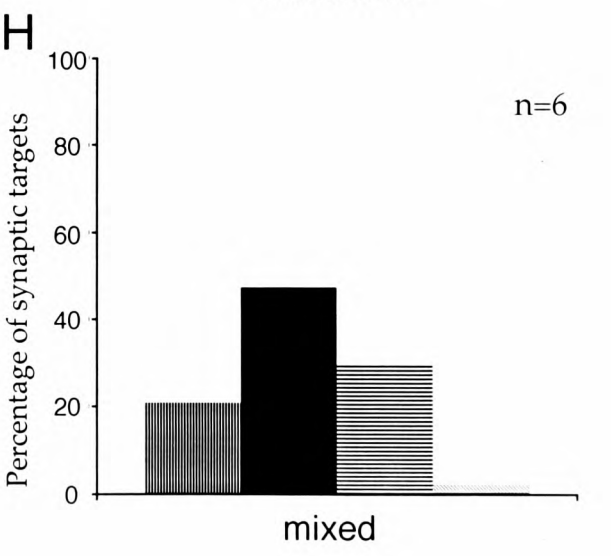
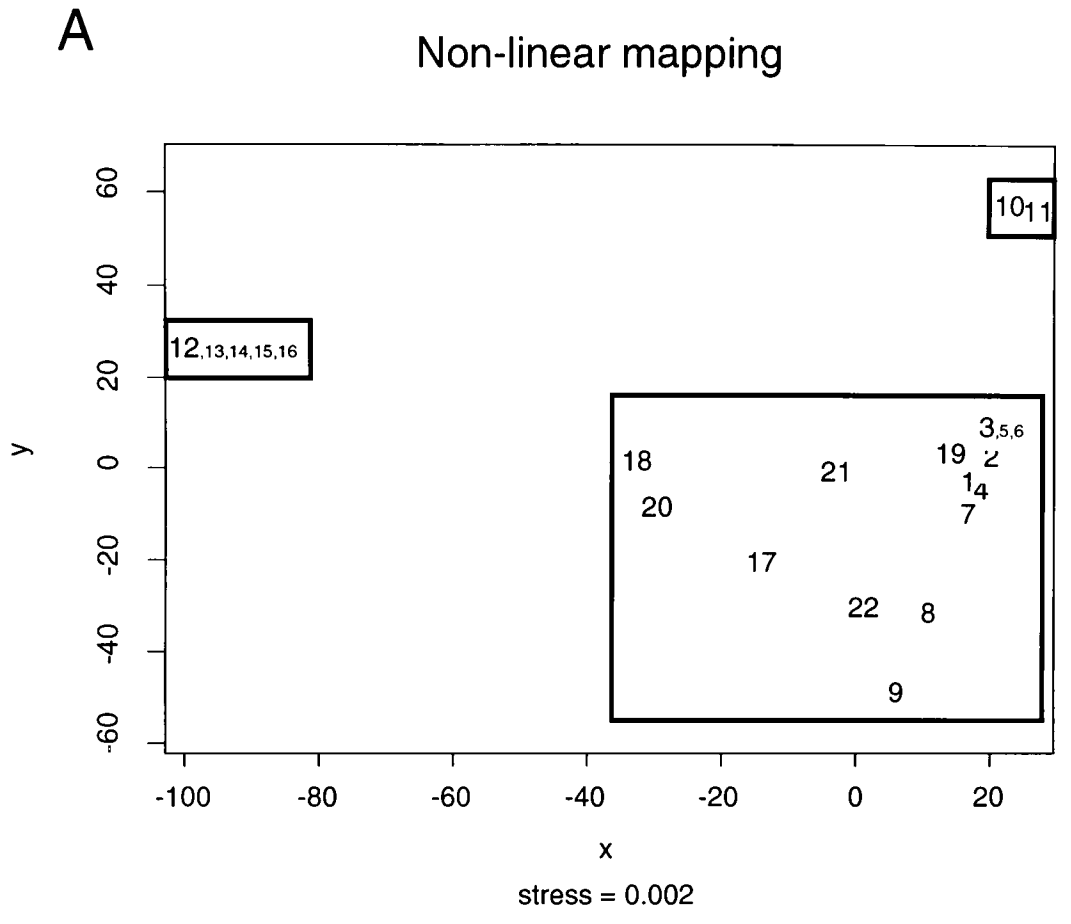

H
Percentage of synaptic targets
n=6
mixed

Figure 3.9 Two dimensional representation (non-linear) and tree matrix dendrogram of cells based on proportion of synaptic output onto each of 4 postsynaptic target structures. Each of the twenty two cells in table 3.1 was represented in a 4 dimensional matrix form (see text) which were then mapped in an x-y plot (A). The plot shows three discrete clusters (boxes) which correspond to the axo-axonic cells (12-16), bistratified cells (10, 11) and basket / mixed cells (1-9, 17-22). Where more than one cell was projected onto a single position in the plot (i.e. cells had identical efferent target profile), their position is indicated by the first (large) number, the preceding numbers (small script) indicating the other cells which lay at the same point. (B) The same data represented in hierarchical form as a dendrogram. The numbers indicate cells shown in table 3.1. The first branch separates the axo-axonic cells form the bistratified, basket and mixed cells, whist the second branch separates the bistratified cells from the basket and mixed cells. Note that subsequent branches fail to separate the basket cells from the mixed cells. Scales indicates terms of dissimilarity.

A


Non-linear mapping
y
x
60
40
20
0
-20
-40
-60
-100
-80
-60
-40
-20
0
20
10 11
12,13,14,15,16
3,5,6
19
2
18
21
1
4
20
7
17
22
8
9
stress = 0.002

B

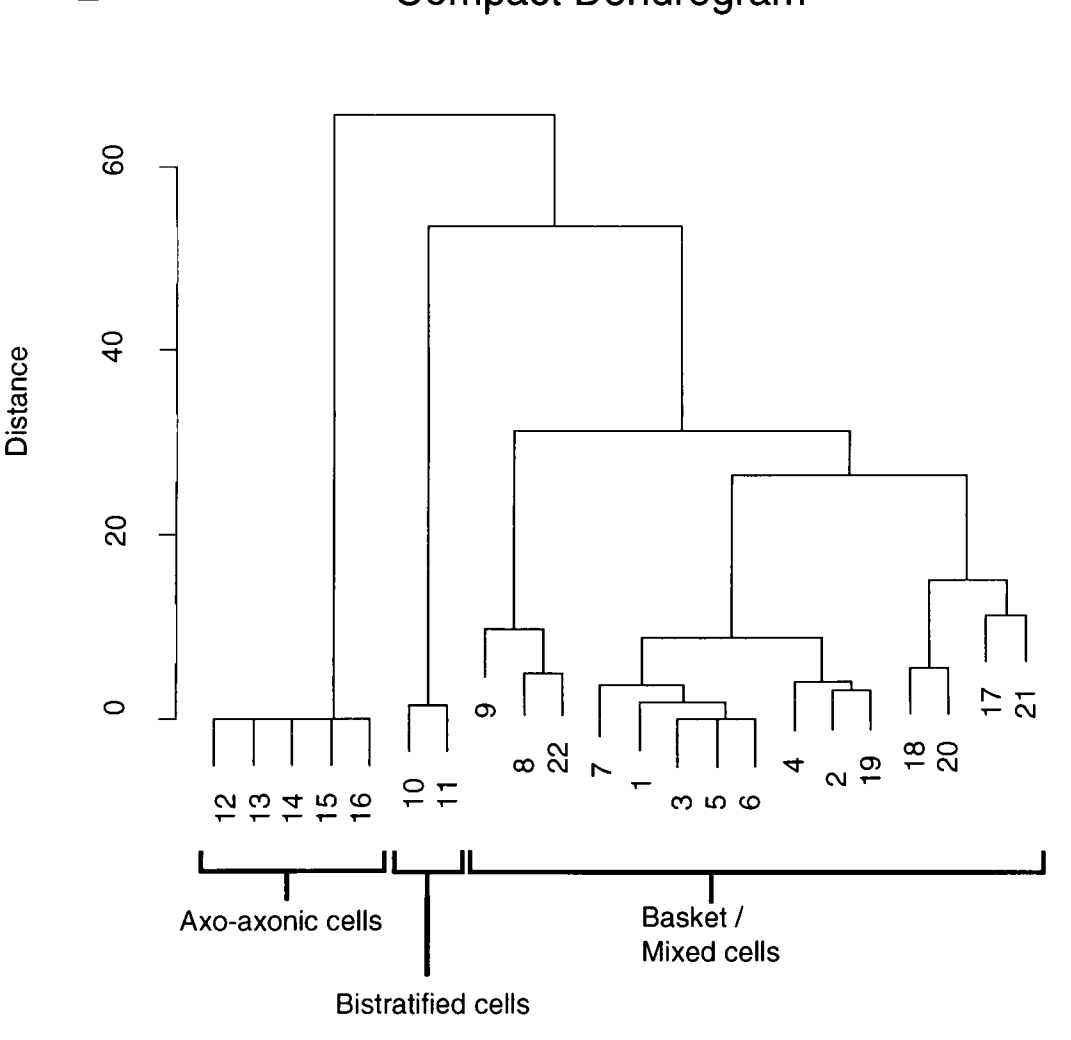
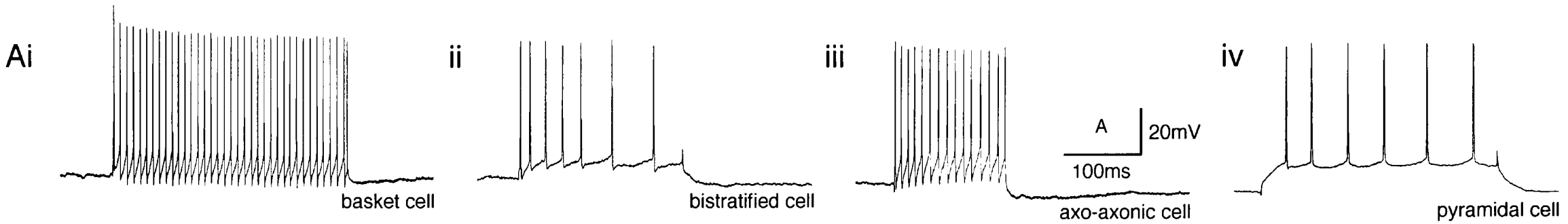
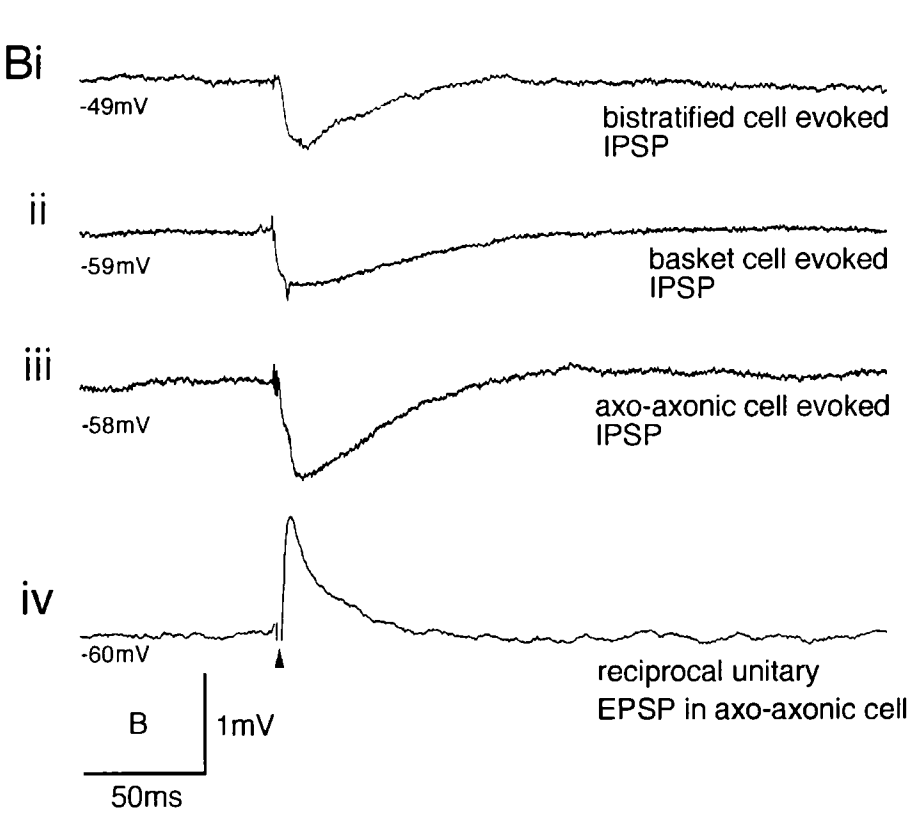
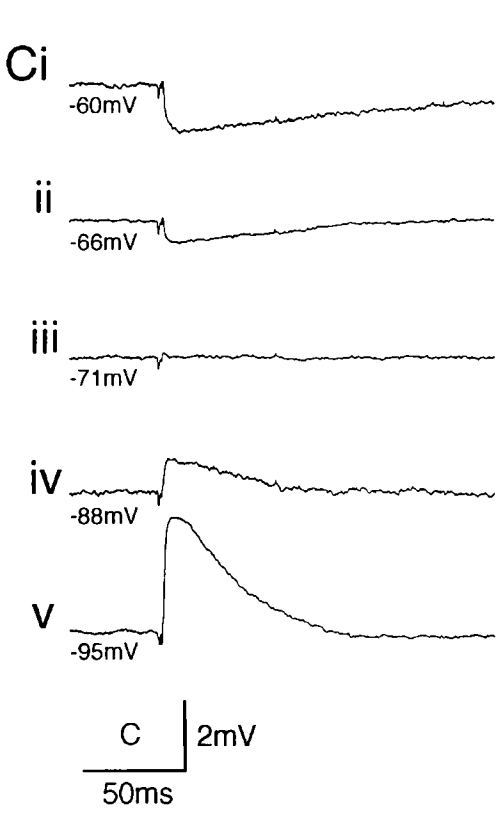

Compact Dendrogram
Distance
60
40
20
0
12
13
14
15
16
10
11
9
8
22
7
1
3
5
6
4
2
19
18
20
17
21
Axo-axonic cells
Bistratified cells
Basket /
Mixed cells

Figure 3.10 Characteristic firing properties of CA1 local-circuit neurones and their unitary responses evoked in pyramidal cells.

(A) Shows firing patterns in basket (i), bistratified (ii), axo-axonic cells (iii) and for comparative purposes, a pyramidal cell (iv). Note that the firing of basket and axo-axonic cells are generally non adapting or weakly adapting whereas bistratified and pyramidal cell action potentials are generally more strongly adapting. The main action potential parameters and membrane properties for each cell type are summarised of table 3.2. (B) Action potentials evoked in bistratified (i), basket (ii) and axo-axonic cells (iii) elicit unitary hyperpolarising IPSPs in simultaneously recorded pyramidal cells. In turn, action potentials evoked in a CA1 pyramidal cells elicit a fast EPSP in a simultaneously recorded and reciprocally connected axo-axonic cell (iv). (C) An example of the voltage dependence of basket cell-evoked IPSPs in a synaptically coupled pyramidal cell. Note that as the cell is hyperpolarised from -60mV to -95mV, the amplitude decreases and then reverses. These data area illustrated graphically in D, where IPSP amplitude is plotted against membrane potential showing a linear relationship ($R= 0.989$, least mean square method; $P < 0.01$, Pearson's R table). All synaptic responses shown are averages >50 sweeps.


Ai
basket cell
ii
bistratified cell
iii
A
20mV
100ms
axo-axonic cell
iv
pyramidal cell


Bi
-49mV
bistratified cell evoked IPSP
ii
-59mV
basket cell evoked IPSP
iii
-58mV
axo-axonic cell evoked IPSP
iv
-60mV
reciprocal unitary EPSP in axo-axonic cell
B
1mV
50ms


Ci
-60mV
ii
-66mV
iii
-71mV
iv
-88mV
v
-95mV
C
2mV
50ms

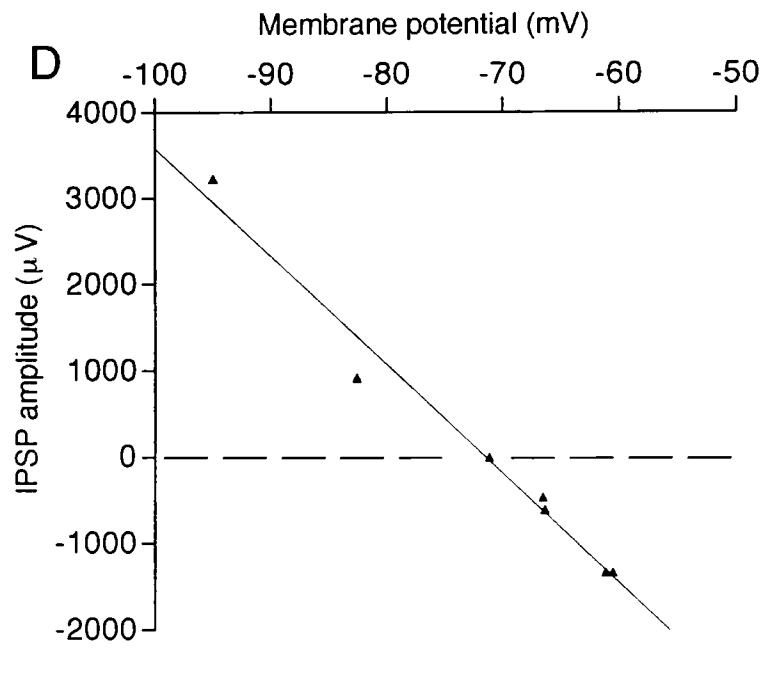

D
Membrane potential (mV)
-100
-90
-80
-70
-60
-50
4000
3000
2000
1000
0
-1000
-2000
IPSP amplitude (μV)

Table 3.1 Segregation of cell types based on efferent synaptic target profile.

TABLE 3.1 Segregation of cell types based on efferent synaptic target profile

Interneurone type	Overall random synaptic target pattern							
	soma		dendrite		spine		AIS*	
Basket cells	n	%	n	%	n	%	n	%
16/11/93/4	29	48	30	49	2	3	0	0
03/06/94/2	5	45	6	55	0	0	0	0
16/06/94/3	5	50	5	50	0	0	0	0
20/06/94/1	10	40	14	56	1	4	0	0
05/07/94/1	5	50	5	50	0	0	0	0
15/07/94/1	5	50	5	50	0	0	0	0
23/11/94/1	7	54	6	46	0	0	0	0
05/12/94/1	16	70	7	30	0	0	0	0
15/12/94/1	5	83	1	17	0	0	0	0
mean		**54**		**45**		**1**		**0**
Bistratified cells								
30/11/94/1	0	0	8	80	2	20	0	0
07/06/95/1	0	0	9	82	2	18	0	0
mean		**0**		**81**		**19**		**0**
Axo-axonic cells								
01/11/93/1	0	0	0	0	0	0	10	100
08/07/94/1	0	0	0	0	0	0	12	100
13/07/94/2	0	0	0	0	0	0	11	100
29/11/94/1	0	0	0	0	0	0	11	100
13/12/94/1	0	0	0	0	0	0	11	100
mean		**0**		**0**		**0**		**100**
Mixed cells								
02/11/93/5	5	56	2	22	0	0	2	22
17/11/93/2	8	36	5	23	0	0	9	41
19/05/94/3	9	43	11	52	0	0	1	5
10/06/94/1	7	41	3	18	1	6	6	35
12/07/94/1	10	42	9	38	1	4	4	16
16/09/94/2	8	67	3	25	0	0	1	8
mean		**47.5**		**29.5**		**2**		**21**

AIS* - axon initial segment

Table 3.2 Summary of morphological and physiological features of basket, bistratified cells and axo-axonic cells in the CA1 area.

This table summarises the key anatomical features, synaptic target profile, passive membrane properties, action potential properties and properties of evoked responses in synaptically coupled pyramidal cells. Other that the electron microscopically determined postsynaptic target profile, no one feature can reliably distinguish cell types. However, there are a number of distinguishing features* which do show subtle differences between cell types and which may be useful as indicators.

TABLE 3.2 : Summary of morphological and physiological properties of basket, bistratified and axo-axonic cells in area CA1 of the rat hippocampus

Anatomy	**Basket cells**	**Bistratified cells**	**Axo-axonic cells**
dendrites			
- location*	all layers	all layers except SL-M	all layers, tuft in SL-M
- appearance	aspiny / varicose	aspiny / varicose	aspiny / varicose
Axon			
- location*	SP (mainly)	SO / SR	SP / SO
- targets*	soma / proximal dendritic shafts	dendritic shafts / spines	axon initial segments
Physiological properties			
Input resistance (MΩ)	51.3±25.9	63.9±55.8	86.0±36.8
Time constant (ms)	13.7±9.8	16.3±6.6	12.9±2.2
Action potential - amplitude (mV)	58.0±7.1	49.5±7.8	54.8±5.8
- duration (ms)*	0.37±0.13	0.78±0.15	0.57±0.15
Spike frequency adaptation	weak / variable	moderate / variable	weak / variable
Fast after-hyperpolarisation	present	present	present
Postsynaptic effect	fast IPSP (n=10)	fast IPSP (n=3)	fast IPSP (n=5)
Average amplitude (μV)	577±402 at -59.0±3.6mV	933±250 at -56.6±10.8mV	396±215 at -54.0±4.7mV
10-90% Rise time (ms)	5.1±4.9	9.7±5.5	4.2±2.4
Duration at half-amplitude(ms)	46.2±37.9	48.6±20.7	24.6±7.5
Decay τ (ms; single exponential)	28.4±10.4	52.4±19.3	23.5±5.0

* key distinguishing features

Chapter 4. Properties of unitary IPSPs evoked by anatomically identified basket cells in the rat hippocampus

4.1 Introduction

Hippocampal interneurones were recognised early as the major source of locally generated inhibition which is exerted on excitatory principal cells (Andersen et al., 1963; 1964a, b). Far from being homogeneous, these γ-aminobutyric acid (GABA) releasing local-circuit neurones show great diversity with respect to their content of various neurochemical markers, expression of neurotransmitter receptors and their afferent and efferent connections (see chapter 1). As is evident from the previous chapter, local-circuit interneurones in the hippocampal CA1 area whose cell bodies are restricted to stratum pyramidale may differ markedly with respect to both their dendritic and axonal distributions. Although the connectional rules of inhibitory microcircuits are gradually emerging in parallel with the advent of sophisticated techniques, the functional role of specific GABAergic mechanisms is far from being understood.

A major technical advance for investigating possible roles of interneurones was made by employing double recording techniques to reveal the postsynaptic effect of a single inhibitory neurone on a monosynaptically coupled principal cell (Knowles and Schwartzkroin, 1981; Miles and Wong, 1984, 1987; Lacaille et al., 1987; Lacaille and Schwartzkroin, 1988b; Miles, 1990; Scharfman et al., 1990). As it is not possible to recognise different classes of GABAergic interneurones unambiguously on physiological grounds (Buhl et al., 1996), intracellularly recorded neurones must be therefore identified anatomically to ascertain their identity on the basis of their efferent connections (Han et al., 1993; Gulyás et al., 1993a; Buhl et al., 1994a, b). Moreover, the synaptic effect of different cell types is determined not only by the location, but also by the number of synaptic release sites. Thus the anatomical characterisation of connections which mediate unitary interactions between synaptically coupled pairs of neurones can reveal the role of

structural differences which may shape postsynaptic responses (Korn et al., 1982; Gulyás et al., 1993a; Buhl et al., 1994a).

The previous chapter introduced several classes of local-circuit interneurone which were identified in the hippocampal CA1 area by an intracellular labelling study and demonstrated the postsynaptic effects they mediate. This chapter describes a more detailed investigation into the synaptic actions for one class of CA1 interneurone - the *basket cell.*. As before, dual intracellular recordings were made with biocytin containing microelectrodes from synaptically connected inhibitory and pyramidal cell pairs in subfields CA1 and CA3 of the rat hippocampus. However, subsequent physiological analysis was restricted to the category of cells which had an efferent target profile of predominantly somatic and proximal dendritic synapses.

4.2 Materials and methods

Young adult female Wistar rats (<150g) were used. Detailed description of the preparation of hippocampal slices, electrophysiological recording, biocytin labelling, and the subsequent correlated light and electron microscopic methods are given in chapter 2. Putative interneurones were identified using previously established physiological criteria (Knowles & Schwartzkroin, 1981). When a stable recording was obtained, a search was made for synaptically coupled cells displaying the properties of hippocampal principal cells. The putative interneurone was made to fire by depolarising current injection and synaptic coupling tested using on-line spike-triggered averaging. Capacitive coupling was eliminated on-line using a modified axoprobe amplifier (section 2.2). Diffusion of biocytin during recordings generally resulted in adequate filling. Slices were processed for light and electron microscopy as described (sections 2.3.1 and 2.3.3). Electron microscopy was carried out at Jozsef Attila University, Szeged, Hungary in collaboration with Dr K. Halasy.

4.3 Results

4.3.1 Physiological properties of pre- and postsynaptic cells

The data presented below is based on a total of 14 physiologically as well as anatomically identified basket cells (cell numbers 1-6, 8-9, 11, 18, 22, 16, 40, 44 on table 2.1) which elicited unitary IPSPs in 24 pyramidal cells, the discrepancy of numbers being due to the fact that in several instances paired recordings were obtained between a single presynaptic neurone and several successively recorded principal cells. No attempt was made to precisely determine the number of paired recordings without obvious signs of synaptic coupling. On a subjective basis however, it appeared that the overall proportion of inhibitory interactions was relatively high, in the range between 20 - 50%, once a stable recording had been

obtained from a cell which displayed the physiological properties of an, as yet morphologically unidentified, interneurone.

Basket cells had a mean resting membrane potential of -64.0 ±5.5 mV and non-overshooting action potentials with an amplitude of 60.0 ±8.0 mV, whereas pyramidal cells had a slightly less negative resting membrane potential of -61.0 ±5.4 mV and overshooting action potentials (73.9 ±6.4 mV). The average action potential duration of basket cells (0.376 ±0.118 ms) was considerably shorter than in pyramidal cells (0.948 ±0.179 ms). Basket cells had a mean input resistance of 48.1 ±31.6 MΩ vs. 58.2 ±19.0 MΩ in pyramidal cells and a mean time constant of 11.2 ±8.2 ms which was shorter than that of pyramidal cells (15.9 ±3.7 ms). When the physiological properties of pre- and postsynaptic cells were compared with a non-parametric statistical test (Mann-Whitney U-test), three parameters were found to be significantly different, membrane time constant ($p < 0.02$), action potential amplitude ($p < 0.0005$) and action potential duration ($p < 0.0001$). In contrast, resting membrane potential and input resistance did not differ significantly ($p > 0.05$).

In contrast to the obvious differences between basket and pyramidal cell properties it must be emphasised that it was not feasible to discriminate reliably, on physiological grounds, between the different types of local-circuit neurone which reside in the pyramidal cell layer of area CA1 (Buhl et al., 1996). Stringent anatomical verification was therefore considered essential and recordings without adequate morphological recovery (for criteria see below) were therefore not analysed.

4.3.2 Anatomical definition of CA1 basket cells

Throughout much of the literature it appears that the term 'basket cell' is frequently used as a rather ill-defined denominator for a variety of GABAergic local-circuit neurones which reside in and around the cell body layer of the

hippocampus. Intracellular labelling of these neurones has however revealed that they generally fall into fairly well defined categories, largely determined by the target selectivity of their axonal output (e.g. Somogyi et al., 1983a, 1985; Halasy and Somogyi, 1993; Han et al., 1993; Buhl et al., 1994a). Basket cells, as originally described by Ramon y Cajal (1893) and Lorente de No (1934), have much of their axon confined to the principal cell layer and its immediate surround. The terminal branches of *several* such cells may form pericellular 'baskets' around the somata of principal cells. However, since axo-axonic cells in Ammon's horn (Somogyi et al., 1985; Gulyás et al., 1993a; Buhl et al., 1994b) may have a similar axonal arborization pattern, more stringent criteria were therefore required to unambiguously identify particular classes of local-circuit cells (Somogyi et al., 1983a, 1985; Halasy and Somogyi, 1993, Gulyás et al., 1993a). In the present study basket cells were thus more rigorously defined as *GABAergic interneurones with a synaptic target profile enriched in somatic contacts* (>30%). In this respect, basket cells differ from other local-circuit neurones, for example axo-axonic or bistratified cells, which very rarely terminate on principal cell bodies (Buhl et al., 1994a).

4.3.3 Morphological features of basket cells

Biocytin labelled basket cells in the Ammonic subfields gave rise to several primary dendrites that dichotomously branched into secondary and tertiary processes which fanned out into the strata radiatum and lacunosum-moleculare as well as oriens (Figure 4.2). Most of the dendrites were predominantly smooth and beaded, only rarely displaying a few spines. Provided the cells were sufficiently well labelled (10 of 14 cells), most of the apical dendrites could be traced into the stratum lacunosum-moleculare but rarely branched there, thus differing from axo-axonic cells which frequently form a prominent apical tuft (Li et al., 1992; Buhl et al., 1994b). As a general feature, basket cell basal dendrites deeply invaded the

alvear white matter, thus differing from concomitantly recorded pyramidal cells which have their basal dendrites predominantly contained within stratum oriens.

The axon of basket cells usually emerged from the cell body and ascended into the stratum radiatum, where it branched repeatedly into several major, frequently myelinated (data not shown) branches which then proceeded along the cell body layer. After successive further branching, preterminal and terminal axons then formed a dense meshwork of fibres criss-crossing the cell body layer and proximal regions of the strata radiatum and oriens. In the light microscope, varicose axons frequently appeared to be wrapped around unlabelled cell bodies and/or followed the initial portion of the proximal apical dendrites. The proximal apical dendrite seemed to be a preferred site of termination, as evident from the accumulation of varicose branches at the border of strata radiatum and pyramidale (Figures 4.2). What has been described in Golgi studies as "pericellular nests or baskets" is rarely evident, as this peculiar phenomenon may be attributed to the bulk impregnation of up to 25 individual basket cell axons, which were recently estimated to converge on a single postsynaptic cell (Buhl et al., 1994a).

4.3.4 Postsynaptic targets of basket cells

Postsynaptic recordings which displayed the physiological properties of principal cells could be invariably allocated to an individually labelled or a cluster of biocytin filled pyramidal cells. In 6 instances, a single pyramidal cell could be unequivocally matched with the placement of the second microelectrode, whereas this proved to be impossible for the remainder of cases. To some extent, the occurrence of multiple labelling could be attributed to the fact that during the course of the experiment several neurones with the characteristics of pyramidal cells had been impaled in succession. In the remainder of cases, however, a cluster of 2-4 pyramidal cells was recovered, even when only one postsynaptic cell had been recorded. In the absence of any obvious electrical coupling, this form of multiple labelling was therefore interpreted, in agreement with previous reports, as resulting

from the diffusion and/or uptake of biocytin into adjoining cells which had been damaged by the recording electrode (Gulyás et al., 1993a; Buhl et al., 1994b).

In the electron microscope, biocytin labelled basket cell boutons were readily discernible due to their content of an opaque reaction product (see chapter 3, Figure 3.7). Vesicle-containing terminals were followed in serial electron microscopic sections to determine their postsynaptic targets. Synaptic junctions were identified on the basis of the rigid apposition of pre- and postsynaptic membrane, the widening of extracellular space at the synaptic cleft, the slightly electron-dense cleft material, the presence of presynaptic vesicles and, finally, the postsynaptic density, when detectable. All basket cells made type 2 (symmetrical) efferent synapses (Gray, 1959; Blackstad and Flood 1963). Electron microscopic analysis of a random sample of basket cell synaptic junctions (n = 282) showed that they predominantly targeted cell bodies (48.2%) and proximal dendrites (45%) in roughly equal proportions. In contrast, axon initial segments (3.2%) and spines (3.6%) formed a relatively minor proportion of postsynaptic targets (for details see table 4.1). Whenever a single postsynaptic pyramidal cell had been recovered (n=6), the cell body and proximal dendrites were enmeshed in a tangle of basket cell axon. Without exception, light microscopical estimates revealed *several* sites of close membrane apposition between basket cell terminals and postsynaptic target. A precise prediction however proved to be impossible because, for example, portions of the basket axon were visually occluded by the opaque pyramidal soma.

4.3.5 Properties of unitary basket cell-mediated IPSPs

To determine the parameters of unitary IPSPs, presynaptic cells were made to fire single action potentials (Figure 4.1C) by means of either depolarising constant or pulsed current injection at frequencies near 1 Hz. In view of the inherently low signal/noise ratios, postsynaptic responses were averaged prior to measurements (Figures 4.1D, E). Moreover, postsynaptic cells were frequently

depolarised with constant depolarising current to increase the magnitude of the effect.

At an average membrane potential of -57.8 ±4.6 mV unitary IPSPs had a mean amplitude of 450 ±238 μV (n=23), ranging from 124 to 919 μV. The events had a 10-90% rise time of 4.6 ±3.2 ms (n=18) and, measured at half-amplitude, a mean duration of 31.6 ±18.2 ms (n=22). Generally larger effects tended to have longer rise-times and durations. In most instances (n=19) the decay phase of unitary IPSPs could be adequately fitted with a single exponential function (Figure 4.1E) with a mean time constant of 32.4 ±18.0 ms. Likewise, single exponentials were fitted to the decay phase of averages of small (-0.1 nA) current pulses delivered through the recording electrode. With one exception, the injected currents decayed with shorter time constants (20.5 ±9.5 ms) when compared to the respective IPSPs elicited in the same cells. This difference was statistically significant (Mann-Whitney U-test; $p<0.025$).

4.3.6 Voltage dependence and conductance of unitary IPSPs

In all cells tested (n=5) amplitudes of averaged IPSPs decreased at more hyperpolarised membrane potentials (Figure 4.3A). The relationship between membrane voltage and IPSP amplitudes was approximately linear (Figure 4.3B). Therefore, linear regression was employed to calculate the point of response reversal which, on average, was -74.9 ±6.0 mV (n=5). In this respect, it should however, be emphasised that this correlation may only hold for the range of membrane potentials investigated, as previous work indicates increasing non-linearities beyond the point of response reversal (Collingridge et al., 1984; Miles, 1990).

Under current clamp recording conditions, an estimate of the *average* IPSP conductance G_{IPSP} may be obtained using a procedure originally derived from Ginsborg (1973) and subsequently adopted by others (for details see Miles and

Wong, 1984; Benardo, 1994). In brief, using the experimentally determined values for input resistance and the slope of the IPSP-amplitude/membrane voltage relationship (Figure 4.3B) the mean unitary IPSP conductance was estimated to be 0.95 ± 0.29 nS, ranging from 0.52 to 1.16 nS.

4.3.7 Receptor pharmacology of unitary IPSPs

The pharmacological profile of unitary basket cell IPSPs was investigated in 3 instances. Before drug application, the control IPSPs (ranging from 141 to 476 μV) were monitored for a 10 min. period to ascertain that they remained stationary (Figure 4.3Cb). Throughout the entire procedure presynaptic cells were made to discharge at 1 Hz and the pyramidal cell membrane potentials were manually adjusted with small DC current injections to remain constant, generally not deviating in excess of ±1 mV. Initially, the slices were superfused with a mixture of the non-NMDA receptor antagonist CNQX (5 or 10 μM) and NMDA receptor antagonist AP5 (30 μM; Figure 4.3Cc). In the presence of the excitatory amino acid blockers, the responses showed a small but consistent increase in amplitude (8.3 ±2.5% change of *normalised* amplitudes). Following addition of the $GABA_B$ receptor antagonist CGP 35845A (1 μM [n=1] or 4 μM [n=2]) to the bath, a further average increase of 26.3 ±19.9% of the normalised mean IPSP amplitudes was observed. It is however noteworthy that the increase in response amplitude was largely confined to 2 cells (37.5%[33% & 42%]), whereas in the third example the monitored increase (4%; Figures 4.3Cd, f) was marginal. In all instances, superimposition of the traces obtained in the presence of the excitatory amino acid blockers and following addition of the $GABA_B$ receptor antagonist revealed that the decay of the averaged IPSPs remained virtually unchanged (Figure 4.3Cf). Finally, addition of bicuculline (10 or 13 μM) reduced the amplitude to 15.5 ±3.1% of the response obtained in the presence of excitatory amino acid blockers. Neuronal input

resistances (all cells >40 MΩ) were monitored throughout and showed only minor fluctuations.

4.3.8 Summation of IPSPs and use-dependent depression

High frequency trains of presynaptic discharge (Figure 4.4Aa) invariably resulted in an initial summation of the postsynaptic response (n=5; Figures 4.4Ab, c). Up to four IPSPs were effective in approximately doubling the amplitude of single action potential triggered events. The first IPSP usually resulted in the largest amplitude increase, whereas the contribution of successive events decreased. Then, despite maintained presynaptic activity, the response remained stationary, until it gradually declined and eventually reached a steady-state level (Figure 4.4Ab).

The phenomenon of frequency-dependent tonic depression was further investigated at lower presynaptic firing rates. The results illustrated in Figures 4.4Bb and Bc indicate that presynaptic firing rates in the range of 1 Hz may already result in a depression of the postsynaptic response. In both the examples illustrated (Figures 4.4B, C) an approximately 10 fold increase of the presynaptic firing rate resulted in a >50% reduction of the IPSP amplitude (Figures 4.4Be, Cd). For the cell shown in figure 4.4C this effect could be antagonised in the presence of 5μM CNQX and 30μM AP5 by bath applying 1μM of the $GABA_B$ antagonist CGP 55845A (Figure 4.4D).

4.3.9 Reliability of unitary IPSPs

The amplitudes of unitary IPSPs appeared to fluctuate at all connections tested, although much of the intrinsic variability of the signal may have been due to the superimposition of recording noise. However, superimposition of successive events clearly indicated a low number or complete absence of release failures

(Figures 4.5B, C) although the amplitude of individual events seemed to fluctuate around the average of the postsynaptic response (Figures 4.5B, D).

4.3.10 Postinhibitory facilitation and rebound action potentials

When elicited by single action potentials or brief bursts of basket cell discharge, the averaged postsynaptic response of 4 pyramidal cells was followed by a distinct depolarising overshoot, here referred to as postinhibitory facilitation. The respective IPSPs had a mean amplitude of 414 ±344 μV and were followed by a depolarising wave which, on average, went 210 ±219 μV above the pre-event baseline level. When measured from single action potential elicited averages, the humps attained their maximum positivity at 130 ± 33 ms after the presynaptic action potential.

All postsynaptic cells had overshooting action potentials and appeared to be, in physiological terms, healthy cells (mean action potential amplitude 77 ±7 mV; input resistance 51 ±19 MΩ). Interestingly, all cells which displayed postinhibitory action potentials had been depolarised to membrane potentials close to firing threshold (-54.4 ±1.6 mV) and were seen to sporadically discharge action potentials. Perhaps due to the limited sample size, the difference in membrane potential of basket cell effects with versus those without a depolarising hump (-59 ±4.6 mV) was statistically not significant (Mann-Whitney U-test; p=0.088).

Averages of postsynaptic effects such as the one shown in Figure 4.6B were obtained by excluding sweeps which were contaminated by action potentials. Subsequently a complementary approach was adopted by excluding from a string of *successive* sweeps all events when the hump was subthreshold and additionally only those, where the pyramidal cell discharge *preceded* the basket cell action potential by less than 70 ms. When superimposing the remaining events it is apparent that the distinctive clustering of pyramidal cell action potentials is highly

non-random and appears to temporally coincide with the occurrence of post-inhibitory facilitation (Figure 4.6C, E).

4.4 Discussion

4.4.1 Identification of pre- and postsynaptic neurones

There is a general consensus across the literature that it is possible to discriminate hippocampal GABAergic local-circuit neurones due to their distinctive firing properties, such as short-duration action potentials, fast membrane time-constants, non-accommodating firing pattern. The results presented above for one subclass, the basket cells, are clearly in support of this notion, as every presumed interneurone was 1/ shown to elicit short-latency GABAergic IPSPs in postsynaptic principal cells 2/ light microscopically identified as a smooth dendritic non-pyramidal cell 3/ shown by electron microscopy to establish symmetrical synaptic contacts predominantly with the somata and proximal dendrites of their respective postsynaptic target cells. It is equally clear however that membrane and firing properties of basket cells are an insufficient criterion to discriminate them from several other types of GABAergic interneurones. Amongst those are axo-axonic cells, which have relatively few distinctive physiological features, such as spike doublets, that would allow their unequivocal discrimination from hippocampal interneurones that reside within or close to the hippocampal cell body layers (Buhl et al., 1994b). It is noteworthy however that this notion of similarity in membrane and firing properties does not necessarily apply to all hippocampal interneurones, as, for example, stratum lacunosum moleculare interneurones do not belong to the physiologically defined group of fast-spiking cells (Kawaguchi and Hama, 1988; Lacaille and Schwartzkroin, 1988a,b)

Therefore, the apparent similarity of interneuronal membrane and firing properties is a relatively poor indicator of their connectional heterogeneity. Consequently, until better discriminatory features can be routinely exploited in

conjunction with intracellular recording experiments, morphological identification of cells remains a necessity when addressing the specific roles of hippocampal interneurones. Moreover, the occasionally deceiving similarity of basket and chandelier cell axonal arbours at the light microscopical level strongly warrants the identification of the different cell types at the electron microscopic level by virtue of their distinctive synaptic target profiles. It appears however, that the dendritic arborizations of basket and axo-axonic cells in the CA1 area are sufficiently distinct to predict the efferent synaptic targets of the respective cell type with a high degree of probability. Basket cells have more numerous radially oriented dendrites in stratum radiatum (Buhl et al., 1994a) than axo-axonic cells, whereas the latter have conspicuous tufts of dendritic branches in stratum lacunosum-moleculare (Somogyi et al., 1985; Li et al., 1992; Buhl et al., 1994a,b) which is generally absent in basket cells.

4.4.2 The monosynaptic nature of unitary basket cell effects

Previous work by Miles (1990) has shown that the activity of a single CA3 pyramidal neurone is sufficient to elicit, via a di-synaptic loop, IPSPs in a concomitantly recorded pyramidal cell. This particular mechanism involves the glutamate evoked excitation of an interneurone brought to firing by local axon collaterals of the pyramidal cell (Miles, 1990). Such a scenario can be excluded in our recordings in view of the fact that the presynaptic cells were identified as *GABAergic* basket cells. Accordingly, unitary basket cell IPSPs remained unaffected in the presence of CNQX and AP5, whereas di-synaptic IPSPs are diminished by excitatory amino acid blockers (Miles, 1990).

Likewise, any arguments in favour of a less well defined polysynaptic pathway appear to be rather unlikely, since the very short latencies of basket cell IPSPs are not compatible with the inevitably longer synaptic and conduction delays required for such a hypothetical circuit. Furthermore, the probability of transmission failures would be expected to increase disproportionally with the

number of synaptic links, whereas most basket cell-mediated interactions showed few if any apparent failures.

4.4.3 Unitary basket cell IPSPs - some consensus data

Paired recording techniques have been previously employed to study unitary inhibitory interactions in the major hippocampal subfields, the dentate gyrus (Scharfman et al., 1990), subfield CA3 (Miles and Wong, 1984, 1987; Miles, 1990) and area CA1 (Knowles and Schwartzkroin, 1981; Lacaille et al., 1987; Lacaille and Schwartzkroin, 1988b). Although anatomical findings would suggest that probably most of the data is derived from a pool of heterogeneous presynaptic cells, a number of general principles have emerged that appear to govern unitary synaptic interactions: First, in most instances the probability of successfully encountering a monosynaptic connection is rather high (>0.3; Knowles and Schwartzkroin, 1981; Miles and Wong 1984; Lacaille et al., 1987), thus reflecting a high degree of divergence of the local inhibitory axonal arbours. For instance, for basket cells in the CA3 area, light microscopic estimates of the bouton numbers arrived at figures ranging from 3484 - 9972 (Gulyás et al., 1993a). If a basket cell were to establish, on average, 10 synaptic contacts with its postsynaptic targets this would suggest approximately 350 - 1,000 postsynaptic cells within the confines of the slice. Comparable values were recently obtained for axo-axonic cells in the CA1 area of the rat (Li et al., 1992; Buhl et al., 1994b). Second, as yet there appears to be no evidence for biphasic dual-component unitary IPSPs. Third, considerable variability was found not only for the average strength of different unitary connections but also for the amplitude distribution of individual events within a given connection (Miles and Wong, 1984; Miles, 1990; Scharfman et al., 1990). Fourth, tetanic stimulation of the presynaptic cell generally results in the summation of several events and is followed by a subsequent decrement in the postsynaptic response (Miles and Wong, 1984; Lacaille et al., 1987; Scharfman et al., 1990).

4.4.4 Receptor pharmacology of basket cell-mediated IPSPs

The rapid onset, fast rise kinetics as well as extrapolated response reversals of unitary basket cell IPSPs strongly suggest that they elicit, in concert with at least 2 further types of GABAergic neurone (Buhl et al., 1994a), the $GABA_A$ receptor-mediated component of compound IPSPs that are commonly observed in response to the stimulation of afferent pathways (Alger and Nicoll, 1979). In marked contrast, the relatively sluggish onset of pharmacologically isolated $GABA_B$ receptor-mediated responses shows a characteristic lag of 6-8 ms which is presumably due to a delay corresponding to the activation of postsynaptic G-proteins (Otis et al., 1993). Moreover, unitary basket cell IPSPs decayed rapidly and generally monoexponentially back to baseline, approximately an order of magnitude faster than $GABA_B$ receptor-mediated potentials (Otis et al., 1993). In view of the kinetic properties of basket cell-mediated IPSPs, it is not surprising that the pre- and postsynaptic $GABA_B$ receptor antagonist CGP 55845A neither *decreased* (for presynaptic effects see below) their amplitude nor appreciably shortened their decay. The dramatic reduction of basket cell-mediated IPSPs by bicuculline would therefore suggest that they were exclusively mediated by the activation of $GABA_A$ receptors. These physiological results are in agreement with the immunocytochemical demonstration of the α_1 and $\beta_{2/3}$ subunits of the $GABA_A$ receptor in somatic synapses of dentate granule cells where dentate basket cells terminate (Nusser et al., 1995)

Despite this seemingly straightforward interpretation of these findings it is nevertheless conceivable that a different scenario of events may lead to $GABA_B$ receptor activation, for example the spillover of GABA to extra- or perisynaptic sites (Solis and Nicoll, 1992; Isaacson et al., 1993; Mody et al., 1994). It is therefore of interest to note that high frequency long-duration trains of action

potentials in basket cells failed to appreciably prolong the decay of summed IPSPs. In support of these findings, the notion of separate populations of GABAergic neurones being responsible for $GABA_A$ and $GABA_B$ receptor-mediated effects has been repeatedly put forward by others. Thus, unitary IPSPs elicited by CA3 pyramidal cell layer interneurones are abolished by the $GABA_A$ receptor antagonist picrotoxin (Miles, 1990), whereas stratum lacunosum-moleculare interneurones in area CA1 has been suggested to evoke slow IPSPs (Lacaille and Schwartzkroin, 1988b). However, a recent study has found all such cells tested to mediate their effect through $GABA_A$ receptor mechanisms (Vida et al., 1997). In the dentate gyrus, spontaneous IPSCs have been shown to selectively activate $GABA_A$ receptors (Otis and Mody, 1992). Furthermore, local application of nipecotic acid, which induces GABA release, via a heteroexchange mechanism, may evoke pure $GABA_A$ or $GABA_B$ responses (Solis and Nicoll, 1992). Finally, in hippocampal neurones the potassium channel blocker 4-aminopyridine may result in the isolated appearance of either fast or slow spontaneous IPSPs (Muller and Misgeld, 1990; Misgeld et al., 1992), the latter being sensitive to the $GABA_B$ receptor antagonist 2-hydroxy-saclofen (Segal, 1990).

4.4.5 Presynaptic control of basket cell-mediated GABA release

A wealth of earlier literature indicated that GABAergic inhibition is depressed following repetitive activation of afferent pathways (e.g. McCarren and Alger, 1985; Thompson and Gähwiler, 1989; for review see Thompson, 1994). These findings however are sometimes difficult to interpret in view of the generally disynaptic nature of the evoked IPSPs. This disadvantage can be largely circumvented by focusing on monosynaptically elicited unitary events which permit the analysis of frequency-dependent phenomena on a small number of functionally homogeneous synapses. Under these conditions we found that responses mediated

by *basket cell* synapses show a marked frequency-dependent depression of their postsynaptic response, although the response never faded completely, regardless of the presynaptic discharge frequency. Pharmacological blockade of $GABA_B$ receptors resulted in an amplitude increase of averaged IPSPs already at presynaptic tonic firing rates in the range of 1 Hz. Moreover, an additional response depression due to a further increase in presynaptic frequency could be effectively antagonised by a $GABA_B$ receptor antagonist. The most parsimonious explanation for these findings is, that GABA which is released from *basket cell terminals* not only acts on postsynaptic $GABA_A$ receptors, but also on presynaptic $GABA_B$ autoreceptors which govern neurotransmitter release (Davies et al., 1990; Davies and Collingridge, 1993). It is thus possible that, to some extent, the measurements of IPSP amplitudes and calculated conductance values within this frequency range may have been also affected by the activation of presynaptic $GABA_B$ receptors. As an alternative explanation for frequency dependent-depression of IPSP amplitudes it is conceivable that chloride-loading due to the bulk activation of many GABAergic synapses may lead to a change in the chloride equilibrium potential and thus to a decrease in the response amplitude (Thompson and Gähwiler, 1989). This possibility however seems rather remote considering that unitary events are mediated by a comparatively small number of synaptic contacts, approximately 4% of perisomatically positioned basket cell terminals (Buhl et al., 1994a).

In line with the data emerging from the analysis of unitary events, work on pharmacologically isolated IPSPs (Davies et al., 1990; Nathan and Lambert, 1991; Davies and Collingridge, 1993; Lambert and Wilson, 1993a,b, 1994) and miniature inhibitory postsynaptic currents (IPSCs; Cohen et al., 1992; Behrends and Ten Bruggencate, 1993; Capogna et al., 1993) has provided evidence for the existence of presynaptic $GABA_B$ receptors on the terminals of GABAergic interneurones (Davies and Collingridge, 1993). In addition, presynaptic opioid (Cohen et al., 1992; Capogna et al., 1993; Lambert and Wilson, 1993b) and muscarinic receptors

(Behrends and Ten Bruggencate, 1993) were also shown to be involved in the regulation of transmitter release from GABAergic terminals. As yet however, it is not clear whether anatomically distinct subsets of GABAergic interneurones may differ with respect to the expression of presynaptic receptors as it has been proposed by Lambert and Wilson (1993b). However, Pearce et al (1995) have recently shown a differential presynaptic $GABA_B$ mediated modulation of fast and slow $GABA_A$ receptor mediated IPSCs in CA1 pyramidal cells which may originate from activation of different subtypes of GABAergic interneurone (Pearce, 1993).

4.4.6 Unitary conductance and number of release sites

Buhl and colleagues have previously demonstrated two unitary basket cell IPSPs to be mediated by 10 (Buhl et al. 1994a) and 12 (Buhl et al., 1995) synaptic contacts. Previously, counts of synaptic junctions were found to be in accord with the number of release sites (n), as determined by quantal analysis (Korn et al., 1982; Gulyás et al. 1993b). Quantal models of transmitter release assume that postsynaptic responses occur as integer multiples of an elementary synaptic event, the response to a single quantum (q) of neurotransmitter (Del Castillo and Katz, 1954; for review see Redman, 1990). Ideally the parameter q is determined by studying action potential independent spontaneous release (miniature events) and evoked release at the same synapse (Bekkers, 1994; Paulsen and Heggelund, 1994). In the absence of such data the conductance / amplitude of miniature postsynaptic potentials may be taken as a rough equivalent of q, assuming homogeneity of release sites and that spontaneous release is predominantly monovesicular (Bekkers, 1994). Thus, in area CA1, the averaged GABA-mediated quantal conductance was estimated to be in the range of 258 - 326 pS (Ropert et al., 1990), being very close to the figures which were obtained for conductance changes responsible for inhibitory quantal events in dentate granule cells (200 - 400 pS; Edwards et al., 1990). These values provide an indication that, on average, unitary basket cell-mediated IPSPs with an average conductance of 0.95 ± 0.29nS,

may be due to the synchronous release and summation of not more than 3 - 4 quanta. In view of the approximately 3 times higher number of release sites it would thus appear that the release probability (p) at basket cell terminals is relatively low, in the range of 0.3, thus being similar to the experimentally determined p at inhibitory synapses on the goldfish Mauthner cell (Korn et al., 1982). In spite of p being low, the relatively high n does nevertheless restrict the number of total transmission failures. This is evident by the absence of a discernible failure peak in unitary IPSP amplitude histograms (Miles, 1990; Buhl et al., 1995).

4.4.7 Inhibitory rebound

Already Kandel and Spencer (1961) in their pioneering *in vivo* studies noticed that IPSPs were frequently followed by action potentials, a phenomenon to which they referred to as "rebound excitation". They proposed that rebound excitation may be either mediated by the arrival of late EPSPs or, alternatively, by a similar mechanism as anodal break spikes following hyperpolarising currents. Subsequently, rebound excitation was also noted in conjunction with unitary IPSPs which were mediated by stratum lacunosum-moleculare interneurones (Lacaille and Schwartzkroin, 1988b). As excitatory synaptic mechanisms do not participate in the generation of unitary IPSPs it would thus appear more likely that it is the membrane hyperpolarisation which is responsible for the generation of stratum lacunosum-moleculare and/or basket cell-mediated postinhibitory facilitation. And indeed, a variety of voltage-dependent conductances have been described all of which may result in a postinhibitory overshooting membrane depolarisation, including the deinactivation of sodium or calcium channels (Carbone and Lux, 1984; Stafstrom et al., 1985; Llinás, 1988) or the activation of a hyperpolarisation-activated current such as I_h (Halliwell and Adams, 1982; Maccaferri et al., 1993). The functional implications for rebound facilitation and the interaction of unitary IPSPs with pyramidal cell firing are further discussed in chapter 5 of this thesis.

4.4.8 A distinct functional role for basket cells?

GABAergic basket cells constitute only one of several well-defined classes of hippocampal GABAergic interneurones. Amongst those, it is largely their synaptic target selectivity which renders basket cells a distinct neuronal entity. At the onset of the present study it therefore appeared to be a reasonable assumption that it may be to some extent also their postsynaptic effect which provides the relevant cues to the specific functional role of basket cells. With respect to eliciting fast, perisomatic $GABA_A$ receptor-mediated inhibition, however, basket cells resemble axo-axonic cells (Buhl et al., 1994a) which act through the same postsynaptic receptor type(s), albeit on the axon initial segment of principal cells. Although at first glance this similarity of effects may render the target specificity of peri-somatic GABAergic synapses redundant, these findings do rather indicate that differences of $GABA_A$ receptor-mediated synaptic mechanisms are more subtle than currently assumed. Indeed, recent evidence suggests that the $GABA_A$ receptor subunit composition may differ between axo-axonic and basket cell synapses (Nusser et al., 1996).

Figure 4.1: Physiological identification of interneurone-pyramidal cell pairs. A, during the experiments a search was made for cells which fired either trains of non-accommodating action potentials and/or had short-duration action potentials which were followed by a deep fast afterhyperpolarising potential (fAHP). B, while monitoring the impalement of the presumed interneurone shown in A a second microelectrode was advanced into cells that exhibited the physiological characteristics of pyramidal cells, such as marked spike frequency adaptation and relatively broad action potentials which were followed by a comparatively small fAHP. C, once two stable impalements had been achieved, the cell with interneuronal firing properties was depolarised by small increments of DC current until it fired. D, spike-triggered averaging techniques were then employed to determine whether both cells were synaptically coupled. If so, neurones with the properties shown in A invariably elicited short-latency IPSPs in the postsynaptic cells. E, Unitary IPSPs were always of short duration and their decay phase could be frequently fitted with a single exponential function. Membrane potential in D = -62 mV. The traces in D-E represent an average of 135 sweeps. These 2 cells were identified anatomically using biocytin injections and are shown in Figure 4.2.

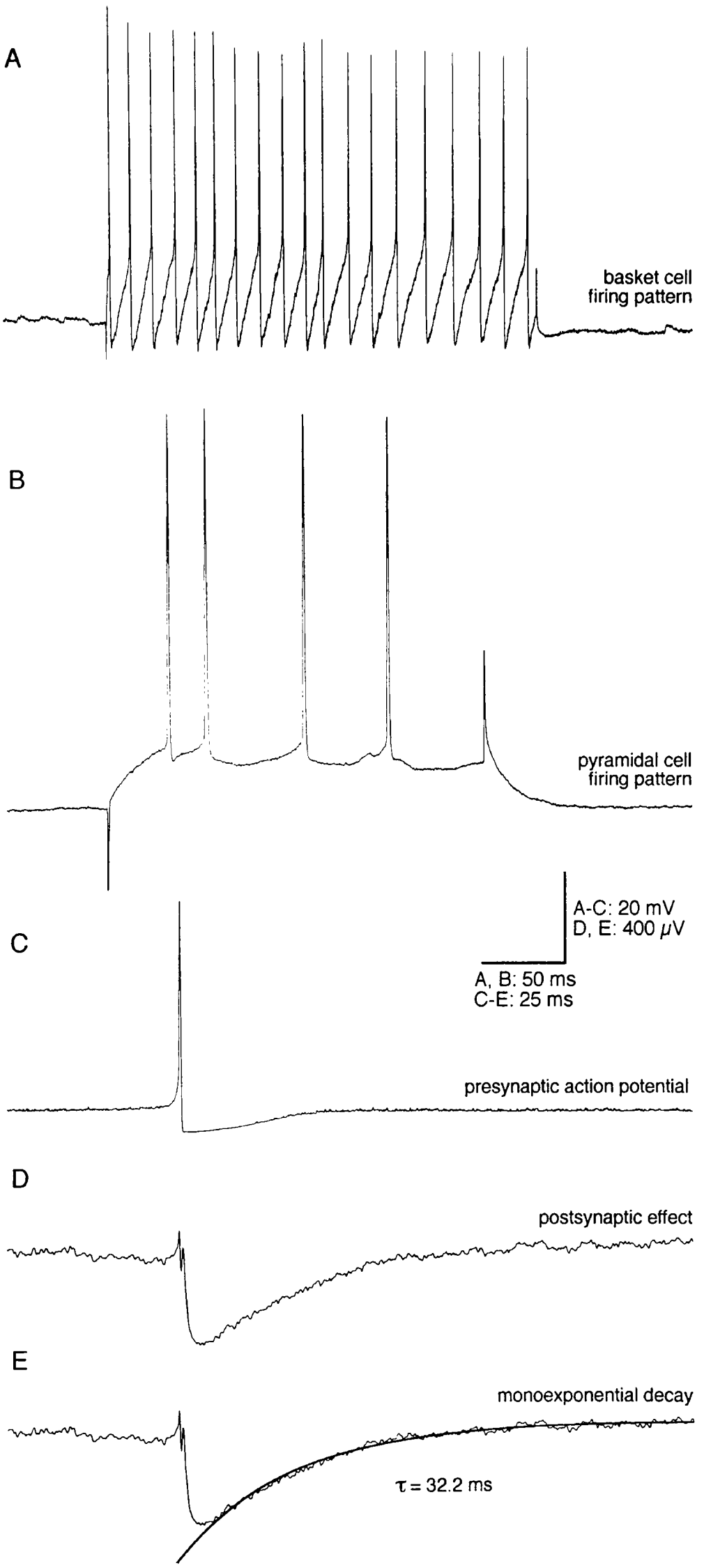

A
basket cell
firing pattern
B
pyramidal cell
firing pattern
A-C: 20 mV
D, E: 400 μV
A, B: 50 ms
C-E: 25 ms
C
presynaptic action potential
D
postsynaptic effect
E
monoexponential decay
τ = 32.2 ms

Figure 4.2: Light microscopic reconstruction of a synaptically connected and intracellularly labelled basket/pyramidal cell pair. Both cells were identified due to their distinctive firing patterns (shown in Figure 4.1A, B). The basket cell (soma, dendrites and axonal arbour shown in black) elicited a short-latency fast IPSP (Figure 4.1D, E) in the postsynaptic pyramidal cell (dendrites and cell body displayed in red; spines not shown). The inhibitory axon emerged from the basket cell soma (arrow) and densely ramified within the cell body layer and the adjacent portions of the strata radiatum (Str. rad.) and oriens (Str. or.). The border of strata radiatum and pyramidale is indicated by line at left and right. Although basket cell dendrites, as a general rule, enter stratum lacunosum-moleculare (Str. lac. mol.) they do not give rise to a prominent apical tuft. Following light microscopical analysis, the synaptic target profile of the inhibitory cell was assessed by means of random electron microscopic bouton sampling. From a total of 61 labelled boutons 29 (48%) were found in synaptic contact with somata, 2 (3%) on spines, whereas the remainder (n=31; 49%) formed synapses with dendrites. Scale bar = 100 μm.

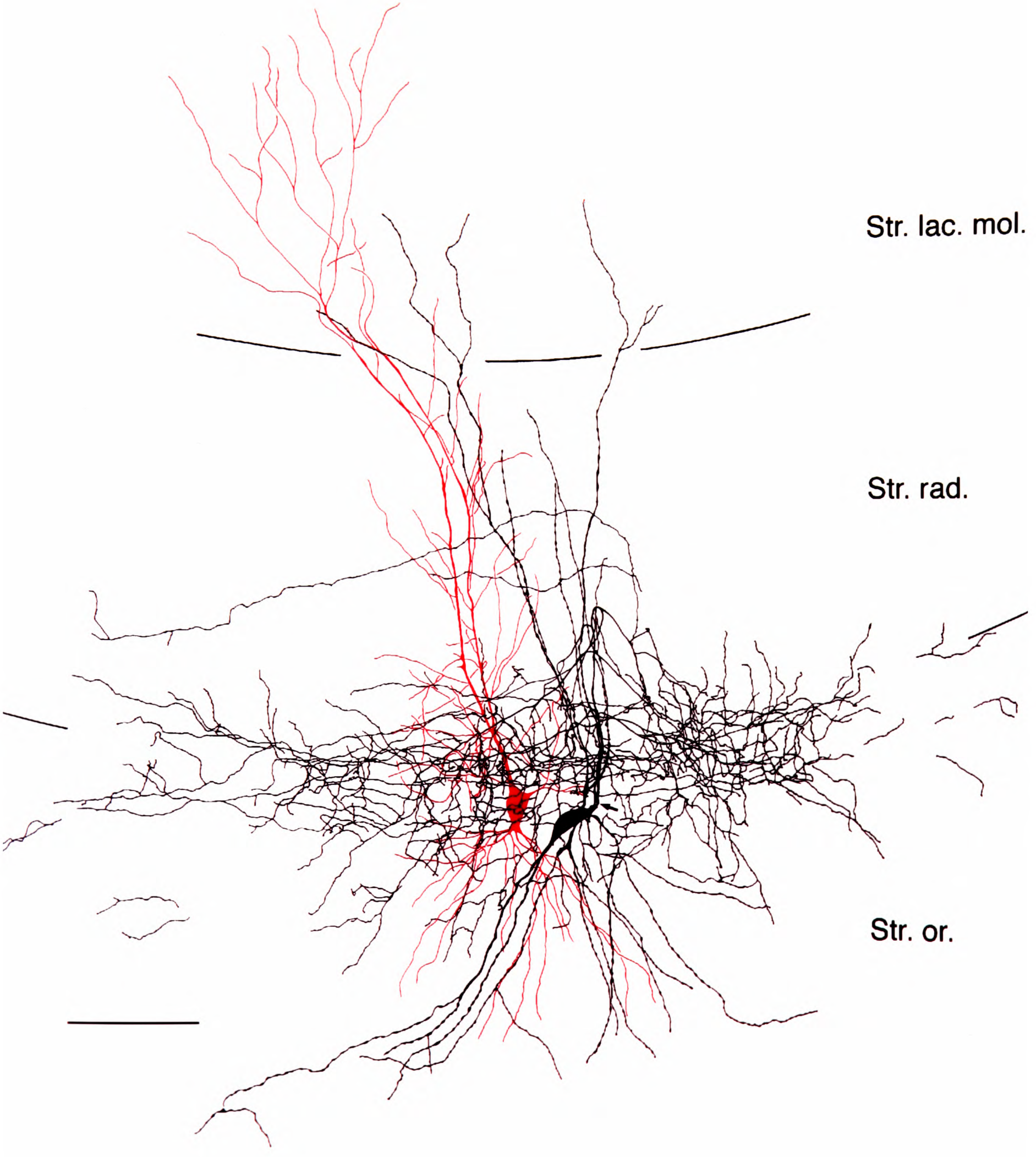
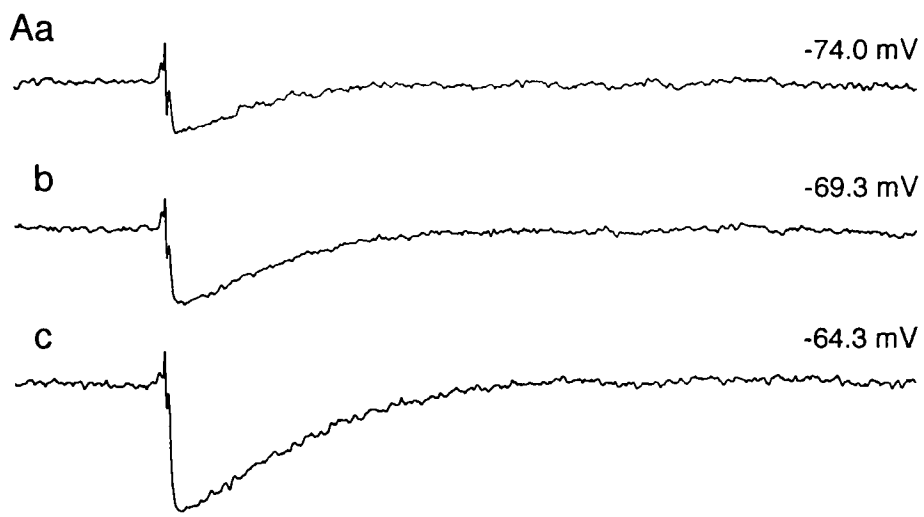
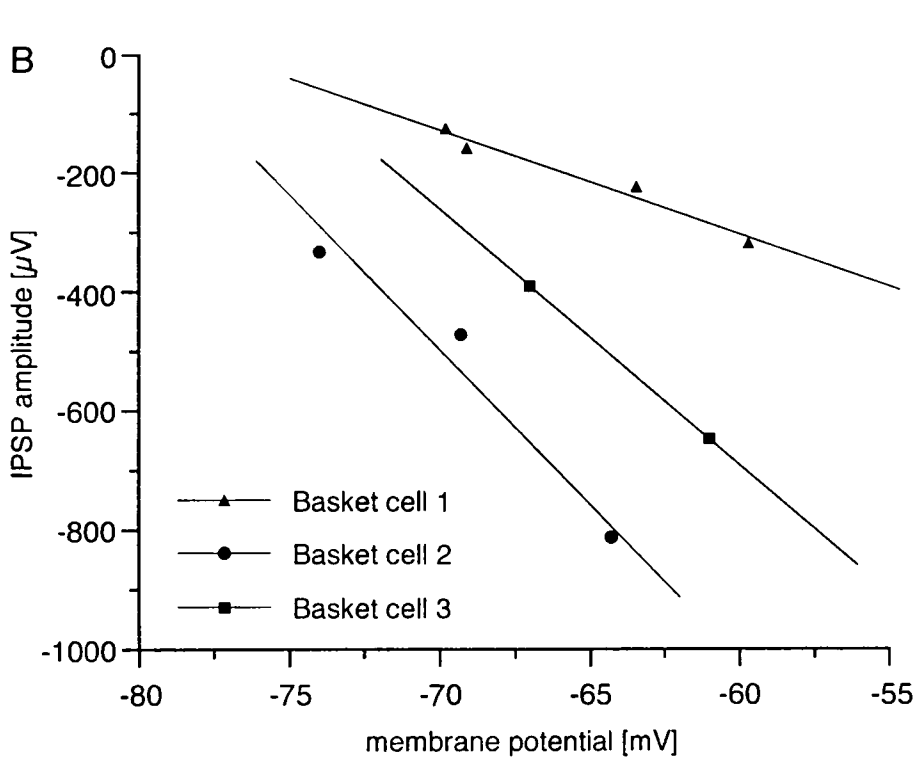

Str. lac. mol.
Str. rad.
Str. or.

Figure 4.3: Voltage-dependence of IPSPs and their pharmacological properties. A, voltage-dependence of a unitary basket cell IPSP. Whenever tested, membrane depolarisation in postsynaptic pyramidal cells resulted in the successive increase of IPSP-amplitudes (Aa-c). B, estimation of IPSP response reversal. Linear regression was employed to fit graphs to the data points and calculate the response reversal of IPSPs. C, pharmacological dissection of unitary basket cell IPSP. Using DC current injections the presynaptic cell was made to fire (Ca), whilst the postsynaptic membrane potential was maintained at -55 ±1 mV throughout the experiment. Cb, once a stable, synaptically connected pair had been obtained, the control response was followed for several minutes until superfusion with the excitatory amino acid blockers CNQX and AP5 was commenced. Cc, basket cell-evoked unitary IPSP following bath application of glutamate receptor antagonists Cd, addition of the selective $GABA_B$ receptor antagonist CGP 55845A resulted in a marginal (4%) increase of the IPSP amplitude. Ce, superfusion of the $GABA_A$ receptor antagonist bicuculline, however, almost completely eliminated the response. Cf, superimposition of the averages shown in Cc-e reveals that the $GABA_B$ antagonist had only a marginal effect on the amplitude, whereas the decay phase of the basket cell-evoked IPSP remained unchanged. All traces shown in A & C represent averages >50 sweeps.


Aa
-74.0 mV
b
-69.3 mV
c
-64.3 mV


B
0
-200
-400
-600
-800
-1000
IPSP amplitude [μV]
-80
-75
-70
-65
-60
-55
membrane potential [mV]
Basket cell 1
Basket cell 2
Basket cell 3

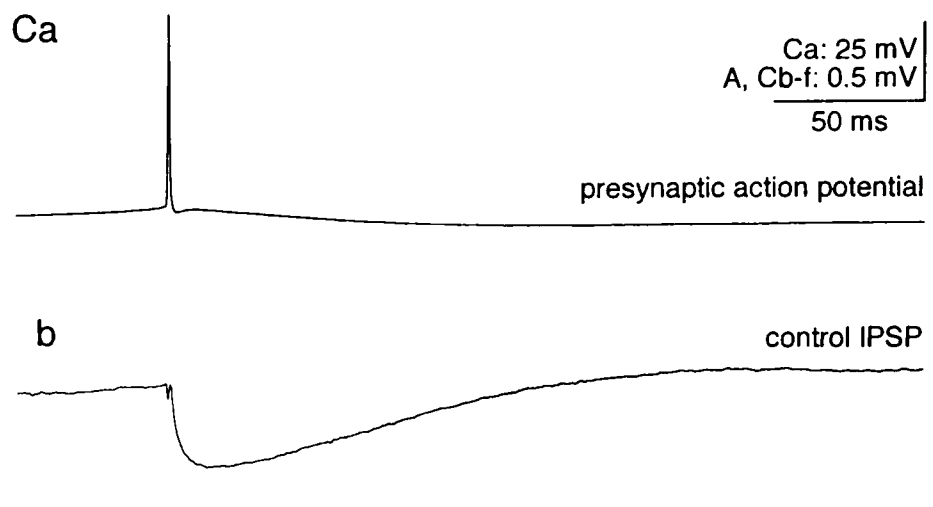

Ca
Ca: 25 mV
A, Cb-f: 0.5 mV
50 ms
presynaptic action potential
b
control IPSP
c
5 μM CNQX & 30 μM AP5
d
4 μM CGP 55845A
e
13 μM bicuculline
f
superimposed averages (c-e)

Figure 4.4: Summation of IPSPs and frequency-dependent attenuation. Aa, a 300 ms train of presynaptic action potentials in a basket cell firing at a non-decrementing frequency >200 Hz. Ab, the average of 8 postsynaptic events in a pyramidal cell revealed an early peak of the response that subsequently declined and levelled at slightly more than half of the peak amplitude. Note the monoexponential decay of the IPSP, which was similar to the decay of single action potential-evoked IPSPs. Ac, expansion of the early response (time window indicated by horizontal bar) shown in Ab. Due to the small variability of interspike intervals in the presynaptic cell the first 6 action potentials (arrows indicate coupling artefacts) superimpose precisely. It is apparent that the peak response is due to the summation of, on average, 4 IPSPs, with some degree of variability in individual events (data not shown). In *b* and *c* electrode coupling artefacts caused by capacitive transients in *a* were clipped for clarity of display. B, the presynaptic rate of discharge may affect the magnitude of the postsynaptic response. A twelvefold increase in presynaptic firing frequency from 0.3 Hz (Ab) to 3.6 Hz (Ad) resulted in a >50% decrease of the IPSP amplitude. Ae superimposition of traces Ab-d. Arrowheads indicate position of spike capacitive artefacts which were removed for clarity. C & D, effect of $GABA_B$ receptor blockade on frequency dependent IPSP depression. Ca presynaptic basket cell action potential. Cb, c A more than tenfold elevation of the presynaptic firing frequency resulted in a substantial reduction of the postsynaptic response, which is apparent upon superimposition (Cd). Da-d, following superinfusion with 1μM CGP 55845A the test was repeated by increasing the presynaptic firing frequency more than fivefold. De superimposition of the traces shown in Db, c reveals the absence of frequency dependent IPSP depression in the presence of the $GABA_B$ receptor antagonist. All traces in B-D represent averages of > 50 responses.

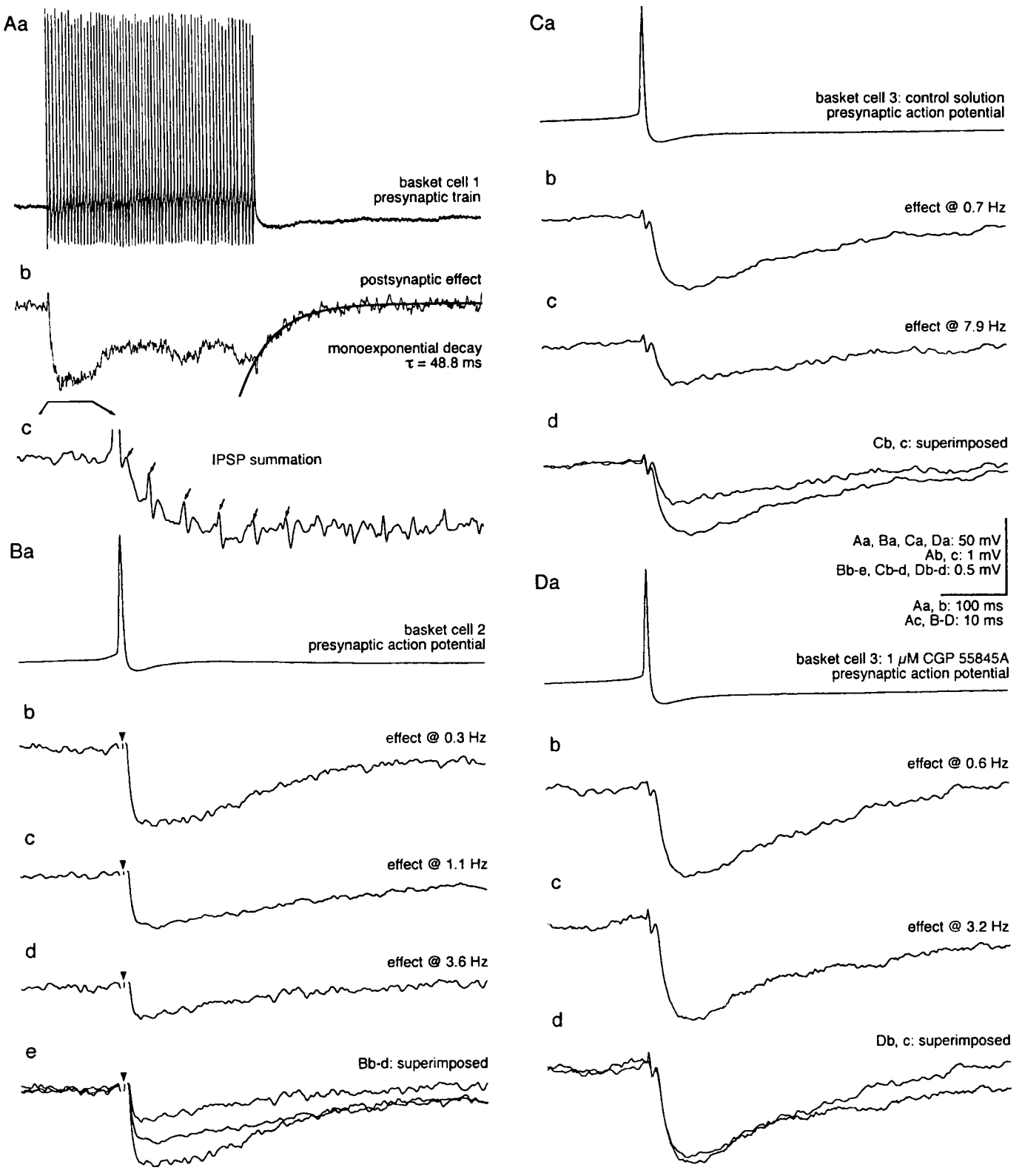

Aa
basket cell 1
presynaptic train
b
postsynaptic effect
monoexponential decay
τ = 48.8 ms
c
IPSP summation
Ba
basket cell 2
presynaptic action potential
b
effect @ 0.3 Hz
c
effect @ 1.1 Hz
d
effect @ 3.6 Hz
e
Bb-d: superimposed
Ca
basket cell 3: control solution
presynaptic action potential
b
effect @ 0.7 Hz
c
effect @ 7.9 Hz
d
Cb, c: superimposed
Aa, Ba, Ca, Da: 50 mV
Ab, c: 1 mV
Bb-e, Cb-d, Db-d: 0.5 mV
Aa, b: 100 ms
Ac, B-D: 10 ms
Da
basket cell 3: 1 μM CGP 55845A
presynaptic action potential
b
effect @ 0.6 Hz
c
effect @ 3.2 Hz
d
Db, c: superimposed

Figure 4.5: Reliability of basket cell mediated unitary IPSPs. A, presynaptic spike of a CA1 basket cell (1207941) B, response variability in 33 consecutively elicited pyramidal cell IPSPs. The presynaptic cell was driven at a frequency of ~1Hz, the postsynaptic pyramidal cell was held at a membrane potential of -64 mV. C, superimposition of all events reveals absence of apparent failures during this period. D, averaged response.

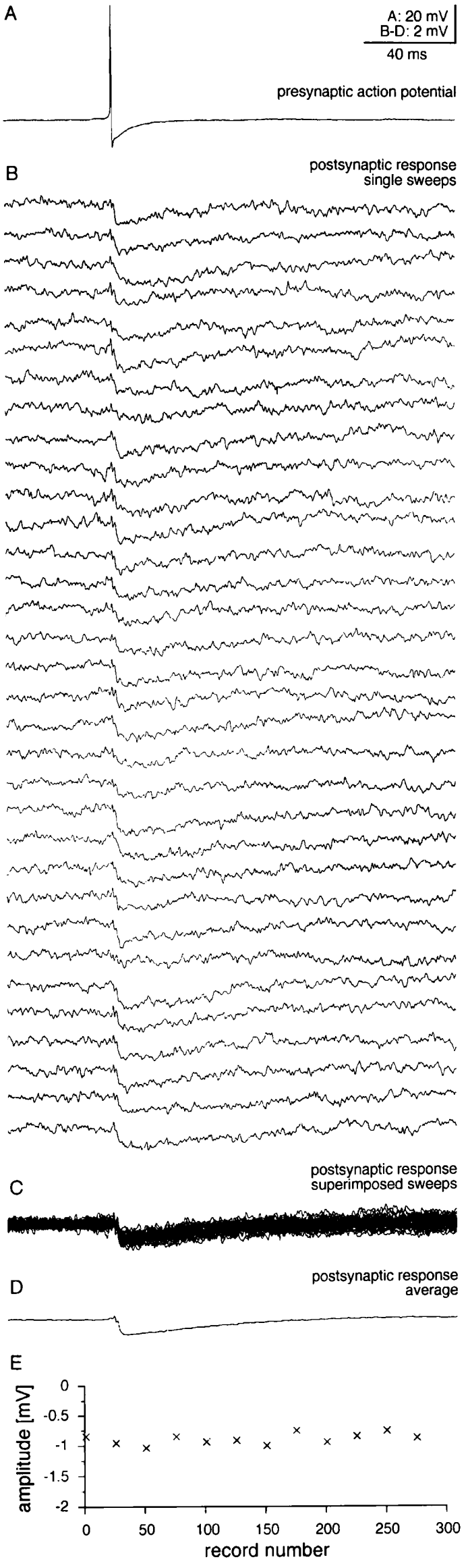

A
A: 20 mV
B-D: 2 mV
40 ms
presynaptic action potential
B
postsynaptic response
single sweeps
C
postsynaptic response
superimposed sweeps
D
postsynaptic response
average
E
amplitude [mV]
0
-0.5
-1
-1.5
-2
0
50
100
150
200
250
300
record number

Figure 4.6: Postinhibitory facilitation and rebound action potentials. A, brief burst of action potentials in a presynaptic basket cell. B, average of postsynaptic response in a synaptically coupled pyramidal cell. By injecting constant depolarising current the pyramidal cell was held close to action potential threshold (membrane potential -54 mV) and was firing sporadically (<1 Hz). Sweeps containing pyramidal cell action potentials were excluded from this average. Note the apparent incremental summation of synaptic events (see also Figure 4.4Ac) which were followed by a large amplitude "hump" which considerably overshot the pre-event baseline level (indicated by stippled line). C, postinhibitory rebound action potentials. Same epoch of recording as shown in B, after excluding all events in which the cell remained below firing threshold. Superimposition of 10 *consecutive* sweeps reveals that the pyramidal cell preferentially discharges during the same time window in which postinhibitory facilitation was observed. D, presynaptic action potential, evoked by a brief depolarising pulse in a different basket cell. E, Distinct clustering of consecutive rebound action potentials in the postsynaptic pyramidal cell.

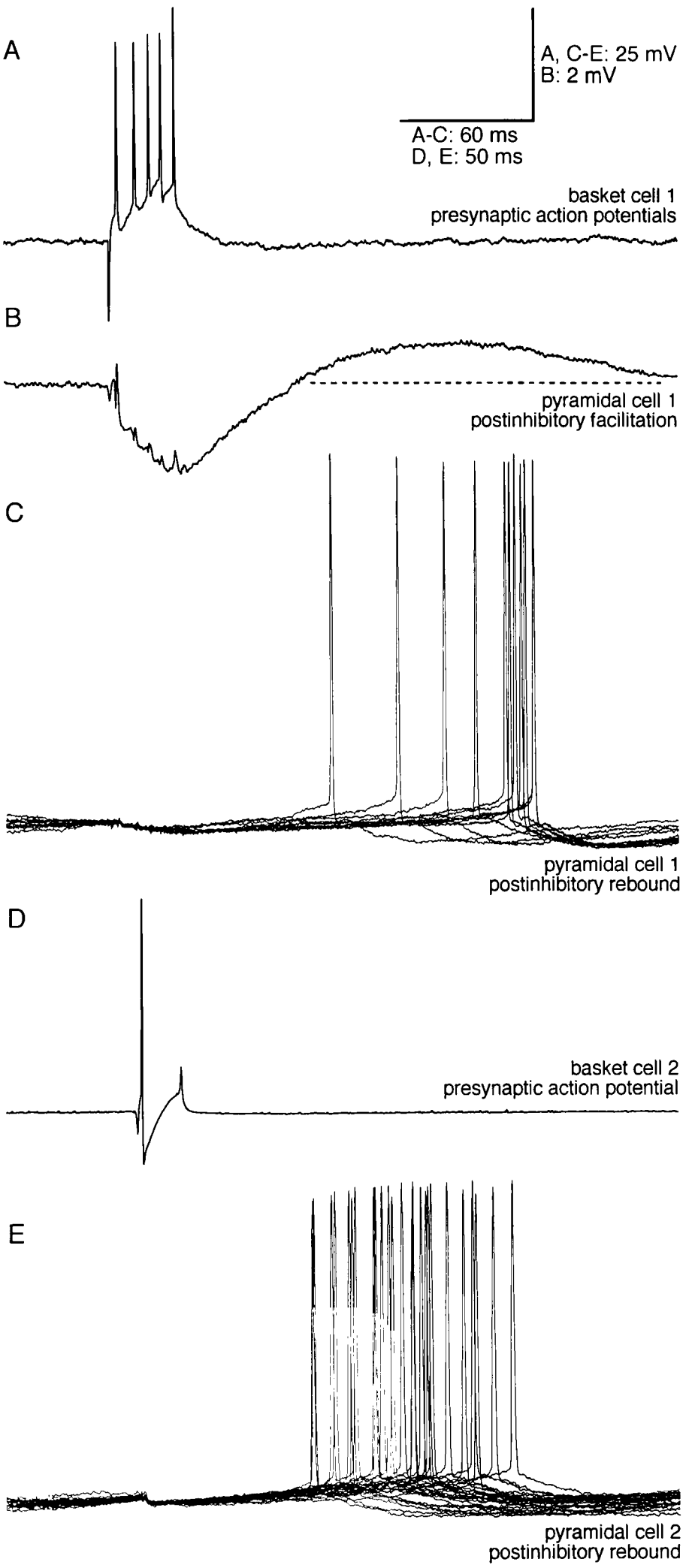

A
A, C-E: 25 mV
B: 2 mV
A-C: 60 ms
D, E: 50 ms
basket cell 1
presynaptic action potentials
B
pyramidal cell 1
postinhibitory facilitation
C
pyramidal cell 1
postinhibitory rebound
D
basket cell 2
presynaptic action potential
E
pyramidal cell 2
postinhibitory rebound

Table 4.1

TABLE 4.1. Location of electron microscopically determined synaptic junctions made by randomly selected labelled basket cell boutons on unlabelled postsynaptic targets

Basket cell	Area	Number of tested synapses (n)					Relative proportion of synapses (%)				
		AIS*	Soma	Dendrite	Spine	Total	AIS	Soma	Dendrite	Spine	Total
1	CA3	3	6	6	2	17	18	35	35	12	100
2	CA1	0	5	7	0	12	0	42	58	0	100
3	CA1	0	19	18	0	37	0	51	49	0	100
4	CA1	0	17	19	5	41	0	42	46	12	100
5	CA1	0	7	5	0	12	0	58	42	0	100
6	CA3	0	14	2	0	16	0	87.5	12.5	0	100
7	CA1	0	5	6	0	11	0	45.5	54.5	0	100
8	CA1	0	29	30	2	61	0	48	49	3	100
9	CA1	0	4	7	0	11	0	36	64	0	100
10	CA1	0	5	6	0	11	0	45.5	54.5	0	100
11	CA1	0	5	5	0	10	0	50	50	0	100
12	CA1	4	10	9	1	24	17	42	37	4	100
13	CA1	0	5	5	0	10	0	50	50	0	100
14	CA1	2	5	2	0	9	22	56	22	0	100
Total		**9**	**136**	**127**	**10**	**282**	**3.2**	**48.2**	**45**	**3.6**	**100**

AIS* - axon initial segment.

Chapter 5. Novel mechanisms of synchronising neuronal activity by individual local-circuit interneurones

5.1 Introduction

Recent years have seen great advances in our understanding of GABAergic synaptic transmission in the central nervous system. In particular, considerable effort has been made investigating GABAergic synaptic interactions from biophysical and pharmacological perspectives (for review see Mody et al., 1994). Despite this wealth of information however, few studies have investigated the interaction of GABAergic synaptic responses with dynamic properties of postsynaptic neurones, such as action potential discharge and other active processes. The traditional "integrate and fire" system of neuronal integration has formed the basis of our current understanding of how individual neurones operate (for review see McCormick, 1990). This system assumes an input-output relationship in which the activity of each neurone in a network is simply a reflection of the excitatory and inhibitory inputs which impinge upon it. In its most simple form, this model of neuronal integration relies on spatial and temporal summation of convergent excitatory signals and a resultant passive depolarisation spreading to the site of action potential initiation, where a regenerative action potential will be produced if the depolarisation is sufficient to reach a minimum voltage threshold. Whether or not an action potential is generated will thus not only depend upon the overall amount of excitatory drive, but also where it arrives on the dendritic arbour (i.e. its placement), the relative timing of convergent inputs (i.e. temporal summation), the passive properties of the postsynaptic membrane (e.g. input resistance and time constant) and finally, the level and placement of inhibitory inputs. However, this system fails to take into account the mainly voltage-gated intrinsic conductances within neurones which are likely to profoundly shape synaptic neuronal responses (Llinás, 1988). Cortical principal neurones are known to support many active conductances in their dendrites (Andreasen and Lambert, 1995; Yuste and Tank, 1996).

In addition to the more traditional function ascribed to inhibitory GABAergic innervation in providing an inhibitory offset to control the level of

excitation, considerable interest is now focused on an additional or more diversified role for GABAergic systems in the central nervous system, namely to control temporal aspects of neuronal activity. In particular, GABAergic mechanisms have been implicated in controlling various patterns of population activity, including hippocampal theta activity (Buzsáki & Eidelberg, 1983; Buzsáki et al., 1983; Ylinen et al., 1995b; Konopacki et al., 1987; Fox, 1989; Stewart & Fox, 1990, Soltész & Deschenes, 1993; Lee et al., 1994), gamma activity (Whittington et al., 1995; Bragin et al., 1995; Ylinen et al., 1995a; Buzsáki et al., 1983; Soltész & Deschenes, 1993), hippocampal sharp waves, and high frequency 'ripple' oscillations (Chrobak & Buzsáki, 1996; Buzsáki et al., 1992). The establishment of such synchronised neuronal activities is considered to be a fundamental principle in the operation of cortical neuronal networks (Singer, 1993). Indeed, such patterns of cortical oscillatory activity at the EEG level (Niedermeyer and Lopes da Silva, 1993) have been correlated to distinct patterns of behaviour. Coherent activity has been implicated in many higher-order processes, including perception (Eckhorn et al., 1988; Gray and Singer, 1989; Gray et al., 1989) and memory encoding (Cook, 1991; Huerta and Lisman, 1993, Lisman and Idiart, 1995; Buzsáki et al., 1992). With respect to an ongoing synchronised oscillation, the precise timing of action potentials represents an attractive candidate mechanism for information coding (Mainen and Sejnowski, 1995; O'Keefe and Recce, 1993; Lisman and Idiart, 1995; Hopfield, 1995).

One form of rhythmic oscillatory activity, theta oscillations (4-7 Hz) represents one of the most prominent synchronous rhythmic events in the brain, and is evident in the hippocampal EEG during exploratory behaviour (Vanderwolf, 1969). Hippocampal theta oscillations have been proposed to serve as a reference for coding by 'place cells' (O'Keefe and Recce, 1993). At the cellular level, intrinsic membrane conductances support theta frequency membrane potential oscillations in individual CA1 pyramidal cells (Leung and Yim, 1991; Garcia-Munoz, 1993). Moreover, intracellular recordings from pyramidal cells during theta

activity have revealed rhythmic chloride-mediated conductances, which originate close to the cell body (Fox, 1989; Soltész and Deschenes, 1993), suggesting that perisomatic $GABA_A$ receptor-mediated synaptic events contribute during intracellular theta oscillatory activity. The divergent axonal output of local-circuit interneurones innervating the perisomatic domain of pyramidal cells (Cajal, 1911; Lorente de No, 1934; Li et al., 1992; Han et al., 1993; Buhl et al., 1994a; Sík et al., 1995), suggest that they are indeed well suited to synchronise the activity of pyramidal cells. In excess of a thousand of which will receive a common synchronous GABAergic input.

The aim of these *in vitro* experiments was to establish the effectiveness of identified GABAergic local-circuit interneurones in governing the activity of pyramidal cells, taking into account both their effect on the overall level of activity of postsynaptic neurones as well as temporal aspect of their activity. In relation to the latter, a paradigm was developed to test, in the absence of patterned excitatory input, whether rhythmic activation of individual GABAergic interneurones can synchronise theta frequency activities in CA1 pyramidal cells in hippocampal slices.

5.2 Materials and methods

The procedures for the preparation of rat hippocampal slices are described in the methods chapter (chapter 2). Dual intracellular recordings were obtained with 2% biocytin / 1.5M KCH_3SO_4 filled electrodes from neurones in the CA1 area and experimental paradigms testing current-discharge relationships, phase-lock activity and synchronisation were designed as follows.

Pyramidal cell current -discharge characteristics were assessed by delivering 300-500ms depolarising current pulses to pyramidal cells in 0.05 - 0.1nA steps ranging between 0.05 and 0.6nA (see Figure 5.1). Each current pulse was repeated 10-30 times at each stimulus intensity at 5s intervals. Every second depolarising current pulse to the pyramidal cell was given concurrent with a

suprathreshold depolarising current injection (0.2-0.5nA; 300-500ms) to the presynaptic interneurone but which preceded the pyramidal cell pulse by 10-50ms. The current-discharge paradigm was automated using a Macintosh Quadra 800 computer with commercially available software (Axo-data; Axon Instruments, CA, USA). All firing frequency measurements refer to the initial firing frequency calculated form the first inter-spike interval. All frequency values shown indicate mean ± standard error.

Phase-locking activity was assessed by tonically depolarising pyramidal cells with suprathreshold intracellular current injection until cells constantly evoked action potentials. Presynaptic interneurones were then made to fire short trains of 3-4 action potentials at frequencies ranging between 2-10Hz to test for entrainment. Autocorrelation analysis was carried out on 5s segments of the pyramidal cell trace immediately prior to and during entrainment to determine the regularity of action potential discharge or subthreshold membrane potential oscillations during entrainment and control conditions. Power spectral analysis of 5-20s sections of trace, high pass filtered 1Hz, was used to determine the frequency of subthreshold membrane potential oscillations. Autocorrelation and power spectral analysis used Axo-graph software (Axon Instruments, CA, USA).

To test the effectiveness of GABA mediated inhibition at synchronising pyramidal cell activities, simultaneous intracellular recordings were made in the presence of AMPA and NMDA receptor antagonists (10μM 6-cyano-7-nitroquinoxaline-2,3-dione and 30μM DL-2-amino-5-phosphopentanoic acid respectively; Tocris Cookson, Bristol, UK), from unconnected pairs of CA1 pyramidal cells separated by ~100μm. Both pyramidal cells were tonically depolarised to fire action potentials constantly, during which IPSPs were evoked by minimal stimulation of stratum pyramidale, using a monopolar sharpened tungsten electrode at a distance of ~100μm lateral from the recording electrodes. The

amplitude of the stimulus was reduced until the evoked IPSP amplitude was approximately equivalent to that produced by one or a few basket cells (IPSP amplitude ~ 2mV; stimulus strength, 3-8V, 100μs). IPSPs were evoked at 0.2-0.5Hz to examine their effect on action potential discharge in both pyramidal cells and at 5Hz to test for phase-locked activities. Cross-correlation analysis of 5s sections of trace prior to and during rhythmic minimal stimulation was used to determine the degree of synchrony in pyramidal cell firing.

5.3 Results

5.3.1 Identification of labelled neurones

Dual intracellular recordings were made from 17 interneurone -to- pyramidal cell pairs. Following histological processing, morphological evaluation revealed all presynaptic cell somata to be situated in stratum pyramidale, giving rise to apical and basal dendrites which were beaded and smooth. The axonal arbour of all presynaptic interneurones ramified within or adjacent to stratum pyramidale, suggesting a predominantly perisomatic synaptic target profile. Further morphological evaluation of randomly selected postsynaptic profiles at the electron microscopic level showed presynaptic cells to be either basket cells (n=8; cell numbers 18, 22, 26, 40, 49, 53, 62 and 64 in table 2.1) or axo-axonic cells (n=2; cells 57 and 63 on table 2.1). Basket cells made symmetrical synapses mainly onto somata (53±15 %; n=50 electron microscopically determined synaptic contacts) and proximal dendrites (44±15 %; n=41 synapses), whilst axo-axonic cells (n=2) terminated exclusively on axon initial segments of pyramidal cells (100%, n=22 synapses). The postsynaptic cells showed morphological features characteristic of pyramidal cells, including highly spinous dendrites (see chapter 3). The number of synaptically coupled pairs exceeds the number of interneurones because the latter could serve as the presynaptic partner for more than one recorded pyramidal cell.

5.3.2 Characteristics of unitary IPSPs

Both basket and axo-axonic cells elicited fast hyperpolarising inhibitory postsynaptic potentials (IPSPs) in simultaneously recorded pyramidal cells (n=17). The characteristics of basket cell mediated unitary IPSPs have been described in detail in chapter 4. Only those basic biophysical characteristics particularly relevant to these experiments are considered further. For the sample of cells included in these experiments, the mean estimated reversal potential was calculated to be -75.5±7.6 mV (n=7 cell pairs) and -70.5±8.6mV (n=6 cell pairs) for basket and axo-axonic cell mediated IPSPs respectively. Using the method derived form Ginsborg (1973), the estimated mean conductance values for basket and axo-axonic cell mediated unitary IPSPs were estimated to be 1.5±0.7 nS (n=6) and 1.2±0.13nS (n=6) respectively. Where tested (n=2), unitary IPSPs were completely blocked by bath application of $GABA_A$ receptor antagonist (2-10 μM bicuculline).

5.3.3 Effect of unitary IPSPs on action potential generation

Action potentials were evoked in pyramidal cells (n=6) by depolarising current pulse injections (0.05-0.50nA; 500ms) delivered via the recording electrode, in or close to the soma. The initial firing frequency was calculated as the inverse of the first inter-spike interval and ranged from 7.1 ± 0.9 Hz to 116.3 ± 9.0 Hz. Figure 5.1 shows characteristic firing responses in a typical pyramidal cell to depolarising current pulses delivered via the somatic recording electrode. Simultaneous activation of the presynaptic basket cell (right traces) causes a delay in action potential generation and a reduction in the overall firing frequency (16.1% decrease in frequency at 0.4nA current intensity, 29.2% decrease in frequency at 0.5nA current intensity). For the pyramidal cells, plots of the initial firing frequency versus the amplitude of current pulses showed the firing frequency to increase with

increasing current injection, the current-discharge relationship being near linear in some cells whilst exhibiting a non-linear (convex shape) relationship in others (Figure 5.2A-F). To assess the effect of basket cell-mediated inhibition on the initial action potential discharge rate, pyramidal cells were depolarised to evoke action potentials whilst simultaneously activating presynaptic basket cells. In 6 of 6 connections tested, basket cell-mediated IPSPs modestly yet significantly ($P<0.05$; Mann-Whitney U test) reduced the initial firing frequency. However, in only 3 of the 6 connections tested could the presynaptic basket cell significantly suppress the initial firing frequency *over the complete* range of current intensities tested (Figure 5.2B,C,D). The effect of basket cell-mediated IPSPs was to shift the current-discharge plots to the right (Figures 5.2A-F). The non-linearity of the current-discharge relationships and the low number of stimulus intensities sampled meant that the slope of the current-discharge relationship and the effect of basket cell-mediated inhibition on that slope could not be expressed quantitatively in a simple way.

5.3.4 Effect of unitary IPSPs on the timing of action potentials

To assess the effect of unitary IPSPs on the timing of pyramidal cell action potentials, pyramidal cells were depolarised to fire at frequencies in the theta frequency range (4-7Hz) by constant depolarising current injection through the somatic recording electrode. Concomitant IPSPs were evoked by stimulating presynaptic interneurones by brief intracellular depolarising current pulses. Rhythmic activation of presynaptic basket and axo-axonic interneurones at 1-8 Hz instantly phase-locked firing in simultaneously recorded postsynaptic pyramidal cells (n=7 of 7 cells tested; Figure 5.3Ai). During entrainment, interneurones and their respective postsynaptic pyramidal cells fired alternately. Such entrainment was robust and lasted for as long as the presynaptic basket or axo-axonic cell was stimulated. Moreover, individual basket and axo-axonic cells could phase-lock the

activity of pyramidal cells at harmonic or sub-harmonic frequencies to the discharge rate of the interneurone. In those cases, the pyramidal cells could for example, fire two or three action potentials between consecutive interneurone action potentials or, alternatively, fire between every second interneurone action potential (not shown). Autocorrelation analysis (Figure 5.3Aii-iii) showed that during periods of entrainment, pyramidal cells generally fired more regularly than during periods immediately prior to or following entrainment. By phasing the pyramidal cell activity, the interneurone could either *decrease or increase* (by up to 54%) the firing rate of the pyramidal cell ($p<0.05$, Mann-Whitney U test).

At membrane potentials close to action potential threshold, 8 of 8 pyramidal cells tested exhibited subthreshold membrane potential oscillations as previously described (Leung and Yim, 1991). Power spectral analysis (Figure 5.4) revealed such oscillations to occur within the theta frequency range (3-7Hz). Hyperpolarisation of the pyramidal cells by with constant current injection resulted in the disappearance of such oscillations as described (Leung and Yim, 1991). Subthreshold membrane potential oscillations were also entrained by rhythmic activation of single basket and axo-axonic cells (n=5 of 5; Figure 5.3Bi). Autocorrelation analysis (Figure 5.3Bii-iii) showed that during periods of entrainment, sub-threshold membrane potential oscillations in pyramidal cells were more regular than periods immediately prior to or following basket cell firing. Thus, basket and axo-axonic cells could phase individual pyramidal cell activities both at sub- and suprathreshold levels.

5.3.5 Mechanisms underlying inhibitory phasing of pyramidal cells

To elucidate the mechanism underlying inhibitory phasing of pyramidal neurones, unitary IPSPs were evoked at different membrane potentials. At depolarised membrane potentials, where firing occurred sporadically in the

pyramidal cell, single spikes or short trains of action potentials in the inhibitory interneurone evoked hyperpolarising IPSPs in the pyramidal neurone, frequently followed by 'rebound' action potentials (n=10 of 13; Figure 5.5Ai). These action potentials preferentially occurred in a time window corresponding to the depolarising overshoot following IPSPs at subthreshold membrane potentials (Figure 5.5Aii). Such rebound depolarisations following unitary IPSPs were abolished at more hyperpolarised membrane potentials (Figure 5.5Aiii). Brief hyperpolarising current pulses mimicking IPSPs were delivered via the somatic recording electrode and evoked similar rebound depolarisation and action potentials (n=8; Figure 5.5Bi-ii). Like in the case of the 'post-inhibitory rebound', hyperpolarisation of the pyramidal cell resulted in abolition of the rebound depolarisation.

Since these membrane potential oscillations and the rebound depolarisation occurred over a similar voltage range close to action potential threshold, we investigated whether the rebound discharge observed here might be due to interaction with intrinsic oscillatory mechanisms. In pyramidal cells tonically depolarised so to constantly fire action potentials, unitary perisomatic IPSPs were repeatedly evoked. The synaptic response suppressed, but thereafter *facilitated* action potential discharge in the pyramidal cell (n=10 of 13; Figure 5.5Ci-ii). Following single IPSPs, multiple subsequent clusters of action potentials were apparent, when successive sweeps were superimposed. To further investigate the interaction of unitary IPSPs with sub-threshold oscillatory mechanisms, pyramidal cells were depolarised to near action potential threshold, where sub-threshold membrane potentials became apparent (Figure 5.5Di) and unitary IPSPs were evoked by delivering brief depolarising intracellular current injections to basket and axo-axonic cells. Both types of presynaptic neurone were effective in *resetting* the *phase* sub-threshold membrane potential oscillations and could even initiate oscillatory activity during periods of quiescence (Figure 5.5Di-iv).

5.3.6 Synchronisation of pyramidal cell activity

To examine whether through the GABAergic mechanisms described above, single local-circuit interneurones can synchronise the activity of principal cells, we tested in the presence of excitatory amino acid receptor blockers, whether minimal stimulation of GABAergic interneurones could synchronise the firing of two spontaneously active pyramidal cells. Dual intracellular recordings were made from unconnected pairs of pyramidal cells separated by ~100μm in the presence of AMPA and NMDA receptor antagonists (10μM 6-cyano-7-nitroquinoxaline-2,3-dione and 30μM DL-2-amino-5-phosphopentanoic acid respectively).

Both pyramidal cells were tonically depolarised to constantly fire action potentials, during which IPSPs evoked by minimal stimulation reset the regular firing of both cells (n=5 ; Figure 5.6A). Moreover, repeated minimal stimulation at theta frequencies phase-locked both neurones (Figure 5.6Bi) effectively synchronising their discharge. Cross-correlation analysis of the activities of both pyramidal cells indicates the increased synchrony during rhythmic minimal stimulation (Figure 5.6Bii-iii).

5.4 Discussion

The main finding of these experiments was, that individual basket and axo-axonic cells were highly effective at modifying action potential generation in synaptically coupled pyramidal cells. A surprising aspect of this control however, was that whilst perisomatic inhibition by individual cells appears to only modestly modulate the overall *discharge rate* of pyramidal cells, perisomatic inhibition appears particularly effective at modifying the exact *timing* of action potential generation. By interacting with intrinsic membrane conductances in pyramidal cells, powerfully tuned mechanisms appear to be in place which afford the relatively small increase in conductance associated with perisomatic synaptic input from a single

basket or axo-axonic cell to powerfully sculpt temporal aspects of pyramidal cell activity.

5.4.1 Basket cell-mediated suppression of pyramidal cell firing

As expected, increasing levels of depolarising current injection in pyramidal neurones causes an increase in the firing rate (Figures 5.1&5.2). The current-discharge plots shown in figure 5.2 indicate that these relationships can be linear or non-linear in character as has been described previously (Lanthorn et al., 1984). The physiological input-output relationship of cortical neurones has not been well characterised to date because there is no method for measuring the synaptic input to a cell whilst simultaneously recording the corresponding spiking output. Because of such technical difficulties, it is necessary to inject a known current (input) via a recording microelectrode (usually in the soma) and correlate the firing output with the artificially injected 'input'. Unfortunately, this simple design of experiment fails to realise the complexities of processing in dendritic structures, active conductances in the dendrites and the temporal signature of synaptic inputs. These difficulties aside however, this paradigm does give a crude picture of gross input-output (current-discharge) relationships.

The effectiveness of individual basket cells at suppressing the firing rate of pyramidal cells is clear from the current-discharge plots where, at specific stimulation intensities, concomitant activation of basket cells significantly reduces the mean initial firing frequency. However, in only three of the connections did such a reduction occur over the complete range of stimulus intensities tested. Theoretical studies predict that inhibition close to the action potential initiation zone will be effective at suppressing firing activities only at low stimulus intensities and that such inhibition will be saturated at higher stimulation intensities (Douglas & Martin, 1990). The current-discharge relationships described in figure 5.2 show no such trend, although the range of stimulus intensities tested was limited. One

complicating factor however, is that the firing responses in all pyramidal neurones tested showed accommodation in the firing frequency (Figure 5.1) the conductances for which were not included in the aforementioned simulation. It is therefore not clear from the data described here whether the GABAergic inhibition was acting only on the generation of fast action potentials or whether it was also influencing other conductances which shape firing responses. In relation to this point, it is interesting to note that dendritic inhibition has little effect on fast sodium spikes, yet is particularly effective at suppressing underlying slow calcium spikes (Miles et al., 1996). Another interesting aspect of these results relating to the mechanisms underlying inhibition of firing concerns shunting versus hyperpolarising inhibition (Coombs et al., 1955). Theoretical studies also indicate that different forms of inhibition will produce different effects on the current-discharge relationship. Whilst hyperpolarising inhibition produces a linear subtraction of firing rate (see Bloomfield, 1974; Amthor & Grzywacz, 1991), the resultant firing rate being determined by the sum of excitation coupled to a negative offset, shunting inhibition multiplies any amount of excitation by some fixed fraction. It is thus predicted that hyperpolarising inhibition will shift the current-discharge relationship curve to the right, whilst shunting inhibition will decrease the slope of the input-output plot. Such differences may be important in terms of the placement of the GABAergic synapses, as hyperpolarising inhibition will be detected some distance from the synapses, whereas the large increase in conductance required for shunting inhibition will only be effective locally. As the current-discharge plots generally appeared to show a shift to the right and no apparent systematic change in slope (except 5.2D), this agrees with the notion of basket cell-mediated hyperpolarisation passively propagating to the action potential trigger zone - the axon initial segment (Stuart & Sakmann, 1994), providing a hyperpolarising 'subtractive' inhibition. However, the current-discharge relationship could not be quantified satisfactorily given the low number of points sampled, its non-linearity and the many additional factors that have to be considered including frequency range, input resistance,

strength and kinetics of evoked inhibition and firing pattern of pre- and postsynaptic cells (e.g. bursting versus regular firing). Clearly, the importance of the placement of GABAergic synapses (e.g. from basket versus axo-axonic cells) in relation to their effectiveness over action potential generation at the axon initial segment needs further detailed investigation.

5.4.2 Unitary IPSPs control the timing of pyramidal cell activities

In contrast to the effect of basket and axo-axonic cells on the overall discharge rate of pyramidal cells, their effect on the timing of action potentials was dramatic and robust. That rhythmic activation of individual presynaptic basket and axo-axonic cells instantly and reliably phase-locked the activity of pyramidal cells suggests that a key role for certain 'inhibitory' GABAergic local-circuit interneurones may be to sculpt temporally the activity of pyramidal cells. Evidence suggesting such a functional role comes from the alternating firing patterns of basket and pyramidal cells during theta activity *in vivo* (Ylinen et al., 1995b) as seen during periods of entrainment in vitro (Figure 5.3). Moreover, the effectiveness of basket and axo-axonic cells at synchronising pyramidal cell activities at both sub- and suprathreshold levels may also provide a mechanism to synchronise subthreshold membrane potential oscillations seen in the majority of pyramidal cells during theta activity *in vivo* and which are also phase related to the extracellular theta EEG pattern (Buzsáki & Eidelberg, 1983; Ylinen et al., 1995b).

Previous theoretical studies have predicted that neocortical GABAergic interneurones may phase-lock principal cell firing in the gamma frequency range (Lytton & Sejnowski, 1991). Although these studies have modelled a slightly different system (gamma frequency spectrum (~40Hz) in neocortical pyramidal cells), the authors estimated that the small conductances associated with individual GABAergic inputs would require the concerted action of several GABAergic basket cells to adequately entrain pyramidal cells activities. These experiments however indicate that individual interneurones with mean conductances around 1.5nS are sufficient to entrain pyramidal cell firing. The effectiveness of individual basket and axo-axonic cells in this study are thus surprising and suggest the presence of powerfully tuned mechanisms, whereby synaptic responses elicited by basket and

axo-axonic cells interact with intrinsic mechanisms underlying action potential discharge in pyramidal cells.

5.4.3 Mechanisms underlying inhibitory phasing of pyramidal cells

The effect of basket and axo-axonic cell-evoked IPSPs was to *suppress* but thereafter to *facilitate* action potential generation, so that a cluster of 'rebound' action potentials occurred following a period of inhibition. This rebound cluster of action potentials preferentially occurred in a period after the IPSP which coincided temporally with the previously described 'post-inhibitory facilitation' or 'rebound depolarisation' (Andersen et al., 1963 ; Kandel & Spencer, 1961) seen at sub-threshold membrane potentials. This rebound depolarisation only occurred at membrane potentials close to action potential threshold and disappeared upon hyperpolarisation of the pyramidal cells suggesting, that the hyperpolarisation associated with the IPSP was interacting with intrinsic voltage-gated conductances to produce the period of rebound depolarisation and action potentials. This was confirmed by injecting brief hyperpolarising current pulses with the somatic recording electrode, mimicking IPSPs, which produced similar rebound action potentials and depolarising overshoots. The exact ionic conductance responsible for such rebound overshoots remains to be established. Prime candidate mechanisms mediating the rebound depolarisation include the deinactivation of sodium and / or calcium channels (Carbone & Lux, 1984; Stafstrom et al., 1985; Llinás, 1988) as well as the activation of the hyperpolarisation activated current I_h (Halliwell & Adams, 1982; Maccaferri et al., 1993). However, since the rebound depolarisation only occurred at membrane potentials in a narrow range close to action potential threshold and where subthreshold membrane potential oscillations were also apparent, it is tempting to speculate that similar ionic mechanisms underlie both phenomena. Indeed, figure 5.5D indicates that the rebound depolarisation seen in

averaged synaptic responses is at least in part due to resetting the phase of sub-threshold membrane potential oscillations. Several voltage-dependent conductances have been reported to be involved in theta frequency sub-threshold membrane potential oscillations in CA1 pyramidal cells (Leung & Yim, 1991; Garcia-Munoz et al., 1993) as well as other cortical neurones (Alonso & Llinás, 1989; Llinás, 1988; Amitai, 1994). The exact contribution of individual types of ion channel remains to be established using detailed pharmacological tests.

That pyramidal cells exhibit rhythmic sub-threshold oscillations and fire regularly suggests that each pyramidal cell possesses its own 'pacemaker' activity and that the effect of perisomatic IPSPs may be to reset and thereby phase this activity. Since several spike clusters occur following perisomatic IPSPs suggests that the hyperpolarising response resets an intrinsic rhythmic state, rather than simply delaying the onset of action potential generation (Figure 5.5C). Such an action of IPSPs is apparent from the ability of IPSPs to reset or initiate sub-threshold oscillations (Figure 5.5D).

5.4.4 Functional implications

The entrainment of pyramidal cells by single basket and axo-axonic cells, both at sub- and supra-threshold membrane potentials, suggests that synchronisation of pyramidal cell activity may be a fundamental functional role for these interneurones. Minimal stimulation of GABAergic interneurones was shown to synchronise the firing of two spontaneously active pyramidal cells. Indeed, one single IPSP reset regular firing in both pyramidal cells whilst rhythmic minimal stimulation at theta frequencies phase-locked both neurones (Figure 5.6). Given the divergent nature of local-circuit interneurones (Li et al., 1992; Buhl et al., 1994a; Sík et al., 1995; Halasy et al., 1996), single basket or axo-axonic cells will synchronise the activity of very large principal cell populations which they innervate. The exact contribution of different subtypes of interneurone remains to

be established as they may be differentially active during different behavioural states. Anatomically identified basket cells have been reported to fire phase-related to extracellularly recorded theta oscillations (Ylinen et al., 1995b), whereas no such data are yet available for axo-axonic cells. As suggested by rhythmically occurring IPSPs in basket cells during theta activity (Ylinen et al., 1995b), the basket cells themselves may be phased by GABAergic inputs from the medial septum (Freund and Antal, 1988), or from other interneurones in the hippocampal network. In addition, periodic excitation through recurrent axon collaterals from the pyramidal cells (Buhl et al., 1994a; Gulyás et al., 1993b) would strengthen rhythmic basket cell discharges, suggesting a functionally relevant role for such a feedback loop (Andersen et al., 1963) in synchronisation of cortical pyramidal cells (Andersen and Eccles, 1962). The results suggest that post-inhibitory 'rebound' activation of cortical principal cells must be considered as a fundamental facet in the functional repertoire of GABAergic interneurones acting on $GABA_A$ receptors (Mody et al., 1994). The interaction of the synaptic events with intrinsic conductances provides a powerful mechanism, such that one single interneurone is sufficient to synchronise a large neuronal population. Given the ubiquitous nature of perisomatic GABAergic innervation throughout cortical structures (Somogyi, 1989), GABAergic phasing may represent a general mechanism for synchronisation of cortical activity (Lytton and Sejnowski, 1991). Indeed, intracellular recordings *in vivo* show that, at several distinct frequencies, rhythmic oscillatory activity is associated with periodic IPSPs, both in the hippocampus (Soltész and Deschenes, 1993; Ylinen et al., 1995a,b) and the neocortex (Steriade et al., 1993). Moreover, recent evidence indicates that interneurones which terminate onto pyramidal cell dendrites may subserve a key role in synchronising oscillatory activities in dendrites (Paulsen & Vida, 1996). Such control over dendritic oscillations may be important in temporally gating excitatory inputs (Lampl & Yarom, 1993) and modulating their plasticity (Huerta & Lisman, 1993, 1995, 1996a,b). Hippocampal interneurones are known to exhibit pacemaker currents (Maccaferri & McBain, 1996).

In conclusion, the data presented here supports the mounting consensus that, in addition to the more classical role of providing an inhibitory drive in opposition to excitation, local-circuit GABAergic interneurones can effectively control temporal aspects of hippocampal principal cell activity. They directly demonstrate that individual interneurones can exert a profound influence over the temporal activity of pyramidal cells by the polarising effect of the relatively small synaptic conductance interacting with voltage-gated intrinsic conductances , in turn, modulating the timing of the very large conductances associated with firing activities of principal cells. Thus, by phasing and resetting rhythmic activity in a large population of pyramidal cells, I suggest that subsets of cortical interneurones serve key roles in synchronising principal cell activity, thus providing temporal references relative to which specific information may be coded.

Figure 5.1 Effect of basket cell-mediated inhibition on current-induced discharge in a CA1 pyramidal cell.

(A) Traces indicate basket cell membrane potential during control (no current injection) and test (0.5nA depolarising current pulse) periods. (B) Representative responses in postsynaptic pyramidal cell to depolarising current steps (amplitudes to left of traces) before (control) and during (test) basket cell discharge. Note that generation of action potentials is delayed and the firing frequency is reduced during simultaneous activation of the presynaptic basket cell. Input resistance of pyramidal cell = 46MΩ; mean estimated conductance of basket cell-mediated unitary IPSP at this connection = 1.1nS. Action potentials are truncated due to sampling rate.

A

50mV

100ms

presynaptic basket cell

I_{inj}

B

0.3nA

postsynaptic pyramidal cell

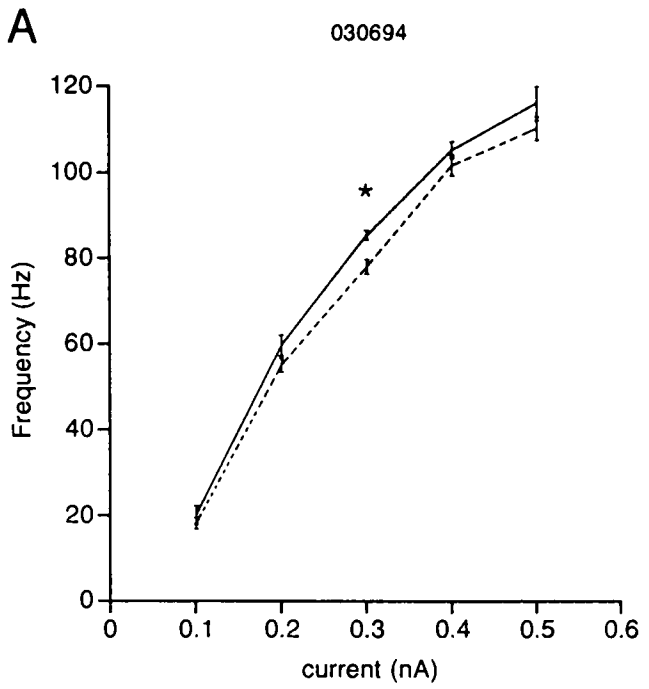
0.4nA

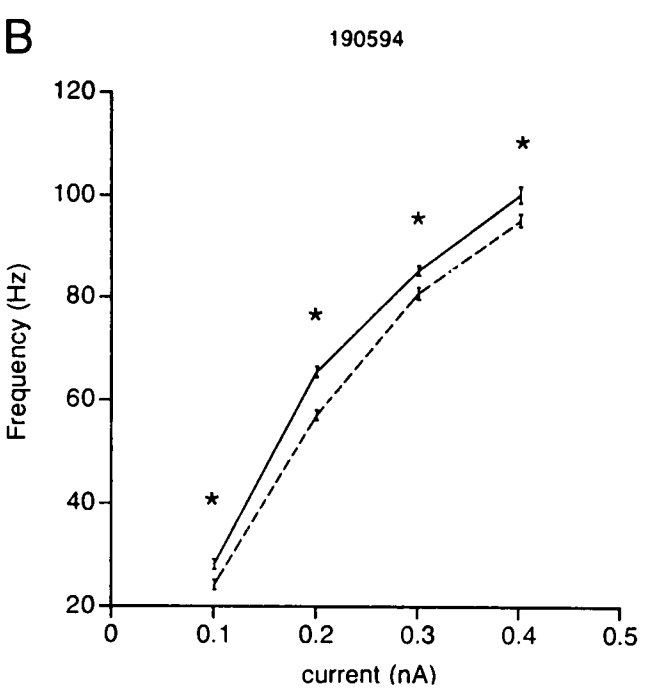
0.5nA

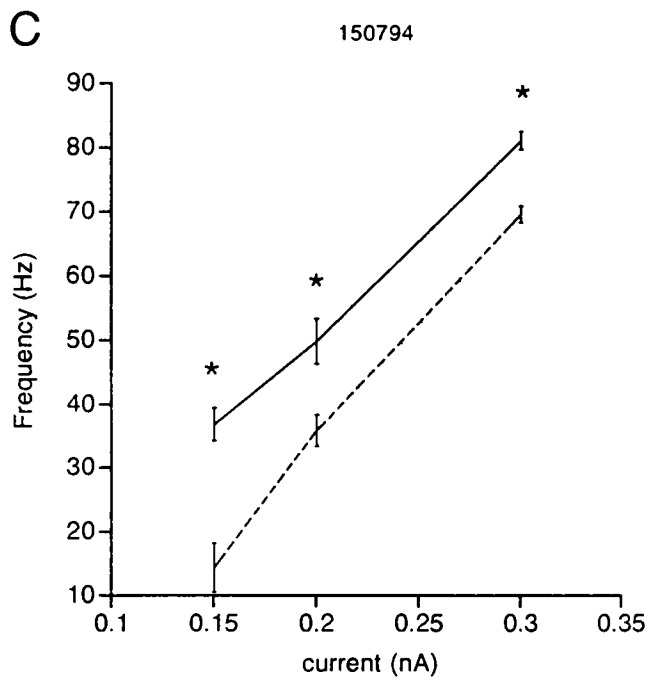
I_{inj}

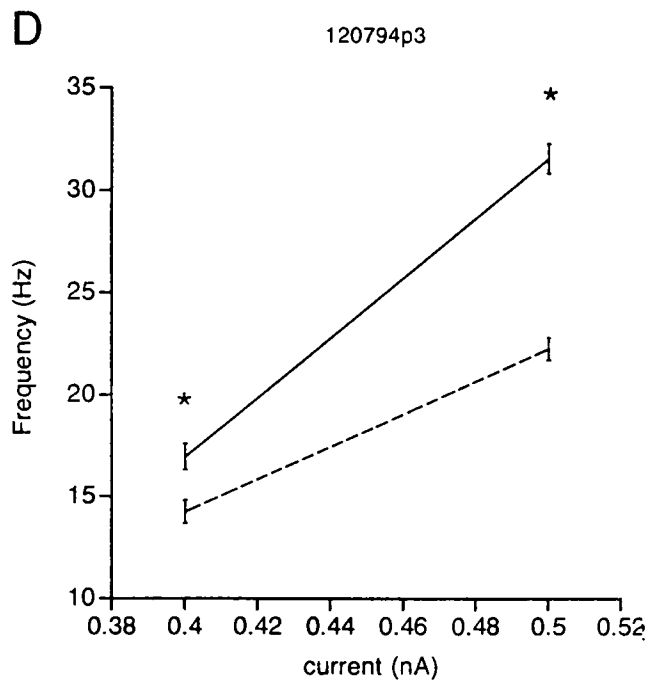
Figure 5.2 Suppression of pyramidal cell firing by basket cell-mediated IPSPs. (A-F) Graphs of initial firing frequency (Hz) of pyramidal cell action potentials plotted against the amplitude of the current pulse injected via the somatic recording electrode (nA) producing the firing response. Solid lines represent control plots. Dotted lines show current-discharge relationship during concurrent activation of individual presynaptic basket cells. Note that activation of the basket cells shifts the current-discharge plots to the right.

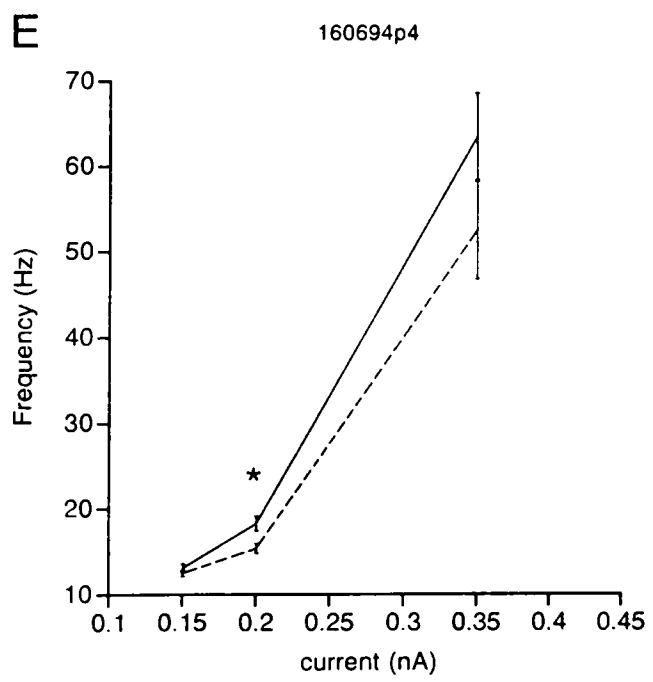
Frequency measurements were derived from the reciprocal of the first inter-spike interval and are given as the mean ($n \geq 5$ pulses) $\pm$ standard error (error bars). Asterisks represent significant differences between control and test frequencies ($P < 0.05$; Mann-Whitney U test).


A
030694
Frequency (Hz)
current (nA)


B
190594
Frequency (Hz)
current (nA)


C
150794
Frequency (Hz)
current (nA)


D
120794p3
Frequency (Hz)
current (nA)


E
160694p4
Frequency (Hz)
current (nA)

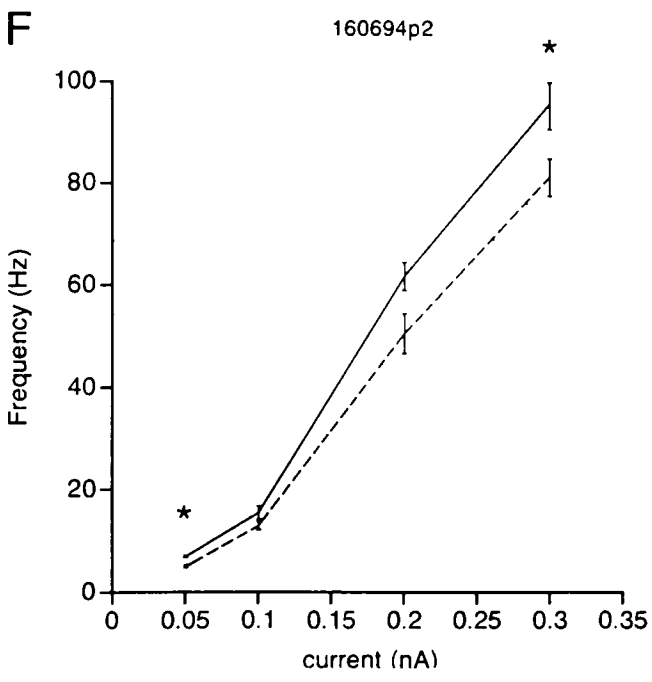
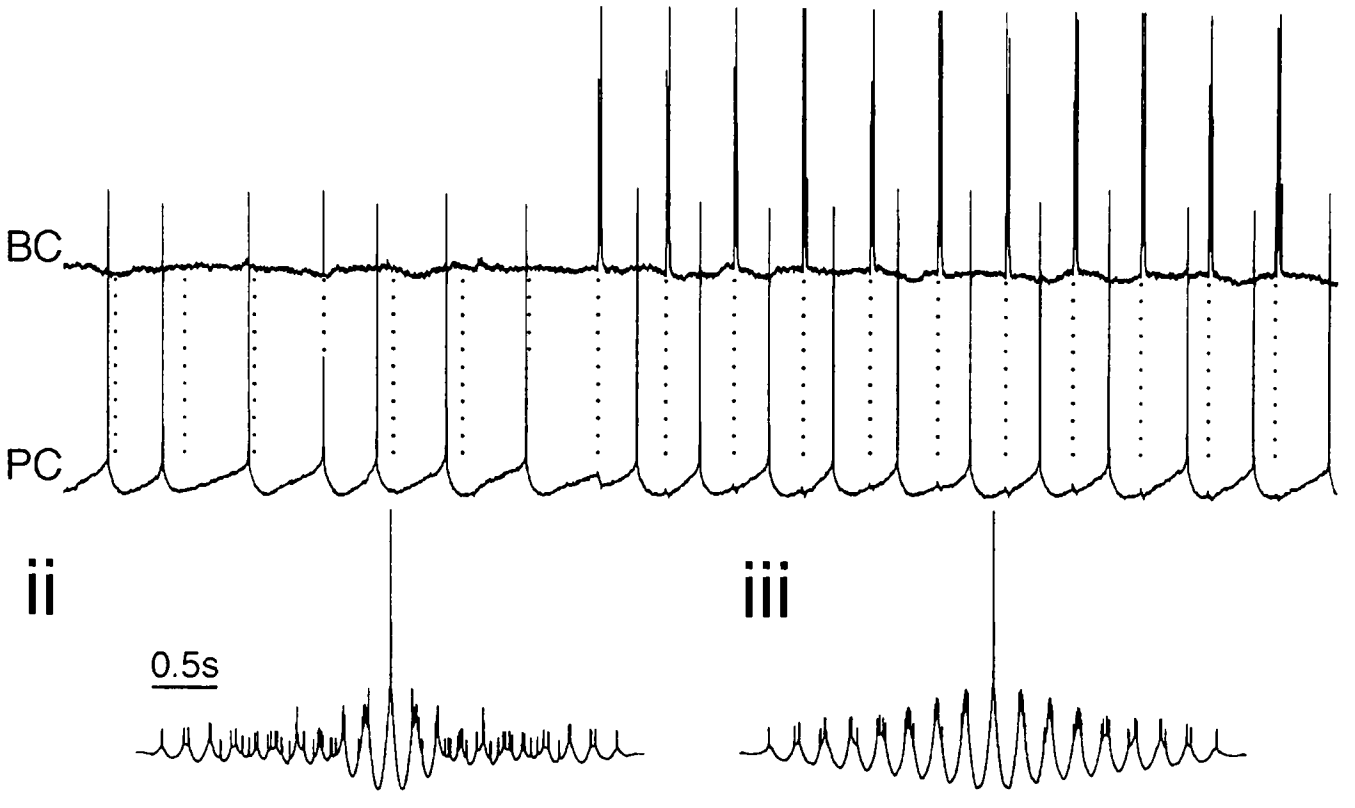

F
160694p2
Frequency (Hz)
current (nA)

Figure 5.3 Phase-locking of pyramidal cell discharge by a single presynaptic basket cell.

(Ai) The firing of a pyramidal cell (lower trace), depolarised by constant current injection, becomes instantly entrained by periodic activation (4.7 Hz) of short trains of 3-4 action potentials in the presynaptic basket cell (upper trace, action potentials truncated). Dotted lines indicate intervals of 0.21 s. In all 5 basket and 2 axo-axonic cell to pyramidal cell connections tested for entrainment, the postsynaptic pyramidal cell became instantly phase-locked to the interneurone activity, firing at opposite phase to the interneurone. By entraining the postsynaptic pyramidal cell, the interneurones could decrease or increase the mean discharge rate of the pyramidal cell. Autocorrelation of the trace prior to (Aii) and during (Aiii) regular basket cell activity shows an increased rhythmicity of pyramidal cell firing during periodic activation of the interneurone. (Bi) Effect of periodic rhythmic discharge of a single basket cell on sub-threshold membrane potential oscillations in a pyramidal cell. Dotted lines indicate intervals of 0.26 s. Autocorrelograms of the trace prior to (Bii) and following entrainment (Biii) show an increased rhythmicity during periodic activation of the interneurone.

Ai



Bi

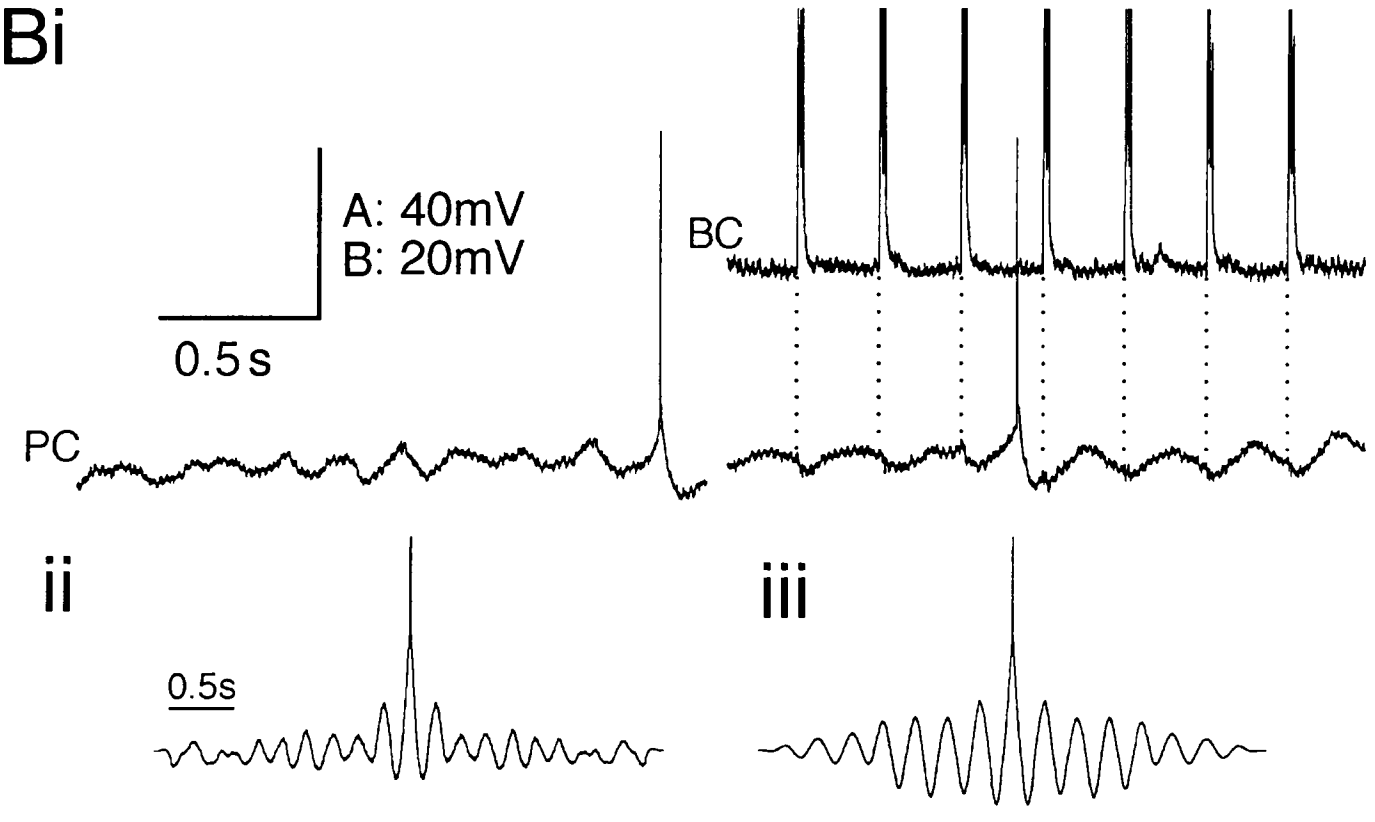
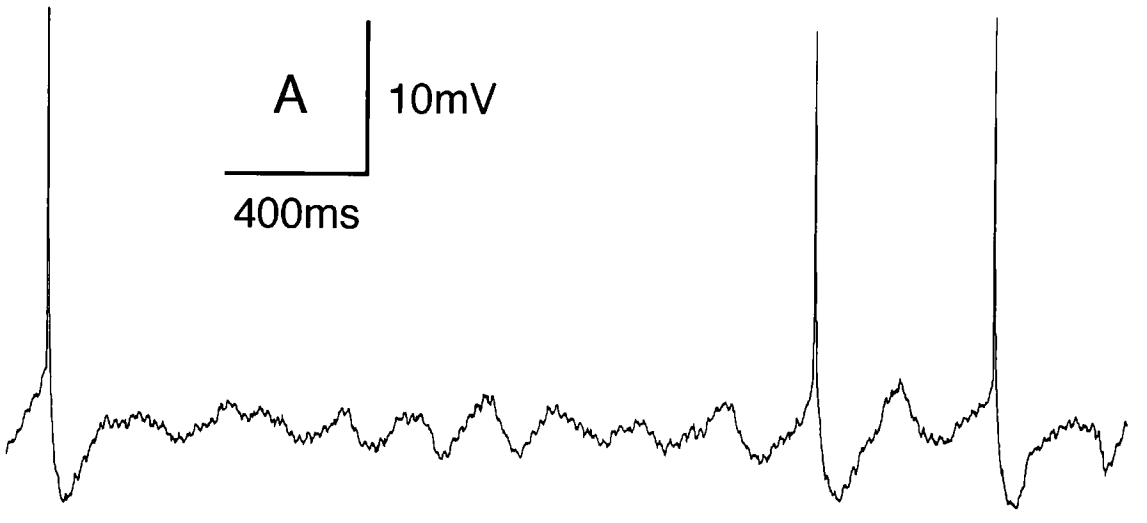


Figure 5.4 Subthreshold membrane potential oscillations

(A) Pyramidal cells depolarised to action potential threshold (-49.6mV) by constant current injection, reveal action potentials and subthreshold membrane potential oscillations. (B) Power spectral analysis reveals a prominent peak, indicating a dominant oscillatory frequency of 5Hz. Subthreshold membrane potential oscillations (frequency range 3-7Hz) were apparent in all 8 of 8 cells tested. Action potentials are truncated due to sampling rate and filtering.

A


A
10mV
400ms

B

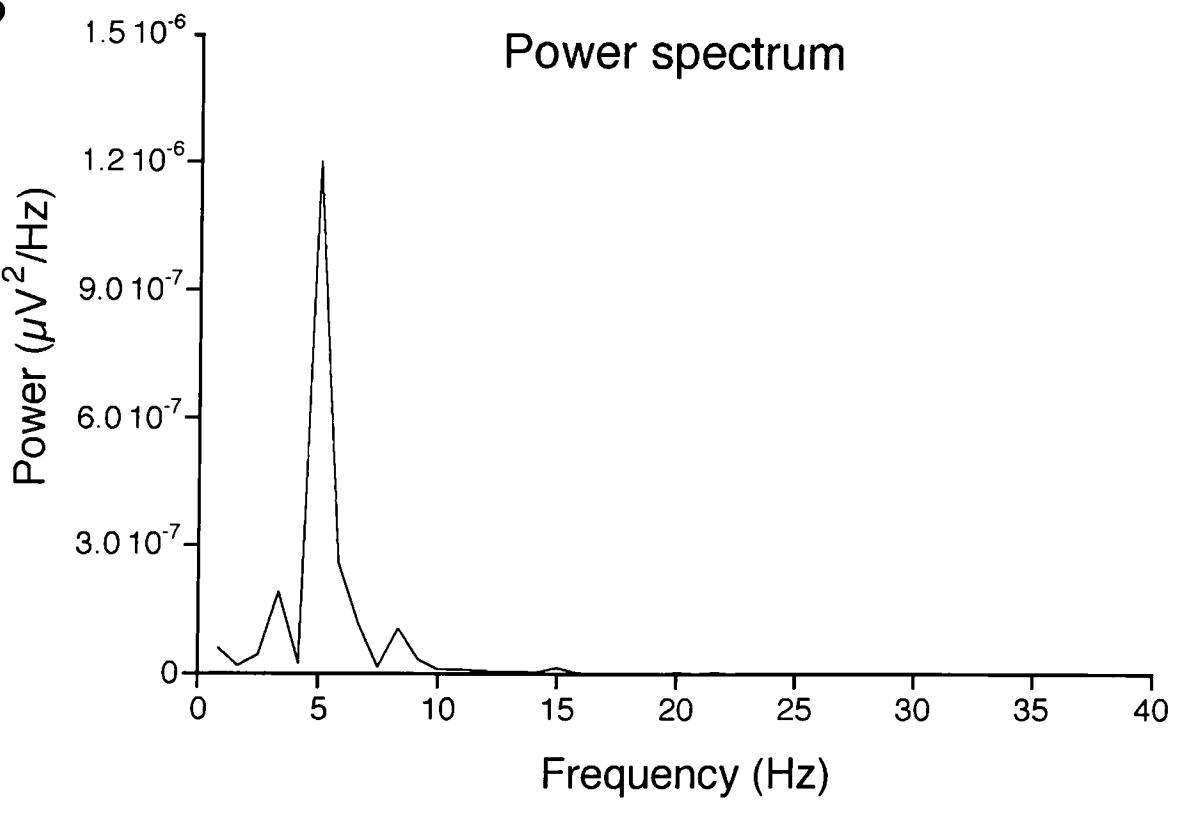

Power spectrum
1.5 10-6
1.2 10-6
9.0 10-7
6.0 10-7
3.0 10-7
0
Power (μV2/Hz)
0
5
10
15
20
25
30
35
40
Frequency (Hz)

Figure 5.5 Mechanism underlying phasing of pyramidal cells.
(A) Effect of a short train of 3-4 action potentials (position indicated by filled arrow) elicited by the presynaptic basket cell in a pyramidal cell at varying membrane potentials. (Ai) Superimposition of 12 consecutive sweeps in which the IPSP was followed by an action potential. (Aii) Average of 23 sweeps showing subthreshold rebound depolarisation following the IPSP. Note that the action potentials shown in (Ai) cluster in a region temporally coinciding with the rise of the depolarising overshoot. (Aiii) Postsynaptic response evoked at a more hyperpolarised membrane potential showing a mono-exponential decay and no depolarising overshoot. (B) Effect of brief hyperpolarising current pulses in a pyramidal cell. (Bi) Superimposition of 5 single sweeps in which a small hyperpolarising current pulse (0.05 nA) elicited a rebound action potential. (Bii) Average of 333 sweeps showing subthreshold rebound depolarisation following a short hyperpolarising current pulse. (Biii) Identical current pulses at more hyperpolarised membrane potentials failed to produce a depolarising overshoot.
(C) Effect of unitary IPSPs on the firing of the postsynaptic pyramidal cell. (Ci) shows 19 consecutive sweeps aligned on the rising phase of single action potentials (trigger point indicated by filled triangle) evoked at 0.75 Hz in the presynaptic basket cell. (Cii) is the corresponding spike histogram for a total of 132 sweeps with 572 spikes. Note the regular occurrence of peaks in histogram following the IPSP. Bin width, 20 ms. (D) Effect of unitary IPSP on subthreshold membrane potential oscillations of a postsynaptic pyramidal cell. (Di) Single sweep showing subthreshold membrane potential oscillations of the pyramidal cell. (Dii) Three superimposed sweeps demonstrating the effect of single unitary IPSPs (triangle) on subthreshold oscillations in the pyramidal cell. The positive peak of each cycle has been marked with an open circle. At whichever phase or membrane potential the IPSP occurred, the IPSP effectively reset the oscillation. (Diii) Single sweep demonstrating that a unitary IPSP can initiate oscillations in the pyramidal cell, when no obvious oscillatory activity was present prior to the IPSP. (Div) Average of 15 sweeps without action potentials. Subthreshold oscillatory activity occurring at random phases resulted in a flat pre-event base-line. The IPSP was followed by a characteristic waveform, consistent with the IPSP resetting an intrinsic oscillatory state.

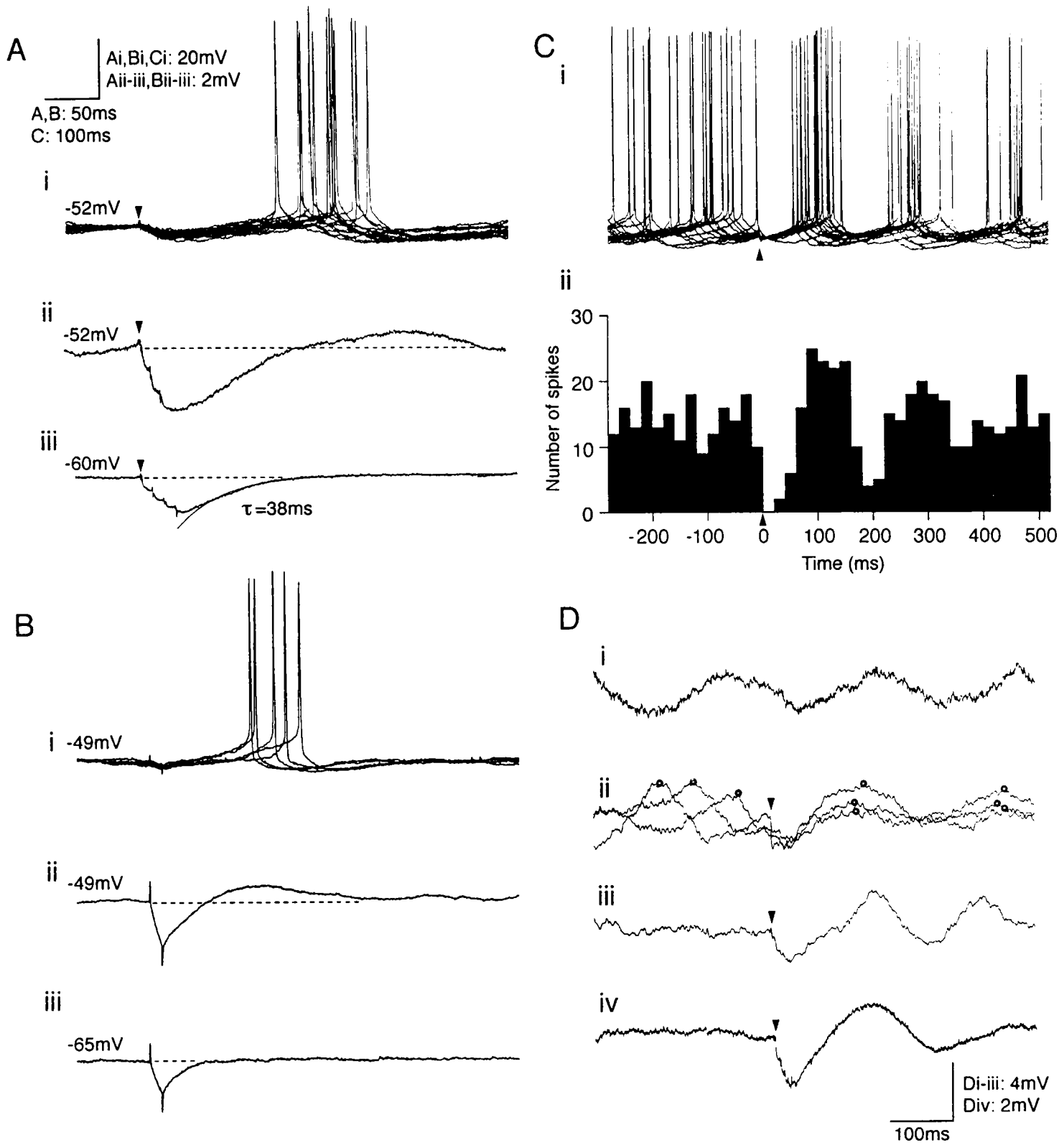
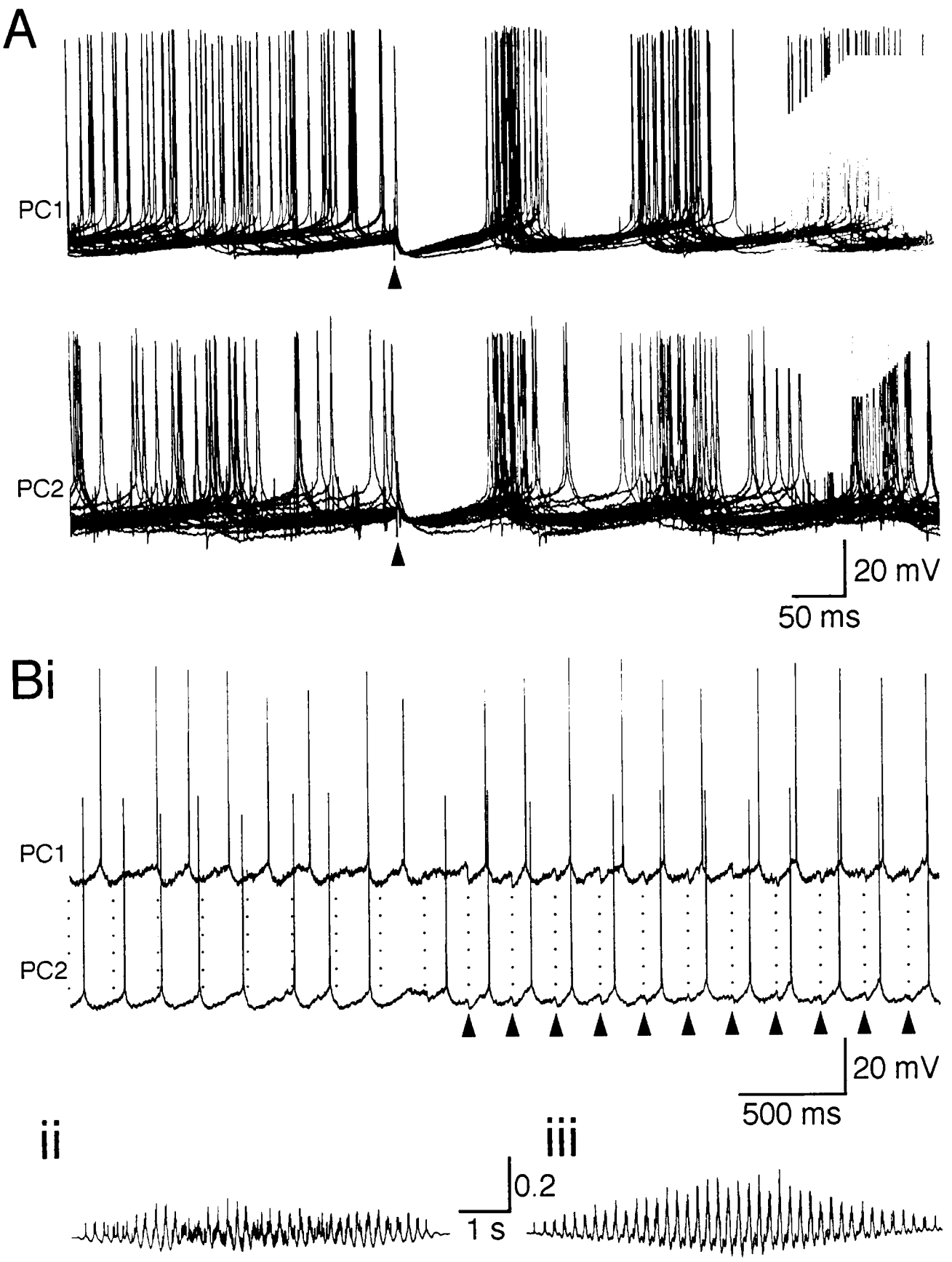

A
Ai,Bi,Ci: 20mV
Aii-iii,Bii-iii: 2mV
A,B: 50ms
C: 100ms
i
-52mV
ii
-52mV
iii
-60mV
τ=38ms
B
i -49mV
ii -49mV
iii
-65mV
C
i
ii
Number of spikes
30
20
10
0
-200 -100 0 100 200 300 400 500
Time (ms)
D
i
ii
iii
iv
Di-iii: 4mV
Div: 2mV
100ms

Figure 5.6 Synchronisation of pyramidal cell firing in the presence of ionotropic glutamate receptor antagonists.

(A) Two simultaneously recorded pyramidal neurones were depolarised to elicit action potentials during which single IPSPs (triangle), evoked at 0.2-0.5 Hz by minimal stimulation, reset the regular firing of both cells (30 consecutive sweeps, n=5). The stimulation strength was adjusted to evoke an IPSP of an amplitude approximately equivalent (<2 mV) to that produced by an individual, intracellularly recorded interneurone. In addition, rebound depolarisation as in Figure 5.5aii could be evoked in both pyramidal cells (data not shown).

(Bi) Rhythmic IPSPs evoked by minimal stimulation at 5 Hz (triangles) synchronise the firing of two simultaneously recorded pyramidal neurones. Dotted lines indicate intervals of 0.2 s. (Bii) Cross-correlogram for the two neurones in a 5 s period prior to rhythmic minimal stimulation. (Biii) Corresponding cross-correlogram for a 5 s period following the start of rhythmic minimal stimulation. Note more pronounced cross-correlation during entrainment.


A
PC1
PC2
20 mV
50 ms
Bi
PC1
PC2
20 mV
500 ms
ii
iii
0.2
1 s

Chapter 6. Common sources of GABAergic input to interneurones and pyramidal cells

6.1 Introduction

Much effort in recent years has been devoted to characterising GABAergic mechanisms in the hippocampus, mainly in terms of the effect on principal cells (reviewed by Thompson, 1994). However, GABAergic interneurones are themselves also under GABAergic control. They show both fast (putative $GABA_A$) and slow (putative $GABA_B$) IPSPs (Misgeld and Frotscher, 1986; Lacaille et al., 1987; Scharfman et al., 1990; Lacaille, 1991, Buhl et al., 1994a,b, 1996; Sík et al., 1995) which are currently assumed to originate from three main sources. These include a selective extrinsic input from GABAergic cells in the medial septum (Freund and Antal, 1988; Gulyás et al., 1990; Miettinen et al., 1992; Ascady et al., 1993); intrinsic inputs from hippocampal GABAergic interneurones, which also innervate principal cells (Nunzi et al., 1985; Harris et al., 1985; Sík et al., 1995); and recently described GABAergic interneurones, which selectively target other interneurones (Acsády et al., 1996b; Gulyás et al., 1996).

Although some physiological evidence suggests the existence of an interconnected network(s) of inhibitory interneurones (Lacaille and Schwartzkroin, 1988b; Michelson and Wong, 1991, Scharfman et al., 1990, Whittington et al., 1995), electrophysiological studies of GABAergic interneurones, to date, have focused almost exclusively on their influence over the local population of principal cells (Knowles and Schwartzkroin, 1981; Miles and Wong, 1984, 1987; Lacaille et al., 1987; Lacaille and Schwartzkroin, 1988b; Miles, 1990; Scharfman et al., 1990; Buhl et al., 1994a, 1995). Therefore, the mechanism and site of action of GABAergic cells on other interneurones remain to be established. The experiments described in this chapter, dual intracellular recording techniques in conjunction with biocytin labelling were employed to identify directly those types of interneurones in area CA1 of the rat hippocampus which innervate other interneurones in addition to pyramidal cells. Moreover, I sought to establish whether both the physiology as well as the anatomy of such synaptic interactions differ from those with pyramidal cells.

6.2 Materials and methods

Detailed description of the preparation of hippocampal slices, electrophysiological recording, biocytin labelling, and the subsequent correlated light and electron microscopic methods are given in chapter 2. In brief, intracellular recordings were obtained in 400μm transverse hippocampal slices of adult (>150g) female Wistar rats. Slices were maintained at 34-35°C on a nylon mesh at the interface between oxygenated artificial cerebrospinal fluid (ACSF, see 2.1.3) and a humidified atmosphere saturated with 95% O_2 and 5% CO_2. The flow rate was adjusted to 1.5-2ml min^{-1}. Micropipettes were filled with 2% biocytin in 1.5M KCH_3SO_4 and bevelled to a d.c. resistance ranging between 60-150MΩ. Putative interneurones were identified using previously established physiological criteria (Knowles & Schwartzkroin, 1981). When a stable recording was obtained, a search was made for synaptically coupled interneurones and pyramidal cells. Cells were made to fire action potentials by depolarising current injection and synaptic coupling tested using on-line using spike-triggered averaging. Capacitive coupling was eliminated on-line, using a modified axoprobe amplifier (section 2.2). Diffusion of biocytin during recordings generally resulted in adequate filling. Slices were processed for light and electron microscopy as described (section 2.3). The majority of electron microscopy was carried out at Jozsef Attila university, Szeged, Hungary in collaboration with Dr. K. Halasy. All values are shown as mean ± S.D.

6.3 Results

Following dual intracellular recordings between local-circuit interneurones and pyramidal cells in area CA1 of the rat hippocampus, on three occasions the presynaptic local-circuit interneurone could also be tested for synaptic coupling with other CA1 interneurones. This chapter presents the synaptic interactions of these three interneurones (cells 30, 35, 65 on table 2.1) with other hippocampal CA1

interneurones as well as pyramidal cells from a combined electrophysiological and morphological perspective.

6.3.1 Basket cell-to-bistratified cell pair

6.3.1.1 Anatomical analysis

Following simultaneous recording of two fast-spiking putative local-circuit interneurones, visualisation of the biocytin labelling confirmed that both cells share morphological features common to many GABAergic interneurones. Both cells had fusiform somata located in stratum pyramidale, approximately 150 μm apart (Figure 6.1). Their somata gave rise to several basal and apical dendrites which were smooth and beaded in appearance. However, the two cells differed with respect to the extent that their apical dendrites ramified within the molecular layer. Whilst the presynaptic cell had extensive dendrites which fanned out, traversing stratum radiatum before branching in a dichotomous manner within stratum lacunosum-moleculare, the apical dendrites of the postsynaptic neurone ramified extensively within stratum radiatum, but without extending into the molecular layer. These latter dendritic features are highly characteristic of bistratified cells (Buhl et al., 1994a, Halasy et al., 1996).

The axon of both cells branched extensively, giving rise to multiple local collaterals. A partial reconstruction of their axons is shown on Figure 6.1. The axon of the presynaptic cell was confined mainly to an area in and adjacent to stratum pyramidale (omitted for clarity of display). A representative portion of this axon was examined at the electron microscopic level, allowing evaluation of a randomly selected sample of boutons and their postsynaptic targets (n=12). This cell made synapses with somata (50% of synaptic targets examined) of pyramidal cells and proximal dendritic shafts. Such selective innervation of the perisomatic

domain of its target neurones confirms this cell to be a basket cell (Buhl et al., 1995).

By continually following the axon from the presynaptic basket cell, several axonal branches were found to project towards the labelled postsynaptic interneurone where several boutons appeared to be apposed to its somatic and proximal dendritic membrane. A total of 11 suspected sites of synaptic contact were predicted at the light microscopic level. A block containing all presumed sites of contact was re-embedded and serial ultra-thin sections were cut for further evaluation at the electron microscopic level (Figure 6.2). Of the 11 boutons tested, ten were confirmed to form symmetrical (type 2) synaptic contacts (Gray, 1959; Blackstad and Flood, 1963), whereas one bouton did not form a synapse with the postsynaptic neurone. In two instances, a single bouton made two synaptic junctions (Figure 6.1 inset, bouton 2), so that the presynaptic basket cell established a total of 12 synapses with the soma (n=7) and proximal apical (n=2) as well as basal (n=3) dendritic shafts of the postsynaptic interneurone.

The axon of the postsynaptic cell was weakly filled and could be only partially visualised. Due to the difference in biocytin filling, the axonal branches of the two cells could be identified and differentiated clearly. Unusually, two separate axons emerged from the soma, one projecting into stratum radiatum where it branched extensively, whilst the other ramified close to the border between strata pyramidale and radiatum. From this apparent innervation of the dendritic layers and from its characteristic dendritic arbour, this cell was identified as a bistratified cell (Buhl et al., 1994a, Halasy et al., 1996).

6.3.1.2 Synaptic coupling

Action potentials evoked in the basket cell (Figure 6.3A) were found to elicit hyperpolarising IPSPs in the postsynaptic bistratified cell (Figure 6.3B, IPSP amplitude 0.37mV at -55mV membrane potential). Evoked IPSPs had fast kinetics

(rise time ~1ms) and were of short-duration (duration 5.6ms at half-amplitude). In contrast to the basket-to-bistratified cell interaction, action potentials evoked in the bistratified cell failed to elicit detectable reciprocal synaptic responses in the basket cell (data not shown).

On withdrawal of the microelectrode from the bistratified cell, two pyramidal cells (P1 and P2) were subsequently impaled whilst maintaining the same presynaptic basket cell on the other microelectrode. Prior to morphological verification following biocytin visualisation, pyramidal cells were tentatively distinguished from local-circuit interneurones by their distinctive firing response to a depolarising current injection, which occurred in the form of a strongly accommodating train of action potentials. Moreover, pyramidal cell action potentials were generally overshooting, broader and lacked the fast, deep after-hyperpolarisation seen in interneurones (data not shown). For both pyramidal cells, activation of the common presynaptic basket cell elicited hyperpolarising IPSPs (Figure 6.3C,D; averaged IPSP amplitudes 0.31mV and 0.28mV at -57mV and -60mV membrane potential for P1 and P2 respectively), which also had fast kinetics (rise time 2.6ms and 3.2ms; duration 21ms and 16.4ms for P1 and P2, respectively).

6.3.2 Basket cell - to - fast-spiking interneurone pair

6.3.2.1 Anatomical analysis

Following simultaneous recording from two fast-spiking putative local-circuit interneurones, visualisation of the biocytin labelling revealed only a single filled cell in a position corresponding to the first (presynaptic) recording microelectrode. Failure to recover the second biocytin-injected cell may have resulted from inadequate amounts of biocytin entering the cell, owing to the relatively short impalement period. However, the characteristic response to a

depolarising current pulse in the form of a rapid train of very brief, non-accommodating action potentials with fast, deep after-hyperpolarisations (Figure 6.6F), strongly indicates that the postsynaptic cell was an interneurone. Unfortunately, in the absence of morphological verification, the exact type of interneurone cannot be determined from physiological characteristics alone (see Buhl et al., 1996).

Evaluation of the morphologically recovered putative presynaptic cell and subsequent reconstruction (Figure 6.4) showed the multipolar soma (red) located in stratum pyramidale giving rise to an extensive, stellate-like dendritic arbour (red). Dendrites extended radially into strata oriens, pyramidale and radiatum, but no dendrite entered stratum lacunosum-moleculare. The dendrites were smooth and beaded and did not branch except in stratum oriens, close to the alveus (Figures 6.4, 6.5A).

Reconstruction of the axon (black) showed this cell to possess an unusually dense axonal arbour, which was most dense in stratum pyramidale, but which also extensively ramified in both strata oriens and lower radiatum (Figures 6.4, 6.5A). In addition, the lateral extent of the axonal arbour was considerable, covering almost 900μm of the CA1 subfield and implying a highly divergent output. Within stratum pyramidale, the axon appeared to target somata, occasionally forming 'pericellular baskets' (Figure 6.5B) which, at the light microscopic level, indicated that the cell was a basket cell. However, an unusual feature of this cell was that the axon frequently formed vertically elongated axonal terminal branches which extended from stratum pyramidale into stratum radiatum. These branches appeared to run alongside apical dendritic trunks, forming multiple boutons along their length (Figure 6.5C). Electron microscopic evaluation revealed the postsynaptic targets (n=25, Figure 6.5D,E) to be somata of pyramidal cells(40%), proximal dendritic shafts (56%) and spines (4%). Such perisomatic innervation of postsynaptic target neurones confirms this cell to be a basket cell, although several of its features differ from all basket cells previously reported in the CA1 area.

6.3.2.2 Synaptic coupling

Action potentials (duration at half amplitude 0.40ms) evoked in the presynaptic basket cell (Figure 6.6A) were found to elicit hyperpolarising IPSPs (amplitude 0.3mV at -61mV membrane potential) with fast kinetics (rise time 15.2; duration at half-amplitude 49.6ms) in the postsynaptic interneurone (Figure 6.6B). As with the previous interneurone pair, activation of the second interneurone failed to elicit any detectable reciprocal synaptic response (data not shown). A short train of fast (80Hz), non-accommodating action potentials (amplitude 60mV) evoked by a depolarising current pulse in the presynaptic basket cell, resulted in a summated IPSP in the postsynaptic interneurone (Figure 6.6E). After reaching a plateau (summated IPSP amplitude 0.85mV at -65mV), the synaptic response diminished in spite of the continued activation of the presynaptic basket cell. However, like the effect seen in pyramidal cells during repetitive high frequency activation of presynaptic basket cells (Buhl et al., 1995), the synaptic response never completely faded.

Upon withdrawal of the microelectrode from the postsynaptic interneurone an adjacent pyramidal cell (identified as such by its distinctive electophysiological characteristics, see above) was subsequently impaled. Activation of the common presynaptic basket cell elicited hyperpolarising IPSPs (Figure 6.6C, IPSP amplitude 0.6mV at -57mV membrane potential) with fast kinetics (rise time 11.8ms; duration 38ms) similar to those produced in the postsynaptic interneurone.

6.3.3 Stratum lacunosum-moleculare / radiatum border interneurone - to - bistratified cell pair

6.3.3.1 Anatomical analysis

After simultaneous recording of a fast-spiking putative interneurone and a second fast-spiking interneurone, followed by a putative pyramidal cell, subsequent visualisation of biocytin labelling revealed three cells, all in good correspondence with the respective recording sites (Figure 6.7). Consistent with the electrophysiological data, two of the cells (red) revealed morphological characteristics of local-circuit interneurones whilst, the third (black) was a CA1 pyramidal cell.

The soma of the first impaled cell (upper red) was located in stratum radiatum, close to the border with the stratum lacunosum-moleculare (LM-R interneurone). This soma gave rise to several main dendrites which ramified both in strata radiatum and lacunosum-moleculare where they branched, though not extensively. Dendrites were mostly smooth, but some proximal main dendritic trunks protruded large thorn-like processes similar to a type of interneurone described previously (Lacaille and Schwartzkroin, 1988a,b). The LM-R interneurone axon was weakly filled, but nevertheless could be seen to ramify in stratum radiatum. The postsynaptic target profile of the LM-R interneurone was not determined. However, since most of the axon was contained in the stratum radiatum, it seems likely that it innervated mainly dendritic targets.

The second (postsynaptic, see below) interneurone (lower red) soma was located in stratum pyramidale and gave rise to smooth, slightly beaded dendrites ramifying in stratum oriens and radiatum, but not projecting into stratum lacunosum-moleculare. These characteristics are consistent with the cell being a bistratified type interneurone (Buhl et al., 1994a, Halasy et al., 1996). Labelling of the axon was weak and could not be traced far. Evaluation of randomly selected

boutons and their postsynaptic profiles at the electron microscopic level (n=11) showed this cell to innervate dendritic shafts (82%) and dendritic spines (18%), thus confirming the notion from the dendritic branching pattern that this interneurone was a bistratified cell, innervating the dendritic domain (Figure 6.8).

The third cell (Figure 6.7, black) was identified as a CA1 pyramidal cell whose soma was located in stratum pyramidale and whose apical and basal tuft of highly spinous dendrites extended and branched extensively in all layers of the CA1 subfield. The axon of the pyramidal cell (arrowhead indicates main axon) coursed towards the alveus where it branched, sending collaterals towards both the fimbria and the subiculum.

6.3.3.2 Synaptic coupling

Short trains of 8-10 action potentials were evoked in the SR-LM interneurone when testing for synaptic responses in the simultaneously recorded bistratified and pyramidal cells. This protocol was adopted as previous data have indicated that single action potentials are often insufficient to elicit any detectable response mediated by single SR-LM interneurones (Lacaille & Schwartzkroin, 1988b). The LM-R interneurone was found to be synaptically coupled to both the bistratified cell and the subsequently recorded pyramidal cell (Figure 6.8). Synaptic responses were similar in each case and were in the form of summated hyperpolarising IPSPs (peak amplitude 0.48 at -61mV and 0.46mV at -60mV for the bistratified and pyramidal cells respectively). No reciprocal synaptic coupling was observed in either cell pair (not shown). Because of the summated nature of synaptic responses, kinetic measurements of such responses were not obtained.

6.4 Discussion

This study demonstrates directly that local-circuit interneurones located in the CA1 area of the rat hippocampus receive a GABAergic input from several discrete intrinsic sources. Moreover, individual interneurones may provide a common divergent output to both principal cells and other interneurones, whilst retaining target selectivity towards a particular membrane domain. Indeed, both the number and placement of synapses provided by a basket cell to a bistratified cell were similar to those provided to pyramidal cells by other basket cells (Buhl et al., 1994a, 1995). In agreement, the kinetics and amplitudes of the postsynaptic responses were similar in both pyramidal cell and interneurone targets and were consistent with $GABA_A$ receptor-mediated synaptic responses.

6.4.1 Identification of pre- and postsynaptic neurones

All recovered fast-spiking cells shared common morphological features, including smooth, aspinous dendrites and dense local axon, which formed symmetrical type synapses. These results are consistent with the consensus that many local-circuit interneurones can be distinguished from principal cells by their distinctive firing and other salient membrane properties alone (Ashwood et al., 1984; Schwartzkroin and Kunkel, 1985; Misgeld and Frotscher, 1986; Kawaguchi and Hama, 1987a,b; Lacaille and Schwartzkroin, 1988a; Scharfman et al., 1990; Buhl et al., 1994a,b, 1995, 1996). However, specific morphological subtypes of interneurone cannot be reliably differentiated from each other solely on the basis of their intrinsic membrane properties (Buhl et al., 1994a, 1995, 1996) and therefore identification requires assessment at the light and electron microscopic levels (Halasy et al., 1996). The two basket cells identified in this study appear to represent different subclasses of basket cells, based on their dissimilar dendritic and axonal morphology. Indeed, the basket cell shown in Figure 6.4 is quite different

from those described in previous studies (Buhl et al., 1994a, 1995, Halasy et al., 1996) and appears to resemble more closely a "trilaminar cell" described previously by Sík et al. (1995) or the "wide axonal basket cell" described in the CA3 area by Gulyás et al.(1993a). Such differences in axonal and dendritic patterns may reflect different subtypes of basket cell that are known to exist, based on differential immunoreactivity to neurochemical markers (Nunzi et al., 1985; Harris et al., 1985; Sík et al., 1995). Likewise, the LM-R interneurone described in Figure 6.7 represents only one example of a number of different interneurones which are known to occur at the stratum radiatum / lacunosum-moleculare border (Vida et al., 1997).

6.4.2 Properties of postsynaptic responses

Hippocampal interneurones are known to express a range of $GABA_A$ receptor subunits (Zimprich et al., 1991; Gao and Fritschy, 1994; Nusser et al., 1995) and produce both fast (putative $GABA_A$) and slow (putative $GABA_B$) IPSPs (Misgeld and Frotscher, 1986; Lacaille et al., 1987; Scharfman et al., 1990; Lacaille, 1991, Buhl et al., 1994a, 1996; Sík et al., 1995), indicating that GABAergic neurones are themselves under GABAergic control. This study indicates that synaptic responses mediated by basket cells are similar in both pyramidal cells and other interneurones and their properties are consistent with unitary IPSPs described previously (Knowles and Schwartzkroin, 1981; Miles and Wong, 1984, 1987; Lacaille et al., 1987; Lacaille and Schwartzkroin, 1988b; Miles, 1990; Scharfman et al., 1990; Buhl et al., 1994a, 1995; Cobb et al., 1995).

In the absence of pharmacological verification, the finding that all unitary synaptic responses were hyperpolarising in the range of membrane potentials tested (-55 to -65mV) and had relatively fast kinetics is highly suggestive of a $GABA_A$ receptor mediated effect as previously demonstrated in pyramidal cells (Miles, 1990; Buhl et al., 1994a, 1995). It therefore seems likely that responses elicited by

individual interneurones in both pyramidal cells and other interneurones are mediated by similar receptor mechanisms. However, $GABA_A$ receptor subunits may not be uniformly expressed across different subtypes of interneurone (Gao and Fritschy, 1994; Nusser et al., 1995). In the future, detailed pharmacology of interneurone - to - interneurone connections may therefore reveal functional differences corresponding to different $GABA_A$ receptors with varying subunit composition.

The hyperpolarising nature of the unitary synaptic responses seen in this study is at variance with earlier studies addressing interneurone - to- interneurone network interactions in which the authors described a $GABA_A$ receptor mediated excitatory effect over other interneurones (Michelson and Wong, 1991, 1994). However, the hyperpolarising nature of the responses seen here is consistent with other studies which examined unitary interactions between unidentified pairs of putative interneurones (Lacaille and Schwartzkroin, 1988b; Scharfman et al., 1990). The previously reported depolarising responses evoked by population activity (Michelson and Wong, 1991, 1994) could be due to changes in the intracellular concentration of chloride and bicarbonate ions in the cells after synchronous activation of very large numbers of synapses (Staley et al., 1995).

The synaptic response mediated by the LM-R interneurone needs special consideration. Previous studies have shown that single action potentials elicited in presynaptic SR-LM interneurones may fail to evoke any postsynaptic response, whereas a short train of action potentials produces summated hyperpolarising synaptic responses with slow rise and decay kinetics (Lacaille and Schwartzkroin, 1988a,b), which may indicate different receptor mechanisms. However, summated responses evoked by trains of action potentials make accurate kinetic measurements difficult to obtain and interpret. Moreover, recent evidence shows that interneurones in stratum lacunosum-moleculare are morphologically more heterogeneous than previously supposed and their hyperpolarising postsynaptic responses can be abolished by $GABA_A$ receptor antagonists (Vida et al., 1997).

6.4.3 Sources of GABAergic input

GABAergic interneurones receive GABAergic input from three main sources. The primary extrinsic source originates from GABAergic cells in the medial septum which selectively target several classes of hippocampal interneurone (Freund and Antal, 1988; Gulyás et al., 1990; Miettinen et al., 1992; Acsády et al., 1993). The second source is from several recently described populations of hippocampal interneurones which selectively target some types of hippocampal interneurone, whilst avoiding others (Acsády et al., 1996b; Gulyás et al., 1996). These different sets of GABAergic cell can be identified by the presence of distinct neurochemical markers, such as calretinin and vasoactive intestinal peptide, and reveal a high degree of cross-talk amongst different interneurone types. In contrast, data reported here show that other types of interneurone mainly target principal cells, but also provide an intrinsic source of input onto other interneurones. These cells represent the third main source of GABAergic input onto hippocampal interneurones and include those immunoreactive for parvalbumin and cholecystokinin (Nunzi et al., 1985; Harris et al., 1985; Sík et al., 1995). By innervating both other interneurones as well as principal cells, all three presynaptic cells described in this study belong to this third category. The results indicate that the strength of synaptic connections given to postsynaptic pyramidal cells is approximately equivalent to that given to interneurones, since both the amplitude of evoked responses and the number of synapses provided by a single basket cell to a postsynaptic bistratified cell are similar to those received by individual pyramidal cells in the rat hippocampus (Buhl et al., 1994a, 1995). Although the selectivity of a single interneurone towards one type of postsynaptic cell over another cannot be established from these data, a previous study suggested an individual interneurone to innervate both other interneurones and pyramidal cells at a ratio (Sík et al., 1995) equivalent to which the two cell types occur in the hippocampus (Aika et al., 1994), thus implying no preference for one postsynaptic target cell over the other.

6.4.4 Functional implications

The existence of extensive synaptic cross-talk between GABAergic interneurones adds further complexity to the way we view hippocampal microcircuitry. Indeed, interconnectivity amongst interneurones may serve a role in controlling both spatial and temporal aspects of inhibition. The traditional view of an inhibitory neurone innervating a second such cell is that the consequent downstream effect would be one of disinhibition. Indeed, recent evidence suggests that the GABAergic septo-hippocampal input onto hippocampal interneurones does suppress spontaneous IPSP activity in pyramidal cells (Tóth et al., 1995). In the case of one class of interneurone evoking fast inhibition in another, however, it is possible to change the balance of inhibition from one membrane domain of a principal neurone to another (Gulyas et al., 1996. Switches in spatial aspects of inhibition have been reported to occur *in vivo* during exploratory behaviour in the dentate gyrus, where perisomatic inhibition is decreased when dendritic inhibition is increased (Moser, 1996).

A second role for interconnectivity amongst interneurones is predictable, given the observations that many types of interneurone fire within characteristic frequency bands during specific behavioural states (see Freund and Buzsáki, 1996). Rhythmic firing, coupled with the complex postsynaptic responses that assist coherence in the population (chapter 5), greatly extends the role of GABAergic neurones. Neuronal integration and coding is based both on the magnitude and temporal structure of responses (Mainen and Sejnowski, 1995; Kruger and Becker, 1991; Engel et al., 1992). The latter is implemented through the interaction of numerous voltage-gated intrinsic conductances within neurones, which profoundly shape neuronal responses and may endow individual neurones with intrinsic oscillatory properties, which may, in turn, facilitate coherent population activities (Llinás, 1988). Interconnected interneurone networks may therefore form a system of coupled oscillators, leading to emergent network

properties (Buzsáki and Chrobak, 1995; Whittington et al., 1995) which may provide a co-ordinated temporal structure across areas of the hippocampus, relative to which specific information is coded.

FIGURE 6.1: Intracellularly labelled basket cell -to- bistratified cell pair. The light microscopic reconstruction shows the presynaptic basket cell (soma and dendrites in grey, partially reconstructed axon in black) and the nearby postsynaptic interneurone (red) which has the characteristics of a bistratified cell. Arrows indicate the main axons originating from each cell. The postsynaptic bistratified cell gives rise to two main axons, which emerge from the basal portion of the soma. The inset indicates all electron microscopically identified sites of synaptic contact (n=12; see figure 6.2) made by 10 boutons of the presynaptic basket cell axon onto the postsynaptic bistratified cell. In two instances (marked with an asterisk), a single bouton formed two release sites, so that in total, seven synaptic contacts were made onto the soma and the remaining 5 onto proximal dendritic shafts. Electron microscopic evaluation of randomly selected synaptic terminals (n=12) showed that the basket cell innervated somata (50% of targets tested) and proximal dendritic shafts (50%) of unlabelled pyramidal cells. SP=stratum pyramidale, SR=stratum radiatum; Scale bar: 100µm

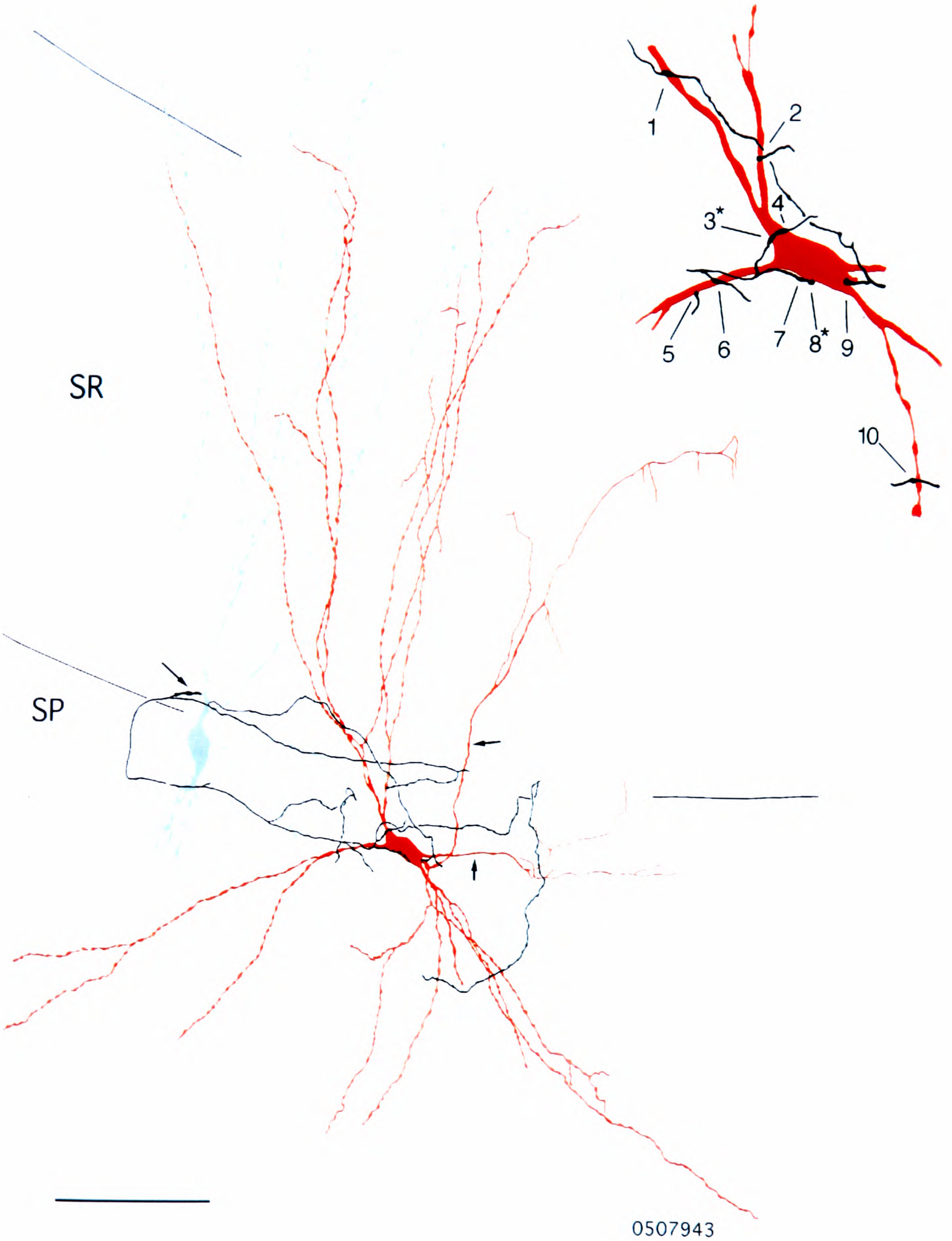

SR
SP
1
2
3*
4
5
6
7
8*
9
10
0507943

FIGURE 6.2: Light and electron micrographs of selected basket cell synaptic contacts onto the postsynaptic bistratified cell (shown in figure 6.1). Bouton numbers correspond to those in Figure 6.1 inset. (A) Light micrograph showing basket cell axon crossing the apical portion of the bistratified cell soma and forming two boutons, b3* and b4. (B,C) Electron micrographs of boutons b3* and b4 respectively, making symmetrical synaptic contacts (arrows) with the bistratified cell soma (SO). Bouton 3* forms two synaptic junctions. (D) Light micrograph of bouton 8 (arrow) in close apposition to the bistratified cell soma. (E) The corresponding electron micrograph confirms the presence of a symmetrical synaptic contact (arrow). The opposite side of the same bouton makes a second symmetrical synapse (open arrow) with an adjacent pyramidal cell soma (PS). (F) Light micrograph showing the basket cell axon forming a bouton (arrow, b2) close to a proximal apical dendrite of the postsynaptic bistratified cell. (G) Corresponding electron micrograph of the bouton (b2) showing the synaptic contact (arrow) with the dendrite (d). An adjacent unlabelled synaptic terminal also gives synaptic input (open arrow) to the bistratified cell. (H) Light micrograph of a basket cell bouton (arrow; b10) in close apposition to a basal dendrite of the postsynaptic bistratified cell. (I) The corresponding electron micrograph shows b10 forming a symmetrical synaptic contact (arrow) with the dendrite (d). Scale bars: A,D,F,H 2μm; B,C,E,G,I 0.5μm

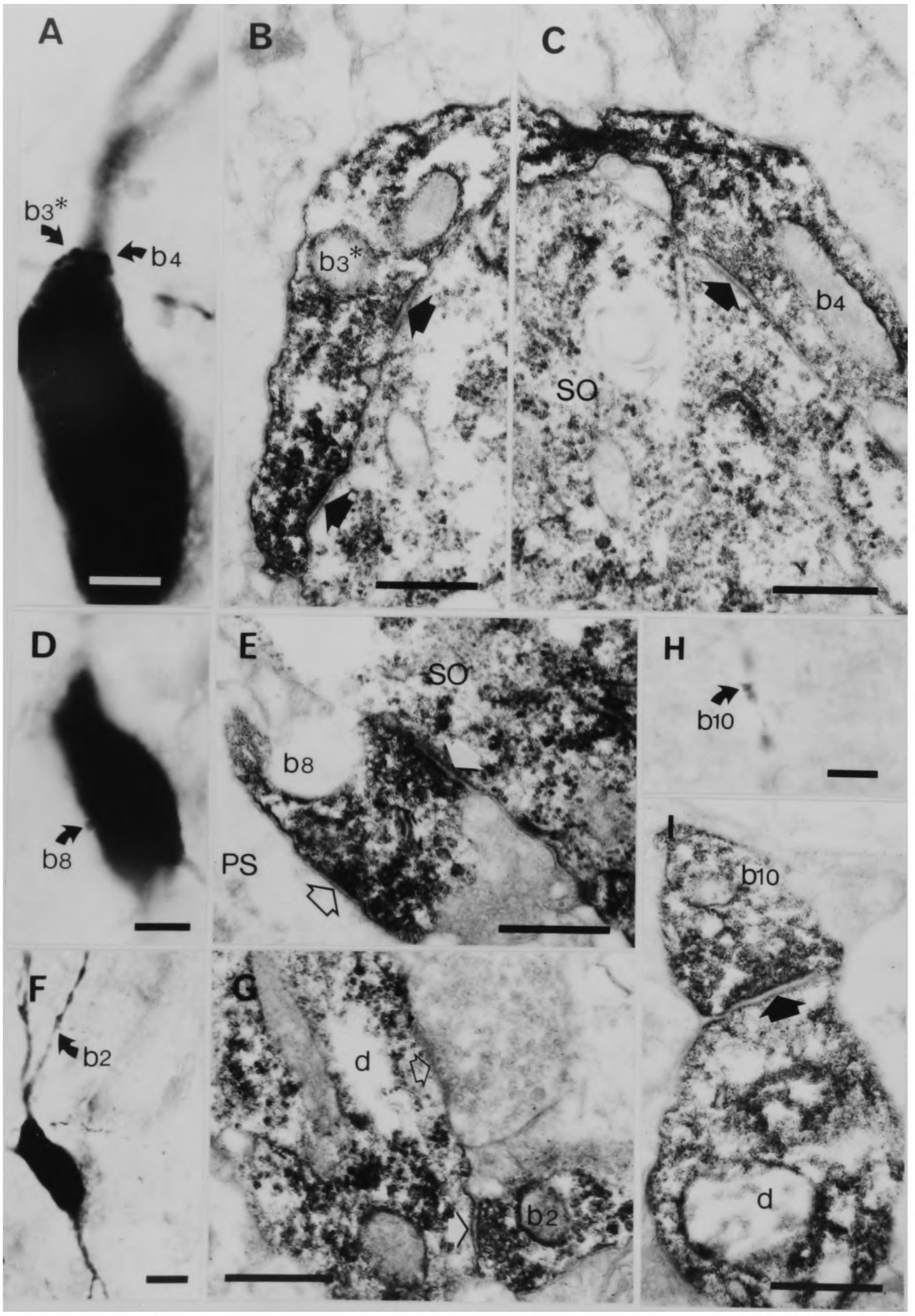

A
b3*
b4
B
b3*
C
b4
SO
D
b8
E
SO
b8
PS
H
b10
b10
d
F
b2
G
d
b2

FIGURE 6.3: Synaptic responses in a bistratified cell (I2) and two pyramidal cells (P1, P2), following activation of a common presynaptic basket cell (I1). Action potentials (A, single sweep) evoked in the presynaptic basket cell shown in Figure 6.1 elicit fast hyperpolarising IPSPs in the simultaneously recorded bistratified cell (B; average of 82 sweeps). Following subsequent sequential impalement of nearby pyramidal cells, activation of the same presynaptic basket cell elicited fast hyperpolarising responses (C, average of 34 sweeps; D, average of 24 sweeps).

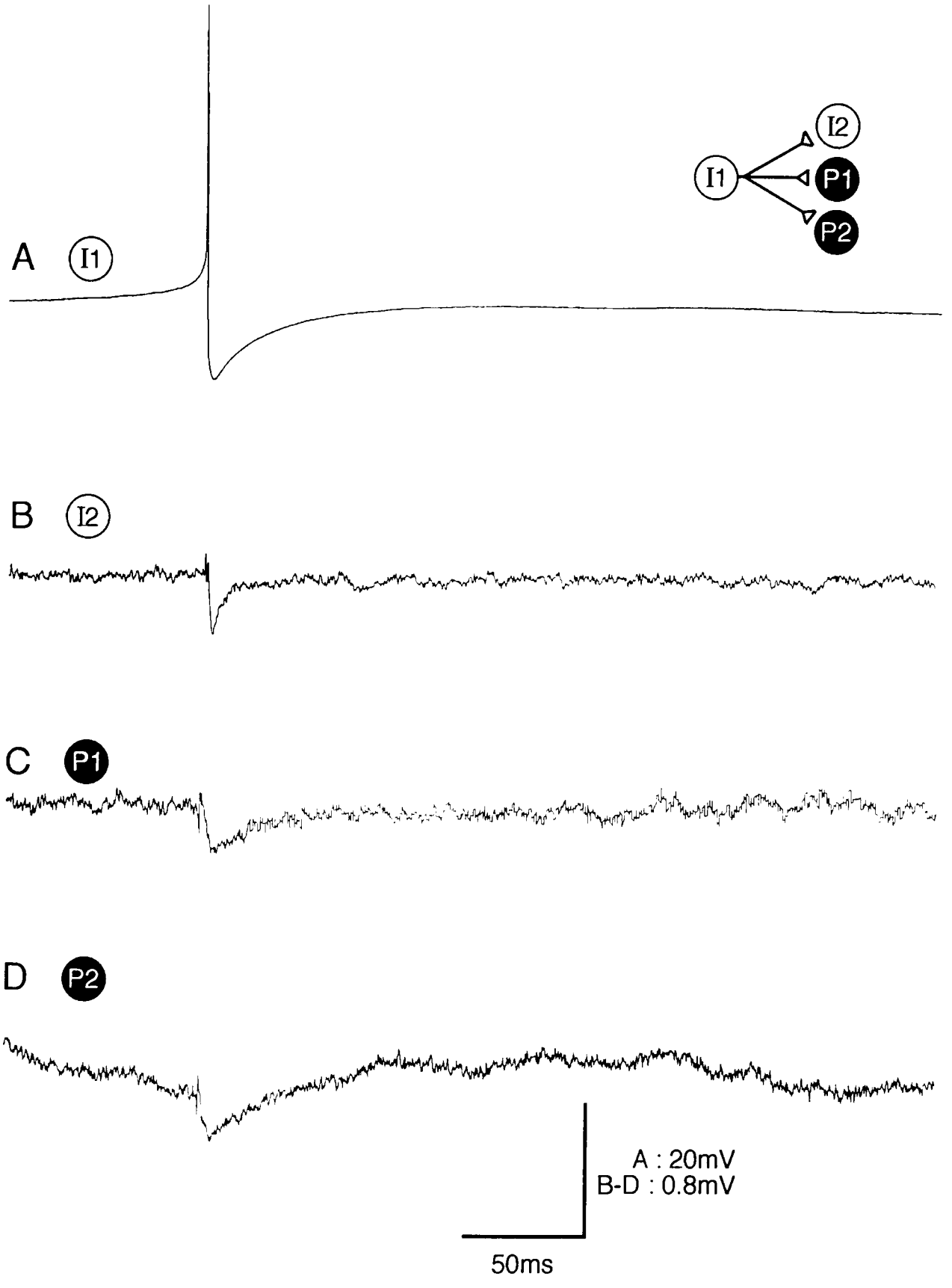

A
I1
I2
P1
P2
B
I2
C
P1
D
P2
A : 20mV
B-D : 0.8mV
50ms

FIGURE 6.4: Reconstruction of a novel type of basket cell showing, the soma, dendrites (red) and the axon (black). The soma is located in stratum pyramidale, giving rise to smooth, aspinous dendrites which extend radially into strata oriens, pyramidale (SP) and radiatum (SR). Note the unusually dense axonal arbour which extends laterally ~ 900μm in the CA1 subfield, but is restricted mainly to stratum pyramidale and adjoining regions of strata oriens and radiatum. Arrows indicate characteristic vertically orientated axon collaterals. Electron microscopic evaluation of randomly selected postsynaptic profiles (n=25) showed this cell to innervate somata (40%), proximal dendrites (56%) and dendritic spines (4%), confirming its basket cell status. Scale bar: 100μm

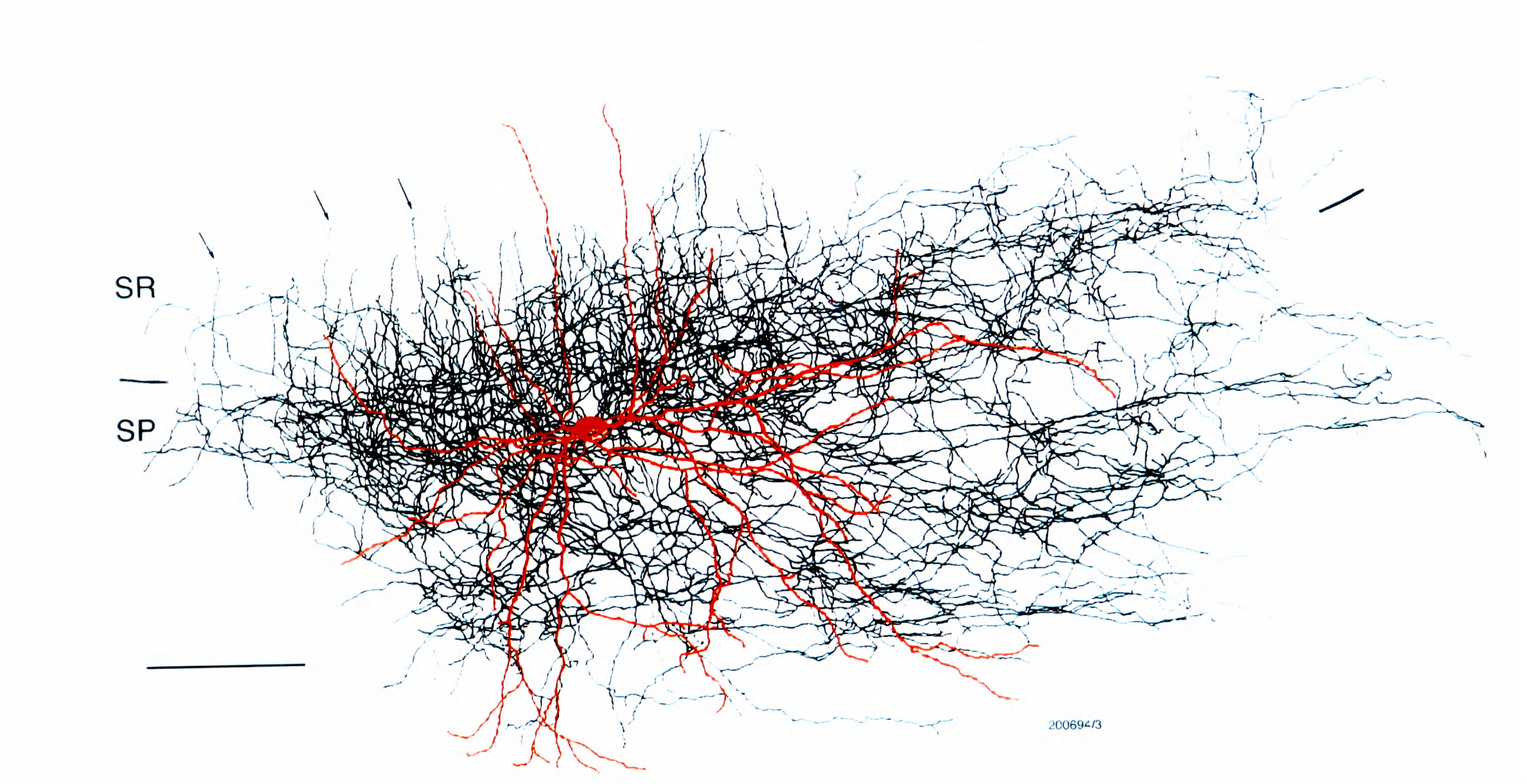
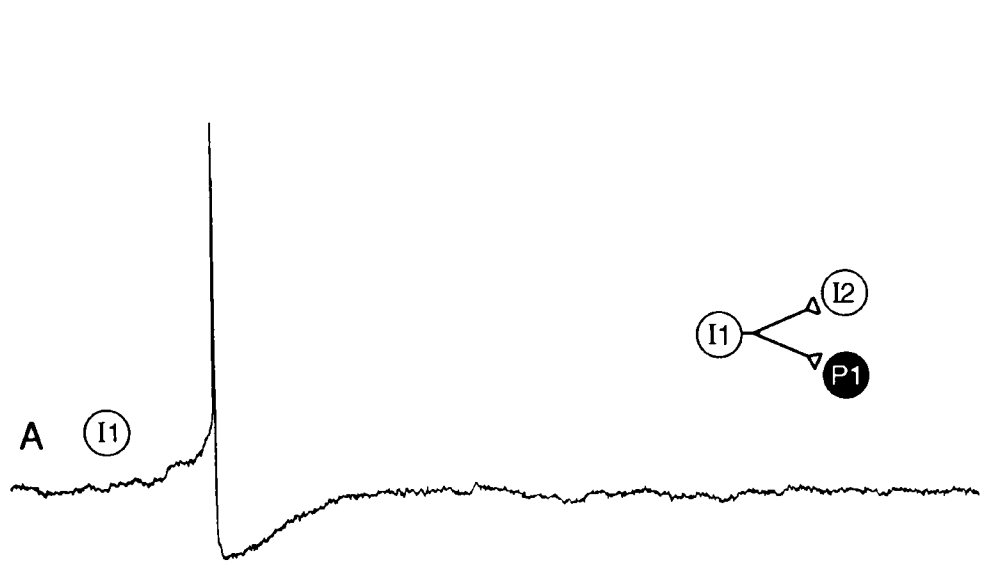

SR
SP
2006943

FIGURE 6.5: Light and electron micrographs of the basket cell shown in Figure 6.4 and its postsynaptic targets. (A) Light microscopic montage of the basket cell. At higher magnification, axons were seen to form characteristic 'perisomatic baskets' (B) and vertically elongated collaterals (C) which appeared to follow unlabelled apical dendrites (arrows), forming multiple boutons. (D,E) Electron micrographs of labelled basket cell boutons (b), forming synaptic junctions (arrows) with an unlabelled pyramidal cell soma (som) and a proximal apical dendrite (d). SO=stratum oriens, SP=stratum pyramidale, SR=stratum radiatum

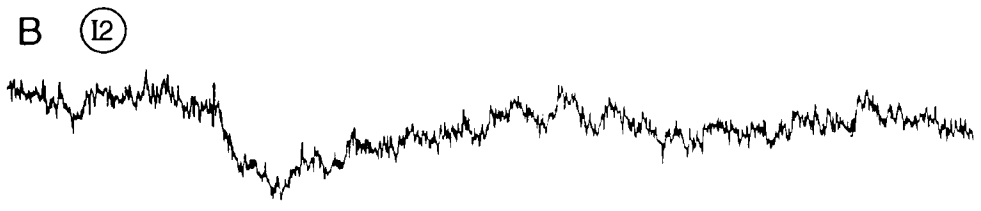
Scale bars: A, 50μm; B 20μm; C, 10μm; D-E, 0.5μm

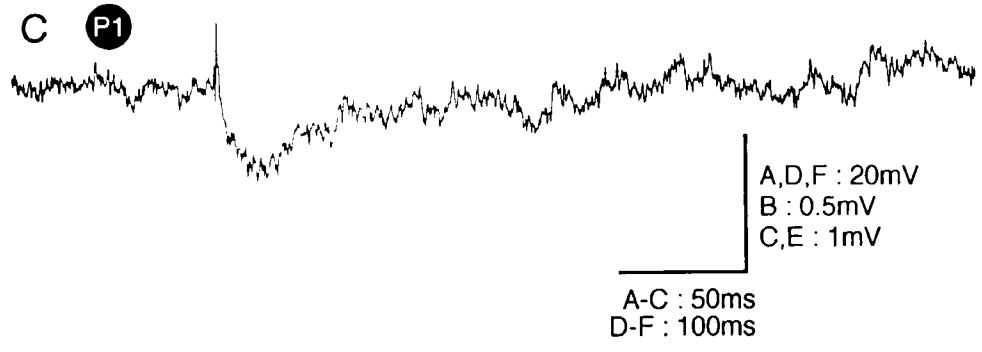

A
SR
SP
SO
B
C
D
b
som
E
b
d

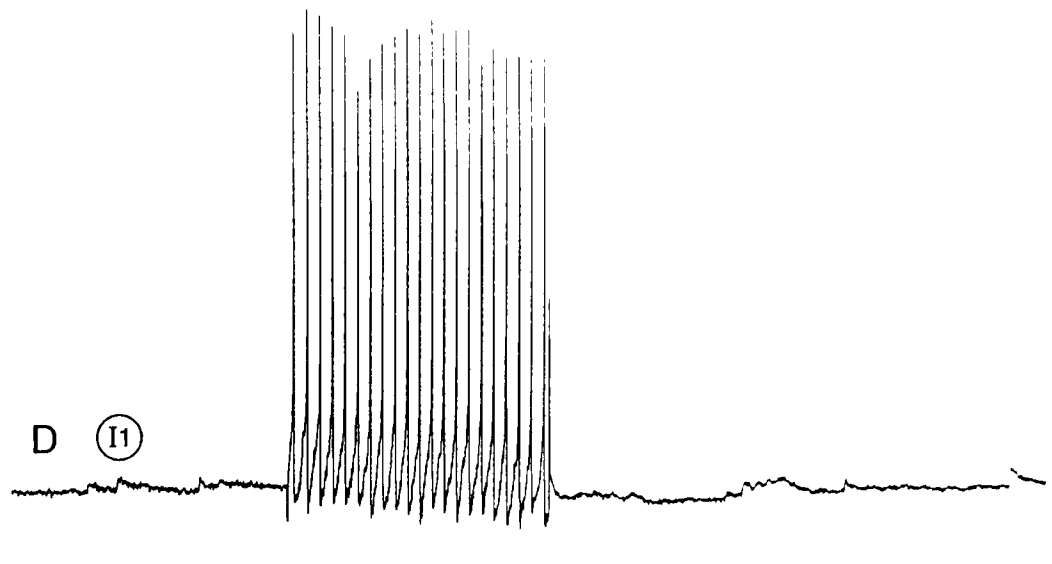
FIGURE 6.6: Basket cell-evoked unitary synaptic responses in consecutively recorded interneurone and pyramidal cell. (A) Action potential (duration at half-amplitude 0.4ms) evoked in the basket cell shown in Figure 6.5 and 6.6 elicits fast hyperpolarising IPSPs in a simultaneously recorded interneurone (B; average of 85 sweeps) and in a subsequently recorded pyramidal cell (C, average of 34 sweeps). (D) A train of action potentials (80Hz) evoked in the presynaptic basket cell (200ms, 0.5nA depolarising current pulse) elicit a summated fast hyperpolarising IPSP in the postsynaptic interneurone (E; average of 8 sweeps). Note that the initial 5-6 IPSPs summate before the synaptic response fatigues (F). A similar intracellular depolarising current injection (300ms, 0.2nA) produces the same characteristic fast-spiking response (102Hz, action potential duration at half-amplitude 0.4ms) in the postsynaptic interneurone. Inset: Schematic diagram of synaptic interactions. Reciprocal synaptic coupling was not observed at either connection (data not shown).


A
I1

I2
I1
P1


B
I2


C
P1
A,D,F : 20mV
B : 0.5mV
C,E : 1mV
A-C : 50ms
D-F : 100ms


D
I1


E
I2

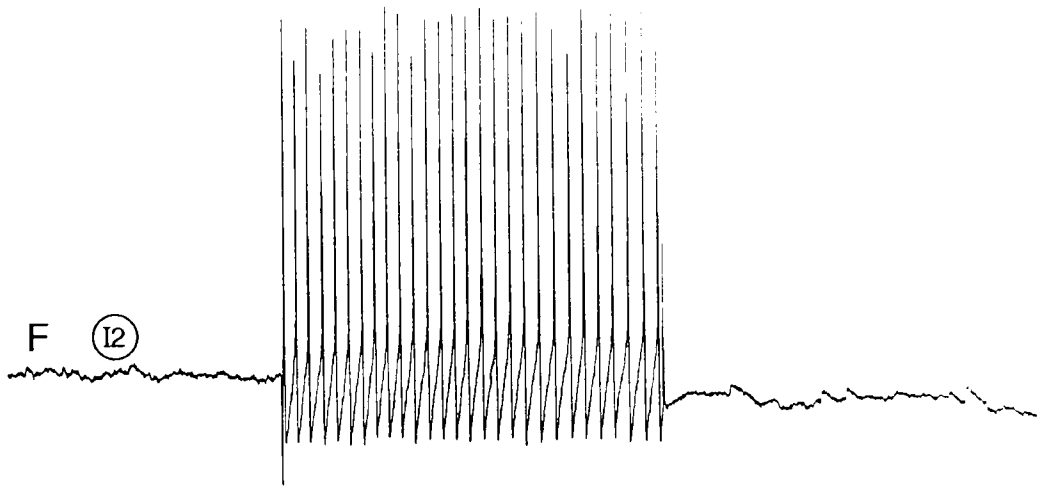

F
I2

FIGURE 6.7: Camera-lucida reconstruction of a LM-R interneurone and postsynaptic bistratified and pyramidal cells. The soma of the presynaptic LM-R cell (top left; in red) is situated in stratum radiatum (SR) close to the border with stratum lacunosum-moleculare (SL-M). Dendrites (incomplete) project into both strata radiatum and lacunosum-moleculare. The postsynaptic bistratified cell (bottom, red) and pyramidal cell (black) somata are situated in stratum pyramidale (SP). Apical dendrites of the bistratified cell are beaded and confined to stratum radiatum, whereas the spiny pyramidal cell dendrites extensively ramify in all layers. The main axons (arrowheads) of the bistratified and pyramidal cells were only partially reconstructed. Scale bar: 100μm

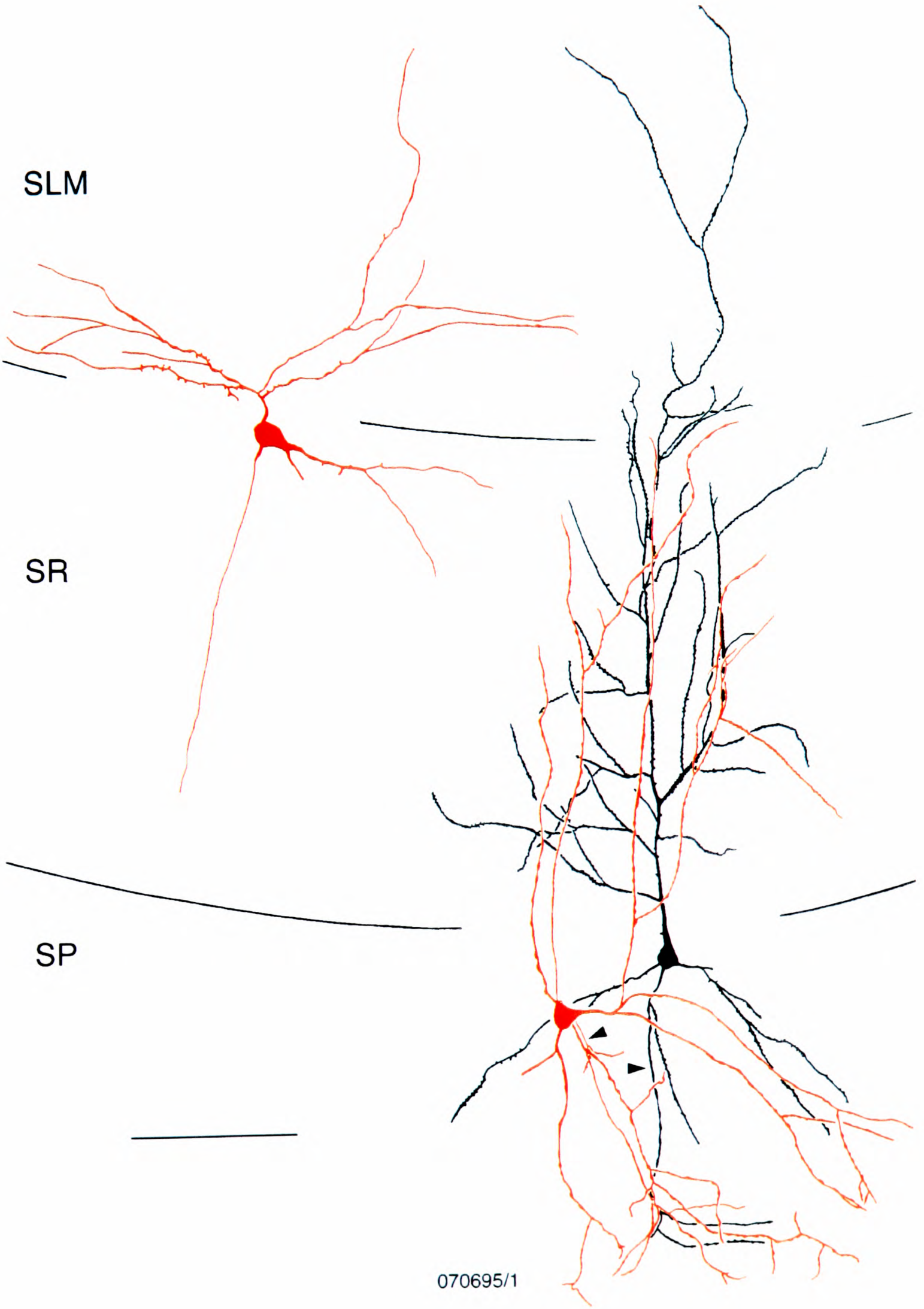
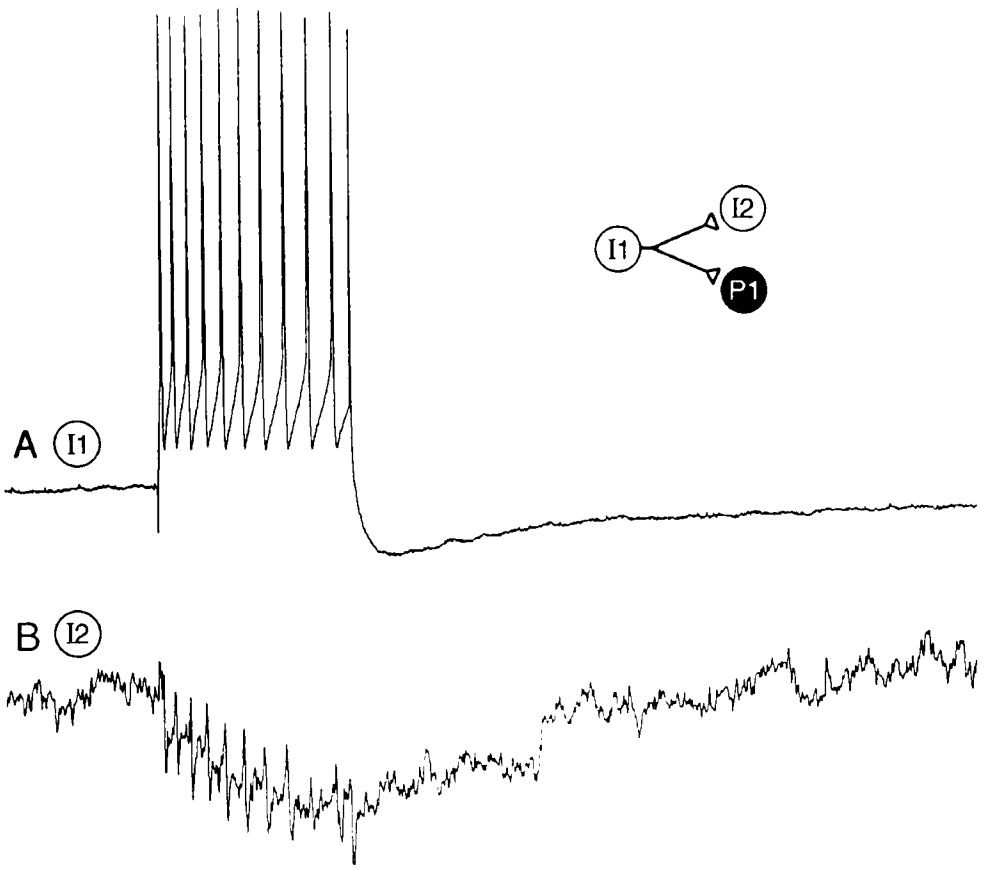

SLM
SR
SP
070695/1

FIGURE 6.8: Synaptic response recorded in a bistratified and pyramidal cell, following activation of a common presynaptic LM-R interneurone. (A) A short train of action potentials evoked in the presynaptic LM-R interneurone (shown in Figure 6.7) elicits a fast hyperpolarising synaptic response in the simultaneously recorded bistratified cell (B; average of 49 sweeps). Repeated activation of the same presynaptic LM-R interneurone (C) elicits similar fast hyperpolarising responses in a subsequently recorded pyramidal cell (D; average of 106 sweeps). Inset: summary of synaptic interactions, where I1, I2 and P1 correspond to presynaptic LM-R interneurone, postsynaptic bistratified cell and pyramidal cell, respectively. No reciprocal synaptic coupling was observed (data not shown).


I2
I1
P1
A I1
B I2

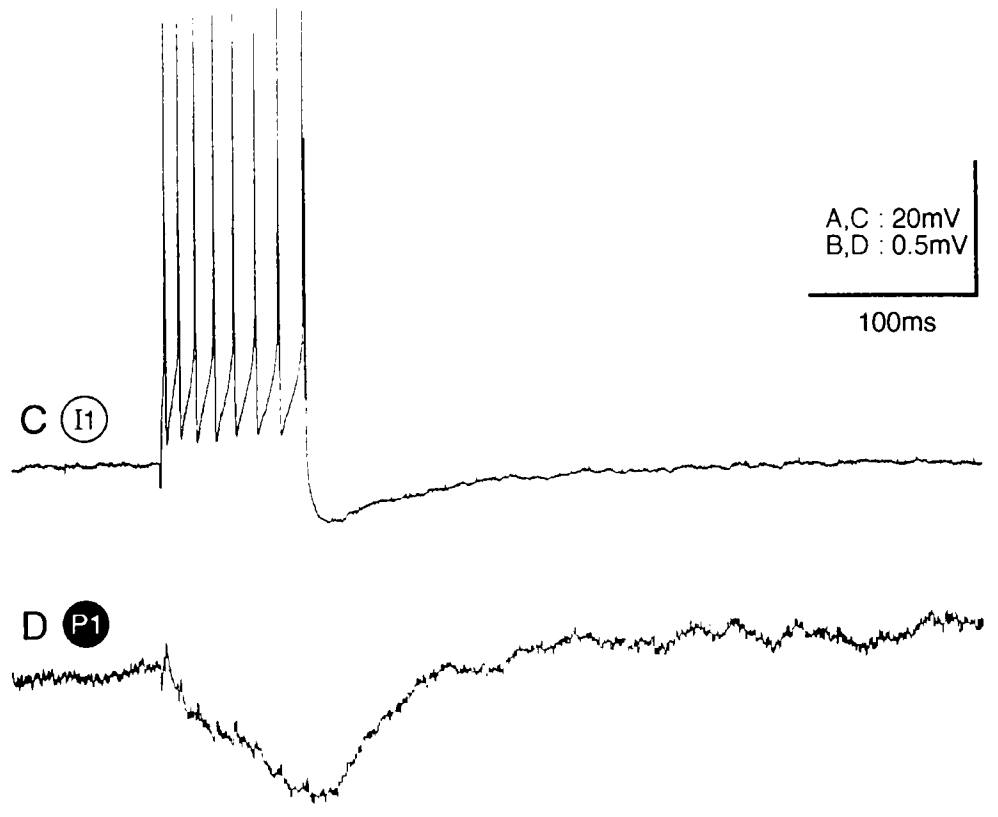

A,C : 20mV
B,D : 0.5mV
100ms
C I1
D P1

TABLE 6.1: Summary of unitary postsynaptic response amplitude and kinetics. Rise times were measured as the time difference of 10 and 90% of the respective peak-amplitude. Duration of responses were determined at half-amplitude.

Presynaptic cell (code)	Postsynaptic cell	IPSP amplitude (mV)	Holding potential (mV)	IPSP 10-90% rise time (ms)	IPSP duration at 1/2 amplitude (ms)
basket cell (I1) (050794/3)	bistratified cell (I2)	0.37	-55	1.0	5.6
	pyramidal cell (P1)	0.31	-57	2.6	21.0
	pyramidal cell (P2)	0.28	-60	3.2	16.4
basket cell (I1) (200694/3)	fast-spiking interneurone (I2)	0.30	-61	15.2	49.6
	pyramidal cell (P1)	0.60	-57	11.8	38.0
SR-LM interneurone (I1) (070695/1)	bistratified cell (I2)	0.48*	-61	n/a	n/a
	pyramidal cell (P1)	0.46*	-60	n/a	n/a

* indicates summated response

n/a - not appilcable

Chapter 7. General discussion

7.1 Overview

These studies were primarily conducted to elucidate the microcircuitry of the hippocampus and to characterise unitary interactions which take place between identified neurones with particular reference to GABAergic interneurones. This thesis presented several experimental findings that advance current concepts of hippocampal microcircuitry. Of particular importance are the novel insights gained regarding the interaction of GABAergic synaptic transmission with action potential generation and subthreshold membrane potential oscillations in pyramidal cells. The following findings are discussed as relevant for considering the functional role of GABAergic systems in the hippocampus :

1. GABAergic interneurones in the hippocampal CA1 area differ with respect to their axonal and dendritic morphology as well as their efferent synaptic target profile, with different cells selectively targeting functionally different membrane domains of their postsynaptic neurones. The same GABAergic interneurones form symmetrical (inhibitory) type synaptic junctions and innervate pyramidal cells as well as other interneurones.

2. Unitary synaptic transmission is mediated by $GABA_A$ type receptors, is reliable (i.e. few transmission failures) and is mediated by multiple synaptic junctions.

3. Single cell-evoked IPSPs are usually hyperpolarising, reverse close to the chloride equilibrium potential and have fast kinetics.

4. Hyperpolarising IPSPs interact with intrinsic conductances to phase action potential generation, subthreshold membrane potential oscillations and evoke postinhibitory facilitation.

5. Through these mechanisms, GABAergic interneurones can effectively synchronise the activity of pyramidal cells.

7.1.1 Diversity of GABAergic interneurones

Intracellular labelling of individual local-circuit interneurones in the CA1 area revealed a heterogeneous population of cells which differed with respect to their dendritic and axonal morphology and their efferent synaptic target profile (chapter 3). This latter difference was most striking and demonstrates that distinct classes of GABAergic interneurones selectively innervate different functional domains of pyramidal cells. The characterisation of cell types in the CA1 area extends previous intracellular labelling studies, (Kawaguchi and Hama, 1988; Kunkel et al., 1988; Lacaille and Schwartzkroin, 1988a; Li et al., 1992; Buhl et al., 1994a,b, 1995, 1996; McBain et al., 1994; Sík et al., 1994, 1995; Halasy et al., 1996; Vida et al., 1997) and provides a quantitative and objective method for differentiating cells types based on their efferent synaptic target profile.

The differences in the extent to which dendrites ramified in different layers of the CA1 area also suggest, that different interneurones are differentially activated by different excitatory pathways. This also has important functional consequences, as it suggests that some interneurones are more strongly activated by perforant path input, whilst others are mainly activated by Schaffer collateral / associational inputs. It is known that stratum oriens interneurones which innervate the molecular layer are almost exclusively activated by recurrent axon collaterals of CA1 pyramidal cells (Blasco-Ibanez and Freund, 1995; Maccaferri and McBain, 1995), whereas those with their dendrites restricted to the area above the pyramidal cell layer are presumably predominantly activated in a feedforward manner. Taken together, these data suggest that distinct excitatory inputs to different dendritic domains of pyramidal cells may produce different responses not only because of the

electrotonic structure of the pyramidal cell dendrites (Rall, 1977), but also because these inputs concomitantly activate distinct GABAergic inputs to specific domains of the same neurone.

7.1.2 Synaptic interaction of GABAergic interneurones

An interesting aspect of the investigated unitary interactions mediated by GABAergic interneurones is that all evoked synaptic responses appeared to be solely mediated by $GABA_A$ receptors. Extracellular bulk stimulation of afferent pathways in the CA1 area typically evoke both fast $GABA_A$ and slow $GABA_B$ mediated IPSPs (Alger and Nicoll, 1982a,b ; Newberry and Nicoll, 1984a; Empson and Heinemann, 1995). Indeed, it has been suggested that $GABA_B$ receptor-mediated IPSPs are mainly evoked on dendritic portions of pyramidal cells in a feedforward manner (Davies et al., 1990; Solis and Nicoll, 1992). Therefore, there appears a difference between pathway activation which produces both $GABA_A$ and $GABA_B$ receptor-mediated IPSPs, and unitary IPSPs (i.e. those evoked by a single presynaptic cell) which my data and those of others (Miles, 1990; Buhl et al., 1994a, 1995) show to be mediated by $GABA_A$ receptors. These finding may be explained in a number ways. Firstly, it is possible that a distinct and as yet untested population of interneurones exists, which mediates its postsynaptic effect through $GABA_B$ receptors (Benardo, 1994). Alternatively, it is possible that the conductance change associated with a unitary $GABA_B$ receptor-mediated event is so small that the voltage deflection produced is below the resolution level of my intracellular recording technique. A third possibility is that $GABA_B$ receptors are situated extrasynaptically and are only activated upon GABA spillover following the simultaneous activation of several interneurones (Isaacson et al., 1993; Mody et al., 1994). Such 'intrinsic neuromodulation' represents an important but less recognised mode of modifying local-circuits and is considered to be important in central pattern generation (Katz and Frost, 1996). An interesting point in this

respect is that the data described in chapter 4 suggest that GABA release from basket cell terminals is under control of presynaptic $GABA_B$ receptors. Thus, $GABA_B$ receptors appear to be present at the synapses under investigation, at least as far as the presynaptic element is concerned. Clearly, further studies are required to resolve the issues concerning the activation of postsynaptic $GABA_B$ receptors.

7.1.3 Distinct functional roles for different types of GABAergic interneurones ?

In spite of the striking finding that GABAergic interneurones described in this study subdivide the surface of their postsynaptic target cells, the unitary postsynaptic responses, recorded in the form of hyperpolarising IPSPs with fast rise and decay kinetics, appeared qualitatively rather similar. Thus, the division of function, implicit in the morphology, was not reflected by any dramatic differences in the postsynaptic response, as measured by changes in voltage across the somatic membrane. It therefore appears, that more subtle experimental paradigms have to be devised to test the functional compartmentalisation of GABAergic inputs onto pyramidal cells. Indeed, with the realisation that most neurones in the central nervous system are richly endowed with active conductances, it is difficult to accurately predict the response to a particular synaptic input (Llinás, 1988). This complexity is especially well illustrated, when considering 'inhibitory' input to hippocampal principal cells. Whilst perisomatic inhibition seems particularly effective at governing action potential generation (Andersen et al., 1963; Cobb et al., 1995; Miles et al., 1996), dendritic inhibition can counteract locally generated EPSPs (Staley and Mody, 1992), enhance (Magee et al., 1995) or inhibit dendritic calcium conductances (Miles et al., 1996), control the propagation of sodium action potential to the dendrites (Spruston et al., 1995) and control oscillatory processes in the dendrites (Paulsen and Vida, 1996). Moreover, when the temporal aspect of neuronal activities are taken into account, the postsynaptic consequences of

GABAergic input become even more complex. Thus the role of GABAergic inhibition appears to be diverse and, it will require much detailed and carefully planned experiments to unravel functionally significant effects.

The demonstration that perisomatic IPSPs interact with intrinsic conductances to effectively phase action potential generation and subthreshold membrane potential oscillations (chapter 5) was a successful attempt to address such functional questions. These experiments revealed the existence of powerfully tuned mechanisms, whereby the relatively small conductance associated with a single GABAergic input can effectively entrain the firing of pyramidal cells. Moreover, by extrapolating the anatomical data that each GABAergic interneurone innervates many hundreds of pyramidal cells (Li et al., 1992; Sík et al., 1995; Halasy et al., 1996), it is reasonable to speculate that an individual interneurone has the capacity to synchronise the activity of a very large population of pyramidal cells. Indeed, experiments demonstrated that a common GABAergic input effectively entrained the activity of two simultaneously recorded pyramidal cells. The maintenance of synchrony requires that at the synapses of basket cells, synaptic transmissions is reliable. The relatively large number of synapses formed between basket cells and somata and proximal dendrites of their postsynaptic targets may provide an anatomical correlate to such reliable transmission. Moreover, though not tested systematically, the fast timecourse of the unitary IPSPs seemed well matched to that of the theta frequency membrane potential oscillations, so as to facilitate entrainment, yet not to destabilise intrinsic rhythmic activities. *In vivo*, anatomically identified basket cells are known to fire short trains of action potentials which occur at theta frequencies during extracellularly recorded theta activity (Ylinen et al., 1995b). The stimulation paradigm of the basket cells during the synchronisation experiments *in vitro* were thus mimicking their firing pattern that is known to occur *in vivo*. Thus, this type of experiment is designed to establish the underlying synaptic mechanisms and anatomical correlates of observations seen in the whole brain. Unfortunately, the effectiveness of dendritically terminating cells at

entraining pyramidal cell activity could not yet be tested. This information would be of great importance in elucidating differences in function for different types of interneurone. Likewise, high frequency activation of basket cells was shown to modestly suppress pyramidal cell firing frequency, whereas the effectiveness of axo-axonic cells has not yet been tested experimentally. It therefore remains to be seen whether there exist differences between basket and axo-axonic cells with respect to suppressing action potential generation. Theoretical studies predict that the more highly localised axo-axonic input would be better placed to elicit shunting inhibition, whereas the more diffuse basket cell input would favour hyperpolarising inhibition (see chapter 5), although these differences remain to be demonstrated. It is known however, that dendritically terminating interneurones have little effect on action potentials generated by somatic current injection (Miles et al., 1996).

That GABAergic interneurones provide a common divergent output to both principal cells and other interneurones, whilst retaining target selectivity towards a particular membrane domain (chapter 6) adds further complexity to the way we view hippocampal microcircuits. Indeed, interconnectivity amongst interneurones may serve a role in controlling both spatial and temporal aspects of inhibition. The traditional view of an inhibitory neurone innervating a second such cell is that the downstream effect would be one of disinhibition. Such a mechanism could mediate changes in the balance of inhibition from one membrane domain of a principal neurone to another, such as from dendritic to perisomatic inhibition. This would be achieved by direct input to the perisomatic domain of pyramidal cells concurrent with a reduction of inhibition at the dendritic membrane, achieved by the same basket cell inhibiting the activity of dendrite-targeting interneurones. Such switches in spatial aspects of inhibition have been reported to occur *in vivo* during exploratory behaviour (Moser, 1996).

A second role for interconnectivity amongst interneurones is predicted by observations that many types of interneurone fire within characteristic frequency bands during specific behavioural states (see Freund and Buzsáki, 1996).

Interneurones are themselves known to support intrinsic oscillatory mechanisms (Maccaferri and McBain, 1996). Interconnected interneurone networks may therefore form a system of coupled oscillators leading to emergent network properties (Buzsáki and Chrobak, 1995; Whittington et al., 1995) amongst sub-populations of interneurones.

7.1.4 Modelling of hippocampal circuits

Detailed morphological studies into the neuronal circuitry of the hippocampus have been under way for over a century and physiologists have analysed the electrical properties of hippocampal neurones and their gross synaptic interactions for many decades. Despite this wealth of information that has accumulated, much of this biological data has not been exploited by current models of hippocampal function which tend mainly to consider excitatory connectivity (for example see Treves and Rolls, 1994). Whilst some attempt is being made to incorporate biophysical, connectional and synaptic properties (Traub et al., 1987a,b, 1989, 1991,1994; Traub and Miles, 1991, 1995), clearly, more realistic models incorporating known biological data are required for a better understanding of how information is processed in the hippocampus (Traub and Miles 1991).

7.2 Technical considerations

The questions addressed in this thesis were all carried out by experiments in the brain slice preparation (Yamamoto and McIlwain, 1966; Skrede and Westgaard, 1971). The use of acutely prepared brain slices is justified in this context as these experiments primarily focused upon local synaptic interactions whose circuitry remain mostly intact in the transverse slice. Moreover, the animals used in these experiments were young adults (age ~1.5 to 3 months) and were thus likely to be fully developed with respect to their neuronal circuitry. Clearly, light microscopic

reconstruction of labelled neurones revealed filled processes to be cut at the surface of the tissue. However, most recordings were made from cells close to the middle of the slice thickness and recent estimates indicate that the majority of dendrites and more than 50 percent of the axonal arbour are contained in horizontal 400µm thick slices, when comparing interneurones labelled *in vitro* with those labelled *in vivo* conditions (Li et al., 1992, 1994; Buckmaster and Schwartzkroin, 1995a,b ; Sík et al., 1995; Ylinen et al., 1995b; Halasy et al., 1996). Thus, the filled cells in the slice were suitable for examining dendritic branching and axonal stratification, although no attempt was made to quantify dendritic and axonal lengths due to the unknown degree of truncation of the labelled cells. The degree of tissue expansion / shrinkage from the living state to the epoxy resin embedded state is not yet known for the tissue described in these experiments. However, identical fixation methods and histological processing in neocortical tissue was shown to produce no appreciable change in tissue volume from the *in situ* state (Tamás et al., 1996).

Brain slices undergo dramatic changes in their metabolic status during preparation, presumably due to tissue damage at the cut surfaces of the slices, but gradually recover towards the intact brain status within the first hour (Whittingham et al., 1984). This recovery is roughly paralleled by changes in evoked synaptic responses, which, by one hour, approach those of intact brain recordings in whole animals, and may operate for many hours. Indeed, acute slices from 7-week old rats are reported to survive three weeks when maintained in culture medium (Frey et al., 1993). In all experiments described in this study, slices were prepared in medium in which all sodium chloride had been replaced by equiosmolar sucrose, so to reduce the acute toxicity associated with slice preparation (Aghajanian and Rasmussen, 1989). Moreover, all recordings described in these experiments were made after a 1 hour recovery period and lasted from tens of minutes to several hours. In general, results form *in vitro* work should be confirmed by *in vivo* recordings, to evaluate the physiological relevance of the phenomenon under study. However, technical difficulties make the study of unitary events difficult to achieve

in vivo, although this difficulty is more than offset by the power of the dual intracellular technique and thus the preparation and methods used in these experiments were well-suited for studying the mechanisms of synaptic interaction. It should be noted however that the hippocampal slice is devoid of several of its major afferent inputs including those providing neuromodulatory transmitters from mid- and forebrain nuclei which may dramatically affect the electrophysiological properties of neurones and synaptic transmission, through effects on the postsynaptic response and presynaptic transmitter release (see McCormick, 1990).

All experiments described in this study were carried out on rat tissue. It should therefore be noted, that considerable differences exist between species with regard to various properties of interneurones (see Freund and Buzsáki, 1996). As differences are apparent in species as close as rat and mouse, care should be taken, when comparing findings in one species with those from another. Moreover, as most anatomical and physiological studies are carried out on rodent (mainly rat) species, care should be taken when drawing comparisons to morphological and electrophysiological findings from guinea pig (D'Erchia et al., 1996) and other non-rodent species. Despite this, however, it is likely that the fundamental principles such as the functional parcellation of GABAergic inputs and the action of GABAergic synapses at particular functional membrane domains is likely to be conserved (Somogyi, 1977; Somogyi et al., 1982, 1983a,b, 1985; Gulyás et al., 1993a; Han et al., 1993; Buhl et al., 1994a, 1995; Halasy et al., 1996). Indeed, the limited data available to compare carnivore, primate and rodent hippocampal interneurones suggest, that the dendritic and axonal features are remarkably conserved, whereas neurochemical characteristics show more variability (see Freund and Buzsáki, 1996).

7.3 Future directions

The anatomical and physiological studies performed, using the techniques described in this thesis, have provided novel results which elucidate the component neurones of the hippocampal CA1 area and the microcircuits they form. New insights have emerged into synaptic communication between neurones and how synaptic responses affect the activity of postsynaptic cells. The advent of the whole-cell patch clamp technique (Hamill et al., 1981) has revolutionised the study of synaptic communication and has already greatly facilitated the study of unitary synaptic interactions (Edwards et al., 1990; Jonas et al., 1993; Markram and Tsodyks, 1996; Morin et al., 1996). In particular, the low signal to noise ratio afforded by the technique would allow much more detailed investigation into the efficacy of identified GABAergic synapses, including their presynaptic control (Lambert and Wilson, 1993b, 1994; Thompson, 1994), the kinetics of postsynaptic responses evoked by different subtypes of interneurone (Morin et al., 1996) and their quantal properties (Edwards et al., 1990; Jonas et al., 1993). Moreover, improved resolution would also allow more detailed pharmacological studies into the synaptic effects mediated by different sets of interneurone. Pharmacological evidence presently suggests that interneurones which innervate the perisomatic region of pyramidal cells may have a different pharmacological profile from those targeting more distal membrane areas (Pearce, 1993). Moreover, recent immunocytochemical evidence suggests that $GABA_A$ receptors on somata and dendrites may differ form those at the axon initial segment, with respect to the expression of the $\alpha 2$ subunit responsible for type II benzodiazepine pharmacological profile (Nusser et al., 1996). The above difference suggests that synaptic effects mediated by axo-axonic cells may differ from other interneurones in terms of their sensitivity to agents acting at the benzodiazepine binding site. Investigating such differences by pharmacological means should be a priority for future studies and may eventually be of clinical significance.

With regard to establishing the functional role of different classes of local-circuit interneurone within the hippocampus, new experimental paradigms have to be devised in order to test specific functions, such as the ability of dendritically terminating interneurones to modulate EPSPs and intrinsic conductances in the dendrites and for axo-axonic cells to control action potential initiation at the axon initial segment. Much is still to be learned about how identified subtypes of interneurone are active *in vivo* but studies to date suggest that they are differentially active during different behavioural states during which their firing patterns vary (Buzsáki et al., 1983; Buzsáki & Eidelberg, 1983; Buzsáki et al., 1992; Lee et al., 1994; Bragin et al., 1995; Ylinen et al., 1995a,b; Chrobak & Buzsáki, 1996; see also Freund and Buzsáki, 1996). By acquiring such information, it will be possible to artificially evoke these characteristic, often rhythmic, firing patterns in individual interneurones to establish the postsynaptic consequence in their target neurones. It is also of considerable interest how such distinctive firing patterns are brought about. It is likely, that there are multiple neuromodulatory effects which shape firing patterns (Madison and Nicoll, 1982, 1984, 1986) and synaptic communication. Evidence supporting this comes from the observation that hippocampal theta activity is associated with phasic cholinergic and GABAergic inputs (Stewart and Fox, 1990).

The past two decades have seen enormous strides in unravelling the circuitry of the hippocampal formation and much progress has been made towards understanding the function of different cell types and circuits. Indeed, with the advent of intracellular recording techniques, the investigation of GABAergic interneurones has seen somewhat of a renaissance since the days of Raymon y Cajal. However, a major problem associated with such a rapid accumulation of so much new information, is that differences amongst cells become apparent based upon a large number of factors such as morphology, connections with other neurones, expression of various neurochemical markers and physiological characteristics obtained both *in vitro* and *in vivo* (reviewed by Freund and Buzsáki,

1996). For a synthesis, a further level of analysis is required to correlate electrophysiological, connectional, morphological and immunocytochemical data. This would be best achieved through studies which combine cellular recording and subsequent visualisation of neurones with elucidating the expression of distinct neurochemical markers and identifying afferent and efferent connections. Furthermore, to understand their firing patterns and differential involvement in network activities during different behavioural states, more combined cellular recording / labelling studies have to be carried out in the whole animal. However, these technically challenging experiments to identify correlated characteristics will also require more thorough analysis to be developed. Multivariate analysis (Krzanowski, 1988) in particular should greatly aid the taxonomy of interneurones, to provide a more complete definition of cell types.

A more detailed knowledge of the components which make up GABAergic network, together with a more thorough understanding of synaptic interactions will greatly facilitate our comprehension of how the cortical network operates. Moreover, the possibility of functionally distinct GABAergic cells carrying out a variety of tasks might open up a whole new era in the rational design of pharmacological tools which permit the fine tuning of specific aspects of inhibition in the brain.

References

Acsády, L., Arabadzisz, D. and Freund, T. F. (1996a) Correlated morphological and neurochemical features identify different subsets of vasoactive intestinal polypeptide-immunoreactive interneurons in rat hippocampus. *Neuroscience,* **73,** 299-315.

Acsády, L., Görcs, T. J. and Freund, T. F. (1996b) Different populations of vasoactive intestinal polypeptide-immunoreactive interneurons are specialized to control pyramidal cells or interneurons in the hippocampus. *Neuroscience,* **73,** 317-334.

Acsády, L., Halasy, K. and Freund, T. F. (1993) Calretinin is present in non-pyramidal cells of the rat hippocampus. III. Their inputs from the median raphe and medial septal nuclei. *Neuroscience,* **52,** 829-841.

Aghajanian, G. K. and Rasmussen, K. (1989) Intracellular studies in the facial nucleus illustrating a simple new method for obtaining viable motoneurons in adult rat brain slices. *Synapse,* **3,** 331-338.

Aika, Y., Ren, J. Q., Kosaka, K. and Kosaka, T. (1994) Quantitative analysis of GABA-like-immunoreactive and parvalbumin-containing neurons in the CA1 region of the rat hippocampus using a stereological method, the disector. *Exp. Brain Res.,* **99,** 267-276.

Alger, B. E. and Nicoll, R. A. (1982a) Feed-forward dendritic inhibition in rat hippocampal pyramidal cells studied in vitro. *J. Physiol. (Lond),* **328,** 105-123.

Alger, B. E. and Nicoll, R. A. (1979) GABA-mediated biphasic inhibitory responses in hippocampus. *Nature,* **281,** 315-317.

Alger, B. E. and Nicoll, R. A. (1982b) Pharmacological evidence for two kinds of GABA receptor on rat hippocampal pyramidal cells studied in vitro. *J. Physiol. (Lond),* **328,** 125-141.

Alonso, A. and Llinás, R. R. (1989) Subthreshold Na^+-dependent theta-like rhythmicity in stellate cells of entorhinal cortex layer II. *Nature,* **342,** 175-177.

Amaral, D. G. (1978) A Golgi study of cell types in the hilar region of the hippocampus in the rat. *J. Comp. Neurol.,* **182,** 851-914.

Amaral, D. G. and Witter, M. P. (1995) Hippocampal formation. In. Paxinos, G. (ed.) *The rat nervous system.* Academic Press, London, pp. 443-493.

Amitai, Y. (1994) Membrane potential oscillations underlying firing patterns in neocortical neurons. *Neuroscience,* **63,** 151-161.

Amthor, F. R. and Grzywacz, N. M. (1991) Nonlinearity of the inhibition underlying retinal directional selectivity. *Vis. Neurosci.,* **6,** 197-206.

Andersen, P. and Eccles, J. (1962) Inhibitory phasing of neuronal discharge. *Nature,* **195,** 645-647.

Andersen, P., Eccles, J. C. and Løyning, Y. (1964a) Location of postsynaptic inhibitory synapses on hippocampal pyramids. *J. Neurophysiol.,* **27,** 592-607.

Andersen, P., Eccles, J. C. and Løyning, Y. (1964b) Pathway of postsynaptic inhibition in the hippocampus. *J. Neurophysiol.,* **27,** 608-619.

Andersen, P., Eccles, J. C. and Løyning, Y. (1963) Recurrent inhibition in the hippocampus with identification of the inhibitory cells and its synapses. *Nature,* **198,** 540-542.

Andersen, P. and Lomo, T. (1966) Mode of activation of hippocampal pyramidal cells by excitatory synapses on dendrites. *Exp. Brain Res.*, **2,** 247-260.

Andreasen, M. and Lambert, J. D. C. (1995) Regenerative properties of pyramidal cell dendrites in area CA1 of the rat hippocampus. *J. Physiol. (Lond),* **483,** 421-441.

Arancio, O., Korn, H., Gulyás, A., Freund, T. and Miles, R. (1994) Excitatory synaptic connections onto rat hippocampal inhibitory cells may involve a single transmitter release site. *J. Physiol. (Lond),* **481,** 395-405.

Ascher, P. and Nowak, L. (1987) Electrophysiological studies of NMDA receptors. *Trends Neurosci.,* **10,** 284-288.

Ashwood, T. J., Lancaster, B. and Wheal, H. V. (1984) In vivo and in vitro studies on putative interneurones in the rat hippocampus: possible mediators of feed-forward inhibition. *Brain Res.,* **293,** 279-291.

Assaf, S. Y. and Miller, J. J. (1978) The role of a raphe serotonin system in the control of septal unit activity and hippocampal desynchronization. *Neuroscience,* **3,** 539-550.

Ault, B. and Nadler, J. V. (1982) Baclofen selectively inhibits transmission at synapses made by axons of CA3 pyramidal cells in the hippocampal slice. *J Pharmacol. Exp. Ther.,* **223,** 291-297.

Bakst, I., Avendano, C., Morrison, J. H. and Amaral, D. G. (1986) An experimental analysis of the origins of somatostatin-like immunoreactivity in the dentate gyrus of the rat. *J. Neurosci.,* **6,** 1452-1462.

Baude, A., Nusser, Z., Roberts, J. D. B., Mulvihill, E., Mcilhinney, R. A. J. and Somogyi, P. (1993) The metabotropic glutamate receptor (mGluR1 alpha) is

concentrated at perisynaptic membrane of neuronal subpopulations as detected by immunogold reaction. *Neuron,* **11,** 771-787.

Behrends, J. C. and TenBruggencate, G. (1993) Cholinergic modulation of synaptic inhibition in the guinea pig hippocampus *in vitro* - excitation of GABAergic interneurons and inhibition of GABA-Release. *J. Neurophysiol.,* **69,** 626-629.

Bekkers, J. M. (1994) Quantal analysis of synaptic transmission in the central nervous system. *Curr. Opin. Neurobiol.,* **4**, 360-365.

Benardo, L. S. (1994) Separate activation of fast and slow inhibitory postsynaptic potentials in rat neocortex *in vitro*. *J. Physiol. (Lond),* **476,** 203-215.

Blackstad, T. W. (1956) Commissural connections of the entorhinal areas in the rat, with special reference to their mode of termination. *J. Comp. Neurol.,* **105,** 417-537.

Blackstad, T. W.and Flood, P. R. (1963)Ultrastructure of hippocampal axo-somatic synapses. *Nature*, **198**, 542-543.

Blasco-Ibanez, J. M. and Freund, T. F. (1995) Synaptic input of horizontal interneurons in stratum oriens of the hippocampal CA1 subfield: structural basis of feed-back activation. *Eur .J. Neurosci.,* **7,** 2170-2180.

Bliss, T. V. P. and Collingridge, G. L. (1993) A synaptic model of memory - Long-Term potentiation in the hippocampus. *Nature,* **361,** 31-39.

Blomfield, S. (1974) Arithmetical operations performed by nerve cells. *Brain Res.,* **69,** 115-124.

Bonanno, G. and Raiteri, M. (1993) Multiple $GABA_B$ receptors. *Trends Pharm. Sci.*, **14,** 259-261.

Bormann, J. and Feigenspan, A. (1995) $GABA_C$ receptors. *Trends Neurosci.*, **18,** 515-519.

Bowery, N. G., Hill, D. R., Hudson, A. L., Doble, A., Middlemiss, D. N., Shaw, J. and Turnbull, M. (1980) (-)Baclofen decreases neurotransmitter release in the mammalian CNS by an action at a novel GABA receptor. *Nature,* **283,** 92-94.

Bowery, N. G., Hudson, A. L. and Price, G. W. (1987) $GABA_A$ and $GABA_B$ receptor site distribution in the rat central nervous system. *Neuroscience,* **20,** 365-383.

Bragin, A., Jando, G., Nadasdy, Z., Hetke, J., Wise, K. and Buzsáki, G. (1995) Gamma (40-100 Hz) oscillation in the hippocampus of the behaving rat. *J. Neurosci.,* **15,** 47-60.

Brock, L. G., Coombs, J. S. and Eccles, J. C. (1952) The recording of potentials from motorneurones with an intracellular electrode. *J. Physiol. (Lond),* **117,** 431-460.

Brown, T. H. and Zador, A. M. (1990) Hippocampus. In. Shepherd, G. M.(ed.) *The synaptic organisation of the brain.* Oxford, New York. pp346-388.

Buckmaster, P. S., Kunkel, D. D., Robbins, R. J. and Schwartzkroin, P. A. (1994) Somatostatin-immunoreactivity in the hippocampus of mouse, rat, guinea pig, and rabbit. *Hippocampus,* **4,** 167-180.

Buckmaster, P. S. and Schwartzkroin, P. A. (1995a) Interneurons and inhibition in the dentate gyrus of the rat in vivo. *J. Neurosci.*, **15,** 774-789.

Buckmaster, P. S. and Schwartzkroin, P. A. (1995b) Physiological and morphological heterogeneity of dentate gyrus-hilus interneurons in the gerbil hippocampus in vivo. *Eur. J. Neurosci.*, **7,** 1393-1402.

Buhl, E. H., Cobb, S. R., Halasy, K. and Somogyi, P. (1995) Properties of unitary IPSPs evoked by anatomically identified basket cells in the rat hippocampus. *Eur. J. Neurosci.*, **7,** 1989-2004.

Buhl, E. H., Halasy, K. and Somogyi, P. (1994a) Diverse sources of hippocampal unitary inhibitory postsynaptic potentials and the number of synaptic release sites. *Nature,* **368,** 823-828.

Buhl, E. H., Han Z.-S., Lörinczi, Z., Stezhka, V. V., Karnup, S. V. and Somogyi, P. (1994b) Physiological properties of anatomically identified axo-axonic cells in the rat hippocampus. *J. Neurophysiol.*, **71,** 1289-1307.

Buhl, E. H., Szilágyi, T., Halasy, K. and Somogyi, P. (1996) Physiological properties of anatomically identified basket and bistratified cells in the CA1 area of the rat hippocampus. *Hippocampus,* **6,** 294-305.

Buzsáki, G. and Chrobak, J. J. (1995) Temporal structure in spatially organized neuronal ensembles: a role for interneuronal networks. *Current Biology.*, **5**, 504-510.

Buzsáki, G. and Eidelberg, E. (1983) Phase relations of hippocampal projection cells and interneurons to theta activity in the anesthetized rat. *Brain Res.*, **266,** 334-339.

Buzsáki, G., Horvath, Z., Urioste, R., Hetke, J. and Wise, K. (1992) High-frequency network oscillation in the hippocampus. *Science,* **256,** 1025-1027.

Buzsáki, G., Leung, L. -W S. and Vanderwolf, C. H. (1983) Cellular bases of hippocampal EEG in the behaving rat. *Brain Res. Rev.,* **6,** 139-171.

Buzsáki, G., Penttonen, M., Nadásdy, Z. and Bragin, A. (1996) Pattern and inhibition-dependent invasion of pyramidal cell dendrites by fast spikes in the hippocampus *in vivo*. *Proc. Natl. Acad. Sci. U.S.A.,* In press

Capogna, M., Gähwiler, B. H. and Thompson, S. M. (1993) Mechanism of m-opioid receptor-mediated presynaptic inhibition in the rat hippocampus *in vitro*. *J. Physiol. (Lond),* **470,** 539-558.

Carbone, E. and Lux, H. D. (1984) A low voltage-activated, fully inactivating Ca channel in vertebrate sensory neurones. *Nature,* **310,** 501-502.

Chittajallu, R., Vignes, M., Dev, K. K., Barnes, J. M., Collingridge, G. L. and Henley, J. M. (1996) Regulation of glutamate release by presynaptic kainate receptors in the hippocampus. *Nature,* **379,** 78-81.

Chrobak, J. J. and Buzsáki, G. (1996) High-frequency oscillations in the output networks of the hippocampal-entorhinal axis of the freely behaving rat. *J. Neurosci.,* **16,** 3056-3066.

Cobb, S. R., Buhl, E. H., Halasy, K., Paulsen, O. and Somogyi, P. (1995) Synchronization of neuronal activity in hippocampus by individual GABAergic interneurons. *Nature,* **378,** 75-78.

Cohen, G. A., Doze, V. A. and Madison, D. V. (Aug 1992) Opioid Inhibition of GABA Release from Presynaptic Terminals of Rat Hippocampal Interneurons. *Neuron,* **9,** 325-335.

Collingridge, G. L., Gage, P. W. and Robertson, B. (1984) Inhibitory post-synaptic currents in rat hippocampal CA1 neurones. *J. Physiol. (Lond),* **356,** 551-564.

Colling, S. B. and Wheal, H. V. (1994) Fast sodium action potentials are generated in the distal apical dendrites of rat hippocampal CA1 pyramidal cells. *Neurosci. Letts.,* **172,** 73-76.

Cook, J. E. (1991) Correlated activity in the CNS: a role on every timescale? *Trends Neurosci.,* **14,** 397-401.

Coombs, J. S., Eccles, J. C. and Fatt, P. (1955) The inhibitory suppression of reflex discharges from motoneurones. *J. Physiol. (Lond),* **130,** 396-413.

Davies, C. H. and Collingridge, G. L. (1993) The physiological regulation of synaptic inhibition by $GABA_B$ autoreceptors in rat hippocampus. *J. Physiol. (Lond),* **472,** 245-265.

Davies, C. H., Davies, S. N. and Collingridge, G. L. (1990) Paired-pulse depression of monosynaptic GABA-mediated inhibitory postsynaptic responses in rat hippocampus. *J. Physiol. (Lond),* **424,** 513-531.

Davies, C. H., Starkey, S. J., Pozza, M. F. and Collingridge, G. L. (1991) $GABA_B$ autoreceptors regulate the induction of LTP. *Nature,* **349,** 609-611.

Deisz, R. A. and Prince, D. A. (1989) Frequency-dependent depression of inhibition in guinea-pig neocortex in vitro by $GABA_B$ receptor feed-back on GABA release. *J. Physiol. (Lond),* **412,** 513-541.

del Castillo, J. and Katz, B. (1954) Quantal components of the end-plate potential. *J. Physiol. (Lond),* **124**, 560-573.

Deller, T. and Leránth, C. (1990) Synaptic connections of neuropeptide Y (NPY) immunoreactive neurons in the hilar area of the rat hippocampus. *J. Comp. Neurol.*, **300,** 433-447.

D'Erchia, A. M., Gissi, C., Pesole, G., Saccone, C. and Aranson, U. (1996) The guinea pig is not a rodent. *Nature*, **381**, 597-600.

Douglas, R. J. and Martin, K. A. C. (1990) Control of neuronal output by inhibition at the axon initial segment. *Neural Comp.*, **2,** 283-292.

Dunlap, K. (1981) Two types of g-aminobutyric acid receptor on embryonic sensory neurons. *Br. J. Pharmacol.*, **74,** 579-585.

Dutar, P. and Nicoll, R. A. (1988) A physiological role for $GABA_B$ receptors in the central nervous system. *Nature,* **332,** 156-158.

Eccles, J. C. (1982) The synapse: from electrical to chemical transmission. *Ann Rev. Neurosci.*, **5,** 325-329.

Eccles, J. C. and McGeer, P. L. (1979) Ionotropic and metabotropic neurotransmission. *Trends Neurosci.*, **2,** 39-40.

Eckhorn, R., Bauer, R., Jordan, W., Brosch, M., Kruse, W., Munk, M. and Reitboeck, H. J. (1988) Coherent oscillations: a mechanism of feature linking in the visual cortex? Multiple electrode and correlation analyses in the cat. *Biol. Cybern.*, **60,** 121-130.

Edwards, F. A., Konnerth, A. and Sakmann, B. (1990) Quantal analysis of inhibitory synaptic transmission in the dentate gyrus of rat hippocampal slices: a patch-clamp study. *J. Physiol. (Lond),* **430,** 213-249.

Empson, R. M. and Heinemann, U. (1995) Perforant path connections to area CA1 are predominantly inhibitory in the rat hippocampal-entorhinal cortex combined slice preparation. *Hippocampus,* **5,** 104-107.

Engel, A. K., König, P., Kreiter, A. K., Schillen, T. B. and Singer, W. (1992) Temporal coding in the visual cortex: new vistas on integration in the nervous system. *Trends Neurosci.,* **15,** 218-225.

Fox, S. E. (1989) Membrane potential and impedance changes in hippocampal pyramidal cells during theta rhythm. *Exp. Brain Res.,* **77,** 283-294.

Freund, T. F. and Antal, M. (1988) GABA-containing neurons in the septum control inhibitory interneurons in the hippocampus. *Nature,* **336,** 170-173.

Freund, T. F. and Buzsáki (1996) Interneurons of the hippocampus. *Hippocampus,* In press

Freund, T. F. and Gulyás, A. L. (1991) GABAergic interneurons containing calbindin D28K or somatostatin are major targets of GABAergic basal forebrain afferents in the rat neocortex. *J. Comp. Neurol.,* **314,** 187-199.

Freund, T. F., Martin, K. A. C., Smith, A. D. and Somogyi, P. (1983) Glutamate decarboxylase-immunoreactive terminals of Golgi-impregnated axoaxonic cells and of presumed basket cells in synaptic contact with pyramidal neurons of the cat's visual cortex. *J. Comp. Neurol.,* **221,** 263-278.

Frey, U., Huang, Y. -Y and Kandel, E. R. (1993) Effects of cAMP simulate a late stage of LTP in hippocampal CA1 neurons. *Science,* **260,** 1661-1664.

Frotscher, M. (1989) Mossy fiber synapses on glutamate decarboxylase-immunoreactive neurons: evidence for feed-forward inhibition in the CA3 region of the hippocampus. *Exp. Brain Res.,* **75,** 441-445.

Fuortes, M. G. F., Frank, K. and Becker, M. C. (1957) Steps in the production of motoneuron spikes. *J. Gen. Physiol.*, **40,** 735-752.

Gähwiler, B. H. and Brown, D. A. (1985) GABAB-receptor-activated K+ current in voltage-clamped CA3 pyramidal cells in hippocampal cultures. *Proc. Natl. Acad. Sci. U. S .A.*, **82,** 1558-1562.

Gao, B. and Fritschy, J. M. (1994) Selective allocation of $GABA_A$ receptors containing the a1 subunit to neurochemically distinct subpopulations of rat hippocampal interneurons. *Eur. J. Neurosci.*, **6,** 837-853.

Garcia-Munoz, A., Barrio, L. C. and Buno, W. (1993) Membrane potential oscillations in CA1 hippocampal pyramidal neurons invitro: intrinsic rhythms and fluctuations entrained by sinusoidal injected current. *Exp. Brain Res.*, **97,** 325-333.

Ginsborg, B. L. (1973) Electrical changes in the membrane in junctional transmission. *Biochim. Biophys. Acta.*, **300,** 289-317.

Gray, C. M., König, P., Engel, A. K. and Singer, W. (1989) Oscillatory responses in cat visual cortex exhibit inter-columnar synchronization which reflects global stimulus properties. *Nature,* **338,** 334-337.

Gray, C. M. and Singer, W. (1989) Stimulus-specific neuronal oscillations in orientation columns of cat visual cortex. *Proc. Natl. Acad. Sci. USA.*, **86,** 1698-1702.

Gray, E. G. (1959) Axo-somatic and axo-dendritic synapses of the cerebral cortex: an electron microscope study. *J. Anat.*, **93,** 420-433.

Gulyás, A. I., Görcs, T. J. and Freund, T. F. (1990) Innervation of different peptide-containing neurons in the hippocampus by GABAergic septal afferents. *Neuroscience,* **37,** 31-44.

Gulyás, A. I., Hájos, N. and Freund, T. F. (1996) Interneurons containing calretinin are specialized to control other interneurons in the rat hippocampus. *J. Neurosci.,* **16,** 3397-3411.

Gulyás, A. I., Miettinen, R., Jacobowitz, D. M. and Freund, T. F. (1992) Calretinin is present in non-pyramidal cells of the rat hippocampus-I. A new type of neuron specifically associated with the mossy fibre system. *Neuroscience,* **48,** 1-27.

Gulyás, A. I., Miles, R., Sík, A., Tóth, K., Tamamaki, N. and Freund, T. F. (1993b) Hippocampal pyramidal cells excite inhibitory neurons through a single release site. *Nature,* **366,** 683-687.

Gulyás, A. I., Miles, R., Hájos, N. and Freund, T. F. (1993a) Precision and variability in postsynaptic target selection of inhibitory cells in the hippocampal CA3 region. *Eur. J. Neurosci.,* **5,** 1729-1751.

Gulyás, A. I., Tóth, K., Danos, P. and Freund, T. F. (1991) Subpopulations of GABAergic neurons containing parvalbumin, calbindin D28k, and cholecystokinin in the rat hippocampus. *J. Comp. Neurol.,* **312,** 371-378.

Halasy, K., Buhl, E. H., Lörinczi, Z., Tamás, G. and Somogyi, P. (1996) Synaptic target selectivity and input of GABAergic basket and bistratified interneurons in the CA1 area of the rat hippocampus. *Hippocampus,* **6,** 306-329.

Halasy, K., Miettinen, R., Szabat, E. and Freund, T. F. (1992) GABAergic interneurons are the major postsynaptic targets of median raphe afferents in the rat dentate gyrus. *Eur. J. Neurosci.*, **4,** 144-153.

Halasy, K. and Somogyi, P. (1993) Subdivisions in the multiple GABAergic innervation of granule cells in the dentate gyrus of the rat hippocampus. *Eur. J. Neurosci.*, **5,** 411-429.

Halliwell, J. V. and Adams, P. R. (1982) Voltage-clamp analysis of muscarinic excitation in hippocampal neurons. *Brain Res.*, **250,** 71-92.

Hamill, O. P., Marty, A., Neher, E., Sakmann, B. and Sigworth, F. J. (1981) Improved patch-clamp techniques for high-resolution current recording from cells and cell-free membrane patches. *Pflügers Arch.*, **391,** 85-100.

Han, Z. -S, Buhl, E. H., Lörinczi, Z. and Somogyi, P. (1993) A high degree of spatial selectivity in the axonal and dendritic domains of physiologically identified local-circuit neurons in the dentate gyrus of the rat hippocampus. *Eur J. Neurosci.*, **5,** 395-410.

Harris, K. M., Marshall, P. E. and Landis, D. M. D. (1985) Ultrastructural study of cholecystokinin-immunoreactive cells and processes in area CA1 of the rat hippocampus. *J. Comp. Neurol.*, **233,** 147-158.

Hausser, M., Stuart, G., Racca, C. and Sakmann, B. (1995) Axonal initiation and active dendritic propagation of action potentials in substantia nigra. neurons. *Neuron,* **15,** 637-647.

Herreras, O. (1990) Propagating dendritic action potential mediates synaptic transmission in CA1 pyramidal cells in situ. *J. Neurophysiol.*, **64,** 1429-1441.

Hille, B. (1984) Ion channels of excitable membranes. Sunderland, MA: Sinauer Associates.

Hopfield, J. J. (1995) Pattern recognition computation using action potential timing for stimulus representation. *Nature,* **376,** 33-36.

Horikawa, K. and Armstrong, W. E. (1988) A versatile means of intracellular labeling: injection of biocytin and its detection with avidin conjugates. *J. Neurosci. Methods,* **25,** 1-11.

Huerta, P. T. and Lisman, J. E. (1995) Bidirectional synaptic plasticity induced by a single burst during cholinergic theta oscillation in CAl in vitro. *Neuron,* **15,** 1053-1063.

Huerta, P. T. and Lisman, J. E. (1993) Heightened synaptic plasticity of hippocampal CA1 neurons during a cholinergically induced rhythmic state. *Nature,* **364,** 723-725.

Huerta, P. T. and Lisman, J. E. (1996a) Low-frequency stimulation at the troughs of theta-oscillation induces long-term depression of previously potentiated CA1 synapses. *J. Neurophysiol.,* **75,** 877-884.

Huerta, P. T. and Lisman, J. E. (1996b) Synaptic plasticity during the cholinergic theta-frequency oscillation in vitro. *Hippocampus,* **6,** 58-61.

Isaacson, J. S., Solis, J. M. and Nicoll, R. A. (1993) Local and diffuse synaptic actions of GABA in the hippocampus. *Neuron,* **10,** 165-175.

Jefferys, J. G. R. (1995) Nonsynaptic modulation of neuronal activity in the brain: electric currents and extracellular ions. *Physiol. Rev.,* **75,** 689-723.

Jonas, P., Major, G. and Sakmann, B. (1993) Quantal components of unitary EPSCs at the mossy fibre synapse on CA3 pyramidal cells of rat hippocampus. *J. Physiol. (Lond),* **472,** 615-663.

Kandel, E. R. and Spencer, W. A. (1961) Electrophysiology of hippocampal neurons. II. After-potentials and repetitive firing. *J. Neurophysiol.,* **24,** 243-259.

Katsumaru, H., Kosaka, T., Heizmann, C. W. and Hama, K. (1988) Immunocytochemical study of GABAergic neurons containing the calcium-binding protein parvalbumin in the rat hippocampus. *Exp. Brain Res.,* **72,** 347-362.

Katz, P. S. and Frost, W. N. (1996) Intrinsic neuromodulation: altering neuronal circuits from within. *Trends Neurosci.,* **19,** 54-61.

Kawaguchi, Y. and Hama, K. (1987a) Fast-spiking non-pyramidal cells in the hippocampal CA-3 region, dentate gyrus and subiculum of rats. *Brain Res.,* **425,** 351-355.

Kawaguchi, Y. and Hama, K. (1988) Physiological heterogeneity of nonpyramidal cells in rat hippocampal CA1 region. *Exp. Brain Res.,* **72,** 494-502.

Kawaguchi, Y. and Hama, K. (1987b) Two subtypes of non-pyramidal cells in rat hippocampal formation identified by intracellular recording and HRP injection. *Brain Res.,* **411,** 190-195.

Khazipov, R., Congar, P., Ben-Ari, Y. (1995) Hippocampal CA1 lacunosum-moleculare interneurons: modulation of monosynaptic GABAergic IPSCs by presynaptic $GABA_B$ receptors. *J. Neurophysiol.,* **74**, 2126-2137.

Kisvárday, Z. F., Adams, C. B. T. and Smith, A. D. (1986) Synaptic connections of axo-axonic (chandelier) cells in human epileptic temporal cortex. *Neuroscience,* **19,** 1179-1186.

Kisvárday, Z. F., Martin, K. A. C., Whitteridge, D. and Somogyi, P. (1985) Synaptic connections of intracellularly filled clutch cells: a type of small basket cell in the visual cortex of the cat. *J. Comp. Neurol.,* **241,** 111-137.

Knowles, W. D. and Schwartzkroin, P. A. (1981) Local circuit synaptic interactions in hippocampal brain slices. *J. Neurosci.,* **1,** 318-322.

Köhler, C., Chan-Palay, V. and Wu, J-Y (1984) Septal neurons containing glutamic acid decarboxylase immunoreactivity project to the hippocampal region in the rat brain. *Anat. Embryol.,* **169,** 41-44.

Köhler, C. and Chan-Palay, V. (1982) Somatostatin-like immunoreactive neurons in the hippocampus: An immunocytochemical study in the rat. *Neurosci. lett.,* **34,** 259-264.

Konopacki, J., MacIver, M. B., Bland, B. H. and Roth, S. H. (1987) Carbachol-induced EEG 'theta' activity in hippocampal brain slices. *Brain Res.,* **405,** 196-198.

Korn, H., Mallet, A., Triller, A. and Faber, D. S. (1982) Transmission at a central inhibitory synapse. II. Quantal description of release, with a physical correlate for binomial n. *J. Neurophysiol.,* **48,** 679-707.

Kosaka, T., Katsumaru, H., Hama, K., Wu, J-Y and Heizmann, C. W. (1987) GABAergic neurons containing the Ca^{2+}-binding protein parvalbumin in the rat hippocampus and dentate gyrus. *Brain Res.,* **419,** 119-130.

Kosaka, T., Kosaka, K., Tateishi, K., Hamaoka, Y., Yanaihara, N., Wu, J-Y and Hama, K. (1985) GABAergic neurons containing CCK-8-like and/or VIP-like immunoreactivities in the rat hippocampus and dentate gyrus. *J. Comp. Neurol.*, **239,** 420-430.

Kosaka, T., Wu. J. -Y. and Benoit, R. (1988) GABAergic neurons containing somatostatin-like immunoreactivity in the rat hippocampus and dentate gyrus. *Exp. Brain Res.*, **71,** 388-398.

Kravitz, E. A., Kuffler, S. W., Potter, D. D. and van Gelder, N. M. (1963a) Gamma-aminobutyric acid and other blocking compounds in crustacea. II. Peripheral nervous system. *J. Neurophysiol.*, **26,** 729-738.

Kravitz, E. A., Kuffler, S. W. and Potter, D. D. (1963b) Gamma-aminobutyric acid and other blocking compounds in crustacea. III. Their relative concentrations in separated motor and inhibitory axons. *J. Neurophysiol.*, **26,** 739-751.

Krüger, J. and Becker, J. D. (1991) Recognizing the visual stimulus from neuronal discharges. *Trends Neurosci.*, **14,** 282-286.

Krzanowski, W. J. (1988) Principles of multivariate analysis. Clarendon Press, Oxford.

Kunkel, D. D., Lacaille, J. -C and Schwartzkroin, P. A. (1988) Ultrastructure of stratum lacunosum-moleculare interneurons of hippocampal CA1 region. *Synapse,* **2,** 382-394.

Lacaille, J. -C (1991) Postsynaptic potentials mediated by excitatory and inhibitory amino acids in interneurons of stratum pyramidale of the CA1 region of rat hippocampal slices in vitro. *J. Neurophysiol.*, **66,** 1441-1454.

Lacaille, J. -C, Mueller, A. L., Kunkel, D. D. and Schwartzkroin, P. A. (1987) Local circuit interactions between oriens/alveus interneurons and CA1 pyramidal cells in hippocampal slices: electrophysiology and morphology. *J. Neurosci.*, **7,** 1979-1993.

Lacaille, J. -C and Schwartzkroin, P. A. (1988a) Stratum lacunosum-moleculare interneurons of hippocampal CA1 region. I. Intracellular response characteristics, synaptic responses, and morphology. *J. Neurosci.*, **8,** 1400-1410.

Lacaille, J. -C and Schwartzkroin, P. A. (1988b) Stratum lacunosum-moleculare interneurons of hippocampal CA1 region. II. Intrasomatic and intradendritic recordings of local circuit synaptic interactions. *J. Neurosci.*, **8,** 1411-1424.

Lambert, N. A., Borroni, A. M., Grover, L. M. and Teyler, T. J. (1991) Hyperpolarizing and depolarizing $GABA_A$ receptor-mediated dendritic inhibition in area CA1 of the rat hippocampus. *J. Neurophysiol.*, **66,** 1538-48.

Lambert, N. A. and Wilson, W. A. (1993a) Discrimination of post- and presynaptic $GABA_B$ receptor-mediated responses by tetrahydroaminoacridine in area CA3 of the rat hippocampus. *J. Neurophysiol.*, **69,** 630-635.

Lambert, N. A. and Wilson, W. A. (1993b) Heterogeneity in presynaptic regulation of GABA release from hippocampal inhibitory neurons. *Neuron,* **11,** 1057-1067.

Lambert, N. A. and Wilson, W. A. (1994) Temporally distinct mechanisms of use-dependent depression at inhibitory synapses in the rat hippocampus in vitro. *J. Neurophysiol.*, **72,** 121-130.

Lampl, I. and Yarom, Y. (1993) Subthreshold oscillations of the membrane potential: a functional synchronizing and timing device. *J. Neurophysiol.*, **70**, 2181-2186.

Lanthorn, T. H. and Cotman, C. W. (1981) Baclofen selectively inhibits excitatory synaptic transmission in the hippocampus. *Brain Res.*, **225,** 171-178.

Lanthorn, T., Storm, J. and Andersen, P. (1984) Current-to-frequency transduction in CA1 hippocampal pyramidal cells: slow prepotentials dominate the primary range firing. *Exp. Brain Res.*, **53,** 431-443.

Larkman, A. U., Major, G., Stratford, K. J. and Jack, J. J. (1992) Dendritic morphology of pyramidal neurones of the visual cortex of the rat. IV: Electrical geometry. *J. Comp. Neurol.*, **323,** 137-52.

Lee, M. G., Chrobak, J. J., Sík, A., Wiley, R. G. and Buzsáki, G. (1994) Hippocampal theta activity following selective lesion of the septal cholinergic system. *Neuroscience,* **62,** 1033-1047.

Leung, L. W. and Yim, C. Y. (1991) Intrinsic membrane potential oscillations in hippocampal neurons in vitro. *Brain Res.*, **553,** 261-274.

Li, X. -G, Somogyi, P., Ylinen, A. and Buzsáki, G. (1994) The hippocampal CA3 network: an in vivo intracellular labeling study. *J. Comp. Neurol.*, **339,** 181-208.

Li, X-G, Somogyi, P., Tepper, J. M. and Buzsáki, G. (1992) Axonal and dendritic arborization of an intracellularly labeled chandelier cell in the CA1 region of rat hippocampus. *Exp. Brain Res.*, **90,** 519-525.

Lisman, J. E. and Idiart, M. A. P. (1995) Storage of 7±2 short-term memories in oscillatory subcycles. *Science,* **267,** 1512-1515.

Llinás, R. R. (1988) The intrinsic electrophysiological properties of mammalian neurons: Insights into central nervous system functions. *Science,* **242,** 1654-1664.

Llinás, R. and Nicholson, C. (1971) Electrophysiological properties of dendrites and somata in alligator Purkinje cells. *J. Neurophysiol.,* **34,** 532-551.

Lorente de Nó, R. (1934) Studies on the structure of the cerebral cortex. II. Continuation of the study of the ammonic system. *J. Psychol. Neurol.,* **46,** 113-177.

Loy, R., Koziell, D. A., Lindsey, J. D. and Moore, R. Y. (1980) Noradrenergic innervation of the adult rat hippocampal formation. *J. Comp. Neurol.,* **189,** 699-710.

Lüddens, H. and Wisden, W. (1991) Function and pharmacology of multiple $GABA_A$ receptor subunits. *Trends Pharm. Sci.,* **12,** 49-51.

Lytton, W. W. and Sejnowski, T. J. (1991) Simulations of cortical pyramidal neurons synchronized by inhibitory interneurons. *J. Neurophysiol.,* **66,** 1059-1079.

Maccaferri, G., Mangoni, M., Lazzari, A. and DiFrancesco, D. (1993) Properties of the hyperpolarization-activated current in rat hippocampal CA1 pyramidal cells. *J. Neurophysiol.,* **69,** 2129-2136.

Maccaferri, G. and McBain, C. J. (1996) The hyperpolarization-activated current (I_h) contrbutes to pacemaker activity in rat CA1 hippocampal St. oriens/alveus interneurones. *J Physiol(Lond).,* In Press

Maccaferri, G. and McBain, C. J. (1995) Passive propagation of LTD to stratum oriens-alveus inhibitory neurons modulates the temporoammonic input to the hippocampal CA1 region. *Neuron,* **15,** 137-145.

MacDermott, A. B. and Dale, N. (1987) Receptors, ion channels and synaptic potentials underlying the integrative actions of excitatory amino acids. *Trends Neurosci.,* **10,** 280-284.

Madison, D. V. and Nicoll, R. A. (1986) Actions of noradrenaline recorded intracellularly in rat hippocampal CA1 pyramidal neurones, in vitro. *J. Physiol. (Lond),* **372,** 221-244.

Madison, D. V. and Nicoll, R. A. (1984) Control of the repetitive discharge of rat CA 1 pyramidal neurones in vitro. *J. Physiol. (Lond),* **354,** 319-31.

Madison, D. V. and Nicoll, R. A. (1982) Noradrenaline blocks accommodation of pyramidal cell discharge in the hippocampus. *Nature,* **299,** 636-638.

Magee, J. C., Christofi, G., Miyakawa, H., Christie, B., Lasser-Ross, N. and Johnston, D. (1995) Subthreshold synaptic activation of voltage-gated Ca^{2+} channels mediates a localized Ca^{2+} influx into the dendrites of hippocampal pyramidal neurons. *J. Neurophysiol.,* **74,** 1335-1342.

Magee, J. C. and Johnston, D. (1995a) Characterization of single voltage-gated Na^{+} and Ca^{2+} channels in apical dendrites of rat CA1 pyramidal neurons. *J. Physiol. (Lond),* **487,** 67-90.

Magee, J. C. and Johnston, D. (1995b) Synaptic activation of voltage-gated channels in the dendrites of hippocampal pyramidal neurons. *Science,* **268,** 301-304.

Mainen, Z. F. and Sejnowski, T. J. (1996) Influence of dendritic structure on firing pattern in model neocortical neurones. *Nature,* **382,** 363-366.

Mainen, Z. F. and Sejnowski, T. J. (1995) Reliability of spike timing in neocortical neurons. *Science,* **268,** 1503-1506.

Markram, H. and Tsodyks, M. (1996) Redistribution of synaptic efficacy between neocortical pyramidal neurons. *Nature,* **382,** 807-810.

Mason, A. and Larkman, A. (1990) Correlations between morphology and electrophysiology of pyramidal neurons in slices of rat visual cortex. II. Electrophysiology. *J. Neurosci.,* **10,** 1415-1428.

Mason, A., Nicoll, A. and Stratford, K. (1991) Synaptic transmission between individual pyramidal neurons of the rat visual cortex in vitro. *J. Neurosci.,* **11,** 72-84.

McBain, C. J., Dichiara, T. J. and Kauer, J. A. (1994) Activation of metabotropic glutamate receptors differentially affects two classes of hippocampal interneurons and potentiates excitatory synaptic transmission. *J. Neurosci.,* **14,** 4433-4445.

McBain, C. J. and Dingledine, R. (1993) Heterogeneity of synaptic glutamate receptors on CA3 stratum radiatum interneurones of rat hippocampus. *J. Physiol. (Lond),* **462,** 373-392.

McCarren, M. and Alger, B. E. (1985) Use-dependent depression of IPSPs in rat hippocampal pyramidal cells in vitro. *J. Neurophysiol.,* **53,** 557-571.

McCormick, D. A. (1990) Membrane properties and neurotransmitter actions. In. Shepherd, G. M.(ed.) *The synaptic organisation of the brain.* Oxford, New York. pp32-66.

Michelson, H. B. and Wong, R. K. S. (1991) Excitatory synaptic responses mediated by $GABA_A$ receptors in the hippocampus. *Science,* **253,** 1420-1423.

Michelson, H. B. and Wong, R. K. S. (1994) Synchronization of inhibitory neurones in the guinea-pig hippocampus in vitro. *J. Physiol. (Lond),* **477,** 35-45.

Miettinen, R. and Freund, T. F. (1992) Neuropeptide y-containing interneurons in the hippocampus receive synaptic input from median raphe and gabaergic septal afferents. *Neuropeptides,* **22,** 185-193.

Miettinen, R., Gulyás, A. I., Baimbridge, K. G., Jacobowitz, D. M. and Freund, T. F. (1992) Calretinin is present in non-pyramidal cells of the rat hippocampus-II, Co-existence with other calcium binding proteins and GABA. *Neuroscience,* **48,** 29-43.

Miles, R. (1990) Variation in strength of inhibitory synapses in the CA3 region of guinea-pig hippocampus *in vitro. J. Physiol. (Lond),* **431,** 659-676.

Miles, R., Tóth, K., Gulyás, A. I., Hájos, N. and Freund, T. F. (1996) Differences between somatic and dendritic inhibition in the hippocampus. *Neuron,* **16,** 815-823.

Miles, R. and Wong, R. K. S. (1987) Inhibitory control of local excitatory circuits in the guinea-pig hippocampus. *J. Physiol. (Lond),* **388,** 611-629.

Miles, R. and Wong, R. K. S. (1984) Unitary inhibitory synaptic potentials in the guinea-pig hippocampus in vitro. *J. Physiol. (Lond),* **356,** 97-113.

Misgeld, U., Bijak, M. and Brunner, H. (1992) Granule cell inhibition and the activity of hilar neurons. In. Ribak, C. E., Gall, C. M. and Mody, I. (eds.) *The*

dentate gyrus and its role in seizures. Elsevier Science Publishers BV, Amsterdam, pp. 113-118.

Misgeld, U., Bijak, M. and Jarolimek, W. (1995) A physiological role for $GABA_B$ receptors and the effects of baclofen in the mammalian central nervous system. *Prog. Neurobiol.,* **46,** 423-462.

Misgeld, U., Deisz, R. A., Dodt, H. U. and Lux, H. D. (1986) The role of chloride transport in postsynaptic inhibition of hippocampal neurons. *Science,* **232,** 1413-1415.

Misgeld, U. and Frotscher, M. (1986) Postsynaptic-GABAergic inhibition of non-pyramidal neurons in the guinea-pig hippocampus. *Neuroscience,* **19,** 193-206.

Mody, I., De Koninck, Y., Otis, T. S. and Soltész, I. (1994) Bridging the cleft at GABA synapses in the brain. *Trends Neurosci.,* **17,** 517-525.

Möhler, H., Fritschy, J. M., Luscher, B., Rudolph, U., Benson, J. and Benke, D. (1996). The $GABA_A$ receptors from subunits to diverse functions. *Ion Channels.* Vol. 4. pp. 89-113.

Morin, F., Beaulieu, C. and Lacaille, J. -C (1996) Membrane properties and synaptic currents evoked in CA1 interneuron subtypes in rat hippocampal slices. *J. Neurophysiol.,* **76,** 1-16.

Moser, E. I. (1996) Altered inhibition of dentate granule cells during spatial learning in an exploration task. *J. Neurosci.,* **16,** 1247-1259.

Müller, W. and Misgeld, U. (1990) Inhibitory role of dentate hilus neurons in guinea pig hippocampal slice. *J. Neurophysiol.,* **64,** 46-56.

Nakanishi, S. (1994) Metabotropic glutamate receptors: synaptic transmission, modulation, and plasticity. *Neuron,* **13,** 1031-1037.

Nathan, T. and Lambert, J. D. (1991) Depression of the fast IPSP underlies paired-pulse facilitation in area CA1 of the rat hippocampus. *J. Neurophysiol.,* **66,** 1704-1715.

Newberry, N. R. and Nicoll, R. A. (1984a) A bicuculline-resistant inhibitory post-synaptic potential in rat hippocampal pyramidal cells in vitro. *J. Physiol. (Lond),* **348,** 239-54.

Newberry, N. R. and Nicoll, R. A. (1985) Comparison of the action of baclofen with g-aminobutyric acid on rat hippocampal pyramidal cells in vitro. *J. Physiol. (Lond),* **360,** 161-185.

Newberry, N. R. and Nicoll, R. A. (1984b) Direct hyperpolarizing action of baclofen on hippocampal pyramidal cells. *Nature,* **308,** 450-452.

Nicoll, R. A. (1988) The coupling of neurotransmitter receptors to ion channels in the brain. *Science,* **241,** 545-550.

Nicoll, R. A. (1994) Neuroscience - Cajals rational psychology. *Nature,* **368,** 808-809.

Nicoll, R. A. and Dutar, P. (1990) Pre- and postsynaptic $GABA_B$ responses in the hippocampus. In. *$GABA_B$ receptors in mammalian function.* John Wiley & Sons Ltd, pp198-205.

Niedermeyer, E. and Lopes da Silva, F. (1993) Electroencephalography: basic principles, clinical applications, and related fields. Williams and Wilkins, Baltimore.

Nitsch, R., Soriano, E. and Frotscher, M. (1990) The parvalbumin-containing nonpyramidal neurons in the rat hippocampus. *Anat. Embryol.*, **181,** 413-425.

Nunzi, M. G., Gorio, A., Milan, F., Freund, T. F., Somogyi, P. and Smith, A. D. (1985) Cholecystokinin-immunoreactive cells form symmetrical synaptic contacts with pyramidal and non-pyramidal neurons in the hippocampus. *J. Comp. Neurol.*, **237,** 485-505.

Nusser, Z., Roberts, J. D., Baude, A., Richards, J. G., Sieghart, W., and Somogyi, P (1995) Immunocytochemical localization of the α1 and β2/3 subunits of the $GABA_A$ receptor in relation to specific GABAergic synapses in the dentate gyrus. *Eur. J. Neurosci.*, **7**, 630-646.

Nusser, Z., Sieghart, W., Benke, D., Fritschy, J. -M and Somogyi, P. (1996) Differential synaptic localization of two major γ-aminobutyric acid type A receptor subunits on hippocampal pyramidal cells. *Proc. Natl. Acad. Sci. U.S.A.*, In press

O'Keefe, J. and Recce, M. L. (1993) Phase relationship between hippocampal place units and the EEG theta-rhythm. *Hippocampus,* **3,** 317-330.

Otis, T. S., de Koninck, Y. and Mody, I. (1993) Characterization of synaptically elicited $GABA_B$ responses using patch-clamp recordings in rat hippocampal slices. *J. Physiol. (Lond),* **463,** 391-407.

Otis, T. S. and Mody, I. (1992) Differential activation of $GABA_A$ and $GABA_B$ receptors by spontaneously released transmitter. *J. Neurophysiol.*, **67,** 227-235.

Patton, P. E. and McNaughton, B. (1995) Connection matrix of the hippocampal formation.1. The dentate gyrus. *Hippocampus,* **5,** 245-286.

Paulsen, O. and Heggelund, P. (1994) The quantal size at retinogeniculate synapses determined from spontaneous and evoked EPSCs in guinea-pig thalamic slices. *J. Physiol. (Lond),* **480,** 505-11.

Paulsen, O. and Vida, I. (1996) Sustained dendritic oscillations at theta frequencies elicited in CA1 pyramidal cells in rat hippocampal slices. *J. Physiol. (Lond),* In press

Pearce, R. A. (1993) Physiological evidence for two distinct $GABA_A$ responses in rat hippocampus. *Neuron,* **10,** 189-200.

Pearce, R. A., Grunder, S. D. and Faucher, L. D. (1995) Different mechanisms for use-dependent depression of two $GABA_A$-mediated IPSCs in rat hippocampus. *J. Physiol. (Lond),* **484,** 425-435.

Peters, A.,Palay, S. L. and Webster, H. (1991) The Fine Structure of the Nervous System. Oxford University Press, New York.

Petsche, H., Stumpf, C. and Gogolak, G. (1962) The significance of the rabbit's septum as a relay station between the midbrain and the hippocampus. The control of hippocampus arousal activity by septum cells. *Electroenc. Clin. Neurophysiol.,* **14,** 202-211.

Pham, T. M. and Lacaille, J. -C (1996) Multiple postsynaptic actions of GABA via $GABA_B$ receptors on CA1 pyramidal cells of rat hippocampal slices. *J. Neurophysiol.,* **76,** 69-80.

Pin, J. P. and Duvoisin, R. (1995) The metabotropic glutamate receptors: structure and functions. *Neuropharmacology,* **34,** 1-26.

Poolos, N. P. and Kocsis, J. D. (1990) Dendritic action potentials activated by NMDA receptor-mediated EPSPs in CA1 hippocampal pyramidal cells. *Brain Res.*, **524,** 342-346.

Qian, N. and Sejnowski, T. J. (1990) When is an inhibitory synapse effective? *Proc. Natl. Acad. Sci. U.S.A.*, **87,** 8145-8149.

Rall, W. (1977) Core conductor theory and cable properties of neurons. In. Kandel, E. R. (ed.) *The nervous system, Vol. I: cellular biology of neurons, part 1.* American Physiological Society, Bethesda, pp39-97.

Ramon y Cajal, S. (1911) *Histologie du systeme nerveux de l'homme et des vertebres.* Maloine, Paris,

Ramon y Cajal, S. (1893) Estructura del asta de ammon. *Anal Socied Historia natural.*, **XXII,**

Redman, S. (1990) Quantal analysis of synaptic potentials in neurons of the central nervous system. *Physiol. Rev.*, **70,** 165-198.

Reynolds, E. S. (1963) The use of lead citrate at high pH as an electron opaque stain in electron microscopy. *J. Cell. Biol.*, **17,** 208-212.

Ribak, C. E. and Seress, L. (1983) Five types of basket cell in the hippocampal dentate gyrus: a combined Golgi and electron microscopic study. *J. Neurocytol.*, **12,** 577-597.

Ribak, C. E. and Seress, L. (1988) A Golgi-electron microscopic study of fusiform neurons in the hilar region of the dentate gyrus. *J. Comp. Neurol.*, **271,** 67-78.

Robbins, S. L. and Kumar, V. (1987) Basic pathology. W. B. Saunders, Philadelphia.

Robertson, B. and Taylor, W. R. (1986) Effects of gamma-aminobutyric acid and (-)-baclofen on calcium and potassium currents in cat dorsal root ganglion neurones in vitro. *Br. J. Pharmacol.*, **89,** 661-672.

Ropert, N., Miles, R. and Korn, H. (1990) Characteristics of miniature inhibitory postsynaptic currents in CA1 pyramidal neurones of rat hippocampus. *J. Physiol. (Lond),* **428,** 707-722.

Schaffer, K. (1892) Beitrag zur Histologie der Ammonshornformation. *Arch. Mikros. Anat.*, **39,** 611-632.

Scharfman, H. E., Kunkel, D. D. and Schwartzkroin, P. A. (1990) Synaptic connections of dentate granule cells and hilar neurons: results of paired intracellular recordings and intracellular horseradish peroxidase injections. *Neuroscience,* **37,** 693-707.

Schwartzkroin, P. A. (1994) Role of the hippocampus in epilepsy. *Hippocampus,* **4,** 239-242.

Schwartzkroin, P. A. and Kunkel, D. D. (1985) Morphology of identified interneurons in the CA1 regions of guinea pig hippocampus. *J. Comp. Neurol.*, **232,** 205-218.

Segal, M. (1990) A subset of local interneurons generate slow inhibitory postsynaptic potentials in hippocampal neurons. *Brain Res.*, **511,** 163-164.

Segal, M. and Landis, S. (1974) Afferents to the hippocampus of the rat studied with the method of retrograde transport of horseradish peroxidase. *Brain Res.*, **78,** 1-15.

Seress, L. and Ribak, C. E. (1985) A combined Golgi-electron microscopic study of non-pyramidal neurons in the CA1 area of the hippocampus. *J. Neurocytol.*, **14,** 717-730.

Seress, L. and Ribak, C. E. (1990) The synaptic connections of basket cell axons in the developing rat hippocampal formation. *Exp. Brain Res.*, **81,** 500-508.

Sherrington, C. (1906) The integrative action of the nervous system. Yale University Press, New Haven.

Sherrington, C. (1897) A textbook of physiology.In Macmillan, New York,

Sieghart, W. (1995) Structure and pharmacology of g-aminobutyric $acid_A$ receptor subtypes. *Pharm. Revs.*, **47,** 181-234.

Sík, A., Penttonen, M., Ylinen, A. and Buzsáki, G. (1995) Hippocampal CA1 interneurons: an in vivo intracellular labeling study. *J. Neurosci.*, **15,** 6651-6665.

Sík, A., Ylinen, A., Penttonen, M. and Buzsáki, G. (1994) Inhibitory CA1-CA3-hilar region feedback in the hippocampus. *Science,* **265,** 1722-1724.

Singer, W. (1993) Synchronization of cortical activity and its putative role in information processing and learning. *Annu. Rev. Physiol.*, **55,** 349-374.

Skrede, K. K. and Westgaard, R. H. (1971) The transverse hippocampal slice: a well-defined cortical structure maintained in vitro. *Brain Res.*, **35,** 589-593.

Sloviter, R. S. (1989) Calcium-binding protein (calbindin-D_{28k}) and parvalbumin immunocytochemistry: Localization in the rat hippocampus with specific reference to the selective vulnerability of hippocampal neurons to seizure activity. *J. Comp. Neurol.*, **280,** 183-196.

Sloviter, R. S. and Nilaver, G. (1987) Immunocytochemical localization of GABA, cholecystokinin, vasoactive intestinal polypeptide-, and somatostatin-like immunoreactivity in the area dentata and hippocampus of the rat. *J. Comp. Neurol.,* **256,** 42-60.

Solis, J. M. and Nicoll, R. A. (1992) Postsynaptic action of endogenous GABA released by nipecotic acid in the hippocampus. *Neurosci. Lett.,* **147,** 16-20.

Soltész, I. and Crunelli, V. (1992) A role for low-frequency, rhythmic synaptic potentials in the synchronization of cat thalamocortical cells. *J. Physiol.,* **457,** 257-276.

Soltész, I. and Deschênes, M. (1993) Low- and high-frequency membrane potential oscillations during theta activity in CA1 and CA3 pyramidal neurons of the rat hippocampus under ketamine-xylazine anesthesia. *J. Neurophysiol.,* **70,** 97-116.

Soltész, I., Smetters, D. K. and Mody, I. (1995) Tonic inhibition originates from synapses close to the soma. *Neuron,* **14,** 1273-1283.

Somogyi, P. (1977) A specific 'axo-axonal' interneuron in the visual cortex of the rat. *Brain Res.,* **136,** 345-350.

Somogyi, P. (1989) Synaptic organisation of GABAergic neurons and $GABA_A$ receptors in the lateral geniculate nucleus and visual cortex. In Lam, D. K-T and Gilbert, C. D. (ed.), *Neural Mechanisms of Visual Perception. Proc Retina Res Found Symp.* Portfolio Publ, The Woodlands, Texas, pp. 35-62.

Somogyi, P., Freund, T. F. and Cowey, A. (1982) The axo-axonic interneuron in the cerebral cortex of the rat, cat and monkey. *Neuroscience,* **7,** 2577-2607.

Somogyi, P., Freund, T. F., Hodgson, A. J., Somogyi, J., Beroukas, D. and Chubb, I. W. (1985) Identified axo-axonic cells are immunoreactive for GABA in the hippocampus and visual cortex of the cat. *Brain Res.*, **332,** 143-149.

Somogyi, P., Hodgson, A. J., Smith, A. D., Nunzi, M. G., Gorio, A. and Wu, J. -Y. (1984) Different populations of GABAergic neurons in the visual cortex and hippocampus of cat contain somatostatin- or cholecystokinin-immunoreactive material. *J. Neurosci.*, **4,** 2590-2603.

Somogyi, P., Nunzi, M. G., Gorio, A. and Smith, A. D. (1983a) A new type of specific interneuron in the monkey hippocampus forming synapses exclusively with the axon initial segments of pyramidal cells. *Brain Res.*, **259,** 137-142.

Somogyi, P., Smith, A. D., Nunzi, M. G., Gorio, A., Takagi, H. and Wu, J. -Y. (1983b) Glutamate decarboxylase immunoreactivity in the hippocampus of the cat: distribution of immunoreactive synaptic terminals with special reference to the axon initial segment of pyramidal neurons. *J. Neurosci.*, **3,** 1450-1468.

Soriano, E. and Frotscher, M. (1989) A GABAergic axo-axonic cell in the fascia dentata controls the main excitatory hippocampal pathway. *Brain Res.*, **503,** 170-174.

Soriano, E., Nitsch, R. and Frotscher, M. (1990) Axo-axonic chandelier cells in the rat fascia dentata: Golgi-electron microscopy and immunocytochemical studies. *J. Comp. Neurol.*, **293,** 1-25.

Spruston, N., Schiller, Y., Stuart, G. and Sakmann, B. (1995) Activity-dependent action potential invasion and calcium influx into hippocampal CA1 dendrites. *Science,* **268,** 297-300.

Squire, L. R., Schimamura, A. P. and Amaral, D. G. (1989) Memory and the hippocampus.In. Byrne, J. H. and Berry, W. O. (eds.) *Neural models of placticity: experimental and theoretical approaches.* Academic Press, San Diego, pp. 208-239.

Stafstrom, C. E., Schwindt, P. C., Chubb, M. C. and Crill, W. E. (1985) Properties of persistent sodium conductance and calcium conductance of layer V neurons from cat sensorimotor cortex in vitro. *J. Neurophysiol.,* **53,** 153-170.

Staley, K. J. and Mody, I. (1992) Shunting of excitatory input to dentate gyrus granule cells by a depolarizing $GABA_A$ receptor-mediated postsynaptic conductance. *J. Neurophysiol.,* **68,** 197-212.

Staley, K. J., Soldo, B. L. and Proctor, W. R. (1995) Ionic mechanisms of neuronal excitation by inhibitory $GABA_A$ receptors. *Science,* **269,** 977-81.

Steriade, M., Nunez, A. and Amzica, F. (1993) A novel slow (<1 Hz) oscillation of neocortical neurons in vivo: depolarizing and hyperpolarizing components. *J. Neurosci.,* **13,** 3252-3265.

Stewart, M. and Fox, S. E. (1990) Do septal neurons pace the hippocampal theta rhythm? *Trends Neurosci.,* **13,** 163-168.

Stuart, G. J. and Sakmann, B. (1994) Active propagation of somatic action potentials into neocortical pyramidal cell dendrites. *Nature,* **367,** 69-72.

Swanson, L. W., Köhler, C. and Björklund, A. (1987) The limbic region. I: The septohippocampal system. In Björklund, A.,Hökfelt, T. and Swanson, L. W. (ed.), *Handbook of Chemical Neuroanatomy.* Elsevier, Amsterdam, pp. 125-277.

Tamás, G., Buhl, E. H. and Somogyi, P. (1996) Fast IPSPs elicited via multiple synaptic release sites by distinct types of GABAergic neurone in the cat visual cortex. *J. Physiol. (Lond),* Submitted.

Tarczy-Hornoch, K., Martin, K., Jack, J. and Stratford, K. (1996) Paired recording of synaptic interactions involving inhibitory neurones in layer 4 of cat visual cortex in vitro. *J. Physiol. (Lond),* In press

Thompson, S. M. (1994) Modulation of inhibitory synaptic transmission in the hippocampus. *Prog. Neurobiol.,* **42,** 575-609.

Thompson, S. M., Capogna, M. and Scanziani, M. (1993) Presynaptic inhibition in the hippocampus. *Trends Neurosci.,* **16,** 222-227.

Thompson, S. M. and Gähwiler, B. H. (1989) Activity-dependent disinhibition. I. Repetitive stimulation reduces IPSP driving force and conductance in the hippocampus in vitro. *J. Neurophysiol.,* **61,** 501-511.

Thompson, S. M. and Gähwiler, B. H. (1992) Comparison of the actions of baclofen at pre- and postsynaptic receptors in the rat hippocampus *in vitro*. *J. Physiol. (Lond),* **451,** 329-345.

Thomson, A. M. and Radpour, S. (1991) Excitatory connections between CA1 pyramidal cells revealed by spike triggered averaging in slices of rat hippocampus are partially NMDA receptor mediated. *Eur. J. Neurosci.,* **3,** 587-601.

Tóth, K. and Freund, T. F. (1992) Calbindin D_{28k}-containing nonpyramidal cells in the rat hippocampus: their immunoreactivity for GABA and projection to the medial septum. *Neuroscience,* **49,** 793-805.

Traub, R. D., Jefferys, J. G. R., Miles, R., Whittington, M. A. and Tóth, K. (1994) A branching dendritic model of a rodent CA3 pyramidal neurone. *J. Physiol. (Lond),* **481,** 79-95.

Traub, R. D., Miles, R. and Wong, R. K. S. (1989) Model of the origin of rhythmic population oscillations in the hippocampal slice. *Science,* **243,** 1319-1325.

Traub, R. D., Miles, R., Wong, R. K. S., Schulman, L. S. and Schneiderman, J. H. (1987a) Models of synchronized hippocampal bursts in the presence of inhibition. II. Ongoing spontaneous population events. *J. Neurophysiol.,* **58,** 752-764.

Traub, R. D., Miles, R. and Wong, R. K. S. (1987b) Models of synchronized hippocampal bursts in the presence of inhibition. I. Single population events. *J. Neurophysiol.,* **58,** 739-751.

Traub, R. D. and Miles, R. (1991) Neuronal networks of the hippocampus. Cambridge University Press, Cambridge.

Traub, R. D. and Miles, R. (1995) Pyramidal cell to inhibitory cell spike transduction explicable by active dendritic conductances in inhibitory cell. *J. Comput. Neurosci.,* **2,** 291-298.

Traub, R. D., Wong, R. K., Miles, R. and Michelson, H. (1991) A model of a CA3 hippocampal pyramidal neuron incorporating voltage-clamp data on intrinsic conductances. *J. Neurophysiol.,* **66,** 635-650.

Treves, A. and Rolls, E. T. (1994) Computational analysis of the role of the hippocampus in memory. *Hippocampus,* **4,** 374-391.

Turner, R. W., Meyers, D. E. R. and Barker, J. L. (1993) Fast pre-potential generation in rat hippocampal CA1 pyramidal neurons. *Neuroscience,* **53,** 949-959.

Turner, R. W., Meyers, D. E. R. and Barker, J. L. (1989) Localization of tetrodotoxin-sensitive field potentials of CA1 pyramidal cells in the rat hippocampus. *J. Neurophysiol.,* **62,** 1375-1387.

Turner, R. W., Meyers, D. E. R., Richardson, T. L. and Barker, J. L. (1991) The site for initiation of action potential discharge over the somatodendritic axis of rat hippocampal CA1 pyramidal neurons. *J. Neurosci.,* **11,** 2270-2280.

Vanderwolf, C. H. (1969) Hippocampal electrical activity and voluntary movement in the rat. *Electroencephalogr. Clin. Neurophysiol.,* **26,** 407-418.

Venables, W. N. and Ripley, B. D. (1994) Modern applied statistics with S-Plus. Springer-Verlag, New York.

Verdoorn, T. A., Draguhn, A., Ymer, S., Seeburg, P. H. and Sakmann, B. (1990) Functional properties of recombinant rat $GABA_A$ receptors depend upon subunit composition. *Neuron,* **4,** 919-928.

Vida, I., Buhl, E. H., Halasy, K., Szinyei, C. and Somogyi, P. (1997) Lacunosum-moleculare interneurones evoke $GABA_A$ receptor mediated IPSPs in pyramidal cells of the hippocampal CA1 area. *J. Neurosci.,* In preparation

Watkins, J. C., Krogsgaard-Larsen, P. and Honoré, T. (1990) Structure-activity relationships in the development of excitatory amino acid receptor agonists and competitive antagonists. *Trends Pharmacol. Sci.,* **11,** 25-33.

Whittington, M. A., Traub, R. D. and Jefferys, J. G. R. (1995) Synchronized oscillations in interneuron networks driven by metabotropic glutamate receptor activation. *Nature,* **373,** 612-615.

Whittingham, T. S., Lust, W. D., Christakis, D. A. and Passonneau, J. V. (1984) Metabolic stability of hippocampal slice preparations during prolonged incubation. *J. Neurochem.,* **43,** 689-696.

Williams, S., Samulack, D. D., Beaulieu, C. and Lacaille, J. -C. (1994) Membrane properties and synaptic responses of interneurones located near the stratum lacunosum-moleculare / radiatum border of area CA1 in whole-cell recordings from rat hippocampal slices. *J. Neurophysiol.,* **71**, 2217-2235.

Wisden, W., Laurie, D. J., Monyer, H. and Seeburg, P. H. (1992) The distribution of 13 $GABA_A$ receptor subunit mRNAs in the rat brain. I. Telencephalon, diencephalon, mesencephalon. *J. Neurosci.,* **12,** 1040-1062.

Woodson, W., Nitecka, L. and Ben-Ari, Y. (1989) Organization of the GABAergic system in the rat hippocampal formation: a quantitative immunocytochemical study. *J. Comp. Neurol.,* **280,** 254-271.

Wouterlood, F. G., Saldana, E. and Witter, M. P. (1990) Projection from the nucleus reuniens thalami to the hippocampal region: light and electron microscopic tracing study in the rat with the anterograde tracer phaseolus vulgaris-leucoagglutinin. *J. Comp. Neurol.,* **296,** 179-203.

Yamamoto, C. and McIlwain, H. (1966) Electrical activities in thin sections from the mammalian brain maintained in chemically-defined media in vitro. *J. Neurochem.,* **13,** 1333-1343.

Ylinen, A., Bragin, A., Nadasdy, Z., Jando, G., Szabo, I., Sík, A. and Buzsáki, G. (1995a) Sharp wave-associated high-frequency oscillation (200 Hz) in the intact hippocampus: network and intracellular mechanisms. *J. Neurosci.,* **15,** 30-46.

Ylinen, A., Soltész, I., Bragin, A., Penttonen, M., Sík, A. and Buzsáki, G. (1995b) Intracellular correlates of hippocampal theta rhythm in identified pyramidal cells, granule cells, and basket cells. *Hippocampus,* **5,** 78-90.

Yuste, R. and Tank, D. W. (1996) Dendritic integration in mammalian neurons, a century after Cajal. *Neuron,* **16,** 701-716.

Zimprich, F., Zezula, J., Sieghart, W. and Lassmann, H. (1991) Immunohistochemical localization of the α1, α2 and α3 subunit of the $GABA_A$ receptor in the rat brain. *Neurosci. Lett.,* **127,** 125-128.

Zola-Morgan, S. and Squire, L. R. (1993) Neuroanatomy of memory. *Ann. Rev. Neurosci.,* **16,** 547-563.